The role of MITF in pigmentation, hypopigmentation syndromes and melanoma

Christine Grill

Thesis for the degree of Philosophiae Doctor
University of Iceland
Faculty of Medicine
School of Health Sciences
November 2013

The role of MITF in pigmentation, hypopigmentation syndromes and melanoma

Christine Grill

Thesis for the degree of Philosophiae Doctor
Supervisor: Prof. Eiríkur Steingrímsson
Doctoral committee:
Prof. Colin Goding
Prof. Guðmundur Hrafn Guðmunsson
Dr. Zophonías Jonsson
Prof. Magnús Karl Magnússon

University of Iceland
School of Health Sciences
Faculty of Medicine
November 2013

Hlutverk MITF í litfrumum,

sortuæxlum og heilkennum sem hafa áhrif á litfrumur

Christine Grill

Ritgerð til doktorsgráðu
Umsjónarkennari: Prof. Eiríkur Steingrímsson
Doktorsnefnd:
Prof. Colin Goding
Prof. Guðmundur Hrafn Guðmunsson
Dr. Zophonías Jonsson
Prof. Magnús Karl Magnússon

Háskóli Íslands
Heilbrigðisvísindasvið
Læknadeild
November 2013

Thesis for a doctoral degree at the University of Iceland. All right reserved. No part of this publication may be reproduced in any form without the prior permission of the copyright holder.

© Author Christine Grill 2013

ISBN 978-9935-9138-9-0

Printing by Háskólaprent (http://haskolaprent.is/)
Reykjavik, Iceland 2013

Dedicated to:

My Mum

Ágrip

Lifrumur (melanocytes) framleiða litinn sem sjá má í húð, hárum og augum manna og dýra. Umritunarþátturinn MITF (Microphthalmia associated transcription factor) er nauðsynlegur fyrir öll skref í þroskun og starfsemi litfruma. Breytingar í starfsemi MITF hafa því áhrif á litarhátt en geta einnig leitt til sortuæxla en það eru krabbamein litfrumanna. Stökkbreytingar hafa fundist í MITF geninu í sjúklingum með Waardenburg heilkenni af gerð 2A (WS2A) og með Tietz heilkennið (TS) en einnig í sortuæxlum. Í ritgerð þessari voru áhrif þeirra stökkbreytinga sem lýst hefur verið í MITF geninu í WS2A, TS og sortuæxlum skoðuð með tilliti til áhrifa á starfsemi próteinsins. Skoðuð voru áhrif á umritunarvirkni, DNA bindigetu, staðsetningu í kjarna og getu til að mynda klón. Niðurstöðurnar sýna að flestar WS2A og TS stökkbreytingarnar leiða til próteina sem geta hvorki bundist DNA né virkjað umritun. Nokkrar stökkbreytinganna sýndu þó sömu virkni og villigerðar-MITF. Tvær stökkbreytinganna, R203K og S298P, eru líklega náttúrulegir breytileikar sem ekki valda WS2A eða TS. Niðurstöðurnar sýna í fyrsta sinn hvaða áhrif þessar stökkbreytingar hafa á starfsemi MITF. Þær stökkbreytingar í MITF sem fundist hafa í sortuæxlum hafa engin áhrif á DNA bindigetu og minniháttar áhrif á umritunarvirkni; sumar breytinganna sýndu aukna getu til að mynda klón.

Einnig var skoðað hlutverk IRF4 (interferon regulatory factor 4) í litfrumum. Nýlegar rannsóknir hafa sýnt að einbasabreytileikar í IRF4 tengjast hára- og augnlit, freknum og getunni til að taka lit í sól. Tjáning IRF4 er undir stjórn MITF. Hér sýnum við að MITF og IRF4 vinna saman að því að virkja tjáningu Týrósínasa, ensíms sem gegnir lykilhlutverki í framleiðslu litarefnisins melanín. Niðurstöður okkar sýna að IRF4 hefur áhrif á litarhátt manna með því að stjórna tjáningu týrósínasa í samstarfi við MITF.

Lykilorð: MITF, litarháttur, Waardenburg heilkenni, sortuæxli, IRF4.

Abstract

Melanocytes are pigment producing cells, responsible for skin-, hair- and eye color. Microphthalmia-associated transcription factor, MITF, is a master regulator of melanocytes, regulating their development, function and survival. Hence, alterations of MITF result in changes in pigmentation but can also lead to severe pathologies such as melanoma, the cancer arising from melanocytes. MITF mutations have been identified in patients with hypopigmentation syndromes Waardenburg syndrome type 2A (WS2A) and Tietz syndrome (TS) as well as in patients with melanoma. Here, MITF mutations associated with WS2A, TS and melanoma were investigated in respect to their biochemical effects. The effects of these mutations on transcription activation potential of melanocyte-specific promoters, DNA-binding ability, nuclear localization and clonogenic potential were determined. The results suggest that most of the mutations associated with WS2A and TS fail to activate melanocyte-specific promoters and to bind DNA; nuclear localization was unaffected. Interestingly, some mutations behaved similarly to wild type MITF. Two of the mutations, R203K and S298P, are most likely neutral variants and not causative mutations of WS2A. Mutations associated with melanoma, behave very similar as wild type MITF regarding their transcription activation potential and DNA-binding ability. This study provides a first and important insight in how these mutations behave regarding their transcription activation potential and DNA binding.

We further investigate the role of IRF4, interferon regulatory factor 4, in pigmentation. Previous genome-wide association studies have associated a single nucleotide polymorphism in intron 4 of IRF4 with hair- and eye color, tanning ability and freckles. Also, it has been shown that IRF4 expression is activated by MITF. Here we show that MITF and IRF4 cooperate to activate expression of tyrosinase, the key enzyme in melanogenesis. This shows that IRF4 regulates human pigmentation by cooperating with MITF in order to activate TYR expression.

Keywords: MITF, pigmentation, Waardenburg syndrome, melanoma and IRF4.

Acknowledgements

I would like to express my very great appreciation to Prof. Eiríkur Steingrímsson who, as my supervisor guided me through various stages of my PhD studies. I thank him for his patience, support and critical opinion throughout my studies. He is an inspirational figure and I am grateful that I have been a PhD student of his laboratory. Further, I would like to thank all current and former members of the laboratory of Prof. Eiríkur Steingrímsson; Christian Praetorius, Kristín Bergsteinsdóttir, Alexander Schepsky, Benedikta Hafliðadóttir, Margrét H. Ögmundsdóttir and Erna Magnúsdóttir. I would like to thank all the co-authors of the publications. I wish to acknowledge the help provided by colleagues from the Biomedical Centre, BMC; Guðrún Valdimarsdóttir, Anne Richter, Stefán Þ. Sigurðsson, Hans Guttormor Þormar, Pétur Henry Petersen, Sif Jónsdóttir and Jónína Jóhannsdóttir. I would like to thank my PhD committee, Prof. Colin Goding, Prof. Guðmundur Hrafn Guðmundsson, Prof, Magnús Karl Magnússon and Dr. Zophonías Jónsson for their opinions on my PhD studies. In particular, I would like to thank Prof. Colin Goding who, as a leader of the pigment cell and melanoma community has been an inspirational scientific figure and I appreciated all his comments on the manuscript. Also I wish to thank Prof. Lionel Larue, Prof. Heinz Arnheiter and Prof. Robert Cornell for vivid discussions of my research projects at scientific meetings.

My family, my parents, I thank them from the bottom of my heart for their continuous support throughout the years.

Over the last several years, many people helped me along my PhD studies and I would like to thank all of them for being so helpful and patient.

Contents

List of abbreviations

3'UTR – 3' untranslated region

5'UTR – 5' untranslated region

A – adenine

Ab – antibody

AICD – activation-induced cell death

AICDA – activation-induced cytidine deaminase

AKT – protein kinase B (the AKT oncogene was isolated from the directly transforming murine retrovirus AKT8, which was isolated from an AKR mouse thymoma cell line)

ALCL – anaplastic large-cell lymphoma

ALL – acute lymphoblastic leukemia

APC – antigen presenting cell

ARL – AIDS-related lymphoma (AIDS=acquired immunodeficiency syndrome)

ASIP – agouti signaling protein

ATL – acute T-cell lymphoma

BAX – Bcl2-associated X protein

BCC – basal cell carcinoma

BCL6 – B-cell lymphoma 6

BCRA1 – breast cancer type 1 susceptibility protein 1

Blimp-1 – B-lymphocyte maturation protein

Bp – base pair bp

C – cytosine

cAMP – cyclic adenosine monophosphate

CAT – chloramphenicol acetyltransferase

CBP – cyclic-AMP response element binding protein

CD – cysteinylDOPA

CDKN2a – cycline-dependent kinase inhibitor 2 a = p16

ChIP – chromatin immunoprecipitation

CHL – chronic Hodgkin's lymphoma

CLL – chronic lymphocytic leukemia

CMM – cutaneous malignant melanoma

CR – conserved region

DC – dendritic cell

DCT – dopachrome tautomerase

DHFR – Dihydrofolate reductase

DHI – 5,6-dihydroxyindole

DHICA – 5,6-dihydroxyindole-2-carboxylic acid

DIA1 – diaphanous-related formin

DLBCL – diffuse large B-cell lymphoma

DNA – deoxyribonucleic acid

DQ – dopaquinone

EMSA – electrophoretic mobility shift assay

ER – endoplasmatic reticulum

FL – follicular lymphoma

FOXD3 – forkhead box transcriptional repressor

G – guanine

GC – germinal center

GSK3β - glycogen synthase kinase 3 β

GWAS – genome-wide association studies

HEK – human embryonic kidney cells

HERC2 – hect domain and RCC1-like domain 2

HGF – hepatocyte growth factor

HIF1α – hypoxia-inducible factor 1α

HIV – human immunodeficiency virus

HL – Hodgkin's lymphoma

HLM – haematolymphoid malignancies

HPFS – Health Professionals Follow-Up Study

HRS (cells) – Hodgkin and Reed-Sternberg (cells)

IgVH – immunoglobin (V=variable; H=heavy chain)

IHC – immunohistochemistry

INF-α – interferon alpha

IRF4 – interferon regulatory factor 4

ISRE – interferon-specific response element

LCMV – lymphocytic choriomeningitis

LEF-1 – lymphoid enhancer binding-protein 1

LPS – lipopolysaccharide

LSIRF – lymphoid specific member of the interferon regulatory factor family

MALT – mucosal associated lymphoid tissue

MAP – mitogen-activated protein

MAPK – mitogen-activated protein kinase

MATP – membrane associated transporter protein

MC1R – Melanocortin 1 receptor

MCL – mantle cell lymphoma

miRNA – micro RNA

MITF – microphthalmia associated transcription factor

ML-IAP – melanoma inhibitor of apoptosis

MM - malignant melanoma

MM2 – matrix metalloprotease 2

mRNA – messenger ribonucleic acid

α-MSH – α-melanocyte stimulating hormone

MTAP – methylthioadenosine phosphorylase

MTX – Methotrexate

MZL – marginal zone lymphoma

NHL – Non-Hodgkin lymphoma

NHS – Nurse's Health Study

NK (cells) – natural killer (cells)

NLPHL – nodular lymphocytic predominant Hodgkin's lymphoma

OA – ocular albinism

OCA2 – oculocutaneous albinism 2

OR – odds ratio

OS(R) – overall survival (rate)

PAX 3 – paired box 3

PBL – plasmablastic lymphoma

PCFCL – primary cutaneous follicle center lymphoma

PDGF-C – platelet derived growth factor C

PI3K – phosphatidylinositol-3-kinase

PIP – PU.1 interaction partner

POU3F2 – POU domain class 3 transcription factor 2

PRDM1 – PR-domain containing protein 1

PTCL – peripheral T-cell lymphoma

PTEN – phosphatase and tensin homologe deleted on chromosome 10

Q-MEGA – the Queensland Study of Melanoma; Environmental and Genetic Associations

qPCR – quantitative pPCR (polymerase chain reaction)

RB – retinoblastoma

RSK-1 – p90 ribosomal s6 kinase

RT PCR – real time PCR

RTK – receptor-tyrosine kinase

SAE – SUMO1-activating enzyme

SCC – squamous cell carcinoma

SF – steel factor / Kit ligand

shRNA – small hairpin RNA

siRNA – small interference RNA

SILV – silver (mouse homologue to human PMEL17)

SLC24A4 – solute carrier 24 A 4

SLL – small lymphocytic lymphoma

Slt – slaty

SNP – single nucleotide polymorphism

SOX10 – sry-related HMG box 10

SRY – sex-determining region Y

STAT3 – signal transducer and activator of transcription 3

T – thymine

TBX2 – T-box 2

TF – transcription factor

TFAP2α – transcription factor activating enhancer-binding protein 2 alpha

TFE3 – transcription factor for immunoglobin heavy-chain enhancer 3

TFEB – transcription factor EB

TFEC – transcription factor EC

Th (cell) – T-helper (cell)

TMECG – 3-O-(3,4,5-trimethoxybenzoyl)-(-)-epicatechin

TRAP – tartrate-resistant acid phosphatase

TS – Tietz syndrome

TYR – tyrosinase

TYRO3 – protein tyrosine kinase 3

TYRP1 – tyrosinase-related protein 1

UVR – ultra violet radiation

VEGF-C – vascular endothelial growth factor C

VT – variant type

WNT – wingless type

WS2 – Waardenburg syndrome type 2

WT – wild type

XBP-1 – X-box binding protein

List of Figures

List of Tables

List of Papers

Paper I:

MITF mutations associated with pigment deficiency syndromes and melanoma have different effects on protein function. Grill C, Bergsteinsdóttir K, Ogmundsdóttir MH, Pogenberg V, Schepsky A, Wilmanns M, Pingault V, Steingrímsson E. Hum Mol Genet. 2013 Nov 1;22(21):4357-67. doi: 10.1093/hmg/ddt285. Epub 2013 Jun 20.

Paper II:

IRF4 affects human pigmentation by regulating expression of tyrosinase through an MITF and TFAP2A-dependent pathway. Praetorius C., Grill C., Stacey SN., Metcalf AM., Robinson KC., Gorkin DU., Van Otterloo E., Kim RSQ., Mishva PJ., Davis SR., Guo T., Zaidi MR., Sigurdsson MJ., Melzer PS., Merlino G., Larue L., Loftus S., Adams DR., Pavan WJ., McCallion AS., Cornell RA., Smith AG., Fisher DE., Strum RA., Steingrimsson E. Accepted by Cell and scheduled for publication 21st of November 2013.

Declaration of contribution

With the guidance and supervision of Prof. Eiríkur Steingrímsson, Christine Grill planned and carried out the manual work shown in the thesis. The thesis has been written by Christine Grill.

Paper I: Christine Grill, Eiríkur Steingrímsson and Veronique Pingault conceived and designed this study; Christine Grill designed and recreated 21 mutants, performed the co-transfection assays, the clonogenic assays, the Western blots and the sequence alignments; Christine Grill and Kristín Bergsteinsdóttir performed the EMSA studies; Margrét H. Ögmundsdóttir and Alexander Schepsky designed and recreated 5 mutants; Vivian Pogenberg and Matthias Wilmanns contributed the structure of MITF for Figure 1B; Christine Grill and Eiríkur Steingrímsson wrote the manuscript.

Paper II: Eiríkur Steingrímsson conceived and designed this study and wrote the manuscript; Christine Grill showed the cooperative effects of MITF and IRF4 on TYR by several transcription activation assays and determined the effects of mutations of this cooperation. Christian Praetorius performed the knock down studies, the ChIP, the transcription activation assay on intron 4; Richard Sturm and students provided valuable information regarding the IRF4 polymorphism; Robert Cornell and students performed the work in zebrafish; David E. Fisher, Lionel Larue and students performed work in mice; William Pavan and students provided DNAse-sequencing data; Martin I. Sigurdsson provided the allele frequency of the SNP; Simon N. Stacey contributed information from Decode Genetics.

1. INTRODUCTION

Pigmentation is one of the most demonstrable phenotypes in the animal kingdom as demonstrated by the variable skin, eye and hair color as well as different pigmentation patterns observed in nature. Pigmentation of human skin and hair is largely determined by the amount and type of melanin pigment produced in melanocytes. The regulation of the process of melanogenesis is therefore essential for pigmentation. The number of melanocytes or body site distribution or density of melanocytes is less important (reviewed in Sturm, 2009).

1.1. Melanocytes

Melanocytes arise in the neural crest. Neural crest cells from the axial level of the trunk differentiate primarily into neurons, glia or melanocytes. The neurogenic and the melanogenic cell populations have distinct migratory properties. Neurogenic neural crest cells migrate ventrally along the neural tube whereas the melanoblasts (non-pigmented precursors of melanocytes) migrate dorsolaterally between the somites and the ectoderm. They then invade the ectoderm where they differentiate into melanocytes. Melanoblasts then migrate to the epidermis and hair follicles, their final destination, where they differentiate into melanocytes, mature pigment producing cells. Melanocytes are also found in the choroid of the eye, heart and brain (reviewed in Goding, 2007; Thomas & Erickson, 2008). Alternatively and just recently described, melanocytes are also produced from nerves innervating the skin (immature glial cells) (Adameyko et al., 2009; reviewed in Ernfors, 2010). Ernfors and colleagues describe two waves of melanocytes differentiation; the first wave describes the differentiation of melanocytes migrating the dorsolateral pathway and the second wave of melanocyte differentiation describes the melanocytes migrating the ventral pathway. The melanocytes from the second wave are thought to originate from Schwan cell precursors and that the growing nerve might serve as a stem cell nice (Adameyko et al., 2009; reviewed in Ernfors, 2010).

1.1.1. Melanogenesis

Melanosomes are membrane-bound organelles which are exclusively produced in melanocytes and in retinal pigment epithelial cells (reviewed in Kondo & Hearing, 2011; reviewed in Lin et al., 2007). Melanin pigments are synthesized within melanosomes

(Schiaffino, 2010). Melanosomes are part of the secretory/endocytic pathway, but are different from lysosomes, because melanosomes are responsible for specific functions unrelated to degradation (Schiaffino, 2010). Melanosome biogenesis originates from endosomal precursors, followed by several maturation stages. Each maturation stage is characterized by specific morphology and melanin content (Schiaffino, 2010). Stage I of melanosome biogenesis corresponds to endosomal precursors whereas stage II are non-pigmented immature organelles and stage III are partially pigmented immature organelles. Stage IV melanosomes correspond to fully melanized mature cell organelles with melanin deposition (Schiaffino, 2010). The structural protein Pmel17 represents the main constituent of the internal matrix of the melanosomes and the membrane transporters MATP/SLC45A2 and SLC24A5 are implicated in the control of pH, osmolarity and calcium content in melanosomes just to mention a few important melanosomal proteins (Schiaffino, 2010). The coordinated migration, distribution, differentiation, proliferation and function of melanoblasts (melanocyte precursors) determine the visible phenotype of skin-, hair- and eye color. The interaction of melanocytes, keratinocytes and fibroblasts in the basal layer of the epidermis is crucial for skin pigmentation (reviewed in Kondo & Hearing, 2011).

Melanogenesis is a biochemical pathway resulting in yellow-to-reddish-brown pheomelanin and black-to-brown eumelanin (reviewed in Kondo & Hearing, 2011). At the top of this pathway is the amino acid tyrosine, which through an oxidation step, catalyzed by the enzyme tyrosinase, becomes dopaquinone (DQ). The first step in eumelanogenesis is the production of cyclodopa from dopaquinone which involves a transient intermediate DOPA (L-3,4-dihydroxyphenylalanine). After a redox exchange with another dopaquinone molecule DOPAchrome is generated. Via an enzyme, the DOPAchrome tautomerase (DCT), DOPAchrome undergoes tautomerisation to produce DHICA (5,6-dihydroxyindole-2-carboxylic acid). In the absence of DCT, 5,6-dihydroxylindole (DHI) is produced. Finally, DHI and DHICA are further oxidized and polymerized to form eumelanin. The last step from DHICA to eumelanin involves tyrosinase and another enzyme, tyrosine-related protein 1 (TYRP1). Pheomelanogenesis also starts with the enzymatic reaction via tyrosinase from tyrosine to DQ, but continues with the reductive addition of cysteine to DQ to produce two cysteinylDOPA (CD) isomers. A redox exchange between CD and DQ results in CD-quiones and DOPA. Through hydration, CD-quiones form ortho-quinonimine. After quinonimide´s are rearranged, 1,4-benzothiazine intermediates are formed, which are finally polymerized to pheomelanin (reviewed in Kondo & Hearing, 2011).

Tyrosinase plays an important role and is a key enzyme in the production of melanin. Tyrosinase is a glycoprotein that matures in the endoplasmatic reticulum (ER) which provides a protective folding environment. Once the ER ensures correct folding of tyrosinase, it is subsequently sorted to the cis-Golgi. In the trans-Golgi network, tyrosinase becomes further modified by additional loadings of sugars and coppers. Subsequently tyrosinase is transported to melanosomes where it reaches the premelanosome compartment which matures to pigment producing melanosomes (reviewed in Wang & Hebert, 2006).

During the 'late stage' of melanosome biogenesis, when pigment production is complete, the melanosomes bind to microtubules and undergo actin-dependent transport toward the cell periphery, followed by the transfer to the adjacent keratinocytes. The transport and transfer process of melanosomes are critical to the distribution of melanin pigments in the skin (reviewed in Kondo & Hearing, 2011). The process by which melanosomes are transferred to keratinocytes is not fully understood although various hypotheses have been proposed including exocytosis, cytophagocytosis, fusion and membrane vesicle transport. Similar to synapses in neural systems, a pigmentary synapse must exist between melanocytes and keratinocytes (reviewed in Yamaguchi & Hearing, 2009).

Dysfunction of melanogenesis, either through lack or hyperactivation of enzymes catalyzing the biochemical reactions or through deregulation of those enzymes, results in pigmentation disorders, but also natural human pigmentation (reviewed in Kondo & Hearing, 2011). For example, mutations in tyrosinase result in oculocutaneous albinism type1 (OCA1) (reviewed in Oetting et al., 2003).

1.1.2. The αMSH pathway – regulatory pathway of pigmentation

In response to ultraviolet radiation, keratinocytes secrete factors that regulate melanocyte survival, differentiation, proliferation and mobility, stimulating melanocytes to produce melanin (reviewed in Gray-Schopfer et al., 2007). The signaling pathway triggered by α-MSH (α-melanocyte stimulating hormone) is thought to represent one of the most important regulators of pigmentation (reviewed in Chin et al., 2006). α-MSH is a pro-opiomelanocortin peptide (Busca & Ballotti, 2000). It binds the transmembrane receptor MC1R (αMSH receptor) of melanocytes and induces the activation of the αS-coupled G protein leading to the activation of adenylyl cyclase which results in increased synthesis of cAMP (cyclic adenosine monophosphate). cAMP binds to the two sites of the regulatory subunit of protein kinase A

(PKA) which activates the catalytic subunit. PKA translocates to the nucleus where it phosphorylates and activates the transcription factor CREB (cAMP response element binding protein). CREB, in the nucleus, binds the CRE sequence (cAMP response element 5'-TGACCTCA-3') and activates target genes. One of those target genes is MITF which in turn binds to the M-box of tyrosinase, tyrosine-related protein 1 (TYRP1) and dopachrometautomerase (DCT) (reviewed in Busca & Ballotti, 2000; reviewed in Steingrimsson et al., 2004; reviewed in Tachibana, 2000). cAMP elevating agents such as forskolin and cholera toxin are able to increase tyrosinase promoter activity by 10- to 20-fold, respectively, further supporting the role of cAMP in melanogenesis (Bertolotto et al., 1996).

1.1.3. Important enzymes during melanogenesis – an introduction

Constitutive pigmentation is a polygenetic trait and many loci affecting pigmentation have been identified in mouse, humans and zebrafish. The European Society of Pigment Cell Research provides information of cloned and non-cloned color genes described in mice and their human and zebrafish homologues (http://www.espcr.org/micemut/). The three related enzymes TYR, TYRP1 and DCT are of particular importance.

1.1.3.1. Identification of Tyrosinase (TYR)

In 1986 Shibahara and colleagues isolated a pigment cell-specific cDNA clone from the B16 mouse melanoma cell line. Transient transfection of the cDNA in K1735 amelanotic melanoma cells resulted in staining with a tyrosinase antibody, suggesting that the isolated cDNA clone was tyrosinase (Shibahara et al., 1986). However, it turned out that Shibahara and colleagues did not clone tyrosinase. Instead he and his colleagues cloned tyrosinase-related protein 1 (TYRP1) (Jackson, 1988). The human tyrosinase gene was cloned out of a human melanoma cell line by Known and colleagues (1987). They cloned a gene coding for 548 amino acids and a molecular weight of 62,16kDa, possessing five glycolysation sites. This gene mapped at or near the mouse albino locus at chromosome 7. It was further shown that newborn mice carrying the lethal albino deletion mutation showed no tyrosinase activity nor had any tyrosinase DNA (Kwon et al., 1987).

1.1.3.2. Tyrosinase-related protein 1 (TYRP1)

As mentioned above, the misidentification of tyrosinase was discovered by Ian Jackson, a research fellow who aligned the sequences of tyrosinase with the sequence discovered by

Shibahara and showed that it is a distinct but related gene. The gene was termed tyrosinase-related protein 1 (TYRP1) and was mapped to the *b* (brown) locus in the mouse (Jackson, 1988). BALB/c mice which are heterozygous for the *b* locus showed four nucleotide differences in the *TYRP1* gene compared to the wild type gene. One of those differences was a G to A variant at base 329 which changes the amino acid sequence from a cysteine residue to a tyrosine, suggesting that it was the causative mutation leading to the brown phenotype. This mutation is adjacent to another cysteine at which a mutation in the analogous position in tyrosinase results in the albino phenotype (Zdarsky et al., 1990). When the melanocyte cell line melan-b, which was derived from a homozygous *brown* mouse embryo, was transfected with wild type TYRP1 cDNA, the cells produced darker pigmentation than the mock-infected cells (Bennett et al., 1990). The *b*-locus encodes a glycoprotein with the activity of a catalase. Because peroxides may be byproducts of melanogenic activity and hydrogen peroxide in particular is known to destroy melanin precursors and melanin, pigmentation is controlled not only by tyrosinase but also by hydroperoxidase. It has been shown that in 'brown light' B^{lt} (a mutation that causes clumping, irregular distribution and reduced number of melanosomes) melanocytes, the *b* locus is inactive and that the B^{lt} mutation caused an increased sensitivity to proteolytic degradation (Halaban & Moellmann, 1990). These results suggest that this enzyme has an important function in the decomposition of hydrogenperoxide to water and oxygen hence controlling melanin content (Halaban & Moellmann, 1990). Interestingly, it seems that TYRP1 is required for the formation of black melanin rather than brown (Hirobe, 1984; Shibahara et al., 1991).

In humans, patients with OCA (oculocutaneous albinism) and mutations in TYRP1 belong to a particular type of OCA, namely OCA type 3 (OCA3) (Boissy et al., 1996). Affected patients have less melanin and electroscopic images revealed that melanosomes looked normal only until stage I and II (non-pigmented immature organelles). The mutation in TYRP1 is a single base pair deletion in exon 6 which leads to an amino acid change which encodes for a stop codon (Boissy et al., 1996).

1.1.3.3. Dopachrome tautomerase (DCT)

Another enzyme important during eumelanogenesis is dopachrome tautomerase (DCT). Mice that are homozygous for the recessive *slaty* mutation (*slt/slt*) have a 3- to 10-fold reduction in DCT enzyme activity and produce a dark grey/brown eumelanin rather than black. The *slaty* mutation arose spontaneously and is a point mutation that changes an arginine to a glutamine

in the first copper binding domain of DCT of two such domains (Jackson et al., 1992). It has been shown that in contrast to tyrosinase and TYRP1, DCT is expressed in melanocyte stem cells residing in the bulge of the hair follicle. DCT knockout mice show a diluted and lighter coat color (Guyonneau et al., 2004). Mice homozygous for the *slaty* mutation and DCT knockout mice both show a diluted coat color compared to the black wild type mice, indicating that the two mutations have a similar effect on eumelanin synthesis (Guyonneau et al., 2004) The *tyrosinase* gene family (*TYR, TYRP1 and DCT*) demonstrates a 40-50% conservation of amino acid identity. However, the intron-exon structure is not fully conserved. Therefore it has been proposed that the tyrosinase gene family triplication is an ancient event (Budd & Jackson, 1995).

1.2. The microphthalmia-associated transcription factor – A master regulator of melanocytes

60 years ago, Paula Hertwig described a mouse with white coat color and small (microphthalmic) eyes. This mouse was an offspring of an inbred albino mouse which descended from an irradiated male and exhibited mast cell deficiencies, inner ear defects and osteopetrosis. Hence, Paula Hertwig named the mouse 'microphthalmus' (reviewed in Arnheiter, 2010). The mutated gene, *microphthalmia-associated transcription factor (MITF),* was first cloned in mouse in 1993 by Hodgkinson and colleagues. The MITF protein is a basic-helix-loop-helix-leucine-zipper (bHLH-ZIP) transcription factor consisting of a basic DNA-binding domain and the helix-loop-helix and zipper dimerization domains. In addition it contains transcription activation domains (reviewed in Hemesath et al., 1994; reviewed in Steingrimsson et al., 2004; Takebayashi et al., 1996).

MITF is expressed in the developing ear, eye and skin but also in mast cells and osteoclasts (Hodgkinson et al., 1993; reviewed in Steingrimsson et al., 2004). The human homolog of MITF was mapped on chromosome 3 (Tachibana et al., 1994). Today, many different *MITF* mutations and their resulting phenotypes have been described in mice and humans. In all cases the mutations affect melanocytes and retinal pigmented epithelial cells and some also affect osteoclasts. In mice, about half of the *MITF* mutations are recessive, producing a phenotype only in homozygous animals (reviewed in Steingrimsson et al., 2004).

MITF is able to bind the canonical E-box sequence CACGTG as a homodimer but also as a heterodimer with the related proteins TFEB, TFE3 and TFEC. MITF acts as a transcription factor and is located in the nucleus where it is able to activate expression of pigment cell-, mast cell- and osteoclast-specific genes. Multiple *MITF* isoforms have been identified (MITF-A, -J, -C, -MC, -E, -H, -D, -B, -M and -CX) and the gene contains several different promoters which are regulated in a cell-specific manner (Li et al., 2010; reviewed in Steingrimsson, 2008; reviewed in Steingrimsson et al., 2004). This thesis will focus on the MITF-M isoform since it is expressed in the melanocytic lineage and melanomas. Interestingly, MITF-M is also expressed at a low level in the eye (choroid, retinal pigment epithelium), mast cells (cultured mast cells and peritoneal mast cells) and the heart (Bharti et al., 2008; Maruotti et al., 2012; Primot et al., 2009).

In addition to the alternative MITF isoforms discussed above several other alternative spliced versions of MITF have been identified (Primot et al., 2009). The inclusion or exclusion of exon 6a (18 bases) lead to two distinct mRNA populations of MITF. These 18 bases encode a 6-amino acid domain which is located just upstream of the basic region (Primot et al., 2009). DNA binding studies have shown that the stability of the DNA-bound complex formed with the MITF protein lacking the 18bp (termed MITF (-)) is 20% lower than that formed with MITF (+). In melanoblasts and melanocytes, MITF (+) is more abundant than MITF (-). In melanoma cell lines, MITF (-) is more abundant than MITF (+). It seems therefore that the regulation of MITF-isoform expression is different in melanoma cells from cultured precursor or differentiated melanocytes (Primot et al., 2009). These MITF-isoforms are independent of NRAS/BRAF mutation status but MEK1 and MEK2 are able to regulate the ratio of MITF (+) and MITF (-). Melanoma cells treated with U0126 (MEK1 inhibitor) showed that the MITF (-) isoform led to increased cell growth compared to the MITF (+) isoform (Primot et al., 2009). These results indicate that MAP kinase signaling regulates the ratio of MITF (+)/(-) expression and that the two MITF isoforms MITF (+) and (-) may differ in their ability to regulate and drive transcription (Primot et al., 2009). Primot et al. showed that levels of MITF (-) were markedly higher in tumor samples than in normal skin samples. These data suggest that a fraction of metastatic melanomas acquire differential expression of the *Mitf* gene (Primot et al., 2009).

Pogenberg and colleagues determined the structure of residues 180-296 of MITF. Isothermal titration calorimetry showed that the MITF(-) isoform binds with less affinity to the E-box and the M-box than the MITF(+) isoform (Pogenberg et al., 2012).

MITF forms leucine zipper-mediated homodimers, which is indicative that the dimerization is a DNA-binding independent event (Pogenberg et al., 2012). Interestingly, the second MITF protomer contains a kink at residues R259 to E260 in the zipper of MITF. This kink establishes a hole in the pattern of the leucine zipper thus restricting dimeric interactions of MITF to MITF itself and to TFE proteins (Pogenberg et al., 2012). DNA-binding studies revealed that deleting the three amino acids making the kink, E260, Q261 and Q262 (or deleting the residues R263-K265) enables heterodimerization with the bHLH zip protein MAX which normally cannot heterodimerize with MITF. This suggests that the three residue shift of the leucine zipper in wild type MITF is important for limiting its ability for heterodimerization (Pogenberg et al., 2012). Analysis of the structure of MITF also revealed that residue I212 showed reduced binding selectivity (I212N) compared to wild type MITF. Further I212N is crucial for target gene specificity, the I212N mutant protein binds the E-box sequence but to a lesser extent to the M-box sequence. These results indicate that I212 is very important for target gene selection and may in fact be a critical determinant in MITF's ability to bind the M-box (Pogenberg et al., 2012).

1.2.1. MITF target genes

MITF regulates a broad variety of genes, including genes involved in pigmentation such as *DCT, TYR, TRPI, MCIR,* and *SILV*, genes involved in cell cycle such as *p16, p21* and *p27*, or genes involved in proliferation (*MET*) and apoptosis (*BCL2*) (Carreira et al., 2006; reviewed in Cheli et al., 2009; Hoek et al., 2008; Strub et al., 2011). In order to identify novel MITF targets to further explain the role of MITF in melanocytes and melanoma, a gene expression study using MITF transfected SKmel28 cells was conducted. This study verified many of the reported MITF target genes but identified 71 additional MITF target genes (Hoek et al., 2008). Among the top five novel targets was *IRF4, interferon regulatory factor 4*, a gene previously shown to be expressed in melanocytes and melanomas (Hoek et al., 2008; Natkunam et al., 2001; Sundram et al., 2003). IRF4 will be discussed in detail in section 1.3. Another study, using ChIP-sequencing of 501 melanoma cells transfected with a HA-MITF, identified multiple MITF occupied loci including DCT, TYR, MCIR, TFAP2α, HIF1α, IRF4 and MITF itself (Strub et al., 2011). More importantly, genes involved in DNA replication, recombination and repair such as *LIG1, MCM2, EME1, BRCA1, FANCA* and *TERT* and genes involved in mitosis such as *CENPF, CENPH, CENPM* and *CENPA* were also identified (Strub et al., 2011). Hence, depletion of MITF leads to defects in mitosis and DNA replication

(Strub et al., 2011). Both studies found that numerous genes encoding SLCs (solute carriers) are occupied by MITF, most notably SLC24A2. This locus contains the 'golden' mutation in zebrafish (hypopigmentation of skin melanophores and retinal pigment epithelium) (Hoek et al., 2008; Strub et al., 2011). A variant in SLC24A2 has been reported to be involved in human pigmentation and is associated with hair color (black to blonde) and tanning ability (Lamason et al., 2005; Nan et al., 2009). Recently, BRCA1 has been implicated as an MITF target gene (Beuret et al., 2011).

1.2.1.1. MITF target genes in melanocyte differentiation: TYR and TYRP1

As mentioned in section 1.1.3., several enzymes are key players in the genesis of melanin. In this section, their transcriptional regulation will be discussed with particular emphasis on the role of MITF.

It has been shown that TYR is highly expressed in the murine melanoma cell line B16, but not in the human placental choriocarcinoma cell line (JEG3 cells) suggesting tissue specificity for melanocytes (Bentley et al., 1994). Sequence alignment of the tyrosinase promoter of human, mouse, quail and turtle revealed that there are conserved elements in these species. The most notable elements which are conserved within these species is an E-box (CATGTG) and an M-box. The M-box sequence is TCATGTGCT, basically an E-box with a flanking T at the 5' end and CT at the 3'end of the CATGTG sequence. Interestingly the E-box is fairly close to the transcription start site (Bentley et al., 1994). Transcription activation assays using various sections of the tyrosinase promoter revealed that the first 150 bp (base pairs) of the promoter showed only 10% of the level of expression shown by a fragment containing the -300 to +80bp region of the promoter. Further shortening including the removal of the first nucleotide of the E-box motif within the M-box, reduced promoter activity to around 5%. These results suggest a strong positive role for the conserved M-box. Interestingly, additional transcriptional activation studies showed that there are positively acting elements as well as a negative regulator element within the tyrosinase promoter. The E-box close to the transcription start site seems to be essential for promoter function whereas mutations affecting the M-box resulted in a decrease of tyrosinase promoter function. Bentley and colleagues showed that MITF was able to activate the tyrosinase promoter whereas it was not able to activate a mutant form of the tyrosinase promoter, lacking the E-box at the initiator region, further suggesting the importance of the E-box at the tyrosinase initiator region (Bentley et al., 1994). Similar results were shown a few years later, that MITF activates the tyrosinase

and the tyrosinase-related protein I (TYRP1) promoters in MeWo human melanoma cells (Yasumoto et al., 1997). Thorough analysis of the TYRP1 promoter revealed the presence of an M-box and cell type specific expression of TYRP1 in B16 melanoma cells but not in NIH3T3 fibroblasts (Lowings et al., 1992). Electrophoretic mobility shift assays (EMSAs) showed that MITF was able to bind DNA with the core sequence CATGTG whereas single or double nucleotide mutations within the CATGTG motif were not bound by MITF (Hemesath et al., 1994). DNA-binding assays showed that MITF protein bound the M-box in the TYRP1 promoter. Creating different mutations within the M-box resulted in complete failure of MITF binding (Yasumoto et al., 1997). MITF was also able to bind the sequence CACGTG, which is found in the *cdc25a* phosphatase gene (Aksan & Goding, 1998).

1.2.1.2. MITF target genes involved in proliferation, survival and cell cycle control

Another MITF target is TBX2, a member of the T-box family which plays a critical role in embryonic development. TBX2 has been implicated in the maintenance of cell identity. TBX2 is expressed in melanoblasts, melanocytes and melanoma cell lines but not in HeLa cells indicating that TBX2 expression is cell-specific. The mouse *Tbx2* promoter contains an E-box (CATGTG) and it has been shown that MITF is able to bind the *Tbx2* promoter element and to activate *Tbx2* expression (Carreira et al., 2000). These findings suggest that the *Tbx2* gene represents a MITF target that is not directly involved in the manufacture of pigment but is rather involved in maintaining cell identity (Carreira et al., 2000). Furthermore, TBX2 binds and represses the *p21* promoter. Depletion of TBX2 leads to activation of p21 expression. p21 contributes to stress-induced growth arrest. These data suggest that TBX2 is a regulator of p21 and that TBX2 is involved in regulation of senescence (via p21) and oncogenesis (Prince et al., 2004). TBX2 is overexpressed in melanomas but a mutant form of TBX2 has been shown to lead to reduced growth, indicating that TBX2 is required to maintain proliferation and suppresses senescence in melanomas (Vance et al., 2005).

Melastatin, also known as TRPM1, has been shown to be expressed in the eye and in melanocytes as well as in benign nevi, dysplastic nevi and melanoma (Miller et al., 2004). Loss of TRPM1 may be an indicator of melanoma aggressiveness since loss of TRPM1 expression was inversely related to tumor thickness (Miller et al., 2004). The TRPM1 promoter contains several MITF binding sites that MITF is able to bind to. Transcriptional activation assays showed that MITF is able to activate the TRPM1 promoter in HEK293 cells

(human embryonic kidney cells) (Miller et al., 2004). Thus, MITF may be an important regulator of TRPM1 in melanocytes and melanoma (Miller et al., 2004).

1.2.1.3. MITF targets playing a role during apoptosis

As mentioned earlier, BCL2 is a target of MITF (McGill et al., 2002). $Bcl2^{-/-}$ mice display profound melanocyte loss shortly after birth, whereas $Bcl2^{+/-}$ mice are fully pigmented and display no age-dependent changes (McGill et al., 2002). Mice heterozygous for vitiligo ($Mitf^{vit/+}$) are black and show no melanocyte loss over time on the other hand homozygous mice for vitiligo $Mitf^{vit/vit}$ develop gradual loss of pigmentation. Crossing $Bcl2^{+/-}$ mice with $Mitf^{vit/+}$, displayed a striking pattern of melanocyte loss over time, starting immediately after birth. These data indicate that Bcl2 and Mitf cooperate genetically in melanocytes (McGill et al., 2002). The Bcl2 promoter contains a MITF binding site (CATGTG) and it has been shown that MITF is able to bind the Bcl2 promoter and to activate it (McGill et al., 2002).

Inhibitor of apoptosis proteins (IAP) is a family of anti-apoptotic regulators that block cell death in response to diverse stimuli (Dynek et al., 2008). The promoter of the gene encoding the melanoma inhibitor of apoptosis ML-IAP contains two functional MITF binding sites. It has been shown that MITF binds to the *ML-IAP* promoter and is able to activate ML-IAP expression. Knockdown of MITF also resulted in decreased ML-IAP expression. These data show that ML-IAP is another target of MITF suggesting that ML-IAP contributes to the prosurvival activity of MITF in melanoma progression (Dynek et al., 2008).

1.2.2. Regulation of MITF expression

As MITF is a critical regulator of melanocyte development, it is important to accurately regulate its expression. Many proteins and pathways have been shown to regulate MITF expression, including SOX10, PAX3, STAT3, FOXD3, BRN2 and TYRO3 as well as CREB as already discussed in section 1.1.2.

1.2.2.1. SOX10

SOX10 is a transcription factor belonging to the SOX family. SOX10 plays a critical role in the specification, migration and survival of all non-ectomesenchymal neural crest derivates including melanocytes. SOX10 directly transactivates the *MITF* gene, both in mouse and human. The MITF promoter contains four SOX10 binding sites (Potterf et al., 2000; reviewed

in Wan et al., 2011). Interestingly, germline mutations in SOX10 and PAX3 (discussed below) share similar clinical pigmentary features with germline MITF mutations in humans (and see in following chapters) (reviewed in Tsao et al., 2012).

1.2.2.2. PAX3

PAX 3 (paired box 3) is a member of the paired class homeodomain family of transcription factors. It plays a role in brain and skeletal muscle formation at embryonic stage of development (reviewed in Wan et al., 2011). PAX3 has been shown to regulate MITF expression by binding to the MITF promoter. Further, PAX3 and SOX10 synergistically activate MITF and both bind to a proximal region of the MITF promoter which contains binding sites for both SOX10 and PAX3 (reviewed in Wan et al., 2011). PAX3 is expressed in melanocytes of normal skin, where it is co-expressed with MITF and MLNA (Medic & Ziman, 2010). Naevi, primary melanoma and metastatic melanoma also showed PAX3 expression (Medic & Ziman, 2010). Interestingly, a proportion of PAX3 positive epidermal melanocytes in normal skin also stained positive for proliferation markers such as Ki-67. These data indicate that PAX3 not only has a role in differentiation but it may also contribute to formation and development of melanocytic lesions (Medic & Ziman, 2010).

1.2.2.3. STAT3

STAT3, signal transducer and activator of transcription 3, is another regulator of MITF, although not as intensively studied as PAX3 or SOX10. STAT3 regulates transcriptional activity of MITF (reviewed in Wan et al., 2011). However, the exact mechanism by which STAT3 regulates MITF remains to be investigated and seems to be more complicated than originally anticipated. It has been shown that protein inhibitor of activated STAT3, PIAS3, directly and specifically interact with MITF and STAT3 resulting in inhibiting their transcriptional activity. Thus, it is seems to be a network of transcription factors, STAT3, PIAS3 and MITF that mediate the regulation of MITF. Additionally, STAT3 has been shown to prevent apoptosis and promote cell proliferation by regulating genes such as Bcl-XL, Mcl-l, c-myc and cyclin D1 (reviewed in Wan et al., 2011).

1.2.2.4. FOXD3

The forkhead box transcriptional repressor, FOXD3, is expressed in the dorsal neural tube during the first wave of neural crest migration and in migrating neural and glial precursors

(Thomas & Erickson, 2009). However, its expression is reduced by the time melanoblasts begin to migrate. It has been shown that FOXD3 represses melanogenesis in the neural crest and that downregulation of FOXD3 results in an increase in the number of differentiating melanocytes (Thomas & Erickson, 2009). FOXD3 is able to repress MITF expression in melanocytes and melanoma cells. FOXD3 does not bind the MITF promoter directly. Rather it prevents the binding of PAX3. Whether FOXD3 directly interacts with PAX3 and how FOXD3 is able to repress MITF remains to be investigated (Thomas & Erickson, 2009).

1.2.2.5. BRN2

The large family of POU transcription factors share a highly homologous region, referred to as POU domain. BRN2 is a member of the POU family and is expressed in melanocytes and in melanoma cell lines (Berlin et al., 2012). Mutating threonine 361 and serine 362 of BRN2 to alanines (termed BRN2AA) results in a non-phosphorylated form of BRN2. Wild type BRN2, termed BRN2TS in this paper, and the BRN2AA mutant have different DNA-binding abilities. Both BRN2 proteins are able to bind to the MITF promoter. Interestingly, only the non-phosphorylatable mutant BRN2AA form was able to bind to the *PAX3* promoter resulting in reduced *PAX3* expression. Cotransfection assays further supported the results of the DNA-binding assays. In melan-a cells it has been shown that both versions of BRN2 are able to repress MITF. In contrast, BRN2 wild type induced the transcription of *PAX3*, but the mutant version (BRN2AA) did not. It seems that phosphorylation of BRN2 is required for *PAX3* transcription but not for MITF repression (Berlin et al. 2012). Whereas the wildtype BRN2 protein induced proliferation but repressed migration, the BRN2AA mutant version reduced proliferation and migration of melanocytes and melanoma cells *in cellulo*. Although BRN2 is not expressed during melanoblast development (until E16.5) it affects melanocyte migration (Berlin et al., 2012).

1.2.2.6. TYRO3

TYRO3 is a protein tyrosine kinase that has been implicated as a novel upstream regulator of MITF (Rudloff & Samuels, 2009). TYRO3 expression was shown to be upregulated in half of the melanoma samples investigated. TYRO3 expression correlated with increased MITF expression levels and it has been suggested that TYRO3 regulates MITF through nuclear translocation of SOX10 (Rudloff & Samuels, 2009).

1.2.3. Post-transcriptional regulation of MITF

1.2.3.1. Phosphorylation

Signaling is known to affect MITF function; hence it is not surprising that the MAPK pathway is an important signaling pathway regulating MITF. Steel factor, SF (also called mast cell growth factor, MGF and stem cell factor, SCF), is the ligand for c-Kit and initiates the MAPK signaling pathway which results in MITF phosphorylation and in an increase in its transactivation potential due to phosphorylation of MITF on serine 73 (Hemesath et al., 1998; Wu et al., 2000). Phosphorylated MITF recruits the coactivator p300. Stimulation of 501 melanoma cells with SF, results in increased MITF protein and reduced stability (Wu et al., 2000). However, this increase of MITF seems to diminish over time. Five hours after SF stimulation, MITF protein diminished significantly (Wu et al., 2000). Interestingly, SF stimulated 501 melanoma cells showed stable MITF protein levels in the presence of a MEK inhibitor throughout the five hour incubation period indicating that SF/c-Kit signals are transmitted through the MAPK pathway (Wu et al., 2000). In order to determine if the observed degradation of MITF after five hours of SF stimulation was due to proteasomal degradation, 501 melanoma cells were treated with proteasome inhibitors. The treatment with proteasome inhibitors prevented SF induced MITF degradation (Wu et al., 2000). Proteins that are degraded due to the proteasomal machinery are ubiquitinylated. MITF was shown to be targeted for ubiquitination after c-Kit stimulation (Wu et al., 2000). Electrophoretic mobility shift assays with wild type MITF and a version of MITF where S73, a potential phosphorylation site, was mutated to alanine showed that both bound the E-box sequence. Interestingly, DNA-binding activity declined after two hours with SF stimulation. This applied to both wild type MITF and the S73 mutant version of MITF. Also, treatment with proteasome inhibitors, to test if there is a difference in proteasomal degradation between wildtype and mutant MITF, had the same effect on wild type MITF and S73A mutant MITF. These results suggest that this phosphorylation site is dispensable for MITF degradation (Wu et al., 2000). Another residue of MITF, serine 409, is phosphorylated by the Rsk-1 kinase. Transcriptional activation assays in NIH3T3 and 501 melanoma cells using the tyrosinase promoter as reporter showed that the single mutants S73A and S409A had reduced transcription activation potential compared to wild type MITF (Wu et al., 2000). However, a S73A/S409A double mutant completely failed to activate tyrosinase expression. These results indicate that c-Kit-induced phosphorylation of MITF increases its transcriptional potential but also makes MITF more susceptible to proteasomal degradation. Although no difference was

observed in DNA-binding ability between wild type MITF and the phosphorylation mutants, the double mutants failed to activate tyrosinase expression (Wu et al., 2000).

In order to investigate the role of the two phosphorylation sites S73 and S409 in melanocytes *in vivo*, BAC transgenes were designed where both residues were mutated to alanine, transgenic mice made and crossed to $MITF^{mi\text{-}vga9}$ mice which are white due to lack of melanocytes and have microphthalmia (Bauer et al., 2009). Three independent lines of S73A were generated and all were able to rescue the $MITFF^{mi\text{-}vga9}$ phenotype (Bauer et al., 2009). Although the rescue was different regarding rescue of eye defects, all mice showed rescue of the coat color leaving only a white belly spot. The double mutant S73A/S409A line was also able to rescue the phenotype of the $MITF^{mi\text{-}vga9}$ mutation fully. These data indicate that these two serines are not essential for MITF function during mouse melanocyte development (Bauer et al., 2009).

In osteoclasts stimulated with RANKL, MITF was shown to be rapidly and persistently phosphorylated at serine 307 (Mansky et al., 2002). This phosphorylation event correlated with the expression of the target gene tartrate-resistant acid phosphatase (TRAP). The phosphorylation of MITF also correlated with persistent activation of p38 MAPK, which utilized MITF as a substrate. These results indicate that phosphorylation of MITF leads to an increase in osteoclast-specific gene expression (Mansky et al., 2002). This might suggest that melanocytes and osteoclasts use different signaling mechanisms to mediate phosphorylation of MITF at different sites.

1.2.3.2. SUMOylation

Small ubiquitin-like modifiers (SUMO) are related to ubiquitin and are of similar three-dimensional structure (reviewed in van der Veen & Ploegh, 2012). They regulate various cellular processes, including nuclear transport and organization, transcription, chromatin remodeling, DNA repair and ribosomal biogenesis (reviewed in van der Veen & Ploegh, 2012). SUMOylation is an enzymatic cascade that resembles ubiquitylation (reviewed in van der Veen & Ploegh, 2012). In vertebrates four SUMO genes have been identified, designated as *SUMO1-4*, whereas SUMO2 and 3 are 97% identical and usually referred to as SUMO2/3 (reviewed in van der Veen & Ploegh, 2012). At first, the SUMO1 protein becomes activated by two enzymes, SAE1 (SUMO1-activating enzyme, subunit 1) and SAE2 (SUMO1-activating enzyme, subunit 2), resulting in the formation of a thioester linkage between the C-terminus of SUMO and a cysteine residue in SAE2 (Desterro et al., 1999). This process is

ATP-dependent. The addition of the SUMO-conjugating enzyme Ubc9 results in efficient transfer of the thioester-linked SUMO1 from SAE2 to Ubc9 (Desterro et al., 1999). Ubc9 becomes linked to the C-terminus of SUMO1 and the ε-amino group of a lysine embedded in ψ-K-X-E consensus sequences of target proteins (ψ marks hydrophobic residues, X stands for any residue). A large number of transcription factors are sumoylated usually leading to attenuation of transcriptional activity. It has been shown that mutations within the sumoylation signature of the glucocorticoid receptor have an effect on transcription activation. Mutants showed increased transcription activation potential compared to wild type glucocorticoid receptor due to impaired sumoylation (Iniguez-Lluhi & Pearce, 2000).

In order to investigate if MITF was modified by SUMO1, HEK293 cells were co-transfected with Flag-tagged SUMO1 and V5-tagged MITF. Co-immunoprecipitation with an anti-V5 antibody and anti-flag revealed that MITF is indeed modified by SUMO1 (Murakami & Arnheiter, 2005). Whole cell lysates which were immunoprecipitated with an anti-V5 antibody showed two slower migrating forms of MITF, suggesting that one or two SUMO proteins are covalently attached to MITF (Murakami & Arnheiter, 2005). Further analysis showed that K182 and K316 in MITF are major sumoylation sites. Interestingly, the ability to bind DNA was not affected by modifying these sites (Murakami & Arnheiter, 2005). However, sumoylation altered transcriptional activity. The double mutant 2KR (K182/316R) showed increased transcriptional activity from a promoter construct containing 4M-boxes compared to wild type MITF or the single mutations (Murakami & Arnheiter, 2005). No difference in transcriptional activation potential of the double mutant was observed with reporter constructs containing TYR or TYRP1 promoter and only a slight increase from DCT and Cathepsin K reporters (Murakami & Arnheiter, 2005). On the other hand, Miller and colleagues showed an increase in transcriptional activity of the double mutant from the TYR and Silver promoters (Miller et al., 2005). These results suggest that sumoylation, which is a dynamic and reversible event, plays a significant role among the multiple mechanisms that regulate MITF during development and in adulthood (Miller et al., 2005; Murakami & Arnheiter, 2005).

1.2.4. An introduction to sporadic and familial melanoma

1.2.4.1. Melanoma

Melanocytes are the precursors of melanoma, the most deadly form of skin cancer. Each year, there are an estimated 2-3 million cases of skin cancer across the world and although melanoma only accounts for approximately 132,000 of these, it is the most dangerous form accounting for most skin cancer deaths. If melanoma is diagnosed early it can be cured by surgical resection. However, metastatic melanoma has poor prognosis, is difficult to treat and existing therapies often lead to development of resistance to the drug (reviewed in Gray-Schopfer et al., 2007). A primary event in melanocytic transformation can be considered a cellular change that contributes to the eventual malignancy. This change occurs as a secondary result of some oncogenic activation through either genetic or epigenetic events leading to a melanocyte with a growth advantage over surrounding cells. Numerous pathways have been found to be involved in primary alteration including proliferative or senescence pathways but also apoptotic pathways (reviewed in Palmieri et al., 2009).

1.2.4.2. Familial melanoma

1.2.4.2.1. CDKN2A and CDK4

Identification of the familial melanoma gene CDKN2A was the result of genetic studies of melanoma-prone families. CDKN2A encodes two distinct proteins, namely INK4a ($p16^{INK4a}$) and ARF (p14). $p16^{INK4a}$ inhibits the G1 cyclin-dependent kinases 4/6 (CDK4/6) resulting in G1 arrest, hence p16 is a negative regulator of the cell cycle. P16 mediated inhibition of CDK4/6 prevents phosphorylayion of the retinoblastoma (RB) protein (functional RB protein is not phosphorylated and in complex with E2F1). On the other hand, CDK4/6, if not inhibited by p16 are able to phosphorylate RB, and inactivate it since it dissociates from E2F1, resulting in cell cycle progression (reviewed in Chin et al., 2006). As a minor note, it has been shown that MITF is able to interact with the RB protein (Yavuzer et al., 1995).

Overexpression of MITF in the mouse fibroblast cell line 10T1/2 resulted in increased growth inhibition and morphological changes consistent with melanocyte differentiation (Loercher et al., 2005). This indicates that MITF has an ability to negatively regulate the cell cycle. Analysis of the INK4A promoter revealed several binding sites for MITF (Loercher et al., 2005). It was shown that MITF binds the p16 promoter and is able to activate its expression. Ectopic expression of MITF resulted in increased p16 protein and mRNA levels (Loercher et

al., 2005). Mutations in two MITF binding sites obliterated activation from the p16 promoter. siRNA against MITF showed decreased p16 protein. Hence, p16 is regulated by MITF and is therefore associated with melanocyte differentiation and cell cycle exit (Loercher et al., 2005).

Other high risk genes are *CDK4/6*, which have been identified in melanoma prone families. Mutations in CDK4 are located in exon 2 such as R24C and R24H. Both mutations are single amino acid changes, substituting an arginine either for a cysteine or a histidine (reviewed in Nelson & Tsao, 2009; Puntervoll et al., 2013).

1.2.4.2.2. The germline mutation E318K in MITF

In a search for familial melanoma genes, a mutation was found in MITF that predisposes to melanoma. Sequencing 62 patients with both melanoma and renal cell carcinoma (RCC) led to the discovery of a novel MITF variant where glutamic acid at position 318 was substituted for lysine (Bertolotto et al., 2011). The frequency of this variant was higher in patients with both melanoma and RCC than in cancer-free controls. Further genotyping of 603 melanoma patients showed that the E318K variant was four times more frequent in melanoma patients than in controls (Bertolotto et al., 2011). Similarly, the variant was more frequent in RCC patients than in controls. When the data of the melanoma and/or RCC patients were pooled, carriers were shown to have a greater than fivefold risk of developing melanoma, RCC or both, as compared to controls (Bertolotto et al., 2011). The E318K variant occurs at a conserved position in MITF, within an IKQE consensus motif that matches very well with the consensus sequence ψKXE for covalent binding of SUMO (Bertolotto et al., 2011). When E318 was replaced by lysine, mimicking the germline mutation, SUMO-modified forms of MITF were severely reduced (Bertolotto et al., 2011). Co-transfection assays showed that the E318K mutant protein had more ability to activate expression of reporter constructs than wildtype MITF (Bertolotto et al., 2011). A combination of E318K with a mutation in another SUMO-site in MITF, K182R, showed even greater transcriptional activity (Bertolotto et al., 2011). In order to investigate whether SUMOylation influenced genome-wide MITF-occupancy of its target genes, chromatin immunoprecipitation coupled to high-throughput sequencing of 501 melanoma cells expressing wild type MITF or the E318K mutant was performed. This revealed that more sites were occupied by the E318K variant than by the wild type protein (22,157 vs. 9,107). HIF1α was one of the loci better occupied by E318K than by wild type (Bertolotto et al., 2011). Cells transfected with E318K construct showed increased

migration and invasion abilities and were able to form more colonies than cells transfected with wild type MITF (Bertolotto et al., 2011). In summary, this novel germline variant of MITF severely impaired MITF SUMOylation and showed more transcription potential as well as certain characteristics consistent with tumorigenic behavior (Bertolotto et al., 2011) SUMOylation as a post-transcriptional process was discussed in section 1.2.3.2.

One month after Bertolotto and colleagues published the identification of E318K, Yokoyama and colleagues also published the identification of E318K as a variant associated with melanoma (Yokoyama et al., 2011). Among cases, the E318K variant was enriched in those with multiple primary melanomas, a family history of melanoma, but not in cases with early age of onset (Yokoyama et al., 2011). In terms of transcriptional activation, E318K was able to activate the TRPM1 promoter better than the wild type MITF protein in the UACC62 human melanoma cell line (Yokoyama et al., 2011).

1.2.5. Signaling pathways associated/dysregulated in melanoma

In order to give a brief overview of signaling pathways involved in melanoma, the most common pathways are described below.

1.2.5.1. Mitogen-activated protein (MAP) kinase signaling

The MAP kinase (MAPK) signal transduction pathway is dysregulated in most melanomas (reviewed in Fecher et al., 2008). In this chapter the MAP kinase pathway is explained in general followed by detailed description of the members of the signaling pathway.

Extracellular signals initiate MAPK signaling through the activation of receptor tyrosine kinases (RTKs) (reviewed in Fecher et al., 2008). Activators of receptor tyrosine kinases such as c-Kit and MET are SCF and HGF, respectively (reviewed in Tsao et al., 2012). RAS is a membrane-bound GTPase which is able to affect signaling when GTP-bound and localized to the plasma membrane (reviewed in Fecher et al., 2008). The RAS/RAF complex, once bound, translocates to the cell membrane and RAF becomes activated. Activated RAF phosphorylates and activates MEK, which phosphorylates and activates ERK (reviewed in Goding, 2000; reviewed in Gray-Schopfer et al., 2007; reviewed in Lennartsson et al., 2005; reviewed in Russo et al., 2009). ERK relays this signal through the phosphorylation of cytoplasmic and nuclear targets. Downstream effects of ERK are broad and include increased proliferation (due to downregulation of cyclin-dependent kinase inhibitors and inactivation of tumor

suppressors) and increased survival and protection against FAS-mediated apoptosis (reviewed in Fecher et al., 2008). ERK activity is not normally present in melanocytes but high constitutive ERK activity has been documented in melanoma cell lines and tumors (reviewed in Fecher et al., 2008).

The RAS proto-oncogenes consist of H-RAS, N-RAS and K-RAS (reviewed in Chin et al., 2006). Activating mutations in the RAS proto-oncogenes are detected in about 10-15% of melanomas. N-RAS is the most frequent RAS family member mutated in the melanocytic lineage, with activating mutations in about 56% of congenital nevi, 33% of primary- and 26% of metastatic melanomas (reviewed in Chin et al., 2006). The most common sites of mutations in NRAS are G12 in the phosphate-binding loop and Q61 in the catalytic unit (Li et al., 2012). Constitutively activated $NRAS^{Q61K}$ is frequently found in nevi and early-stage melanomas (Li et al., 2012). HRAS mutations have been associated with Spitz nevi (reviewed in Tsao et al., 2012). HRAS and KRAS mutations have both been reported in approximately 2% of melanomas (reviewed in Tsao et al., 2012). NRAS mutations have been found in 26% of melanoma samples by whole-genome sequencing (Hodis et al., 2012).

In mammals there are three conserved RAF genes (ARAF, BRAF and CRAF), which are potent activators of ERK protein kinases (reviewed in Palmieri et al., 2009). BRAF is mutated in 59% of melanoma cell lines and 67% of melanoma patients (Brose et al., 2002; Davies et al., 2002). Further analysis of primary tumors revealed that out of the 6 melanoma patients, 5 patients (83%) harbored the $BRAF^{V600E}$ mutation (Davies et al., 2002). Interestingly, almost all mutations occurred at V600 substituting valine for glutamic acid. The $BRAF^{V600E}$ mutation is in exon 15 of *BRAF* and at the protein level, this mutation is within the kinase domain of BRAF, resulting in elevated kinase activity leading to increased phosphorylation of ERK (Davies et al., 2002). These results showed that the $BRAF^{V600E}$ mutation leads to increased activity of the MAPK pathway (Davies et al., 2002). Maldonado and colleagues analyzed 115 primary invasive melanomas for their BRAF status and showed 32 patients had a mutation in BRAF (27,8%). All the mutations in BRAF occurred at position V600E (Maldonado et al., 2003). BRAF was mostly mutated in non-chronic sun damaged skin (54%) such as trunk, extremities and face. In chronic sun damaged skin, BRAF was mutated in only 8% of cases whereas in glabrous skin such as soles, palms and subungual sites BRAF was mutated in 15% of cases and in mucosal melanoma only 10% of cases carried the mutation (Maldonado et al., 2003). A recent study which investigated BRAF and NRAS status in melanoma patients revealed that 47% had BRAF mutations (of those 72% were $BRAF^{V600E}$) and 20% had NRAS

mutations (Jakob et al., 2012). Analysis of overall survival revealed that NRAS patients had the worst outcome with a median survival of 8.2 months from diagnosis of stage IV melanoma, which was significantly shorter than the 15.1 months of wild type patients. BRAF patients who did not receive a BRAF inhibitor had a median survival of 10.3 months. BRAF patients who received BRAF inhibitors such as Vemurafenib survived longer than those who did not receive BRAF inhibitors (further discussed in chapter 1.2.7.) (Jakob et al., 2012). A recent whole-exome sequencing study of 135 melanoma patients showed that BRAF was mutated in 63% of cases (Hodis et al., 2012). It seems the prevalence of mutated BRAF depends on the study population. However, as summarized above the prevalence for mutated BRAF would be approximately 51%.

The identification and implication of BRAF mutations and especially $BRAF^{V600E}$ in melanomas quickly gained interest and led to novel insights. Anchorage independent growth assays showed that melan-a cells are not able to form colonies (Wellbrock et al., 2004). However, melan-a cells expressing $BRAF^{V600E}$ are able to from colonies in soft agar, indicating that $BRAF^{V600E}$ has an effect on anchorage independent growth. $BRAF^{V600E}$ constitutively activates ERK that is essential for proliferation (Wellbrock et al., 2004).

Mutations in ERK1/2 are not very common. However, Hodis and colleagues identified 2 melanoma patients in their cohort (5%) who harbored ERK1 mutation (Hodis et al., 2012).

1.2.5.1.1. BRAF and MITF

MITF has been implicated in the MAPK pathway. ERK has been shown to phosphorylate MITF on S73 (Hemesath et al., 1998; Wu et al., 2000). Phosphorylation of S73 (and also S409) was triggered by c-kit and resulted in short-lived activation of MITF followed by proteasome degradation (Wu et al., 2000). Interestingly, oncogenic BRAF is able to repress MITF expression in immortalized mouse and human melanocytes (Wellbrock & Marais, 2005). Further it was shown that $BRAF^{V600E}$ but not BRAF wild type regulates MITF expression by stimulating its degradation (Wellbrock et al., 2008). Melanoma cells with constitutively active MAPK signaling eg. due to the $BRAF^{V600E}$ mutation, have lower MITF expression because MITF is phosphorylated followed by proteasomal degradation. Treatment of melanoma cell lines with MEK inhibitors showed reduced MITF phosphorylation indicating that ERK activation is necessary for MITF activation in melanoma cells expressing oncogenic BRAF (Wellbrock et al., 2008). BRAF depletion resulted in reduced ERK activity, a reduction of MITF activity and reduced *MITF* mRNA expression, indicating that $BRAF^{V600E}$

also regulates MITF expression. Interestingly it was shown that oncogenic BRAF upregulates MITF transcription through ERK and BRN2. This leads to a constant production of active but unstable MITF protein. In melanoma cells MITF is required downstream of oncogenic BRAF because MITF regulates the expression of important cell cycle regulators such as CDK1 and CDK4 (Wellbrock et al., 2008).

1.2.5.1.2. MET in melanoma and the relationship between MET and MITF

Hepatocyte growth factor/scatter factor (HGF/SF) is a multifunctional cytokine and binds the transmembrane receptor tyrosine kinase MET (Otsuka et al., 1998). HGF/SF is produced by cells of mesenchymal origin, whereas MET is expressed in adult and embryonic epithelium, indicating that HGF/SF functions as a paracrine regulator. Further, it has been shown that HGF/SF is a potent stimulator of melanocytes. MET signaling has been implicated in oncogenesis and acts as a proto-oncogene. MET has been shown to be highly expressed in human and mouse tumors and was correlated with metastatic progression. A number of those tumors co-express HGF/SF suggesting an existence of an autocrine signaling loop. Additionally, HGF/SF is able to stimulate cell movement, extracellular matrix degradation and angiogenesis, all features which could contribute to tumor cell invasion and metastasis. Albino mice, ectopically expressing a HGF/SF transgene, showed that melanocytes were abundant in the dermis, at the dermal-epidermal junction and less consistently in the basal layer of the epidermis (Otsuka et al., 1998). Melanocytes in the transgenic mice were aberrantly clustered in the skin of paws, tail, ears, muzzle, foreskin, penis and dorsal skin as well as in central nervous system and lymph nodes (Otsuka et al., 1998). A portion of the transgenic mice also developed cutaneous malignant melanoma (22%) whereas wild type mice did not develop melanoma at all. Interestingly, the tumors arose preferentially in male mice (17 of 19 were male). RNA levels of HGF/SF and MET were detected in 7 of 9 of the primary tumors, suggesting that the establishment of HGF/SF-MET autocrine loops was a common mechanism. The preferred organs of metastasis were liver, spleen and skin (Otsuka et al., 1998). Immunohistochemical analysis showed that MET is strongly expressed in malignant melanoma, but not so much in normal skin tissue. Further, deeper invasive melanoma samples demonstrated stronger MET staining compared to superficial melanoma (Lee et al., 2011).

A recent study analyzed single cell clones derived from a melanoma patient who was wild type for NRAS but heterozygous for $BRAF^{V600E}$ (Swoboda et al., 2012). Selected lymphoangiogenic clones were grafted into immunodeficient mice, where they induced

lymphoangiogenesis and metastasized into sentinel lymph nodes, whereas non-lymphoangiogenic clones from the same patient did not metastasize (Swoboda et al., 2012). Interestingly, vascular endothelial growth factor C, VEGF-C, platelet derived growth factor C, PDGF-C and MET were highly expressed as shown by transcriptome profiling and Western blot analysis. This suggests that MET is associated with lymphoangiogenesis and mestastasis (Swoboda et al., 2012).

When neonatal melanocytes were stimulated with HGF/SCF it resulted in rapid stimulation/phosphorylation of MITF (McGill et al., 2006). The MITF band shift from a doublet to a single upper band suggested post-translational modification (McGill et al., 2006). This modification requires MAPK signaling to MITF at serine 73 (McGill et al., 2006). As mentioned before, phosphorylation of MITF, subsequently leads to MITF degradation (Wu et al., 2000). After HGF-dependent phosphorylation of MITF, MITF was targeted for proteasomal degradation within 2h of stimulation (McGill et al., 2006). HGF stimulation also increased MET expression. RT PCR showed that MET was induced by MITF but not with a dominant-negative form of MITF (McGill et al., 2006). Using Chromatin-immunoprecipitation, it was shown that MITF binds the MET promoter (McGill et al., 2006). HGF-dependent invasion of melanocytes and melanoma (501) was observed with MITF wild type transfected cells, but not with the dominant-negative form (McGill et al., 2006). To summarize, MET has been implicated in melanoma (Lee et al., 2011; Swoboda et al., 2012) and HGF-dependent phosphorylation of MITF leads subsequently to its degradation (McGill et al., 2006).

αMSH increases MET and MITF expression via cAMP pathway activation in B16 melanoma cells and normal human melanocytes (Beuret et al., 2007). Interestingly, in the human melanoma cell line 501mel no significant increase of MET or MITF expression was observed after αMSH stimulation (Beuret et al., 2007). Using siRNA against MITF demonstrated a significant reduction in MET and tyrosinase expression in B16 and 501 melanoma cells indicating that the cAMP pathway and MITF regulate MET expression (Beuret et al., 2007). To provide further evidence that MITF is able to upregulate MET expression, the melanoma cell line A375 was transfected with MITF resulting in an increase in MET mRNA levels (Beuret et al., 2007). Initial analysis of the MET promoter revealed three E-boxes to which MITF can bind (Beuret et al., 2007). Transcriptional activation assays in B16 cells showed activation of MET by MITF whereas a mutation in the second E-box significantly diminished this effect (Beuret et al., 2007).

1.2.5.2. The phosphatidylinositol-3-kinase (Pi3K) signalling pathway

The Pi3K pathway is activated by RTKs or G-protein coupled receptors such as RAS and has been implicated in cancer pathophysiology due to its role in cell growth, proliferation, motility and survival (reviewed in Fecher et al., 2009). A phosphorylation cascade leads to the activation of AKT which supports cell growth and proliferation, promotes cell cycle progression and cell survival. PTEN (phosphatase and tensin homolog deleted on chromosome 10) acts as a tumor suppressor and negatively regulates AKT and the PI3K pathway. In melanoma, Pi3K pathway activation manifests by functional loss of PTEN or AKT overexpression. Activating BRAF mutations are often accompanied by loss of PTEN (reviewed in Fecher et al., 2009). The $BRAF^{V600E}$ mutation has been shown to cooperate with PTEN loss to induce metastatic melanoma. Mice with a conditional $BRAF^{V600E}$ mutation crossed with mice harboring a PTEN deletion were treated with a MEK inhibitor or with rapamycin (mTOR inhibitor; mTOR is a member of the PI3K pathway and downstream of AKT) or both. Melanoma lesions in vehicle-treated animals progressed steadily over time and expanded in size in all animals (Dankort et al., 2009). Mice treated either with MEK inhibitor or rapamycin as single agents had marked inhibition of tumor growth, but little or no evidence of tumor regression. Interestingly, the combination of MEK inhibitor and rapamycin showed a 20% reduction in tumor size (Dankort et al., 2009).

1.2.5.3. The Wnt signaling pathway

The Wnt signaling pathway plays an important role throughout development, particularly in the neural crest but also in human tumorigenesis and melanocyte lineage-specific expansion (Widlund et al., 2002). The canonical Wnt signaling pathway starts due to the activation of the receptor Frizzled by Wnt ligands and leads to accumulation of β-catenin which can bind to E-cadherins or act as a transcription factor by interacting with TCF/LEF (DNA-binding proteins) in the nucleus (reviewed in Hou & Pavan, 2008; Widlund et al., 2002). In absence of Wnt-signals, β-catenin is targeted for degradation via phosphorylation by a complex consisting of glycogen synthase kinase (GSK)3β and adenomatous polyposis coli protein (APC). However, the presence of Wnt-signals leads to the inactivation of GSK3β and stabilize β-catenin levels, resulting in increased transcription of downstream targets. In human melanoma, stabilizing mutations in β-catenin have been identified leading to aberrant nuclear accumulation of β-catenin (reviewed in Larue & Delmas, 2006). It has been shown that β-catenin is able to bind and regulate the MITF promoter in a lineage-specific manner (Widlund

et al., 2002). Further, β-catenin expression leads to increased MITF protein levels and therefore might contribute to the effects of β-catenin-TCF/LEF on melanoma cell growth or survival (Widlund et al., 2002).

1.2.5.3.1. The relationship between β-catenin, p16 and MITF

Wnt proteins lead to intracellular accumulation of β-catenin and start the downstream signal cascade. Wnt3a is required for expansion of neural crest cells. Hence it is not surprising that dysregulation in Wnt3a signaling causes deficiency of neural crest derivatives including melanocytes (Takeda et al., 2000b). Wnt3a transfected Melan-a mouse melanocytes resulted in an upregulation of MITF indicating that Wnt signaling is involved in melanocyte differentiation. The human *MITF* promoter contains a LEF-1 binding site and it was shown that LEF-1 actually binds the *MITF* promoter (Takeda et al., 2000b). In addition, Wnt3a was able to transactivate the *MITF* promoter. These findings suggest that Wnt3a recruits β-catenin and LEF-1 to the LEF-1 binding site of the *MITF* promoter (Takeda et al., 2000b). Interestingly, it has been shown that MITF interacts directly with β-catenin via the helix domain of MITF (Schepsky et al., 2006). β-catenin strongly activated the TOPFLASH reporter system for β-catenin and Tcf-induced transcription in HEK293 cells (Schepsky et al., 2006). Interestingly, adding MITF reduced this activation indicating that MITF had an inhibitory effect on β-catenin, the more MITF added, the stronger the reduction (Schepsky et al., 2006). Further, MITF and β-catenin cooperate to activate tyrosinase expression. MITF alone was able to activate tyrosinase expression about 13-fold but MITF and β-catenin together activated tyrosinase expression about 50-fold. Chromatin-immunoprecipitation of β-catenin in 501mel cells showed that β-catenin binds the E-box sequences from the tyrosinase (TYR) and tyrosine-related protein 1 (TYRP1) promoters. Knock down of MITF via siRNA in the 501mel cells showed that β-catenin failed to bind the E-box sequences of the TYR and TYRP1 promoters. These results suggest that MITF is able to redirect β-catenin towards MITF-specific promoters (Schepsky et al., 2006).

Mutations in β-catenin that mimic its activation by Wnt signals and lead to its stabilization and translocation from the plasma membrane to the nucleus are found in several cancers including melanoma (Delmas et al., 2007). GSK3β phosphorylates β-catenin on serine (S) or threonine (T) residues. This phosphorylation event leads to the degradation of β-catenin. Hence, mutations affecting the serine or threonine residues will lead to β-catenin stabilization.

Substitution of the ST residues by A results in aggressive fibromatosis and gastrointestinal tumors. Transgenic mice expressing β-catenin containing four ST-A substitutions in melanocytes demonstrated that β-catenin^{STA} was primarily located in the nucleus whereas endogenous β-catenin was detected at cell-cell contacts on the cell surface (Delmas et al., 2007). The β-catenin^{STA} mice did not develop melanoma. However, crossing the β-catenin^{STA} mice with mice producing an oncogenic form of NRAS (NRAS^{Q61K}) in melanocytes resulted in development of melanomas. Those mice had a high incidence of melanomas (85%) with a markedly shorter average latency period (27.6 ± 6.7 weeks) than mice harboring the NRAS^{Q61K} mutation which developed melanomas at 54 ± 21 weeks. The NRAS^{Q61K};β-catenin^{STA} mice developed either one or two primary tumors or multiple (three to nine) tumors. The development of neoplastic lesions in NRAS^{Q61K};β-catenin^{STA} mice is therefore a frequent event (Delmas et al., 2007).

In mice in general, melanocytes are mainly located in the dermis of the pinna (visible part of the ear), in the epidermis of the limbs and tail and in the hair follicles of the hairy parts of the skin. NRAS^{Q61K};β-catenin^{STA} mice developed melanomas on the hairy parts of the body such as neck, back and belly and not on less hairy body parts. This suggests that the melanomas most likely arose from melanocytes within the epidermis and/or hair follicles. β-catenin^{STA} mice harbored less melanocytes and melanoblasts compared to wild type melanocytes. These results suggest that the expression of activated β-catenin results in reduced cell proliferation. Melanocytes from the β-catenin^{STA} mice were cultured and became rapidly immortalized. Melanocyte cell lines could be established from 95% (19/20) of β-catenin^{STA} newborn pup skin, however, only from 31% (6/19) of their wild type littermates, indicating that β-catenin^{STA} expression in melanocytes increased the efficiency of immortalization (Delmas et al., 2007).

Further studies, using the same β-catenin^{STA} (sometimes also called β-catenin*) mice, revealed that these mice had a white belly spot (Gallagher et al., 2012). At this area no melanoblasts were detected which is most likely due to decreased or slower melanoblast migration (Gallagher et al., 2012). Slower migration was also shown *in vitro*, by overexpressing β-catenin^{STA} in human melanocytes and melanoma cells (Gallagher et al., 2012). The conclusion drawn from those studies is that β-catenin^{STA} melanocytes migrate more slowly. The human Mull melanoma cell line expresses moderate levels of MITF and low levels of β-catenin. However, transient expression of β-catenin^{STA} reduced migration compared to wild type.

Crossing β-catenin^{STA} mice with MITF$^{vga9/+}$ mice resulted in mice with white belly spots similar to those of β-catenin^{STA} mice, indicating that the reduction of melanoblast migration by β-catenin during embryogenesis does not result solely from an increase in MITF levels and that there are most likely other MITF-independent targets. Interestingly, β-catenin signals through GSK to reduce migration and β-catenin signaling might increase the metastatic potential of melanoma (Gallagher et al., 2012).

1.2.5.4. The α-MSH pathway regulates HIF1α

cAMP stimulates the expression of the *HIF1α* gene, which encodes for hypoxia-inducible factor 1 α (HIF1α), a master regulator of oxygen homeostasis. HIF1α controls the expression of several genes involved in cancer progression, apoptosis resistance, angiogenesis, invasion and metastasis. HIF1α is inducible by cAMP but the upregulation of HIF1α is cell type specific as it is observed in B16 melanoma cells but not in the fibroblast cell line NIH3T3. Additionally, MITF is able to bind the *HIF1α* promoter and activate its transcription more in B16 cells than in NIH3T3 cells (Busca et al., 2005). Hence it seems that MITF mediates the effect of cAMP on the HIF1α promoter activity and protein expression. Treating B16 melanoma cells (which were stimulated with forskolin to induce cAMP) with an apoptosis-inducing agent showed that cAMP significantly reduced caspase-3 cleavage, indicating that cAMP inhibits apoptosis to a certain degree and implicating a role in pro-survival in melanoma (Busca et al., 2005).

1.2.6. MITF expression and MITF mutations in melanoma

Several studies using immunohistochemistry, revealed that MITF is expressed in almost all malignant melanoma and benign nevi but not in the nuclei of cells in other non-melanocytic lesions; in normal skin, MITF is expressed in melanocytes (Dorvault et al., 2001; King et al., 2001; King et al., 1999; Miettinen et al., 2001; Nonaka et al., 2007; Salti et al., 2000).

Table 1 summarizes studies where MITF expression has been investigated in melanoma samples. Increased *MITF* copy numbers have been detected in malignant melanoma but not in benign nevi (Table 2) (Garraway et al., 2005; Ugurel et al., 2007). In metastatic melanoma *MITF* amplification was associated with decreased 5-year overall survival (OS) (Garraway et al., 2005). Further, *MITF* amplification correlated with a significant increase in MITF protein expression in melanoma (p=0.019) (Garraway et al., 2005). Anchorage-independent growth

assays of human melanocytes showed that over-expressing MITF alone or $BRAF^{V600E}$ alone did not result in the formation of many colonies. However, co-expression of MITF and $BRAF^{V600E}$ resulted in anchorage independent colonies. These results suggest that MITF can function as a melanoma oncogene (Garraway et al., 2005). Recently, Hodis and colleagues performed whole-exome sequencing and showed that the *MITF* gene was amplified in 4% of the investigated melanomas (Hodis et al., 2012).

Table 1. MITF expression in melanoma as determined by immunohistochemistry (IHC)

Study population	Population size	Positive MITF staining*	Comment	Author
malignant melanoma	35	24/35 (68%)	viable area was MITF positive (nuclear); necrotic area was MITF negative	Nonaka et al. 2007
metastatic melanoma	266	235/266 (88%)	nuclear staining	Miettinen et al. 2001
benign melanocytic neoplasms	62	62/62 (100%)	nuclear staining	King et al. 2001
normal skin			melanocytes are positive for MITF	
malignant melanoma	58	58/58 (100%)	nuclear staining	
nonmelanocytic lesions	53	0/53		
malignant melanoma	44	44/44 (100%)	nuclear staining	Dorvault et al. 2001
nonmelanoma malignancies	37	0/37		
malignant melanoma	63	52/63 (82%)	MITF (nuclear stainings) associated with improved survival	Salti et al. 2000
melanoma cell lines	4	4/4 (D5 Ab)	in 501 nuclear MITF staining	King et al. 1999
melanoma in situ	19	19/19	nuclear staining	
metastatic melanoma	7	7/7	nuclear staining	
primary melanoma	50	50/50	nuclear staining	

* Numbers refer to MITF positive tumors over total tumors studied

Table 2. MITF gene amplification in melanoma

Study population	Population size	Positive MITF tumors*	Comment	Author
metastatic melanoma	116	24/104 (23%) 62/104 (60%)	> 4 MITF copies > 3 MITF copies	Ugurel et al. 2007
primary cutanous melanoma	30	3/30 (10%)	amplified (shorter OS)	Garraway et al. 2005
metastatic melanoma	32	7/32 (21%)	amplified (shorter OS)	
benign nevi	10	0/10		

* Numbers refer to tumors showing MITF copy number changes
OS = overall survival

Genomic DNA of 50 metastatic melanoma lines derived from human metastatic melanoma tissue samples showed that of the 50 samples, four had genomic amplifications, four had somatic MITF mutations (E87R, L135V, G244R and D380N) and one had a splice site mutation in exon 2 alteration (see Table 3. Splice site mutation excluded) (Cronin et al., 2009). One MITF mutation was found in a primary tumor (L142F) (Cronin et al., 2009). Transcription activation assays showed that the E87R, L135V, L142F and D380N mutant proteins were able to activate the tyrosinase promoter at levels similar to wild type MITF. The G244R mutant showed reduced activation ability (Cronin et al., 2009).

Table 3. Summary of MITF point mutations found in melanomas

Mutation	Location	Authors	Phenotype/Remarks	Inheritance
E87R	AD	Cronin et al. 2009	metastatic melanoma with BRAF (V600E) mutation	somatic
L135V	AD	Cronin et al. 2009	metastatic melanoma	somatic
L142F	AD	Cronin et al. 2009	metastatic melanoma	somatic
G244R	HLH	Cronin et al. 2009	metastatic melanoma with BRAF (V600E) mutation	somatic
E318K	AD	Bertolotto et al. 2011 Yokoyama et al. 2011	5/62 melanoma and renal cell carcinoma patients harbor the E318K mutation	germline
D380N	AD	Cronin et al. 2009	Metastatic melanoma with BRAF (V600E) mutation	somatic

AD= activation domain, HLH= helix loop helix

MITF fulfills all the criteria of a lineage survival oncogene; (1) MITF plays a crucial role in the melanocyte lineage by regulating their proliferation and survival during development; (2) MITF expression has been shown to be deregulated in melanomas; (3) MITF undergoes amplification in 15-20% of metastatic melanomas; (4) MITF is required for tumor survival; (5) MITF is a transcription factor (reviewed in Garraway & Sellers, 2006). This summarizes that MITF is a ‚prototype' for a lineage survival oncogene and emphasizes the importance of MITF in melanocytes.

1.2.7. Therapy

As mentioned earlier, melanoma is the cancer arising from melanocytes. In the United States, melanoma is the fifth-leading cancer in men and seventh in women and the prognosis of patients with metastatic melanoma remains extremely poor (reviewed in Thumar et al., 2012). It is the fourth most common reported cancer in Australia (reviewed in Law et al., 2012). Due to the aggressiveness, the molecular complexity and heterogeneity of melanoma, the treatment of melanoma patients has been a challenge. Recently however, targeting key members of signalling pathways has been shown to be very promising in melanoma therapy.

Vemurafenib, a BRAF inhibitor, formally known as PLX4032, has been shown to be very effective in melanoma patients who harbour the $BRAF^{V600E}$ mutation. This drug has been approved by the Federal Drug Administration (reviewed in Flaherty et al., 2010; reviewed in Thumar et al., 2012). A recent multicenter phase 2 trial of Vemurafenib was designed to investigate the overall response rate of $BRAF^{V600E}$ melanoma patients as well as duration of response and overall survival (Sosman et al., 2012). Patients received vemurafenib at a dose of 960mg orally twice a day. The overall response rate was 53%, the median duration of response was 6.7 months and the median progression-free survival was 6.8 months. The median overall survival was almost 16 months. The most common adverse effects were arthralgia, rash, alopecia and photosensitivity and less common elevated liver-enzyme levels (Sosman et al., 2012). A certain number of patients (26%) developed cutaneous squamous-cell carcinoma or keratoacanthoma. The lesions occurred within the first 8 to 12 weeks, but were removed effectively without discontinuation of Vemurafenib (Sosman et al., 2012). To summarize, Vemurafenib is effective in melanoma treatment, the adverse effects easily manageable, more clinical trials are in progress and continuous research for more treatment options and targets for specific therapy are in development. Unfortunately, however a great majority of patients receiving Vemurafenib develop resistance (reviewed in Sullivan & Flaherty, 2013). Currently there are two models which explain BRAF resistance; intrinsic and acquired resistance. Intrinsic resistance to oncogenic BRAF inhibitors can be predicted based on 'pre-treatment factors' such as cell cycle regulator levels (e.g. cyclin D), or mutational status of members of other signalling pathways (e.g. PTEN) (reviewed in Sullivan & Flaherty, 2013). Acquired resistance involves non-ERK dependent (ERK still inhibited) or ERK-dependent (ERK reactivated) mechanisms. One of the latter can be explained by the BRAF paradox, where BRAF inhibitors such as vemurafenib inhibit the MAPK pathway in BRAF mutant cells but activate the pathway in cells driven by the MAPK pathway other than the oncogenic BRAF mutation (reviewed in Sullivan & Flaherty, 2013). Further studies, particularly combination-therapy studies such as BRAF/MEK or BRAF/immunotherapy will hopefully eliminate the problem of patients developing resistance (reviewed in Sullivan & Flaherty, 2013). Several combination trials have been performed or are in progress and it seems that combination therapy delays the acquired resistance to a targeted therapy compared to treatment with single agents (Garber, 2013). However, the combination was associated with increased toxicity and costs. In near future, results of several combination phase 3 trial will be evaluated and publicly available (Garber, 2013).

Another recently approved drug in melanoma therapy is Ipilimumab and is the first immunotherapeutic agent to improve overall survival in metastatic melanoma (reviewed in Thumar et al., 2012). In principle, this drug was designed to overcome tumour immune evasion. T-cells express cytotoxic T-lymphocyte-associated antigen 4 (CTLA-4). Ipilimumab is a monoclonal antibody that blocks CTLA-4, resulting in increased T-cell activity and enhanced antitumor activity (reviewed in Finn et al., 2012). Recent phase 3 trials showed an improved overall survival of Ipilimumab versus glycoprotein 100 vaccine. In combination with the BRAF inhibitor Dacarbazine it showed also improvement in overall survival versus the single agent Dacarbazine. The toxicities of the therapy, including immune-related enterocolitis, hepatitis and dermatitis were highly manageable (reviewed in Finn et al., 2012).

1.2.8. The rheostat model

It is well accepted that MITF acts as a lineage survival oncogene in melanoma (Garraway et al., 2005) but also plays an important role in cell cycle regulation in melanocytes (Loercher et al., 2005). It has been shown that depletion of MITF leads to G1 cell cycle arrest (Carreira et al., 2006). Knock down of MITF resulted in a reduction of $p21^{Cip1}$ (cyclin-dependent kinase inhibitor 1A) expression but induced $p27^{Kip1}$ (cyclin-dependent kinase inhibitor) expression. Interestingly, MITF depletion resulted in a change of morphology of the cells resulting in rounder phenotype and in an alteration in F-actin organization (Carreira et al., 2006). Immunofluorescence and immunohistochemical analysis of MITF and $p27^{Kip1}$ in normal skin, benign nevi and primary/metastastic melanomas revealed an inverse correlation between MITF and $p27^{Kip1}$ expression (Carreira et al., 2006). Cycloheximide treatment of cells transfected with siRNA against MITF revealed that p27 was stabilized in MITF-depleted cells indicating that MITF depletion induces a G1 arrest by indirectly increasing $p27^{Kip1}$(Carreira et al., 2006). Further, it has been shown that MITF depletion results in a decrease in SKP2 and DIA1 protein levels (Carreira et al., 2006). Diaphanous-related formin, DIA1, is a Rho effector that plays a key role in F-actin polymerization. DIA1 regulates Skp2. DIA1 expression in MITF-depleted cells resulted in $p27^{Kip1}$ suppression suggesting that Mitf-mediated regulation of DIA1 expression plays a role in determining the invasive and proliferative capacity of melanoma cells (Carreira et al., 2006). Overexpression of MITF in the human melanoma cell line SKMel28 had an effect on cell morphology. The cells had a more elongated morphology compared to the control SKMel28 cells and MITF expressing cells showed reduced proliferation rate (Carreira et al., 2005). Matrigel assays showed that

MITF expression in SKMel28 cells inhibited invasion ability. However, knockdown of MITF lead to increased invasiveness in SKMel28 and 501 melanoma cells (Carreira et al., 2006). It was also shown that the matrix metalloprotease 2, MMP-2, was increased in MITF-depleted cells.

Taken together, this study showed that MITF-depleted cells induce cell cycle arrest via up-regulation of $p27^{Kip1}$ and that MITF regulates Dia1 but increases invasiveness and the expression of matrix metalloprotease 2. These observations lead to the conclusion that Mitf appears to act as a rheostat. The rheostat model provides a framework for understanding the role of MITF in melanoma progression and melanocyte development but more importantly it is a descriptive model to explain the pro- and anti-proliferative roles of MITF (Carreira et al., 2006). As discussed above, short-term depletion of MITF leads to increased Dia1 expression and indirectly to a $p27^{Kip1}$-dependent cell cycle arrest. On the other hand long-term depletion triggers a DNA-damage response resulting in upregulation of p53 and induction of senescence. The ability of MITF to both promote cell division by suppressing $p27^{Kip1}$ expression and to induce senescence and inhibit proliferation via upregulation of $p21^{Cip1}$ and $p16^{INK4a}$ demonstrates the necessity to understand the term 'Mitf activity' (Hoek & Goding, 2010). According to the rheostat model, low level of MITF leads to G1 arrest but cells become more invasive whereas high MITF levels are found in differentiating non-proliferating and non-invasive cells. At this high level, MITF is able to activate its downstream targets and activate pigmentation-associated genes such as tyrosinase. Proliferating cells, expressing MITF at intermediate levels may express MITF-target genes implicated in proliferation and survival such as CDK2 and BCL2. Posttranslational modifications, such as sumoylation and phosphorylation, may play crucial roles to influence MITF activity (Hoek & Goding, 2010).

1.2.8.1. Regulating MITF expression as a melanoma therapy

The rheostat model demonstrates the importance of regulating MITF activity. Saez-Ayala and colleagues have proposed a two-step therapy approach as an antimelanoma strategy (Saez-Ayala et al., 2013). In the first step of melanoma therapy cell invasiveness should be eradicated. Methotrexate (MTX), an inhibitor of dihydrofolate reductase (DHFR), has been shown to increase MITF expression and reduce cell invasiveness in various melanoma cell lines. The increase in MITF expression was accompanied by increased occupancy of the tyrosinase promoter, increased tyrosinase expression and cell morphology changes leading to

a dendritic phenotype (Saez-Ayala et al., 2013). The second step involves the antifolate prodrug 3-O-(3,4,5-trimethoxybenzoyl)-(-)-epicatechin, TMECG (also a potent inhibitor of DHFR), which is activated by the MTX-induced tyrosinase overexpression. MTX and TMECG treated SKMel28 melanoma cells showed reduced proliferation. Melanoma cells treated with higher concentrations of MTX lead to apoptosis. These data indicate that MTX and TMECG act synergistically (Saez-Ayala et al., 2013). Further it was shown that the combination therapy of MTX and TMECG was effective regardless of mutational status of genes such as BRAF, NRAS and MEK. The MTX/TMECG combination therapy was shown to induce S phase-associated DNA-damage and apoptosis in melanoma cells (Saez-Ayala et al., 2013). *In vivo* studies in mice, injected with B16 melanoma cells, showed that MTX/TMECG combination therapy inhibited tumor growth synergistically and resistance to MTX/TMECG was not detected (Saez-Ayala et al., 2013). This study is the first which targets MITF in melanoma treatment in a two-step antimelanoma strategy with very promising results (Saez-Ayala et al., 2013).

1.2.9. Waardenburg- and Tietz syndrome

The auditory-pigmentary syndromes called Waardenburg syndromes are named after the Dutch ophthalmologist and geneticist Petrus J. Waardenburg who firstly described a deaf-mute patient with blepharophimosis (eyelid anomaly) and partial iris atrophy (Waardenburg, 1951). After further research and discussions with colleagues, Petrus J. Waardenburg identified a new human syndrome with the following characteristics; (1) lateral displacement of the medial canthi; (2) prominent broad root of the nose; (3) growing together of eyebrows; (4) white forelock, as a form of partial albinism; (5) heterochromia of the irides and (6) congenital deafness (Waardenburg, 1951). In 1971, Arias subtyped this syndrome Waardenburg syndrome type 1 (WS1 as described by P.J. Waardenburg) and Waardenburg syndrome type 2 (WS2), which has identical features to WS 1 but lacks dystopia canthorum (eyelid anomaly). Today, four different Waardenburg syndromes have been described and their clinical features are summarized in Table 4. WS3 patients have additional musculoskeletal abnormalities and WS4 patients are associated with Hirschsprung‘s disease (intestinal gangliosis). WS2 is autosomal dominantly (AD) inherited, although with a low penetrance. The hearing loss is sensorineural, congenital and usually non-progressive. It can be unilateral or bilateral, however it has been reported that 50% of those with WS2 had a bilateral sensorineural hearing loss. Pigmentation of hair, skin and eye is severely affected in

WS2 patients. Iris heterochromia can be complete or partial. Hypoplastic blue irides are found where there is deficient iris stroma. Diagnostic criteria of WS2 are summarized in Table 5. Further, it has been shown that heterochromia of the irides are more common in WS2 than in WS1 (Liu et al., 1995). A white forelock usually in the midline is very common, but it may be anywhere on the head. The pigmentation defects can affect the eyebrows and eyelashes as well. Hypopigmentation of the skin is congenital and may be found on the face, trunk or limbs (reviewed in Read & Newton, 1997).

Table 4. The four types of Waardenburg syndromes

Type	Inheritance	Disinguishing features	Comment
WS1	AD	dystopia canthorum W>1.95	PAX3 mutations
WS2	AD	no dystopia	MITF or SOX10 mutations
WS3	AD (and sporadic)	hypoplasia of limb muscles, contractures of elbows, fingers	PAX3 mutations
WS4	AR	Hirschsprung's disease	EDN3, EDNRB or SOX10 mutations

AD – autosomal dominant; AR - autosomal recessive

Table 5. Diagnostic criteria for WS2

Major criteria	Minor criteria
congenital sensorineural hearing loss	congenital leucoderma (several areas of hypopigmentated skin)
pigmentary disturbances of iris	synophrys (medial eyebrow flare)
(a) complete heterochromia iridium	broad and high nasal root
(b) partial or segmental heterochromia	hypoplasia of alae nasi
(c) hypoblastic blue eyes	premature greying of hair: scalp hair predominantly white before age 30
hair hypopigmentation: white forelock	
affected first degree relative	

(based on Read and Newton 1997 and Lui et al. 1995)

Using microsatellite polymorphisms, MITF was associated with WS2 (Hughes et al., 1994). Genotyping Waardenburg syndrome patients for MITF revealed that 7 out of 23 WS2 patients harbored MITF mutations (Tassabehji et al., 1995). WS2 patients who harbored MITF mutations have been subtyped WS2A (Nobukuni et al., 1996). Several mutations lead to an amino acid change resulting in a full-length protein. Among these mutations were a serine to proline change at 250, an asparagine exchange to aspartic acid at 278, a serine to proline at 298 and an arginine to lysine at 203. Additionally, one deletion mutation of arginine at residue

217 of MITF was identified (Tassabehji et al., 1995). The phenotypes of all known missense mutations in MITF which result in a full-length protein are summarized in Table 6.

The R217del mutation has been found in a WS2 patient of a Chinese family (Chen et al., 2010). Another MITF mutation at this residue in humans, R217I, which also leads to WS2 has been described (Chen et al., 2010).

In 1960, Walter Tietz presented a family with albinism, blue eyes, deaf-mutism and hypoplasia of the eyebrows. The genetics of the affected family members of this pedigree showed an autosomal dominant fashion with complete penetrance (Tietz, 1963). To date, only two MITF mutations have been associated with Tietz syndrome. Smith and colleagues found a substitution of lysine for asparagine at residue 210 in MITF (N210K). A portion of affected family members (6/19 (31,5%)) were heterozygous for this mutations (Smith et al., 2000). The in-frame deletion of arginine R217 has also been found in a 15-year old male with generalized skin pigment loss, blue irides and blonde hair and eyebrows. Generating this mutation in an expression vector and performing promoter activation assay showed that this mutation was not able to activate the tyrosinase promoter whereas the wild type MITF protein was able to activate the tyrosinase promoter (Shigemura et al., 2010). It seems that WS2A and TS are syndromes with similar clinical features. However, it appears that TS patients have more severe hypopigmentation affecting the skin resulting in a generalized hypopigmentation phenotype. Mice homozygous for the *Mitf*^{mi} mutation have a mutation identical to that found in humans at R217del. This mutation was originally described by Paula Hertwig. These mice have white coat color, small and red eyes, deficiency of mast cells, basophils and natural killer cells (Arnheiter, 2010; Steingrimsson et al., 2004). Additionally the *Mitf*^{mi} mice show spinal ganglia, adrenal medulla, incisors fail to erupt, smaller dermis than in wild type mice, osteopetrosis and inner ear defects (Arnheiter, 2010; Steingrimsson et al., 2004). In summary, mice homozugous for the *Mitf*^{mi} mutation and human patients with TS show similar hypopigmentation defects.

A recent review and update of mutations causing Waardenburg syndrome, identified a novel non-truncated MITF mutation at residue 224 changing an isoleucine to serine (I224S) (reviewed in Pingault et al., 2010). More MITF mutations have been found by Léger and colleagues including K206Q, I212S, E213D, R216K, as well as R217del, N210K and R217I, mostly in a French study population (Leger et al., 2012).

Nobukuni and colleagues identified two *MITF* mutations which result in a truncated MITF protein. Both result in an arginine to a stop codon substitution at, 214 and 259 respectively (Nobukuni et al., 1996). Further, they investigated the DNA binding properties of the mutant proteins to the E-box. These studies revealed that neither of the mutations was able to bind the E-box sequence. In addition to the DNA binding assay, transcription activation assays showed that the R214X and R259X mutant proteins failed to activate gene expression (Nobukuni et al., 1996). Lalwani and colleagues also found the R214X mutation when sequencing MITF in a WS2 affected family (Lalwani et al., 1998).

The S298P mutation has been investigated by DNA-binding and transcriptional activation assays. These studies showed that this protein lacks DNA-binding ability and that it fails to activate the tyrosinase promoter (Takeda et al., 2000a).

Table 6 summarizes all known human MITF mutations found in WS2 and Tietz patients which affect protein function.

Table 6. Summary of all known MITF mutations associated with Waardenburg type 2 and Tietz syndrome

Mutation	Location	Disease	Authors	Phenotype/Remarks	Inheritance
R203K	BR	WS2	Tassabehji et al. 1995	typical WS2. mutation found in proband does not segregate with disease	neutral variant
K206Q	BR	WS2	Léger et al. 2012	36y female; SNHL, white forelock blue irides	familial
N210K	BR	Tietz	Smith et al. 2000	deafness, blonde hair, white eyelashes & eyebrows, cutaneous hypopigmentation	familial
I212M	BR	Tietz/WS2	Welch et al. 2002	blue eyes, hypopigmentation of hair and skin, 14/28 affected members have SNHL	familial
I212S	BR	WS2	Léger et al. 2012	9y male; generalized hypopigmentation, freckles, blue irides, premature graying	familial
E213D	BR	WS2	Léger et al. 2012	33y female; SNHL, white forelock, premature graying, blue irides	de novo
R214X	BR	WS2	Lalwani et al. 1998	SNHL, heterochromia of the irides, premature graying, white forelock, a 3 generation WS2 family	familial
R214X	BR	WS2	Nobukuni et al. 1996	SNHL, heterochromia of the irides, white forelock, early graying	familial
R216K	BR	WS2	Léger et al. 2012	21y female; SNHL, white forelock, fair skin, blue irides	de novo
R217del	BR	Tietz	Léger et al. 2012	3y female; SNHL, generalized hypopigmentation, blue irides	Familial
R217del	BR	WS2	Chen et al. 2010	3 affected families	Familial
R217del	BR	Tietz	Tassabehji et al. 1995	SNHL, blonde/red hair color, pale skin, blue irides; dominant pedigree	Familial
R217del	BR	Tietz	Shigemura et al. 2010	15y male, generalized hypopigmentation, blue irides, blonde hair and eyebrows	Familial
R217I	BR	Tietz	Léger et al. 2012	3y female; SNHL, generalized hypopigmentation, blue irides and white forelock	Familial
R217I	BR	WS2	Chen et al. 2010	SNHL, blue irides, premature graying	de novo
R217G	BR	WS2	Chen et al. 2010	no data available	n/a
I224S	HLH	WS2	Pingault et al. 2010	6y female; SNHL, white forelock, heterochromia of the irides	Familial
S250P	HLH	WS2	Tassabehji et al. 1995	female patient; unilateral hearing loss, premature graying	Familial
Y253C	HLH	WS2	Read et al. 1997	no data available	n/a
R259X	HLH	WS2	Nobukuni et al. 1996	SNHL, heterochromia of the irides, white forelock, early graying	Familial
N278D	ZD	WS2	Tassabehji et al. 1995	female patient; SNHL, inherited from unaffected father	Familial
S298P	AD	WS2	Tassabehji et al. 1995	affected patient comes from a three generation history of WS2	neutral variant

AD= activation domain, BR= basic region, HLH= helix loop helix, ZD= zipper domain, SNHL= sensorineural hearing loss, n/a not available

1.3. Interferon regulatory factor 4 – An introduction

In 1995 Eisenbeis and colleagues isolated the protein PU.1-interaction partner (PIP) from a murine multiple myeloma cell line. PIP is a transcription factor which, in conjunction with PU.1, functions as a transcriptional activator (Eisenbeis et al., 1995). PIP consists of a PEST domain, a region rich in proline, glutamate, serine and threonine. The proline-rich domain represents a potential transcriptional activation domain. PIP has a molecular weight of 51.5 kDa and has been found to be expressed in spleen, thymus and bone marrow as well as in B-cell lines and T-cell lines (Eisenbeis et al., 1995). Almost at the same time that Eisenbeis identified PIP, Matsuyama and colleagues identified a new member of the interferon regulatory factor family in mouse spleen. The new gene was named LSIRF for lymphoid-specific member of the interferon regulatory factor family, and was shown to consist of at least 9 exons (Matsuyama et al., 1995). Surprisingly, LSIRF was not inducible by INFα-, INF-β or by INF-γ. Instead antigen mimetic stimuli like lipopolysaccharide (LPS) and anti-CD3 were able to induce LSRIF expression. DNA-binding assays revealed that LSIRF was able to bind the ISRE-sequence (interferon-specific response element) containing the nucleotide sequence GAAGTGAAACT (Matsuyama et al., 1995). One year after identifying PIP/LSIRF, Grossman and colleagues cloned the complete 5.3kb cDNA and showed that it generates a 450aa protein. Further, they showed that PIP/LSIRF was located on chromosome 6p23-25 and confirmed previous findings that PIP/LSIRF is expressed in B-cells. Interestingly, high levels of PIP/LSIRF mRNA levels were detected in a melanoma cell line and in the skin of newborn mice (Grossman et al., 1996). Although PIP/LSIRF appeared to be lymphocyte restricted, these findings showed also an expression in melanocytes (Grossman et al., 1996). PIP/LSIRF has been re-named interferon regulatory factor 4 (IRF4). Mice deficient for IRF4 show severe immunological features and impairments as listed in Table 7 suggesting that IRF4 is essential for the function and homeostasis of mature B and T lymphocytes (Mittrucker et al., 1997).

DNA-binding assays showed that IRF4 and PU.I form complexes in macrophages and in primary B-cells. IRF4 and PU.I are able to activate transcription of PU.1/IRF4 composite elements (a reporter plasmid containing 4 tandem repeats of Igκ chain 3' enhancer) in macrophages. These data demonstrate that IRF4 is a regulator of transcription in macrophages (Marecki et al., 1999).

Table 7. Features of IRF4 knock out (IRF4-/-) mice

Characteristics of IRF4 -/- mice compared with IRF4 wild type at 10-15 weeks
spleens 3-5 times enlarged in size
lymph nodes 10 times enlarged (because of T- and B- lymphocyte expansion)
CD23B220 B cell population completely absent (block of late B-cell maturation)
absence of germinal centers in B cell follicles
lack of plasma cells in spleen or lamina propria
serum concentrations of all Ig subclasses were reduced at least 99%
antibody production was also absent after TNP-LPS immunization
isolated B-cell stimulation with LPS/IgM showed reduced/no proliferation
T-cell stimulation failed to induce proliferation
IRF4 k.o. mice showed no cytotoxic activity after LCMV infection
Mice developed severe lymphadenopathy (swollen/enlarged lymph nodes)

Based on Mittruecker et al. 1997

1.3.1. IRF4 in pigmentation

As mentioned above, Grossman and colleagues found high IRF4 expression in a melanoma cell line and in the skin of newborn mice (Grossman et al., 1996). Six years after the identification of IRF4, Natkunam and colleagues (2001) investigated IRF4 protein expression in a large number of human malignancies, using a designed tissue microarray containing 265 hematolymphoid and 944 nonhematolymphoid neoplasms. Interestingly, of the solid, non-haematolymphoid disorders and normal tissues investigated, only malignant melanomas (5/22 cases) showed IRF4 staining (Natkunam et al., 2001).

Further evidence that IRF4 is not restricted to lymphocytes came from studies by Sundram and colleagues (2003) who investigated the role of IRF4 in melanomas. They showed that IRF4 expression was high in 86% of conventional primary melanomas (19/22) and 78% of metastatic melanomas (11/14). Benign nevi also showed strong IRF4 expression (Sundram et al., 2003).

In 2007, a genome-wide association study (GWAS) was used to identify sequence variants that influence hair color, freckles and skin sensitivity in the Icelandic and Dutch populations (Sulem et al., 2007). Two SNP´s, single nucleotide polymorphisms, in or near IRF4, rs4959270 and rs1540771, showed association with the presence of freckles. Although strongly correlated, the A allele of rs1540771 showed the stronger association and remained significant. Notably, this allele showed secondary association with brown (rather than blond) hair and with skin that is sensitive to ultraviolet radiation, UVR (Sulem et al., 2007).

Shortly thereafter, another GWAS study showed an association between IRF4 and pigmentation in U.S. women of European ancestry (Han et al., 2008). In the beginning Han and colleagues used a data set consisting only of women of European ancestry. However, this association was also shown in additional data sets (including men). The SNP rs12203592 in intron 4 of the *IRF4* gene was strongly associated with hair color (Han et al., 2008). This SNP is within 69.7kb of the two SNP´s (rs4959270 and rs1540771) that were identified by Sulem et al. (2007). Interestingly, the p-value for association of the IRF4 SNP rs12203592 and natural hair color was more than 13 orders of magnitude smaller than the p-value for any other SNP on chromosome 6 (Han et al., 2008). Further genotyping revealed that the SNP rs12203592 was highly associated with eye color ($6.1x10^{-13}$) (as well as skin color ($6.2x10^{-14}$) and tanning ability ($3.9x10^{-89}$)) (Han et al., 2008). This variant allele was associated with lighter skin color, less tanning ability and blue/light eye color (Han et al., 2008). Another GWAS study dedicated to identify genes contributing to the tanning phenotype was conducted by Nan and colleagues (Nan et al., 2009). They confirmed previous findings that IRF4 was associated with less tanning ability after UV exposure (Nan et al., 2009).

A web-based genome wide association study confirmed result of previous studies (Eriksson et al., 2010). The SNP rs12203592 within *IRF4* was shown to be associated with the presence of freckles, brown hair color and blue/light eye color (Eriksson et al., 2010).

Another GWAS study was conducted to investigate or identify the most highly stratified genes and the mechanism that might have contributed to genetic differences of five European populations; Scotland, Ireland, Sweden, Bulgaria and Portugal (Moskvina et al., 2010). Not surprisingly, genes involved in pigmentation demonstrated high statistical significance. Among those were IRF4 ($p= 3.7x10^{-56}$) with the SNP rs6920655 and OCA2/HERC2 with the SNP rs8041209 ($p= 3.1x10^{-71}$) (Moskvina et al., 2010). Results of this GWAS and others are summarized in Table 8.

Table 8. GWAS studies of pigmentation traits identifying allele variation in IRF4

Study population	Population size	SNP (for IRF4)	Results - association with SNP	Authors
Icelanders Dutch	2718 1214	rs1540771A	brown hair color presence of freckles skin sensitivity to sun exposure	Sulem et al. 2007
U.S. with European ancestry	2287 (initial) 6155 (for SNP)	rs12203592	dark hair color fair skin color less tanning ability blue/light eye color	Han et al. 2008
U.S. with European ancestry	2287	rs12203592	tanning ability	Nan et al. 2009
Scotland Ireland Sweden Bulgaria Portugal	656 1142 620 1129 563	rs6920655	hair color and pigmentation	Moskvina et al. 2010
U.S. with North European ancestry	>1500	rs12203592	presence of freckles brown hair color blue/light eye color	Eriksson et al. 2010

1.3.2. IRF4 in melanoma

In Queensland, Australia, cutaneous malignant melanoma (CMM) is a common cancer in the fair-skinned population with an estimated risk of 5% (Duffy et al., 2009). Within fairer skinned populations, risk varies with the degree of paleness as well as with other pigmentation phenotypes such as hair color and eye color (Duffy et al., 2009). Duffy and colleagues (2009) selected a set of loci which demonstrate polymorphisms in pigmentation traits and tested for association with cutaneous malignant melanoma (CMM) risk (Duffy et al., 2009). The selected loci were *MC1R, OCA2, TYR, TYRP1, IRF4, SLC24A, SLC45A2* and *ASIP*. All investigated loci except *IRF4* and *SLC24A4* were associated with increased risk for CMM. The lack of association between IRF4 and melanoma is surprising since IRF4 shows very strong evidence for association with pigmentation traits including sun sensitivity (Duffy et al. 2009).

Another GWAS study genotyped Australian adolescent twins in whom moles had been counted and measured (Duffy et al., 2010). Nevi or more specifically the number of nevi, contribute to melanoma risk. A previous analysis showed that melanoma risk increased by 2-4% per additional nevus counted (palpable nevi on arms and atypical nevi on body) (Chang et

al., 2009). In this study, the two most significant peaks showing association with melanoma were observed over the MTAP-CDKN2A region on chromosome 9p and IRF4 on chromosome 6p. The SNP rs12203592 for *IRF4* showed the strongest association with nevus counts. The variant allele (rs12203592*T) was associated with an increase in the number of flat nevi, but a decrease of raised nevus counts using adolescent twins as study population (Duffy et al., 2010). Further, including freckle score as a covariate strengthened the negative relationship between the rs12203592*T allele and raised nevi. Interestingly, investigating the parents of the twins showed an opposite direction. Here self-reported nevus count was associated with the C allele (the wild type allele), showing a gene-by-age interaction. To summarize, in adolescents the T polymorphism was associated with higher nevus counts, whereas in adults (their parents) the wild type allele (rs12203592*C) was associated with higher nevus count (Duffy et al., 2010).

In order to investigate if the C allele increases melanoma risk in adults, samples from Australia, UK and Sweden were analyzed, with the result that the C allele was associated with melanoma risk (OR 1.15; $p=4x10^{-3}$), most significantly in the trunk region of the body (OR 1.33; $p=2.5x10^{-5}$) (Duffy et al., 2010) (see Table 9). On the other hand, Gudbjartsson and colleagues (2008) did not find an association of IRF4 with melanoma, using a different SNP (rs6058017)(Gudbjartsson et al., 2008).

A fourth GWAS study focusing on IRF4, identified the variant allele rs12203590*T as a melanoma risk locus but also as a risk allele for basal cell carcinoma (BCC) and squamous cell carcinoma (SCC) (Han et al., 2011).

The latest GWAS study regarding IRF4 and melanoma risk was conducted by Kvaskoff and colleagues (2011) in which they found an association of IRF4 with high nevus count (Kvaskoff et al., 2011). However, no statistically significant association between IRF4 and melanoma was found in adults, although a decreased association of melanoma risk was observed in children and adolescents (Kvaskoff et al., 2011).

Table 9 summarizes the results of the study discussed above and other GWAS studies of melanoma patients identifying allele variation in *IRF4*. The table gives an overview on study population, population size, the used SNP, the association of the SNP and the original publication of the GWAS studies.

Table 9. GWAS of melanoma identifying allele variation in *IRF4*

Study population	Population size	SNP (for IRF4)	Results - association with SNP	Authors
Australian adolescents (Brisbane Twin Nevus Study) and Q-MEGA	1810 and 1882	rs12203592	high nevus count	Kvasskoff et al. 2011
			melanoma risk - decreased in children and adolescents	
U.S. with European ancestry (NHS and HPFS plus two replication sets)	408 Melanoma 537 SCC 513 BCC	rs12203592	associated with melanoma, BCC and SCC	Han et al. 2011
Australian adolescents (Brisbane Twin Nevus Study)	1810	rs12203592	increase of flat nevus counts	Duffy et al. 2010
			decrease of raised nevus counts	
Parents of twins	1470	rs12203592	increased nevus counts for WT	
Australia	1271	rs12203592	higher melanoma risk with the wild type allel (C); most significantly with the trunk	
UK (Leeds)	1821			
Sweden (Karolinska University)	775			
Cutaneous malignant melanoma (CMM; Queensland)	1738	rs12203592	CMM risk; no risk OR 1.04	Duffy et al. 2009
			hair color	
			blue eye color	
			pale skin (light skin color)	

OR = odds ratio

1.3.3. IRF4 in the lymphatic system

As mentioned in the introduction Section 1.3., IRF4 knock-out mice show severe immunological defects (Mittrucker et al., 1997). Klein and colleagues (2006) generated a conditional IRF4 knock-out mouse, in order to investigate the role of IRF4 in post-GC B-cell development and showed that IRF4 deficiency leads to the absence of plasma cells (and to absence of their precursors, plasmablasts), that IRF4 and Blimp-1 act upstream of the transcription factor XBP-1 which is essential for plasma cell development, that those B-cells fail to undergo class switch recombination and that IRF4 is required for memory-to-plasma cell differentiation (Klein et al., 2006). Further, IRF4-deficient B lymphocytes were defective in developing antigen-specific B-cells (Sciammas et al., 2006). It was also shown that IRF4 regulates Aicda and Blimp-1, which are important for antibody secretion and isotype switching, and interacts with Blimp-1, suggesting that Blimp-1 might be a target of IRF4

(Sciammas et al., 2006). Moreover, IRF4 deficiency manifests itself as a severely dysregulated Th-cell (T-helper cell) differentiation (Lohoff et al., 2002). IRF4 was also expressed at low levels in dendritic cells (DC), which are bone marrow-derived professional APCs (antigen-presenting cells) and play critical roles in the induction of both innate and adaptive immunity (Tamura et al., 2005).

1.3.4. IRF4 expression in heamatolymphoid malignancies (HLM)

As mentioned above, IRF4 plays an important role in B-cell development and therefore it is not surprising, that IRF4 expression might be dysregulated in haematolymphoid malignancies such as lymphoma and multiple myeloma. To give an overview on IRF4 expression in HLM several studies are described below. All of them used immunohistochemistry to detect IRF4 expression.

1.3.4.1. Multiple myeloma

Multiple myeloma is the most common primary bone malignancy (reviewed in Nau & Lewis, 2008). Multiple myeloma occurs with increased frequency in older persons (median age of diagnosis is approximately 70 years), and the rate is nearly twice as high in black persons than in white individuals (reviewed in Nau & Lewis, 2008). Plasma cells are responsible for fighting infections. As monoclonal myeloma plasma cells proliferate it will eventually result in an overproduction of paraprotein (or also called M protein). Paraproteins are immunoglobins, therefore overproduction leads to abnormal IgG, IgM, IgA, IgE or IgD and abnormal light chain proteins (κ or λ). Another result of the increased paraprotein production is hyperviscosity of the blood, light chain proteins that cause end-organ damage (most affected are the kidneys) and invasive bone lesions that cause bone pain, osteoporosis and hypercalcemia (reviewed in Nau & Lewis, 2008).

Generating and analyzing cDNA libraries from myeloma patient samples revealed several up- and down-regulated genes compared to nonmyeloma cell lines (Claudio et al., 2002). Among the up-regulated genes was *IRF4*. Further, a myeloma gene-enriched microarray supported the above results, by identifying IRF4 as upregulated in myeloma (Claudio et al., 2002). Another study, conducted by Yamada and colleagues (2001) showed that mRNA transcripts of IRF4 were expressed in B-lymphoblastic and myeloma cell lines (Yamada et al., 2001).

Chromosomal translocations involving the IgH locus on chromosome 14q32 is a common event in multiple myeloma. Analyzing several cell lines of the lymphatic system revealed that 2 multiple myeloma cell lines (SK-MM-1 and XG-7) had a reciprocal balanced translocation in the *IgH* and the *MUM1* loci (2 out of 11 cell lines tested) (Iida et al., 1997). Fluorescence *in situ* hybridization showed that the translocation was specifically between t(6;14)(p25;q32). Western blotting showed that these two cell lines, which harbor the t(6;14) translocation, have a 6-fold overexpression of IRF4 compared to other multiple myeloma cell lines which do not have the translocation (Iida et al., 1997). Hence, these results indicate that the functional consequence of the translocation t(6;14)(p25;q32) is a deregulation of IRF4 expression leading to an increase in IRF4 protein. Further, anchorage-independent growth assays, preformed in rat fibroblasts, showed that IRF4 transfected cells were able to form more colonies than empty vector transfected cells, indicating that IRF4 increases clonogenic potential *in vitro* and may contribute to oncogenesis *in vivo* (Iida et al., 1997). The results of this study have been confirmed by a study conducted by Yoshida and colleagues (Yoshida et al., 1999).

Small hairpin RNAs (shRNA) were used to knock down IRF4 in lymphatic cell lines. This resulted in decreased cell survival in myeloma cell lines, whereas lymphoma cell lines were largely unaffected (Shaffer et al., 2008). IRF4 depletion resulted in increased toxicity (cell death occurred within 3 days) but it did not affect the cell cycle stage (Shaffer et al., 2008). Gene expression profiling revealed that, *MYC* and *PRDM1* are important IRF4 target genes. Further, it was shown that IRF4 bound the promoters of *PRDM1* and *MYC* (Shaffer et al., 2008). Knockdown of IRF4 expression reduced the amount of IRF4 bound to the *MYC* promoter, indicating *MYC* as a direct target of IRF4. Interestingly, knockdown of MYC resulted in decreased IRF4 expression, suggesting a positive regulatory loop in myeloma cells between MYC and IRF4 (Shaffer et al., 2008).

Surprisingly, even though the SNP rs872071 has been associated with increased risk of chronic lymphocytic leukemia (Di Bernardo et al., 2008) it showed no association with multiple myeloma (Pratt et al., 2010).

1.3.4.2. B-cell neoplasm

IRF4 has been shown to be overexpressed in diffuse large B-cell lymphoma (DLBCL) which is the most common of the aggressive non-Hodgkin's lymphomas in the United States

(reviewed in Friedberg & Fisher, 2008). IRF4 expression was observed in 40-50% of DLBCL (Hallack Neto et al., 2009; Hans et al., 2004; van Imhoff et al., 2006; Zinzani et al., 2005).

IRF4 has been shown to be expressed in follicular lymphoma (FL) (Winter et al., 2004), marginal-zone lymphoma (mucosal associated lymphoid tissue (MALT)) (reviewed in Isaacson & Du, 2004), AIDS-related non-Hodgkin lymphoma (AIDS-NHL) (Carbone et al., 2001), primary central nervous system lymphoma (Coupland et al., 2005) and primary cutaneous large B-cell lymphomas (PCLBCL) (Hoefnagel et al., 2005).

1.3.4.2.1 Chronic lymphocytic leukemia (CLL) and acute lymphoblastic leukemia (ALL)

Chronic lymphocytic leukemia (CLL) is the most frequent form of leukemia in Western countries where it accounts for 30% of all leukemias (reviewed in Keating et al., 2003). Numerous immunohistochemical studies have shown that CLL patients show strong IRF4 expression (40-100% IRF4 positive) as summarized in Table 10 (Craig et al., 2008; Michaux et al., 2005; Soma et al., 2006; Uranishi et al., 2005). Interestingly, Ito and colleagues (2002) demonstrated that low IRF4 expression was associated with shorter overall survival rate indicating that higher IRF4 expression is associated with better outcome (Ito et al., 2002). These results have been supported by another study which showed that absence of IRF4 expression in CLL patients was associated with worse overall survival (Chang et al., 2002).

Table 10. IRF4 expression in chronic lymphocytic leukemia (CLL)

Study population	Population size	IRF4 positive expression	Authors
CLL	36	16/36 (44%)	Craig et al. 2008
CLL	28	28/28 (100%)	Soma et al. 2006
B-CLL cell lines	4	2/4 (50%)	Uranishi et al. 2005
CLL	8	8/8 (100%)	Micheaux et al. 2005
CLL	30	12/30 (40%)	Chang et al. 2002
CLL - cell lines	4	2/4 (50%)	Ito et al. 2002
CLL – patients	29	14/29 (48%)	

Genome-wide association studies (GWAS) have shown that the SNPs (single nucleotide polymorphism) rs872071 (located in 3‘ UTR of IRF4) and rs9378805 (10kb centromeric to 3‘ UTR of IRF4) (Crowther-Swanepoel et al., 2010; Di Bernardo et al., 2008; Slager et al.) are associated with increased risk of CLL. This association has been shown for low IRF4 expression.

A recent GWAS of childhood acute lymphoblastic leukemia (ALL) showed that the SNP rs12203590 in intron 4 of IRF4 is associated with increased risk in ALL males (Do et al., 2010). Homozygosity of this particular variant may lead to an increased IRF4 expression. Interestingly, within the intron 4 of IRF4, spanning the SNP rs12203590, is a binding site for the transcription factor TFAP2α. Streptavidin-agarose pulldown assays showed that the variant type of IRF4 binds more weakly to the transcription factor TFAP2α than the wild type. The wild type, harboring the C allele, binds 60% more strongly to TFAP2α than the variant type with the T allele (Do et al., 2010).

1.3.4.3. T-cell neoplasm

Mature T-cell and natural killer cell neoplasms are relatively uncommon, accounting for fewer than 10% of all non-Hodgkin lymphomas on a worldwide basis (reviewed in Jaffe, 2006). IRF4 has been shown to be expressed in 85% of anaplastic large cell lymphoma, ALCL (Wada et al., 2011). Numerous patients of T-cell lymphoproliferative disorders showed extra copies of the *IRF4* locus or showed chromosomal translocation involving *IRF4* (Pham-Ledard et al., 2010; Wada et al., 2011). The translocation t(6;14)(p25;q11.2) was found in patients with peripheral T-cell lymphomas (PTCL) (Feldman et al., 2009).

1.3.4.4 Hodgkin's lymphoma (HL)

Besides DLBCL, Hodgkin lymphoma (HL) is one of the most frequent lymphomas (reviewed in Kuppers, 2009). IRF4 is expressed in almost all investigated HL (Aldinucci et al., 2009; Carbone et al., 2002; Natkunam et al., 2007; Valsami et al., 2007). Further, the SNP rs872071 in the 3'UTR of *IRF4* has been associated with HL and CLL risk; the rs872071-G is the risk allele (Broderick et al., 2009).

1.3.4.5. Mutations of IRF4 in haematolymphoid malignancies

Although translocations and extra copy numbers of *IRF4* are not so uncommon in haematolymphoid malignancies, actual mutations in *IRF4* are rather rare. Recently, two mutations have been found in IRF4 in chronic lymphocytic leukemia (CLL) patients. The mutations which exchange a leucine to either arginine or proline (L116R/P) lead to increased IRF4 mRNA expression and showed increased caspase 3/7 activity (Havelange et al., 2011). Furthermore, genotyping multiple myeloma patients identified the K123R mutation in two out

of 38 multiple myeloma patients. The effects of the K123R mutation have not been further investigated (Chapman et al., 2011).

1.3.4.5.1. IRF4 expression in the lymphatic system – a quick summary

Non-Hodgkin lymphomas (any lymphoma except Hodgkin lymphoma) have been discussed over the last couple of subchapters.

Table 11 shows a summary of IRF4 expression in studies focusing on non-Hodgkin lymphoma (NHL) (Martinez et al., 2008; Natkunam et al., 2001; Tsuboi et al., 2000).

Table 11. IRF4 expression in non-Hodgkin lymphoma (NHL)

Study population	Population size	IRF4 expression	Authors
DLBCL	58	11/58 (19%)	Martinez et al. 2008
MZL	21	6/21 (29%)	
MCL	28	3/28 (11%)	
MM	14	14/14 (100%)	
SLL	49	20/49 (41%)	
PBL	9	9/9 (100)	
DLBCL	70	20/70 (51%)	Natkunam et al. 2001
FL	72	11/72 (17%)	
MZL	12	7/12 (58%)	
MCL	8	2/8 (33%)	
MM	2	2/2 (100%)	
SLL	7	3/7 (43%)	
PTCL	11	8/11 (72%)	
ALCL	4	4/4 (100%)	
DLBCL	41	30/41 (73%)	Tsuboi et al. 2000
CLL	7	3/7 (43%)	
MZL	5	1/5 (20%)	
ATL	5	2/5 (40%)	
ALCL	5	4/5 (80%)	
Multiple myeloma		all (data not shown)	

2. AIMS

2.1. MITF mutations associated with Waardenburg- and Tietz syndrome and melanoma

i. To analyze MITF mutations associated with hypopigmentation syndromes and melanoma with respect to effects on their DNA-binding ability and transcription activation potential

2.2. MITF and IRF4

i. Investigate if MITF and IRF4 interact directly
ii. Determine if MITF and IRF4 co-operate in activating the TYR promoter
iii. Characterize the function of IRF4 as a melanoma oncogene

3. MATERIALS and METHODS

3.1. Conservation of the MITF protein and melanocyte-specific promoter sequences

The MITF protein sequence was retrieved from the ensemble genome browser www.ensembl.org. Sequences of human (ENSG00000187098), mouse (ENSMUSG00000035158) and horse (ENSECAT00000006351) MITF proteins were aligned using the ClustalW program (http://workbench.sdsc.edu). The same tools were used in order to analyze the conservation of E- and M-boxes of MITF between human and mouse.

3.2. Cell culture

HEK293T (ATCC), HEK293 (ATCC), 501mel (a gift from Ruth Halaban, USA), SK-mel 28 (ATCC), MeWo (ATCC), Melan-A (a gift from Dorothy Bennett, UK) and B16 (ATCC) cells were maintained in Dulbecco´s modified Eagle Medium (GIBCO), supplemented with 10% fetal bovine serum, 100U of penicillin/ml and 100µg of streptomycin/ml and cultured in a humidified incubator at 37°C with 5% CO_2. RPMI8266 and U266 cells (a gift from Helga M. Ögmundsdóttir, Iceland) were maintained in RPMI (GIBCO) supplemented with 15% fetal bovine serum, 100U of penicillin/ml and 100µg of streptomycin/ml and cultured in a humidified incubator at 37°C with 5% CO_2.

3.3. Site directed mutagenesis

MITF mutations associated with melanoma and Waardenburg- and Tietz syndrome (see Table 3 and Table 6) were generated in a mouse *Mitf* expression construct (pcDNA 3.1) which produces the melanocyte-specific M-MITF (+) isoform (primers are listed in Table 12). A luciferase reporter plasmid (pGL3 basic vector by Promega) containing the TYR promoter region spanning from +80 to -300 was used to create multiple mutations. All mutations were created by using QuickChange Lightning Site-directed mutagenesis kit from Stratagene. The QuickChange primer design program provided by Agilent Technologies was used to design the primers (see Table 13). All mutants were verified by Sanger sequencing (Applied Biosystems, 3130 Genetic Analyzer).

Table 12. Primer sequences used for mutagenesis of the MITF cDNA

Primer name	Sequence
E87R-F	5'-atgctcactcttaactccaactgtgaaaaa**ag**ggcattttataagtttgag-3'
E87R-R	5'-ctcaaacttataaaatgcc**ct**tttttcacagttggagttaagagtgagcat-3'
L135V-F	5'-gcctggaatcaagttataatgaagaaatt**g**tgggcttgatggatc-3'
L135V-R	5'-gatccatcaagccca**c**aatttcttcattataacttgattccaggc-3'
L142F-F	5'-ttgatggatccggcctt**c**caaatggcaaatacgtt-3'
L142F-R	5'-aacgtatttgccatttg**g**aaggccggatccatcaa-3'
R203K-F	5'-gcaagagcattggctaaagaga**a**gcagaaaaaggaca-3'
R203K-R	5'-tgtccttttctgc**t**tctctttagccaatgctcttgc-3'
K206Q-F	5'-agcattggctaaagagaggcagaaa**c**aggacaatcacaa-3'
K206Q-R	5'-ttgtgattgtcct**g**tttctgcctctctttagccaatgct-3'
N210K-F	5'-agaggcagaaaaaggacaatcacaa**g**ttgattgaacgaag-3'
N210K-R	5'-cttcgttcaatcaa**c**ttgtgattgtccttttctgcctct-3'
I212M-F	5'-gaaaaaggacaatcacaacttgat**g**gaacgaagaagaagatttaacata-3'
I212M-R	5'-tatgttaaatcttcttcttcgttc**c**atcaagttgtgattgtccttttc-3'
I212S-F	5'-ggcagaaaaaggacaatcacaacttga**g**tgaacgaagaagaa-3'
I212S-R	5'-ttcttcttcgttca**c**tcaagttgtgattgtccttttctgcc-3'
E213D1-F	5'-ggcagaaaaaggacaatcacaacttgattga**c**cgaagaagaagattta-3'
E213D1-R	5'-taaatcttcttcttcg**g**tcaatcaagttgtgattgtccttttctgcc-3'
E213D2-F	5'-ggcagaaaaaggacaatcacaacttgattga**t**cgaagaagaagattta-3'
E213D2-R	5'-taaatcttcttcttcg**a**tcaatcaagttgtgattgtccttttctgcc-3'
R214X-F	5'-aaggacaatcacaacttgattgaa**t**gaagaagaagatttaacataaacg-3'
R214X-R	5'-cgtttatgttaaatcttcttcttc**a**ttcaatcaagttgtgattgtcctt-3'
R216K-F	5'-acaatcacaacttgattgaacgaagaa**a**aagatttaacataaacgacc-3'
R216K-R	5'-ggtcgtttatgttaaatctt**t**ttcttcgttcaatcaagttgtgattgt-3'
R217del-F	5'-acaacttgattgaacgaagaagatttaacataaacgaccgcattaa-3'
R217del-R	5'-ttaatgcggtcgtttatgttaaatcttcttcgttcaatcaagttgt-3'
R217I-F	5'-caacttgattgaacgaagaagaa**t**atttaacataaacgaccgcatta-3'
R217I-R	5'-taatgcggtcgtttatgttaaat**a**ttcttcttcgttcaatcaagttg-3'
R217G-F	5'-caacttgattgaacgaagaaga**g**gatttaacataaacgaccgcat-3'
R217G-R	5'-atgcggtcgtttatgttaaatc**c**tcttcttcgttcaatcaagttg-3'
I224S-F	5'-tttaacataaacgaccgca**g**taaggagctaggtactctg-3'
I224S-R	5'-cagagtacctagctcctta**c**tgcggtcgtttatgttaaa-3'
G244R-F	5'-catgcggtggaacaag**a**gaaccattctcaaggc-3'
G244R-R	5'-gccttgagaatggttc**t**cttgttccaccgcatg-3'
S250P-F	5'-aaccattctcaaggcc**c**ctgtggactacatccg-3'
S250P-R	5'-cggatgtagtccacag**g**ggccttgagaatggtt-3'
Y253C-F	5'-ggcctctgtggact**g**catccggaagttgc-3'
Y253C-R	5'-gcaacttccggatg**c**agtccacagaggcc-3'
R259X-F	5'-gactacatccggaagttgcaa**ta**ggaacagcaacgagctaa-3'
R259X-R	5'-ttagctcgttgctgttcc**ta**ttgcaacttccggatgtagtc-3'
N278D-F	5'-ctggagcatgcg**g**accggcacctgc-3'
N278D-R	5'-gcaggtgccggt**c**cgcatgctccag-3'
N278P-F	5'-gctggagcatgcg**cc**ccggcacctgctg-3'
N278P-R	5'-cagcaggtgccgg**gg**cgcatgctccagc-3'
L283P-F	5'-cggcacctgctgc**c**agagtacaggag-3'
L283P-R	5'-ctcctgtactctg**g**gcagcaggtgccg-3'
S298P-F	5'-ggctagagcgcatggactt**c**cccttatcccatc-3'
S298P-R	5'-gatgggataaggg**g**aagtccatgcgctctagcc-3'
E318K-F	5'-ctggtgaatcggatcatcaagcaa**a**aaccagttcttga-3'
E318K-R	5'-tcaagaactggtt**t**ttgcttgatgatccgattcaccag-3'
D380N-F	5'-ggaagacatcctgatg**a**acgatgccctctcacc-3'
D380N-R	5'-ggtgagagggcatcgt**t**catcaggatgtcttcc-3'

Table 13. Primer sequences used for mutagenesis of the TYR promoter

Primer name	Sequence
BS 1 (fwd)	5´ - ggatacgagccaattcgaaa**acc**aagtcagtcatgtgcttttcag - 3´
BS 1 (rev)	5´ - ctgaaaagcacatgactgact**ggt**tttcgaattggctcgtatcccac - 3´
BS 2 (fwd)	5´ - ccaattcgaaagaaaagtcagtcatgtgctt**gct**agaggatgaaagcttaagataaa - 3´
BS 2 (rev)	5´- tttatcttaagctttcatcctct**agc**aagcacatgactgacttttctttcgaattgg - 3´
BS 3 (fwd)	5´- agtcagtcatgtgcttttcagaggatg**ccc**gcttaagataaagactaaaagtgtttg - 3´
BS 3 (rev)	5´- caaacacttttagtctttatcttaagc**ggg**catcctctgaaaagcacatgactgact - 3´
BS 2 x BS 3 (fwd)	5´- cagtcatgtgcttgctcagaggatg**ccc**gcttaagataaagactaaaagtgtt - 3´
BS 2 x BS 3 (rev)	5´- aacacttttagtctttatcttaagc**ggg**catcctctgagcaagcacatgactg - 3´
BS 1 x BS 3 (fwd)	5´ - ggatacgagccaattcgaaaa**cc**aagtcagtcatgtgcttttcag - 3´
BS 1 x BS 3 (rev)	5´- caaacacttttagtctttatcttaagc**ggg**catcctctgaaaagcacatgactgact - 3´
BS 1 x BS 2 x BS 3 (fwd)	5´- cagtcatgtgcttgctcagaggatg**ccc**gcttaagataaagactaaaagtgtt - 3´
BS 1 x BS 2 x BS 3 (rev)	5´- aacacttttagtctttatcttaagc**ggg**catcctctgagcaagcacatgactg - 3´

Bold and underlined sequences indicate site of mutagenesis

3.4. Co-transfection and luciferase assay

For performing reporter gene assays, $1x10^4$ HEK 293T cells were seeded in 96 well plates (BRANDplates – cell grade^{TM}) and transfected with ExGen 500 *in vitro* transfection reagent (Fermentas). Cells were transfected with 35ng of luciferase reporter constructs containing the TYR (Yasumoto et al., 1994), TYRP1 (Lowings et al., 1992), DCT (Murakami & Arnheiter, 2005), 4M-box (Murakami & Arnheiter, 2005), MET (Beuret et al., 2007), p16 (Loercher et al., 2005), p21 (Carreira et al., 2005) or HIF1α (Busca et al., 2005) promoter sequences. All promoter constructs are in the pGL3-basic vector (Promega). Each promoter construct was transfected with 15ng wild type or mutant mouse MITF construct. An HA-IRF4 expression construct (Iida et al., 1997) was used for expressing the IRF4 protein.

pRenilla (1.5ng) was used to normalize luciferase activity. Twenty-four hours after transfection, cells were lysed with passive lysis buffer (Dual luciferase reporter assay system, Promega) and assayed for firefly and *Renilla* luciferase activity according to manufacturer's instructions using a Modulus II microplate reader (Turner Biosystems). Transfection experiments were carried out in six replicates each time and repeated at least twice. Luciferase signals were normalized to corresponding *Renilla* signals and results expressed as fold activation over wild type MITF or empty vector, as appropriate (indicated in figure legends). Outliers were calculated by the quartile method. Error bars show the standard error of mean and significance was calculated via the Student's t-test. P-values < 0.05 were considered statistically significant.

3.5. RNA extraction, cDNA synthesis and RT-PCR (qPCR)

For determining gene expression levels in melanocytes and melanoma, total RNA was extracted using TRIzol reagent (Invitrogen) according to the manufacturer's protocol from HEK293T, 501mel, SK-mel 28, B16, MeWo, RPMI8266 and U266 cells. Cell lysates from a confluent 10cm cell culture dish were used. RNA was quantified using the NanoDrop spectrophometer ND-1000 and the Agilent 2100 Bioanalyzer used to determine RNA quality and integrity. After DNAseI treatment, RNA was purified with the RNEasy Minielute kit (Quiagen). cDNA was generated with the RevertAid First Strand cDNA Synthesis Kit (Fermentas) using a combination of random hexamer and oligo $(dT)_{18}$ primers. PCR was performed according to manufacurer's protocol (cDNA synthesis KIT, Fermentas). Primers used for analyzing endogenous expression of MITF, IRF4 and Tyrosinase are listed in Table 14. The reaction was performed according to the manufacturer's protocol (Fermentas, Maxima^{TM} SYBR Green qPCR). qPCR was performed in duplicates and repeated at least twice (Applied Biosystems, ABI 7500). ΔCt values were calculated by subtracting the average Ct value of β-actin from the average of the sample Ct values.

Table 14. Primers used for RT-PCR (qPCR).

human primers	Sequences	mouse primers	sequences
MITF - F	5´- ctatgcttacgcttaactcca - 3´	MITF – F	5´- caaatgatccagacatgcgg - 3´
MITF – R	5´- tacatcatccatctgcatacag - 3´	MITF - R	5´- tgctccagcttcttctgtc - 3´
IRF4 – F	5´- acagcagttcttgtcagag - 3´	IRF4 – F	5´- cagctcatgtggaacctc - 3´
IRF4 – R	5´- gaggttctacgtgagctg - 3´	IRF4 – R	5´- ggaagaatgacggaggga - 3´
TYR – F	5´- ccatggacaaatccagaaccc – 3	TYR- F	5´- gactcttacatggttcctttca - 3´
TYR – R	5´- ggactagcaaatccttccag - 3´	TYR – R	5´- aaagcctggatctgactct - 3´
b-actin – F	5´- aaatctggcaccacacct - 3´	b- actin – F	5´- taccaactgggacgacat - 3´
b-actin – R	5´- gtctcaaacatgatctgggtc – 3	b- actin – R	5´- gtctcaaacatgatctgggtc - 3´

3.6. Immunoblotting and GST pull-down

In order to investigate if MITF and IRF4 interact GST-pull down and Western blot analyses were performed. HEK293T cells were grown in T175 cell culture flasks (Thermo Scientific) and transfected either with empty vector (pCMV-vector), pCMV-GST-MITF, HA-IRF4 or with pCMV-GST-MITF and HA-IRF4 together using ExGen 500 (Fermentas) transfection reagent. GST pull-down was performed according to the manufacturer's protocol (Pierce). The elution step was performed with sample buffer. Samples were analysed by electrophoresis on 8% SDS-polyacrylamide gel. After electroblotting the proteins on a PVDF

membrane, the membrane was incubated with primary antibody (anti-GST (MERK) and anti-HA (Roche)) overnight at 4°C in PBS with 5% milk. After three washing steps in PBS-T, the membrane was incubated for one hour with protein A/G peroxidase-conjugated secondary antibody (Thermo scientific) followed by signal detection using ECL reagents (Thermo Scientific).

After stripping the membrane at 55°C for 45 minutes followed by extensive washing, the blot was incubated with anti-HA antibody (Roche) overnight at 4°C in PBS with 5% milk. The membrane was incubated for one hour with protein A/G peroxidase conjugated secondary antibody (Thermo scientific), followed by signal detection using ECL reagents (Thermo Scientific).

3.7. Co-immunoprecipitation

Another approach to determine if MITF and IRF4 interact is to use co-immunoprecipitation. HEK293T cells were seeded in four cell culture dishes (Thermo Scientific, Nunc) in a density of 30-50%. The first cell culture dish was transfected with empty 6xcmyc-vector, the second cell culture dish with 6x-cmyc-Mitf, the third with HA-IRF4 expression construct (Iida et al., 1997) and the fourth with 6x-cmyc-Mitf and HA-IRF4 together. Cells were transfected with ExGen 500 (Fermentas) and lysed 48h post-transfection with lysis buffer (50mM Tris-HCl, pH7.6, 5mM $MgCl_2$, 75mM KCl, 0.1% Nonidet p-40). Subsequently the samples were pre-cleared with protein A/G (Fermentas) for 30-60 minutes, incubated with primary myc antibody (9E10, Sigma) or HA antibody (Roche) overnight at 4°C, followed by protein A/G incubation for one hour. Subsequent washing steps were performed with lysis buffer (constantly supplemented with protease inhibitor cocktail (Fermentas)). Samples were eluted in sample buffer and analysed using electrophoresis and immunoblotting (described above). The membrane was incubated with primary antibody (9E10, Sigma or HA antibody, Roche) and processed as described above. After stripping and intensive washing of the membrane, the blot was incubated with HA-antibody (Roche) and Myc-antibody (Sigma).

3.8. Electrophoretic mobility shift assay (EMSA)

Wild type and mutant MITF proteins were synthesized in vitro, using the TNT quick coupled Transcription/Translation system according to manufacturer's protocol (Promega). The TNT produced proteins were analyzed by electrophoresis on an 8% SDS-polyacrylamide gel, electroblotted onto a PVDF membrane and incubated with a MITF antibody (C5, Thermo Scientific) overnight at 4°C in PBS with 5% milk. Protein quantification was determined by intensity comparison of the bands using the Odyssey Infrared Imager (Li-Core). The double stranded oligonucleotides encompassing the MITF binding sequences E-box 5'-AAAGAGTAG**CACGTG**CTACTCAGA-3' and M-box 5'-AAAGAGG**CTCATGTG**CTA-ACCAGA-3' were ^{32}P-dCTP-end-labeled (PerkinElmer) using Klenow fragment (Fermentas) and subsequently purified using Sephadex G50. TNT proteins were incubated with buffer 1 (2mM spermidine, 2mM $MgCl_2$, 10% fetal calf serum, 2ng/µl poly(dI)(dC)) for 15 minutes on ice. For supershifts 0.5µl of MITF antibody (C5, Thermo Scientific) were added and incubated for 30 minutes on ice. The labeled probe was incubated with binding buffer (see Beuret et al., 2007) for a couple of minutes at room temperature and added to the TNT protein-mix. After a 10 minutes incubation period, the DNA-protein complexes were resolved by electrophoresis on a 4.2% non-denaturating polyacrylamide gel in 0.25xTBE buffer. Negative controls included the empty vector (pcDNA3.1) and water. After an overnight incubation on a storage phosphor screen, the gel was scanned on a Typhoon 8610 Variable Mode Imager (Molecular dynamics). Band intensities were calculated using ImageQuant software.

3.9. Soft agar- and clonogenic assay

To test if MITF and/or IRF4 provide cells with growth advantage, anchorage independent soft agar assay and anchorage dependent clonogenic assay were performed. 501mel and HEK293 cells were transfected with empty vector (pCDNA3.1) and with vectors expressing MITF, HA-IRF4 as well as both together using Exgene 500, Fermentas, for 48 hours and subsequently cells were selected with Geneticin G418 (Fermentas). Selection was performed under high concentrations of Geneticin (2mg/ml) for at least one week. A 'mock-plate' of untransfected cells was also included. After antibiotic selection, cells were constantly maintained at low Geneticin concentrations (0.5mg/ml). A soft agar assay was performed in

6-well plates using a 1% bottom agar and 0.8% top agar for SK-Mel28 and 501 melanoma cells and 0.5% top agar for HEK293 cells. Before the cells were seeded (1000, 2000 and 4000 cells per well; see Figure 11) they were counted with a Countess Cell counter (Sigma) and seeded cells (in triplicates) were incubated for 2 weeks. Soft agar was washed carefully with PBS and fixed with 4% paraformaldehyde. Colonies were stained with crystal violet. Quantification of colonies was performed with the clono-counter program (Niyazi et al., 2007). For the clonogenic assay the procedure was very similar, except that cells were seeded directly in 6-well plates. The cells were fixed and stained as described above.

4. RESULTS

4.1. MITF mutations associated with pigment deficiency syndromes and melanoma have different effects on protein function (Paper I).

4.1.1. Human MITF mutations and their location within the protein

Table 1 of Paper I (or Table 3 on page 29 and Table 6 on page 37) summarizes all known human MITF mutations which result in a full length protein which were used in our studies, with the location within the protein, the associated phenotype, mode of inheritance and the original publication describing its identification. All the mutations are missense mutations except for R214X and R259X which result in truncated MITF proteins and were included to serve as negative controls, since we expected them to be functionally inactive. Note that mutations associated with WS2A and TS are mostly located in the basic region, helix-loop-helix- and zipper domains of MITF and only one, the S298P mutation, is located at the carboxyl end of MITF (Figure 1a, Paper I). With respect to the melanoma mutations, only one, the G244R mutation, is located in the helix-loop-helix domain. The remaining mutations are at the amino- or carboxy terminal regions of MITF (Figure 1a, Paper I). The structure of MITF showing the exact location of the mutations associated with WS2A, TS and melanoma is shown in Figure 1b (Paper I). In order to generate MITF proteins carrying the respective mutations, all the MITF mutations were re-created in a mouse MITF-M expression construct, producing a melanocyte-specific MITF-M isoform. Comparison of human and mouse MITF proteins revealed a 94% identity and all the mutant sites are completely conserved (Supplementary Figure 1, Paper I).

4.1.2. DNA-binding properties of MITF mutations

4.1.2.1. Generation of MITF mutant proteins

The primers used to generate the MITF mutations are listed in Table 12. The vector used contains the mouse *Mitf* sequence which produces the melanocyte-specific M-MITF in the pcDNA3.1. vector. Site directed mutagenesis (Stratagene) allowed us to change the nucleotides to create the desired MITF mutations (further description in the Material and Methods section 3.3.)

4.1.2.2. Protein expression

As described in the Material and Methods section 3.8., the MITF mutant proteins were synthesized using the TNT *in vitro* translation system (Promega). The wild type and mutant MITF proteins were analyzed by Western blotting (Supplementary Figure 2A-D, Paper I). Since an *in vitro* translation system was used to create the MITF proteins, only one MITF band is visible (the second band of MITF indicating phosphorylation is missing). The strong single bands indicated that wild type MITF and the mutant MITF protein were expressed. The two MITF mutations resulting in a truncated MITF protein, R214X and R259X, showed different migration behavior in the electrophoresis due to the truncated proteins produced (Supplementary Figure 2B-C, Paper I). The intensities of the MITF mutant protein bands were determined and compared to wild type MITF so that equal amounts of proteins (wild type and mutants) were loaded on the gel used for the electrophoretic mobility shift assay (EMSA).

4.1.2.3. DNA-binding properties of WS2A and TS mutations

In order to investigate the DNA-binding behavior of MITF mutants, electrophoretic mobility shift assay (EMSA) with a double-stranded oligonucleotide containing a central E-box (CACGTG) was used. Figure 2A-C (Paper I) shows three EMSA gels; the first lane of each gel shows the wild type MITF able to bind the E-box, the second lane shows a supershift of the wild type MITF band, created by adding an MITF antibody (C5 Thermo; see material and methods). The last two lanes of each EMSA gel show empty vector (pcDNA3.1) and water that serve as negative controls; only a faint background band was visible. Interestingly, the EMSAs showed that 11 out of 18 WS2A and TS mutants including E313D, R214X, R216K, R217del, R217I, R217G, I224S, S250P, R259X, N278D and L283P failed to bind the E-box probe (Figure 2A-C, all WS2A and TS mutations are indicated in blue, Paper I). Interestingly the mutants R203K, K206Q, N210K, I212M, I212S, Y253C and S298P were able to bind the E-box probe. However, K206Q and Y253C showed reduced DNA-binding ability. The mutations which were able to bind to the E-box (R203K, K206Q, N210K, I212M, I212S and S298P), were also tested for their ability to bind the M-box sequence (CTCATGTG). The M-box probe consists of CT at the 5' end and has a core sequence of CATGTG (Supplementary Figure 3; indicated in blue; Paper I). The mutations R203K, K206Q, N210K, I212M, I212S, and S298P were all able to bind the M-box. However, K206Q and the two I212 mutations (either to M or S) showed less binding to the M-box than to the E-box.

4.1.2.4. DNA-binding properties of melanoma mutations

As summarized in Table 3, several MITF mutations have been found in melanoma patients. The MITF mutations associated with melanoma are indicated in red in Figure 1A (Paper I) and were also included in the DNA-binding assays. All MITF mutations found in melanoma (E87R, L135V, L142F, G244R, E318K and D380N) were able to bind DNA (the E-box) at the same level as wild type MITF (Figure 2A and C, indicated in red; Paper I). Additionally, all MITF mutations associated with melanoma were capable of binding the M-box probe (Supplementary Figure 3; melanoma mutations indicated in red).

4.1.3. Analysis of transcription activation potential

Luciferase reporter gene assays with several different MITF target promoters including TYR, TYRP1, DCT, 4M-box (a synthetic construct with 4 M-boxes in a row) and MET were performed to determine if the MITF mutant proteins are able to activate melanocyte specific promoters as well as the wild type MITF protein. The assays were carried out in HEK293T cells, which do not express MITF endogenously. The luciferase promoter constructs (vector pGL3, Promega) used in the co-transfection assays are described in the material and methods (section 3.4.). All the promoters tested (TYR, TYRP1, DCT, MET and 4M-box) contain MITF binding sites as described in Table 15 and Table 16. The tables compare the sequences of these sites between human and mouse. The underlined sequences emphasis the core sequence of the E- or M-box.

First we determined if the system worked. The MITF protein has been shown to activate TYR, TYRP1, DCT and 4M-box promoters (Paper I); (Bentley et al., 1994; Lowings et al., 1992; Murakami & Arnheiter, 2005). Supplementary Figure 4A (Paper I), shows that wild type MITF activated TYR promoter 90-fold and DCT promoter 60-fold, confirming previous results. Also activated by wild type MITF, but to a lower extent was TYRP1 which showed a 7-fold induction over empty vector, 4M-box which showed a 10-fold activation and MET which showed a 6-fold induction (Supplementary Figure 4B, Paper I).

Table 15. Potential mouse and human MITF binding sites located in the proximal promoters of the indicated genes

Gene	Origin	Location	bp*		Sequence		bp*	E- or M-box
TYR	mouse	5'upstream	-81	AAAA	**CATGTG**	ATAG	-86	E
	human	5' UTR	+412	AAGA	**CATGTG**	ATAA	+417	E
	mouse	5'upstream	-173	TAGT	**CATGTG**	CTTT	-168	M
	human	5' UTR	+320	CAGT	**CATGTG**	CTTT	+325	M
DCT	mouse	5'upstream	-150	GGGT	**CATGTG**	CTAA	-145	M
	human	5'upstream	-147	GGGT	**CATGTG**	CTAA	-142	M
	mouse	5'upstream	-232	GGGA	**CACATG**	AGCC	-227	E
	human	5'upstream	-228	GGAG	**CACATG**	AGCC	-223	E
	mouse	5' UTR	+244	TACA	**CATGTG**	CACA	+249	E
	human	5'upstream	-358	TGCA	**CACATG**	CACA	-353	E
	mouse	5' UTR	+242	TGTA	**CACATG**	TGCA	+247	E
	human	5' UTR	+232	TGTA	**CACATG**	TGCA	+237	E
	mouse	5' UTR	+252	TGCA	**CACGTG**	TAGG	+257	E
	human	5' UTR	+242	TGCA	**CACGTG**	TAAC	+247	E
	mouse	5'upstream	-1219	TGCA	**CACATG**	CACA	-1214	E
	human	5'UTR	+234	TACA	**CATGTG**	CACA	+239	E
TYRP1	mouse	5'upstream	-63	GAGT	**CATGTG**	CTGC	-58	M
	human	5'upstream	-194	GAAT	**CATGTG**	CTGA	-189	M
MET	mouse	5' UTR	+32	CAGA	**CACGTG**	CTGG	+37	E
	human	5'upstream	-193	CAGA	**CACGTG**	CTGG	-188	E

Table 16. Potential MITF binding sites located further upstream in the respective promoters

Gene	Promoter	Location	bp*		Sequence		bp*	E- or M-box
TYR	mouse	5'upstream	-1213	AAAT	**CATGTG**	AGAG	-1208	E
	human	5'upstream	-1549	GCCA	**CATGTG**	GTTA	-1544	E
	human	5'upstream	-1432	AGAT	**CATGTG**	ATGA	-1427	E
	human	5'upstream	-1867	ACAA	**CACGTG**	TAGG	-1862	E
	human	5'upstream	-1551	ATGC	**CACATG**	TGGT	-1546	E
DCT	mouse	5'upstream	-1286	CAAA	**CATGTG**	GGCA	-1281	E
	mouse	5'upstream	-1302	CCTG	**CACATG**	CATA	-1297	E
	mouse	5'UTR	+230	ATTG	**CATGTG**	CGTG	+234	E
	human	5'upstream	-1190	ATTG	**CACATG**	GTCT	-1185	E
TYRP1	mouse	5'upstream	-1815	AGAG	**CATGTG**	GCTA	-1810	E
	human	5'upstream	-61	AATC	**CACGTG**	CACT	-56	E
MET	mouse	5'UTR	+483	TTGG	**CATGTG**	ATCA	+488	E
	mouse	5'UTR	+183	GCCG	**CAGGTG**	ACCC	+188	E
	mouse	5'UTR	+244	GAGC	**CAGATG**	CTGG	+249	E
	mouse	5'UTR	+493	TTGG	**CATGTG**	ATCA	498	E
	mouse	5'upstream	-1123	ATAA	**CACGTG**	TGTG	-1118	E

4.1.3.1. Reduced transcription activation potential of WS2A and TS mutations

Consistent with the results of the DNA-binding assays, the E213D, R214X, R216K, R217del, R217I, R217G, I224S, S250P, R259X, N278D and L283P mutant MITF proteins failed to activate expression from the TYR, DCT, TYRP1 and 4M-box promoter constructs (Figure 3A, Paper I). The R203K, N210K and S298P mutant protein activated the TYR promoter at a higher level than the wild type MITF protein (Figure 3A, Paper I). The K203Q and S298P mutations showed similar transcriptional activity as wild type MITF. Two mutations which showed reduced DNA-binding, K206Q and Y253C, also showed reduced activation potential (Figure 3A, Paper I). Interestingly, the I212M and I212S mutations, failed to activate the tyrosinase promoter construct but showed DNA-binding ability. However, they were able to activate the 4M-box construct at levels similar to wild type MITF but their activation potential on TYRP1 and DCT was reduced (Figure 3A, Paper I).

The MET oncogene promoter construct was also included in our study, and surprisingly, the I212M and E213D mutations were able to hyperactivate from this promoter (Figure 3B, Paper I). The I212S and S298P mutations activated this promoter at levels similar to wild type MITF. The remaining mutations completely failed to activate from the MET promoter (Figure 3B, Paper I).

4.1.3.2. Transcription activation potential of melanoma mutants

In general, most mutations associated with melanoma had similar transcription activation potential as wild type MITF (Figure 3C, Paper I). As shown in Figure 3C (Paper I) all the melanoma mutations were able to activate the tyrosinase promoter construct. The E87R, L135V, L142Q mutations were able to activate the MET promoter but showed slightly reduced transcription activation potential of TYRP1, DCT and 4M-box promoters. The G244R mutation, located in the helix-loop-helix domain of MITF, showed reduced transcription activation potential from the tyrosinase, TYRP1 and MET promoters (Figure 3C, Paper I). The E318K and D380N mutations showed slightly increased transcription activation potential from the tyrosinase promoter construct but also from the 4M-box and MET promoters and only slightly reduced transcription activation potential from the TYRP1 and DCT promoters (Figure 3C, Paper I).

4.1.3.3. Limited effects of MITF on p16 and Hif1α activation

As described in section 1.2.1. *Hif1α* and *p16* have been identified as MITF target genes (Busca et al., 2005; Loercher et al., 2005). Further, it has been shown that MITF is able to bind the p16 promoter and activate p16 expression (Loercher et al., 2005). Similarly, Busca and colleagues showed that Hif1α is transcriptionally activated by MITF and that MITF is able to bind the Hif1α promoter (Busca et al., 2005). We obtained reporter constructs containing p16 (Loercher et al., 2005) and Hif1α promoters (Busca et al., 2005) and tested in co-transfection assays if wild type and mutant MITF proteins were able to activate these constructs. MITF was not able to activate expression from either promoter construct (see Figure 1 and Figure 2). Co-transfection assays of the mutations associated with WS2A and TS and p16 promoter constructs are shown in Figure 1A and melanoma mutations in Figure 1B.

The wild type MITF protein was able to activate Hif1α expression 1.6-fold compared to empty vector (Figure 2). However, the MITF mutants behaved similarly to wild type MITF (Figure 2A (WS2A and TS mutations) and Figure 2B (melanoma mutations)).

As we failed to observe any activation from the p16 promoter with the wild type MITF, we cannot conclude anything about effects of mutants on this promoter. And as we observed only minor effects of MITF on the Hif1α promoter (less than previously reported, (Busca et al., 2005)) we cannot conclude much from this either.

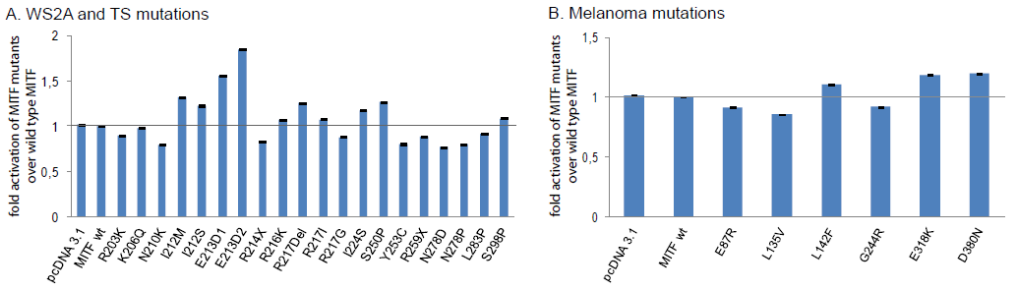

Figure 1. Co-transfection assay of mutant and wild type MITF with the p16 reporter

HEK293T cells transfected with wild type MITF showed no activation from the p16 promoter construct compared to empty vector transfected cells. Error bars show the standard error of mean.
A. WS2A and TS mutations behave similarly to wild type MITF on the p16 reporter.
B. Melanoma mutations behave similarly to wild type MITF on the p16 reporter.

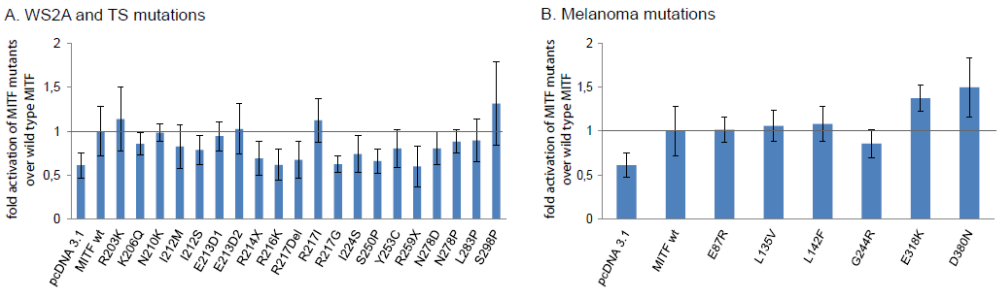

Figure 2. Co-transfection assay of mutant and wild type MITF with the Hif1α promoter

HEK293T cells transfected with wild type MITF showed an induction (1.6-fold) of the Hif1α promoter construct compared to empty vector transfected cells. Error bars show the standard error of mean.
A. WS2A and TS mutations behave similar to wild type MITF on the Hif1α promoter.
B. Melanoma mutations behave similar to wild type MITF on the Hif1α promoter.

4.1.4. Clonogenicity

4.1.4.1. Clonogenicity of melanoma mutations

In order to investigate if MITF mutations associated with melanoma have increased clonogenic potential, stable cell lines were created expressing the melanoma mutations. HEK293 cells were transfected with the melanoma mutations (E87R, L135F, L142Q, G244R, E318K and D380N) and selected with the antibiotic geneticin to create stable cell lines expressing the respective mutations. The stable cell lines were seeded at low density levels, in order to observe the potential of a single cell to form colonies. After one week, when the cells had formed visible but separate colonies, the colonies were stained with Crystal Violet and the colonies counted. Supplementary Figure 5 (Paper I) shows MITF expression in the cell lines. We were unable to generate stable cell lines carrying the L135V and E318K mutations. Even though these mutants were selected, using an antibiotic and although they grew nicely in cell culture, these cells did not express the mutant proteins. At present we do not know why they failed to express MITF. However, all the remaining mutations, E87R, L142F, G244R and D380N expressed MITF protein, as shown by Western blotting (Supplementary Figure 5, Paper I). Figure 4 (Paper I) shows that the E87R and L142F proteins were able to form more colonies than wild type MITF or untransfected HEK293 cells, or empty vector transfected

cells. This difference was statistically significant $p<0.05$. These results are indicative that the N-terminus of MITF might be important for cell proliferation. The G244R and D380N mutations showed no difference compared to wild type MITF with regards to clonogenic behavior (Figure 4, Paper I).

4.1.4.2. Clonogenicity of mutations associated with WS2 and TS

To test the potential of several WS2A and TS mutations in MITF to form colonies, HEK293 cells were transfected with the N210K, I212M, E213D, R217del, Y253C, R259X, L283P and S298P WS2A and TS mutations and selected with geneticin. These WS2A and TS mutants were selected because they affect the various regions of MITF. Expression of MITF protein was determined using Western blotting is shown in Figure 3A. The N210K, I212M, Y253C, L283P, E213D and R217del mutations showed significantly reduced colony formation ability compared to wild type MITF ($p<0.05$). The slight difference between untransfected cells, empty vector and MITF transfected cells is not statistically significant. In summary, these results indicate that MITF mutations associated with WS2A and TS (N210K, I212M, Y253C, L283P, E213D and R217del) show a decrease in proliferations as seen by the lower number of colonies formed. This was rather unexpected as some of these mutations are known to severely affect DNA-binding ability of MITF. For example R217del cannot bind DNA at all. This might suggest a dominant-negative action.

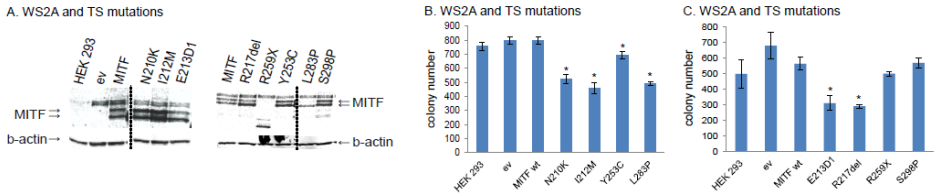

Figure 3. Clonogenic assay of WS2A and TS mutations.

A. Western blot of stable cell lines (HEK293) expressing wild type and mutant MITF proteins.
B. and C. Clonogenicity of selected WS2A and TS mutations, HEK293 cells and MITF wild type transfected cells and empty vector transfected cells. Error bars show the standard error of mean and significance was calculated via the Student's t-test. P-values < 0.05 were considered statistically significant.

4.1.5. Testing for haploinsufficiency

WS2A and TS are autosomal dominantly inherited syndromes (Tietz, 1963; Waardenburg, 1951). The reason for the presence of a WS2A phenotype in heterozygotes is not known but may be explained by a dominant-negative effect of mutated MITF proteins or haploinsufficiency. In order to determine if dominant negative action was responsible, we used cotransfection assays. HEK293T cells were transfected with 50% wild type MITF and 50% mutant MITF DNA together with the TYR promoter. The idea was that dominant negative proteins would interfere with activity of the wild type proteins. Figure 4A shows the results for our analysis of the WS2A and TS mutants, cotransfected with wild type MITF. Interestingly, the R217del mutation failed to show dominant negative activity in our assay. The R203K, K206Q, N210K, E213D, R216K, R217I, R217G, S250P, Y253C, R259X, N278D, N278P and S298P mutants did not show dominant negative behavior. The mutations I212M, I212S, R214 and I224S showed reduced transcriptional activation potential, however, they were still able to activate the TYR promoter by more than 50% compared to wild type MITF. Hence, there results do not indicate that these mutations act in a dominant negative way (Figure 4A). We also included the MITF mutations associated with melanoma and again, no indication of a dominant-negative effect was observed. The assay we used may not be sensitive enough for determining dominant negative action. One reason may be that it is difficult to regulate expression levels transfecting each construct separately. Further it is not possible to control formation of dimers.

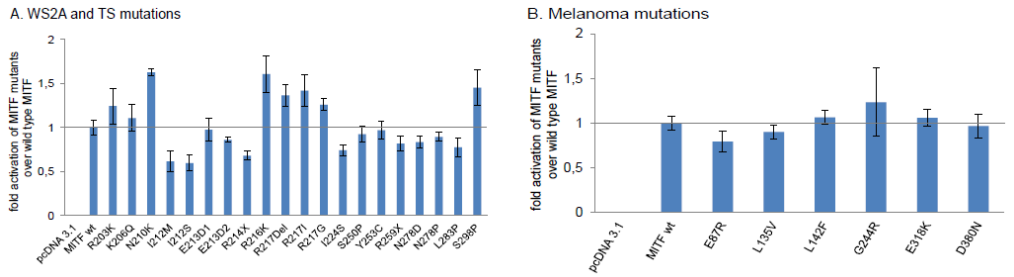

Figure 4. Combination of wild type and mutant MITF in a cotransfection assay indicates haploinsufficiency

A. HEK293T cells were transfected with 7.5ng wild type MITF and 7.5ng mutant MITF (WS2A and TS mutants) DNA and cotransfected with a tyrosinase promoter construct. B. Melanoma mutations cotransfected with wild type MITF (7.5ng and 7.5ng respectively) and the tyrosinase promoter construct.

4.2. The MITF and IRF4 proteins cooperate in inducing tyrosinase expression (Paper II)

4.2.1. MITF and IRF4 cooperate to regulate tyrosinase expression

In order to determine how IRF4 might play a role in pigmentation, promoters of key enzymes in melanogenesis were investigated for potential IRF4 binding sites. A typical ISRE motif (interferon-specific response element) follows the consensus of 5'-GAAANT/C-3' and is present as a monomer or as multimers in the promoters or enhancers of genes (reviewed in Marecki & Fenton, 2002). Only the TYR promoter revealed potential IRF4 binding sites, but not TYRP1 or DCT (Figure 6A shows IRF4 binding sites in the TYR promoter, Paper II). To test if IRF4 can activate tyrosinase expression, HEK293T cells were transfected with MITF or IRF4. The cells were also co-transfected with MITF and IRF4 together where MITF levels were kept constant and IRF4 added in increasing amounts. Figure 5 shows that MITF alone activates TYR about 100-fold as compared to empty vector transfected cells (pCMV). However, IRF4 on its own fails to activate TYR expression. Interestingly, together MITF (15ng) and IRF4 are able to activate TYR cooperatively (134-fold and 146-fold compared to empty vector transfected cells) (see also Figure 6c Paper II). When the first E-box of the TYR promoter was mutated, this leads to reduced ability of MITF to activate TYR expression by 50% and abolishes the synergistic effect of MITF and IRF4 on regulating tyrosinase expression. This strongly indicates that MITF and IRF4 cooperate in activating TYR expression.

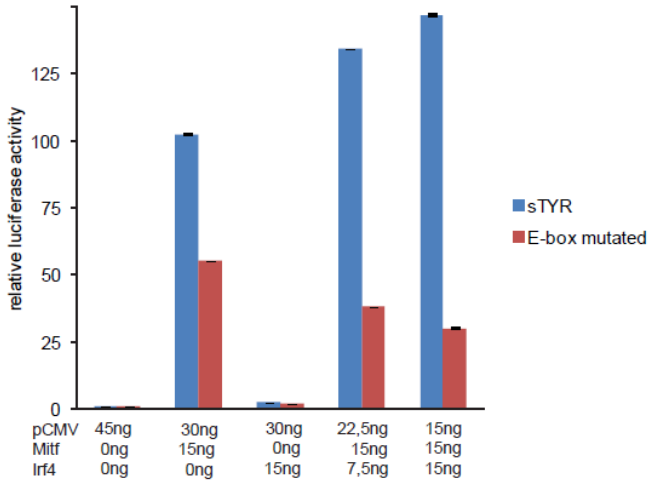

Figure 5. MITF and IRF4 cooperate in regulating tyrosinase expression.

As shown in Figure 6, MITF is able to activate 4M-box, DCT and MET expression. However, no cooperative effects were observed between MITF and IRF4 on these promoter constructs. The same applies for the promoter constructs Hif1α, p16, p21 and TYRP1 (Figure 7). Thus, the cooperative effects are promoter specific.

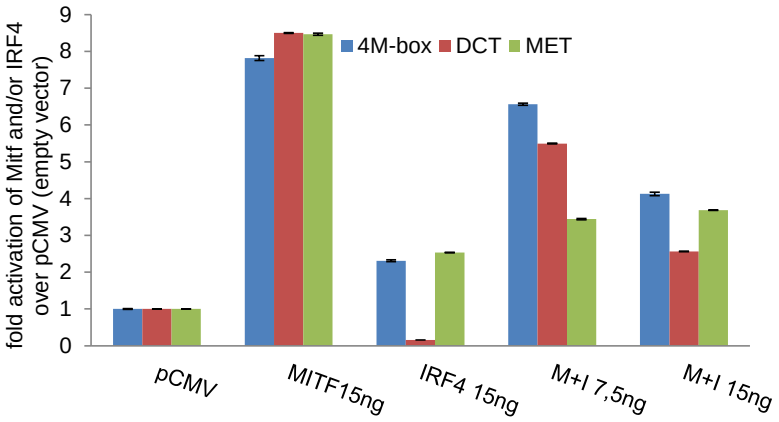

Figure 6. No cooperative effects of MITF & IRF4 on 4M-box, DCT or MET activation.

HEK293T cells were transfected with MITF or IRF4 or MITF and IRF4 together. Blue bars indicate co-transfection assay with the 4M-box reporter construct, red indicates the DCT promoter and green the MET promoter construct.

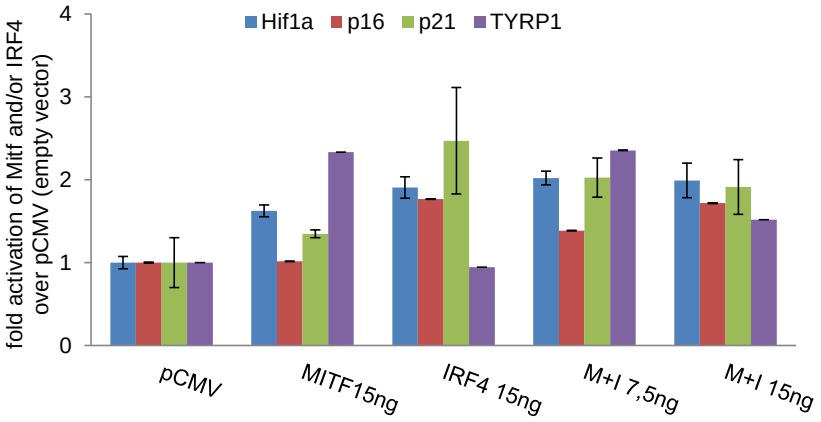

Figure 7. No cooperative effects of MITF & IRF4 on Hif1α, p16, p21 or TYRP1 activation.

HEK293T cells were transfected with MITF or IRF4 or MITF and IRF4 together. Blue bars indicate co-transfection assay with the HIF1α reporter construct, red indicates the p16 -, green the 21 - and purple the TYRP1 promoter.

To further investigate the specificity of the cooperation between MITF and IRF4 on tyrosinase expression, we tested the effects of the MITF white mutation. The *Mitf*$^{Mi\text{-}Wh}$ mutant is caused by an isoleucine to asparagine substitution at residue 212 within MITF and results in a severe heterozygous phenotype (reviewed in Steingrimsson et al., 2004). Mice which are heterozygous for *Mitf*$^{Mi\text{-}Wh}$ have a diluted coat color (light-grey), spots on feet, tail and belly and inner ear defects. Homozygotes exhibit white coat color, small eyes, inner ear defects and reduced fertility (reviewed in Steingrimsson et al., 2004).

Figure 8 shows the cotransfection assay of the + and – isoforms of wild type MITF and the *Mitf*$^{Mi\text{-}Wh}$ mutant together with IRF4 on TYR expression. Although there is no difference between the + and – isoforms, the *Mitf*$^{Mi\text{-}Wh}$ mutation showed significantly reduced transcriptional potential on the TYR promoter compared to wild type MITF. Even though there was some cooperative effect of *Mitf*$^{Mi\text{-}Wh}$ and IRF4 at the highest concentration, this effect was less compared wild type MITF (25-fold and 12-fold, respectively).

Our results indicate that the cooperative effects are specific for MITF and IRF4.

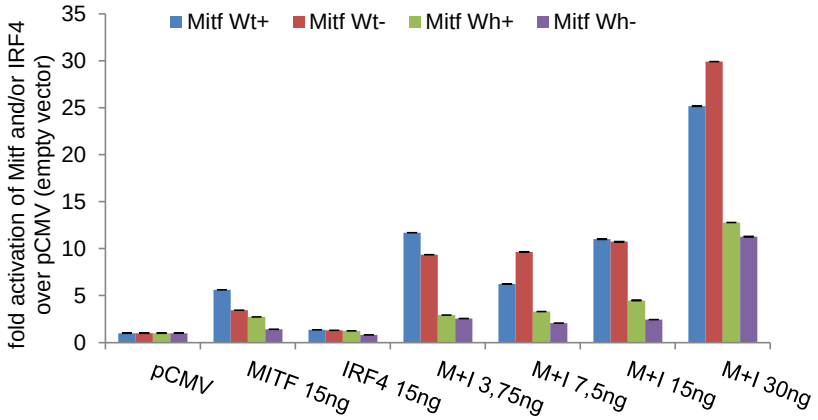

Figure 8. Cotransfection assay of wild type MITF and the MITF$^{Mi\text{-}Wh}$ mutation with IRF4 on TYR expression.

In order to investigate if the observed cooperative effects of MITF and IRF4 are specific for the tyrosinase promoter, the IRF4 binding sites within the tyrosinase promoter were mutated. Figure 6A (Paper II) shows potential IRF4 binding sites within the tyrosinase promoter. Figure 9 shows results of cotransfecting MITF and IRF4 together with constructs where the various potential binding sites in the tyrosinase promoter were mutated. Mutating BS1 did not

influence the cooperative effects of MITF and IRF4. However, destroying BS2 and BS3 eradicates the observed cooperative effects of MITF and IRF4. Additionally, double or triple mutations of these IRF4 binding sites abolished the effects of MITF and IRF4 on transcription activation (Figure 9).

These results indicate that the cooperative effects of MITF and IRF4 on the tyrosinase promoter are mediated through these IRF4 binding sites. As seen in the various cotransfection assays, IRF4 alone has no effect on transcriptional activation of the tyrosinase promoter (Figure 9).

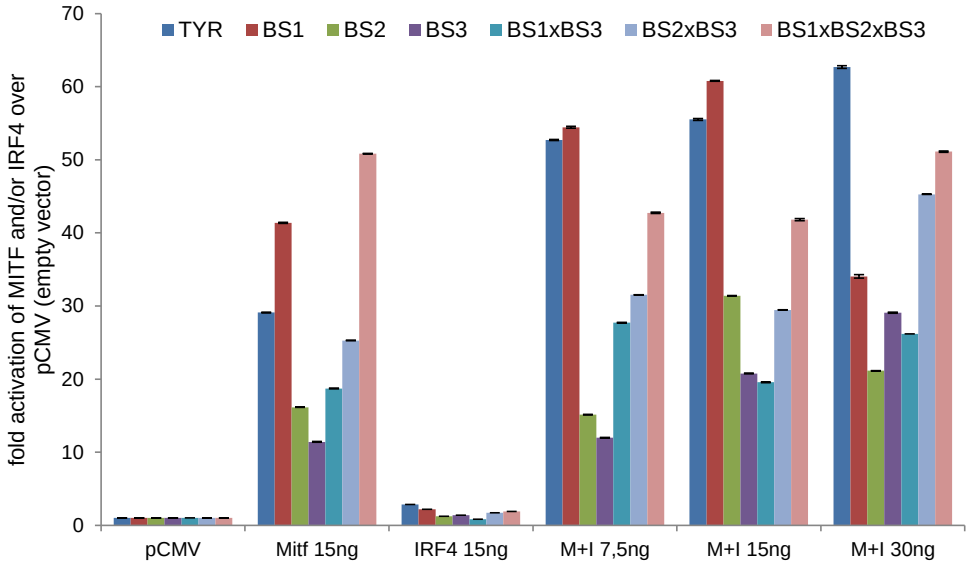

Figure 9. Mutating IRF4 binding sites in the tyrosinase promoter abolishes the cooperative effects of MITF and IRF4

4.2.2. MITF and IRF4 do not interact directly

To investigate if MITF and IRF4 physically interact to mediate the cooperative effects, HEK293T cells were transfected with (1) empty vector (pcDNA3.1), (2) 6xcmyc tagged-MITF, (3) HA tagged-IRF4 and (4) 6xcmyc tagged-MITF and HA tagged-IRF4 together (materials and methods 3.7). Co-immunoprecipitations were performed with anti-HA and anti-myc antibodies. Unfortunately it was not possible to co-immunoprecipitate MITF and IRF4 (data not shown), which indicates that MITF and IRF4 do not interact directly.

4.2.3. The role of IRF4 in melanoma

IRF4 has been shown to be expressed in melanocytes and melanoma (Sundram et al., 2003). However, functional studies to investigate the role of IRF4 in melanocytes and melanoma are rare. We decided to investigate the expression of IRF4 in melanoma cell lines and try to characterize the role of IRF4 in melanoma cells.

4.2.3.1. Expression profile of melanoma cell lines

To address the question if IRF4, but also MITF and TYR, are expressed endogenously in melanoma, qPCR was used to determine their expression in several melanoma cell lines. The melanoma cell lines included were 501mel, SKMel 28, B16 and MeWo and the melanocyte cell line MelanA. Two multiple myeloma cell lines were also tested for endogenous IRF4 expression, since they were expected to express IRF4 at high levels. We also analyzed the HEK293T cell line. RNA was extracted from all cell lines (as described in the material and methods section 3.5.), RNA concentration measured and cDNA generated using 1μg RNA from each cell line. To test for endogenous IRF4, MITF and TYR expression, the primers listed in Table 14 (material and methods section 3.5.) were used. The qPCR was performed at least twice, in duplicates each time; β-actin was used as an internal control. The ΔCt values obtained were calculated by subtracting the average Ct value of β-actin from the average of the sample Ct values. Note that lower ΔCt values are associated with higher expression than high ΔCt values. Table 17 shows endogenous IRF4 expression as ΔCt values. As indicated by the low ΔCt values of SKMel28, 501mel, MeWo and MelanA (a mouse melanocyte cell line) cell lines, these cell lines show IRF4 expression. Interestingly the mouse melanoma cell line B16, the human embryonic kidney cells HEK293T and the multiple myeloma cell line RPMI 8226 do not express IRF4 at high levels. In contrast the multiple myeloma cell line U266 showed high IRF4 expression. The exact ΔCt values (and the ΔCt StDev) are listed in the table below (Table 17). All human melanoma cell lines tested, SKmel28, 501mel and MeWo and the mouse melanocyte and melanoma cell lines express MITF (see Table 17). The HEK293T and the two multiple myeloma cell lines do not express MITF at significant levels. TYR expression was also tested in all these cell lines. High TYR expression was detected in all human and mouse melanoma cell lines including the mouse melanocyte cell line MelanA as shown in Table 17. Endogenous TYR expression was undetectable in the HEK293T cells and the two multiple myeloma cell lines RPMI 8226 and U266. Undetectable means that the

endogenous expression levels of the indicated genes in these cell lines was too low to be detected by this method (Table 17).

Table 17. Endogenous expression of IRF4, MITF and TYR in melanoma cell lines

	IRF4		MITF		TYR	
	ΔCt	ΔCt StDev	ΔCt	ΔCt StDev	ΔCt	ΔCt StDev
SKMel 28	5.25	0.08	3.82	0.06	4.89	0.18
501mel	6.78	0.20	3.06	0.36	2.95	0.36
MeWo	8.48	0.08	4.04	0.17	3.68	0.20
HEK293T	13.99	0.06	9.50	0.07	undetectable	undetectable
RPMI 8226	17.32	0.21	8.69	0.16	undetectable	undetectable
U266	2.67	0.22	12.60	0.12	undetectable	undetectable
MelanA	10.06	0.47	2.97	0.30	1.61	0.46
B16	13.16	0.10	2.41	0.08	4.48	0.16

The ΔCt values obtained were calculated by subtracting the average Ct value of β-actin from the average of the sample Ct values. Note that lower ΔCt values are associated with higher expression than high ΔCt values.

4.2.3.2. Clonogenicity

In order to test for clonogenicity, HEK293 and 501mel cells were transfected with (1) empty vector (pcDNA 3.1), (2) MITF, (3) HA-tagged IRF4 and (4) MITF and HA-tagged IRF4 together. Figure 10 shows results of the clonogenic assay in HEK293 cells. As described in materials and methods, the cells were selected with antibiotic, reseeded in 6-well plates at low cell density. After one week of growth, single cell colonies were visible and distinguishable from each other. The colonies were stained with crystal violet and counted with the Clonocounter program. MITF showed slightly more colony formation potential than empty vector. Interestingly, IRF4 showed significantly more colonies than empty vector (p-value $<2{,}9*10^{-6}$). Also MITF and IRF4 together showed significantly more colonies than empty vector (p-value $<4{,}0*10^{-6}$).

Surprisingly, in 501mel cells, the advantage to form more colonies for IRF4 and MITF together with IRF4 was not observed Figure 10 (right side). One reason could be that 501mel cells express MITF and IRF4 endogenously, whereas the HEK293 do not.

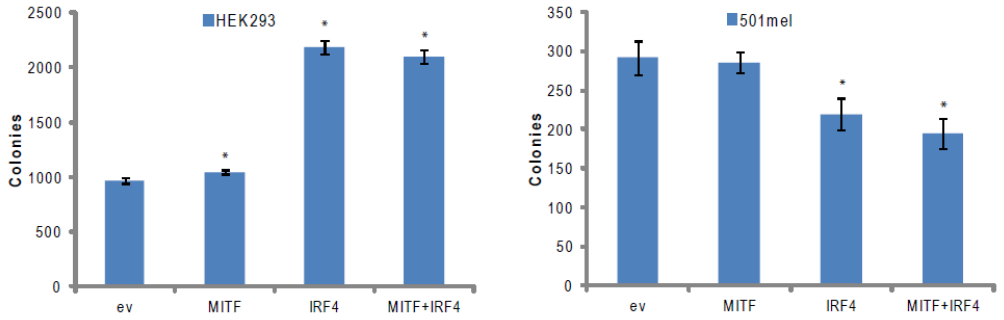

Figure 10. Clonogenic assays of HEK293 and 501mel cells

Cell lines HEK293 (left) and 501mel cells (right) stably expressing MITF, IRF4 or MITF and IRF4 were seeded in low density. After one week formed colonies were counted. Asterisks indicate statistical significance (Students t-test; p-value <0.05).

In an anchorage independent soft agar assay, HEK293 cells were not able to form any colonies (data not shown). 501mel cells did grow in soft agar, however, there was no difference in colony formation when cells were transfected with constructs expressing MITF, IRF4 or both together (Figure 11). Three different cell densities were tested, 1000 cells per well, 2000 cells per well and 4000 cells per well. No statistical difference was observed between cells transfected with MITF, IRF4 or MITF and IRF4 in any of the cell densities seeded (Figure 11). More colonies were formed as more cells were seeded, but transfecting MITF, IRF4 or MITF and IRF4 had no effect (Figure 11).

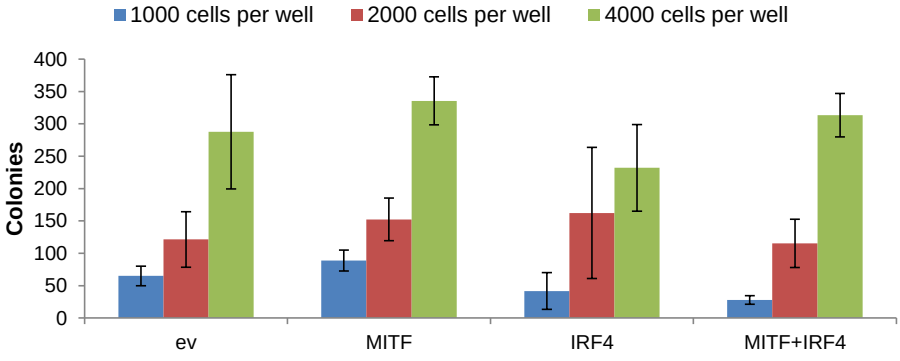

Figure 11. Soft agar assay of 501mel cells.

5. Discussion

The transcription factor MITF, is a master regulator of pigment cells and has been extensively studied over the last two decades (see the following reviews Bell & Levy, 2011; Cheli et al., 2009; Goding, 2007; Steingrimsson et al., 2004; Tsao et al., 2012). Several point mutations in MITF have been identified in melanoma patients and in patients with WS2 and TS (see Table 3 and 6) (Cronin et al., 2009; reviewed in Pingault et al., 2010; reviewed in Tsao et al., 2012). Even though it is well known that MITF mutations are associated with these pathologies, functional studies are rare.

This thesis focused on the analysis of 24 MITF mutations of which 18 are associated with WS2 and TS and 6 with melanoma (see Table 3 and 6 or Table 1 Paper I). Studying the location of these mutations within the MITF protein, it is obvious that mutations associated with WS2 and TS are mainly in the basic region and helix-loop-helix zipper domain whereas melanoma mutations are primarily at the N- and C-terminus of MITF (Figure 1 Paper I). Table 1 (Paper I) summarizes all MITF mutations associated with WS2, TS and melanoma. Clearly there are more studies on WS2 (and TS) patients than on melanoma. More studies investigating MITF mutations in melanoma patients will show, if MITF mutations are common in melanoma patients and where they are located. So far, the G244R mutation is the only melanoma mutation identified, which is located in the helix-loop-helix domain of MITF.

The results of DNA-binding studies and transcriptional activation assays of the 26 MITF mutations are summarized in Table 2 (Paper I). Of the 18 WS2 and TS mutations, 11 failed to bind DNA (E-box) (Figure 2 Paper I). The E213D, R214X, R216K, R217del, R217I, R217G, I224S, S250P, R259X, N278D and L283P mutations did not show DNA binding. Of these, E213D, R214X, R216K, R217del, R217I and R217G affect the basic region of MITF. Therefore it is not surprising that these mutations fail to bind DNA. Interestingly, mutations affecting the HLH-zip domain of MITF such as S250P, R259X, N278D and L283P also failed to bind DNA, suggesting that these domains also contribute to the DNA-binding ability of MITF. Pogenberg and colleagues (2012) showed that the amino acid N278 is important for the formation of hydrogen bonds in one of the heptad repeats of the leucine zipper, ultimately implicating this residue in the connection of the two MITF protomers (Pogenberg et al., 2012). The S250P, N278P and L283P mutations substitute an amino acid for proline, which cannot be incorporated in an α-helix, thus leading to folding disruption of the MITF protein. This in turn, is likely to impair dimerization of MITF and thus DNA-binding. Supporting the

findings of the DNA-binding assays, these mutations failed to activate melanocyte-specific promoters such as TYR, TYRP1, DCT, 4M-box and MET (Figure 3A-B Paper I). The fact that S250P, N278P and L283P cannot bind DNA and are unlikely to dimerize, supports haploinsufficiency as reason for the phenotype.

However, one third of the WS2 and TS mutations were able to bind DNA. The R203K, K206Q, N210K, I212M, I212S, Y253C and S298P mutations showed either reduced or near normal DNA-binding abilities (Figure 2 Paper I). Also, these mutations showed transcription activation potential similar to wild type MITF from the investigated melanocyte specific reporter constructs (Figure 3 Paper I). Investigating the family history of the patient who harbored the R203K mutation showed, that the disease does not co-segregate with the mutation. Thus, the mutation is most likely non-pathological (Tassabehji et al., 1995). Also the N210K mutation showed similar behavior regarding DNA-binding and transcriptional potential as wild type MITF (Figure 2 and 3 Paper I). Originally, this mutation was described in a family diagnosed with Tietz syndrome. Affected family members were born 'snow-white', had blue eye color and congenital hearing loss, however they did gain some pigmentation over time (Smith et al., 2000). Recently, the N210S mutation it has been identified in macchiato Franches-Montagnes horses (Hauswirth et al., 2012). Alignment of human and horse MITF showed that MITF is 97.9% conserved including position 210 (Supplementary Figure 8 paper I). Interestingly, DNA-binding studies showed the N210S had reduced DNA-binding ability (Hauswirth et al., 2012). Hence, we conclude that the N210S mutation has a more severe impact on protein function *in vitro* than the N210K mutation.

The I212M and I212S mutations, showed normal DNA-biding ability on the E-box but reduced ability to bind the M-Box (Figure 2 and Supplemenatry Figure 3, Paper I). These results are consistent with Pogenberg and colleagues (2012), who showed that the I212 position is important for MITF's ability to bind the M-box (Pogenberg et al., 2012). The transcription activation potential of I212M and I212S was reduced from the TYR, TYRP1 and DCT promoter constructs but was similar to wild type MITF when the 4M-box promoter was used. Surprisingly the I212M mutation showed hyperactivation from the MET promoter (Figure 3A-B Paper I). Clearly these results show an imbalance in transcription activation potential of different promoters, which might contribute to WS2A and TS.

Although the E213D mutation was not able to bind DNA and failed to activate TYR, TYRP1, DCT and 4M-box, it showed hyperactivation of the MET promoter (Figure 2B and Figure 3A-

B paper I). So it might be possible that E213D is able to activate MET by a different mechanism than by directly binding DNA. This interesting result requires further work to shed some light in how E213D is able to activate MET, without being able to bind DNA.

One of the most contradictory results was observed with the S298P mutation. It behaved similar to wild type MITF with respect to DNA-binding ability and transcription activation potential (Figure 2 Paper I and Figure 3 Paper I). Interestingly, this mutation is the only WS2 mutation located at the C-terminus of the MITF protein. Takeda and colleagues (2000) showed that a truncated MITF protein consisting of residues 1-293 is not able to transactivate the tyrosinase promoter and failed to bind the E-box sequence CATGTG (Takeda et al., 2000a). When they generated the point mutations S298A and S298P this resulted in severely reduced activation of the tyrosinase promoter whereas the S302A, T303A and S307A mutations showed similar transcription activation potential as wild type MITF (Takeda et al., 2000a). The DNA-binding ability of these mutants showed that S298A and S298P did not bind the E-Box. Interestingly the S302A, T303A and S307A mutations showed near normal DNA-binding ability. It has been suggested that the amino acid S298 of MITF is a substrate for glycogen synthase kinase 3 β (GSK3β), which phosphorylates MITF leading to increased transcription activation potential (Takeda et al., 2000a). Even though the location near S298 resembles the consensus substrate sequence S/T-X-X-X-S/T of GSK3β, it does not fulfill all the criteria to be a substrate for GSK3β (Frame & Cohen, 2001). According to Frame and Cohen (2001) seven criteria need to be established for a protein to be a physiological substrate for GSK3β (Frame & Cohen, 2001). Interestingly, MITF fulfills only one out of these seven criteria, which is that phosphorylation should be abolished by mutagenesis (Frame & Cohen, 2001; Takeda et al., 2000a). Further, the S298 residue has not been formally identified as a site for phosphorylation by GSK3β. Interestingly, the S302A mutation did not affect phosphorylation, even though it is within the potential consensus site for GSK3β. Therefore further studies are needed to investigate if MITF is a true substrate for GSK3β (Frame & Cohen, 2001). The S298P mutation is listed in the Exome Variant Server Database and shows that a C/T polymorphism (rs10493747) is prevalent in European Americans and has a minor allele frequency of 0.046%. Surprisingly, this particular polymorphism was not found in African Americans (Exome Variant Server, July 2013 accessed). The prevalence of all Waardenburg syndromes is 1/42,000 (Read & Newton, 1997). These findings suggest that the SNP (rs10493747) has a higher frequency than all the Waardenburg syndromes combined. Further, the higher prevalence of the SNP and the results shown in Figure 2 and 3 of Paper I

might suggest that the S298P is a rare polymorphism in Caucasians rather than a mutation causing Waardenburg syndrome type 2A.

All the human MITF mutations associated with melanoma (listed in Table 3 and Table 1 of Paper I) were able to bind DNA (E-box and M-box) (Figure 2A and 2C Paper I). Furthermore transcriptional activation assays showed that the MITF mutations associated with melanoma were all transcriptionally active (Figure 3C Paper I). Cronin and colleagues, who originally identified the mutations E87R, 135V, L142F, G244R and D380N mutations also showed that these mutations are transcriptionally active as assayed on the TYR and DCT promoters (Cronin et al., 2009), which is consistent with the results shown in Figure 2 and 3C (paper I). The germline mutation E318K has been shown to be more transcriptionally active than wild-type MITF from the HIF1α and 3M-box (a synthetic construct with 3 M-boxes in a row) promoters. Consistent with our results, the mutant behaved like wild type in activating the MET promoter (Bertolotto et al., 2011 and Figure 3C of Paper I). However, the results for the HIF1α promoter are different. As shown in Figure 2, wild type MITF was able to activate the HIF1α reporter only 2-fold compared to empty vector. One explanation for the unexpectedly little activation of the HIF1α promoter might be that only 15ng of MITF was used for this assay. Bertolotto and colleagues used 100ng of wild type and mutant MITF for their assays (personal communication). However, it makes the interpretation of the results regarding the MITF mutants more difficult. Yokoyama and colleagues showed in UACC62 human melanoma cells, that wild type MITF and the mutant version E318K activated the expression of TRPM1 in a dose-dependent fashion (Yokoyama et al., 2011). The E318K mutant was able to activate TRPM1 promoter better than wild type MITF. In another melanoma cell line, HT144, it was shown that the E318K mutant was able to activate the DCT and MLANA promoters better than wild type MITF. This was not seen in the melanoma cell line C32 (Yokoyama et al., 2011). Figure 1C (Paper I) shows that the increased DCT expression induced by E318K in melanoma cells was not observed in HEK293T cells. In summary, the E318K mutation impairs sumoylation of MITF but shows increased transcriptional activity from some but not all melanocyte specific promoters (Bertolotto et al., 2011; Yokoyama et al., 2011).

MITF, the master regulator of melanocytes has a central role in regulating expression of target genes, which play a role in pigmentation. Hoek and colleagues conducted a study to identify novel MITF target genes and successfully showed that *IRF4* was activated by MITF (Hoek et

al., 2008). Genome-wide association studies (GWAS) focusing on identifying new genes associated with pigmentation and/or melanomas have become increasingly popular over the last decade. GWAS studies have shown that IRF4 is associated with pigmentation traits such as freckles, hair color and eye color (Han et al., 2008; Sulem et al., 2007). Our hypothesis was that MITF is involved in regulating IRF4 expression and, in turn, MITF and IRF4 together regulate expression of pigment genes. Paper II explores the role of MITF and IRF4 in pigmentation and shows that a transcription factor network involving MITF, IRF4 and TFAP2α is able to regulate pigmentation. Figure 5 shows that MITF and IRF4 together cooperate to activate the tyrosinase promoter. This activation was eradicated if the E-box within MITF was destroyed. As expected, the wild type MITF protein was able to activate tyrosinase expression (Figure 5) (Bentley et al., 1994). Interestingly, IRF4 alone has no ability to activate the tyrosinase promoter (Figure 5). MITF and IRF4 together showed cooperative effects on the tyrosinase promoter. Tyrosinase was the only promoter on which cooperation of MITF and IRF4 was observed. Wild type MITF was able to activate the 4M-box, DCT and MET reporter but no cooperation was observed with IRF4 (Figure 6). Additionally, Hif1α, p16, p21 and TYRP1 were also tested, but again MITF and IRF4 did not cooperate to activate these melanocyte-specific promoters. Figure 7 shows that MITF alone was able to activate TYRP1 expression, which has also been shown by Yasumoto and colleagues (Yasumoto et al., 1997). That MITF on its own does not activate the p21 promoter is also well documented, thus it was not surprising that we did not observe an activation of MITF on the p21 promoter (Carreira et al., 2005). MITF is able to interact with retinoblastoma 1 (RB1) and to cooperate on the p21 promoter (Carreira et al., 2005). Interestingly, MITF alone was not able to activate p21 in the C33A cervix cell line. This cell line derived from a retinoblastoma patient, hence negative for endogenous RB1. Cotransfection of MITF and RB1 activated p21 expression (Carreira et al., 2005). Figure 7 shows that MITF alone was not able to activate p21 expression. As for the Hif1α promoter no activation by MITF was observed (Figure 7). Surprisingly, Loercher and colleagues observed an up to 60-fold activation of the p16 promoter by MITF (Loercher et al., 2005). Figure 7 shows that we could not observe this positive effect of MITF on p16 promoter activation.

Multiple mutations within MITF have been identified in the mouse (Steingrimsson et al., 2004). Among these mutations is the Mitf white mutation, $Mitf^{Mi\text{-}Wh}$. This mutation is a single amino acid substitution at location I212 and substitutes isoleucine for an asparagine and causes a severe phenotype in homozygous animals. Heterozygotes have gray coat color and

white belly spot. In fact, this is the most severe heterozygous phenotype observed in any of the known mouse Mitf mutations (Steingrimsson et al., 2004). The I212N mutant protein has been shown to bind better to the E-box than to the M-box (Pogenberg et al., 2012). Transcription activation assays showed that the I212N mutant did not efficiently activate tyrosinase expression (Pogenberg et al., 2012). Very similar characteristics regarding DNA-binding ability and transcription activation potential have been observed with the I212M and I212S mutations (Figure 2C Paper I, Figure 3A Paper I and Supplementary Figure 3 Paper I). In order to test if the cooperative effects of MITF and IRF4 on TYR reporter expression are specific, $Mitf^{Mi\text{-}Wh}$ was used in cotransfection assays. We included the (+) and (-) isoforms of MITF, isoforms which either contain (+) or lack (-) 18 base pairs in exon 6. Interestingly, the cooperative effect of MITF and IRF4 on tyrosinase expression was diminished using the $Mitf^{Mi\text{-}Wh}$ protein whereas no difference was observed with the (+) and (-) isoforms of MITF (Figure 8). In summary this indicates that the cooperative effects of MITF and IRF4 together on tyrosinase is due to MITF. Clearly, mutant versions of MITF eradicate the cooperative effect suggesting that the observed effect is mediated via MITF. Additionally, we showed that mutations within the tyrosinase promoter also affect the cooperative effect of MITF and IRF4 on the tyrosinase promoter (Figure 9).

Although studies show that IRF4 is expressed in melanoma, the role of IRF4 in this disease remains to be investigated (Natkunam et al., 2001; Sundram et al., 2003). Analysis of several cell lines including melanoma (human and mouse), melanocytes (mouse), multiple myeloma – and human embryonic kidney cell lines revealed that endogenous IRF4 expression was high in all of the human melanoma cell lines but not in mouse melanoma cells or melanocytes (Table 17). Interestingly, only one of two multiple myeloma cell lines investigated, the U266 cell line, expressed IRF4 at high levels. MITF and tyrosinase expression was also high in human melanoma cell lines but also in mouse melanoma cells and melanocytes as shown in Table 17. The lack of MITF expression in human embryonic kidney cells (HEK293T) and multiple myeloma cell lines demonstrates the 'melanocyte-specificity' of MITF. Tyrosinase, an MITF target was also absent in these cell lines.

Clonogenic assays showed that in HEK293 cells IRF4 alone, as well as IRF4 and MITF together had a growth advantage over MITF alone. In 501mel cells an opposite effect was observed. IRF4 and MITF together with IRF4 showed a reduced number of colonies formed. Soft agar assays also showed that there was no difference in the number of colonies using MITF, IRF4 or MITF together with IRF4. Hence, we can not determine if IRF4 behaves like

an oncogene in melanoma cells as it has been suggested for rat fibroblasts (Iida et al., 1997). Therefore, further studies need to be conducted to elucidate the role of IRF4 in melanoma. It could also be the case that the role of IRF4 in melanoma is in initiation rather than progression of the disease. In any event, further studies are required to investigate the role of IRF4 in either the genesis or the progression of melanoma.

6. Conclusion

Since the isolation of Mitf, it has become obvious that the MITF protein has a major impact in the development, maintenance and survival of the melanocyte lineage. Thus, mutations in MITF have been identified in hypopigmentation disorders such as WS2A and TS but also in melanoma. This thesis explains the DNA-binding ability and transcription activation potential of MITF mutations associated with these pathologies. Most mutations associated with WS2A and TS fail to bind DNA and activate melanocyte-specific promoters. However, some mutations associated with WS2A, TS and melanoma, behave similar to wild type MITF. Even though the results of this thesis provide first insights, further studies are necessary to understand why some mutations behave like wild type MITF but are associated with these pathologies (hypopigmentation syndromes and melanoma). Certainly, some mutations could be associated with the disease, but not be the causative or activating mutation for the disease. Another possibility could be that the mutations identified in a certain disease are neutral variants. In summary, here we show for the first time, that the mutations associated with these two different diseases, hypopigmentation syndromes and melanoma, have very different effects on the function of the MITF protein. As MITF may be a drug target in melanoma, it is essential to understand how melanoma-associated mutations in the protein affect function in order to contribute to this disease. This affects how we envision MITF as a melanoma drug target. As for the two autosomal dominant inherited auditory-pigment syndromes, no actual treatment plan exists and to change that it is important to understand the origin of those syndromes.

Further, we investigate how MITF regulates pigmentation in humans. Studies using mouse models and GWAS studies showed over the past decades that MITF has a central role in human pigmentation. Additionally, a SNP in intron 4 of IRF4 has been shown to be associated with eye and hair color and tanning ability as well as freckles. Here, we show that MITF and IRF4 together cooperate on the TYR promoter. We could not observe direct MITF interaction with IRF4, however the effects of MITF and IRF4 on TYR promoter were mediated though MITF. We also investigated the role of IRF4 in melanoma. IRF4 is expressed in melanoma and an SNP in IRF4 has been shown to be associated with increased melanoma risk specifically on the trunk. Further studies will be necessary to understand the underlying mechanism of IRF4 in melanoma. Probably, IRF4 contributes to melanoma initiation and is likely to be important in the genesis of melanoma rather than in melanoma progression or advanced stages of melanoma.

References

Adameyko, I., Lallemend, F., Aquino, J. B., Pereira, J. A., Topilko, P., Muller, T., Fritz, N., Beljajeva, A., Mochii, M., Liste, I., Usoskin, D., Suter, U., Birchmeier, C., & Ernfors, P. (2009). Schwann cell precursors from nerve innervation are a cellular origin of melanocytes in skin. *Cell, 139*(2), 366-379.

Aksan, I., & Goding, C. R. (1998). Targeting the microphthalmia basic helix-loop-helix-leucine zipper transcription factor to a subset of E-box elements in vitro and in vivo. *Mol Cell Biol, 18*(12), 6930-6938.

Aldinucci, D., Rapana, B., Olivo, K., Lorenzon, D., Gloghini, A., Colombatti, A., & Carbone, A. (2009). IRF4 is modulated by CD40L and by apoptotic and anti-proliferative signals in Hodgkin lymphoma. *Br J Haematol, 148*(1), 115-118.

Arnheiter, H. (2010). The discovery of the microphthalmia locus and its gene, Mitf. *Pigment Cell Melanoma Res, 23*(6), 729-735.

Bauer, G. L., Praetorius, C., Bergsteinsdottir, K., Hallsson, J. H., Gisladottir, B. K., Schepsky, A., Swing, D. A., O'Sullivan, T. N., Arnheiter, H., Bismuth, K., Debbache, J., Fletcher, C. F., Warming, S., Copeland, N. G., Jenkins, N. A., & Steingrimsson, E. (2009). The Role of MITF Phosphorylation Sites During Coat Color and Eye Development in Mice Analyzed by BAC Transgene Rescue. *Genetics, 183*(2), 581-594.

Bell, R. E., & Levy, C. (2011). The Three M's: Melanoma, MITF and MicroRNA. *Pigment Cell Melanoma Res, 24*(6), 1088-1106.

Bennett, D. C., Huszar, D., Laipis, P. J., Jaenisch, R., & Jackson, I. J. (1990). Phenotypic rescue of mutant brown melanocytes by a retrovirus carrying a wild-type tyrosinase-related protein gene. *Development, 110*(2), 471-475.

Bentley, N. J., Eisen, T., & Goding, C. R. (1994). Melanocyte-specific expression of the human tyrosinase promoter: activation by the microphthalmia gene product and role of the initiator. *Mol Cell Biol, 14*(12), 7996-8006.

Berlin, I., Denat, L., Steunou, A. L., Puig, I., Champeval, D., Colombo, S., Roberts, K., Bonvin, E., Bourgeois, Y., Davidson, I., Delmas, V., Nieto, L., Goding, C. R., & Larue, L. (2012). Phosphorylation of BRN2 modulates its interaction with the Pax3 promoter to control melanocyte migration and proliferation. *Mol Cell Biol, 32*(7), 1237-1247.

Bertolotto, C., Bille, K., Ortonne, J. P., & Ballotti, R. (1996). Regulation of tyrosinase gene expression by cAMP in B16 melanoma cells involves two CATGTG motifs surrounding the TATA box: implication of the microphthalmia gene product. *J Cell Biol, 134*(3), 747-755.

Bertolotto, C., Lesueur, F., Giuliano, S., Strub, T., de Lichy, M., Bille, K., Dessen, P., d'Hayer, B., Mohamdi, H., Remenieras, A., Maubec, E., de la Fouchardiere, A., Molinie, V., Vabres, P., Dalle, S., Poulalhon, N., Martin-Denavit, T., Thomas, L., Andry-Benzaquen, P., Dupin, N., Boitier, F., Rossi, A., Perrot, J. L., Labeille, B., Robert, C., Escudier, B., Caron, O., Brugieres, L., Saule, S., Gardie, B., Gad, S., Richard, S., Couturier, J., Teh, B. T., Ghiorzo, P., Pastorino, L., Puig, S., Badenas, C., Olsson, H., Ingvar, C., Rouleau, E., Lidereau, R., Bahadoran, P., Vielh, P., Corda, E., Blanche, H., Zelenika, D., Galan, P., French Familial Melanoma Study, G., Aubin, F., Bachollet, B., Becuwe, C., Berthet, P., Bignon, Y. J., Bonadona, V., Bonafe, J. L., Bonnet-Dupeyron, M. N., Cambazard, F., Chevrant-Breton, J., Coupier, I., Dalac, S., Demange, L., d'Incan, M., Dugast, C., Faivre, L., Vincent-Fetita, L., Gauthier-Villars, M., Gilbert, B., Grange, F., Grob, J. J., Humbert, P., Janin, N., Joly, P., Kerob, D., Lasset, C., Leroux, D., Levang, J., Limacher, J. M., Livideanu, C., Longy, M.,

Lortholary, A., Stoppa-Lyonnet, D., Mansard, S., Mansuy, L., Marrou, K., Mateus, C., Maugard, C., Meyer, N., Nogues, C., Souteyrand, P., Venat-Bouvet, L., Zattara, H., Chaudru, V., Lenoir, G. M., Lathrop, M., Davidson, I., Avril, M. F., Demenais, F., Ballotti, R., & Bressac-de Paillerets, B. (2011). A SUMOylation-defective MITF germline mutation predisposes to melanoma and renal carcinoma. *Nature, 480*(7375), 94-98.

Beuret, L., Flori, E., Denoyelle, C., Bille, K., Busca, R., Picardo, M., Bertolotto, C., & Ballotti, R. (2007). Up-regulation of MET expression by alpha-melanocyte-stimulating hormone and MITF allows hepatocyte growth factor to protect melanocytes and melanoma cells from apoptosis. *J Biol Chem, 282*(19), 14140-14147.

Beuret, L., Ohanna, M., Strub, T., Allegra, M., Davidson, I., Bertolotto, C., & Ballotti, R. (2011). BRCA1 is a new MITF target gene. *Pigment Cell Melanoma Res, 24*(4), 725-727.

Bharti, K., Liu, W., Csermely, T., Bertuzzi, S., & Arnheiter, H. (2008). Alternative promoter use in eye development: the complex role and regulation of the transcription factor MITF. *Development, 135*(6), 1169-1178.

Boissy, R. E., Zhao, H., Oetting, W. S., Austin, L. M., Wildenberg, S. C., Boissy, Y. L., Zhao, Y., Sturm, R. A., Hearing, V. J., King, R. A., & Nordlund, J. J. (1996). Mutation in and lack of expression of tyrosinase-related protein-1 (TRP-1) in melanocytes from an individual with brown oculocutaneous albinism: a new subtype of albinism classified as "OCA3". *Am J Hum Genet, 58*(6), 1145-1156.

Broderick, P., Cunningham, D., Vijayakrishnan, J., Cooke, R., Ashworth, A., Swerdlow, A., & Houlston, R. (2009). IRF4 polymorphism rs872071 and risk of Hodgkin lymphoma. *Br J Haematol, 148*(3), 413-415.

Brose, M. S., Volpe, P., Feldman, M., Kumar, M., Rishi, I., Gerrero, R., Einhorn, E., Herlyn, M., Minna, J., Nicholson, A., Roth, J. A., Albelda, S. M., Davies, H., Cox, C., Brignell, G., Stephens, P., Futreal, P. A., Wooster, R., Stratton, M. R., & Weber, B. L. (2002). BRAF and RAS mutations in human lung cancer and melanoma. *Cancer Res, 62*(23), 6997-7000.

Budd, P. S., & Jackson, I. J. (1995). Structure of the mouse tyrosinase-related protein-2/dopachrome tautomerase (Tyrp2/Dct) gene and sequence of two novel slaty alleles. *Genomics, 29*(1), 35-43.

Busca, R., & Ballotti, R. (2000). Cyclic AMP a key messenger in the regulation of skin pigmentation. *Pigment Cell Res, 13*(2), 60-69.

Busca, R., Berra, E., Gaggioli, C., Khaled, M., Bille, K., Marchetti, B., Thyss, R., Fitsialos, G., Larribere, L., Bertolotto, C., Virolle, T., Barbry, P., Pouyssegur, J., Ponzio, G., & Ballotti, R. (2005). Hypoxia-inducible factor 1{alpha} is a new target of microphthalmia-associated transcription factor (MITF) in melanoma cells. *J Cell Biol, 170*(1), 49-59.

Carbone, A., Gloghini, A., Aldinucci, D., Gattei, V., Dalla-Favera, R., & Gaidano, G. (2002). Expression pattern of MUM1/IRF4 in the spectrum of pathology of Hodgkin's disease. *Br J Haematol, 117*(2), 366-372.

Carbone, A., Gloghini, A., Larocca, L. M., Capello, D., Pierconti, F., Canzonieri, V., Tirelli, U., Dalla-Favera, R., & Gaidano, G. (2001). Expression profile of MUM1/IRF4, BCL-6, and CD138/syndecan-1 defines novel histogenetic subsets of human immunodeficiency virus-related lymphomas. *Blood, 97*(3), 744-751.

Carreira, S., Goodall, J., Aksan, I., La Rocca, S. A., Galibert, M. D., Denat, L., Larue, L., & Goding, C. R. (2005). Mitf cooperates with Rb1 and activates p21Cip1 expression to regulate cell cycle progression. *Nature, 433*(7027), 764-769.

Carreira, S., Goodall, J., Denat, L., Rodriguez, M., Nuciforo, P., Hoek, K. S., Testori, A., Larue, L., & Goding, C. R. (2006). Mitf regulation of Dia1 controls melanoma proliferation and invasiveness. *Genes Dev, 20*(24), 3426-3439.

Carreira, S., Liu, B., & Goding, C. R. (2000). The gene encoding the T-box factor Tbx2 is a target for the microphthalmia-associated transcription factor in melanocytes. *J Biol Chem, 275*(29), 21920-21927.

Chang, C. C., Lorek, J., Sabath, D. E., Li, Y., Chitambar, C. R., Logan, B., Kampalath, B., & Cleveland, R. P. (2002). Expression of MUM1/IRF4 correlates with clinical outcome in patients with B-cell chronic lymphocytic leukemia. *Blood, 100*(13), 4671-4675.

Chang, Y. M., Newton-Bishop, J. A., Bishop, D. T., Armstrong, B. K., Bataille, V., Bergman, W., Berwick, M., Bracci, P. M., Elwood, J. M., Ernstoff, M. S., Green, A. C., Gruis, N. A., Holly, E. A., Ingvar, C., Kanetsky, P. A., Karagas, M. R., Le Marchand, L., Mackie, R. M., Olsson, H., Osterlind, A., Rebbeck, T. R., Reich, K., Sasieni, P., Siskind, V., Swerdlow, A. J., Titus-Ernstoff, L., Zens, M. S., Ziegler, A., & Barrett, J. H. (2009). A pooled analysis of melanocytic nevus phenotype and the risk of cutaneous melanoma at different latitudes. *Int J Cancer, 124*(2), 420-428.

Chapman, M. A., Lawrence, M. S., Keats, J. J., Cibulskis, K., Sougnez, C., Schinzel, A. C., Harview, C. L., Brunet, J. P., Ahmann, G. J., Adli, M., Anderson, K. C., Ardlie, K. G., Auclair, D., Baker, A., Bergsagel, P. L., Bernstein, B. E., Drier, Y., Fonseca, R., Gabriel, S. B., Hofmeister, C. C., Jagannath, S., Jakubowiak, A. J., Krishnan, A., Levy, J., Liefeld, T., Lonial, S., Mahan, S., Mfuko, B., Monti, S., Perkins, L. M., Onofrio, R., Pugh, T. J., Rajkumar, S. V., Ramos, A. H., Siegel, D. S., Sivachenko, A., Stewart, A. K., Trudel, S., Vij, R., Voet, D., Winckler, W., Zimmerman, T., Carpten, J., Trent, J., Hahn, W. C., Garraway, L. A., Meyerson, M., Lander, E. S., Getz, G., & Golub, T. R. (2011). Initial genome sequencing and analysis of multiple myeloma. *Nature, 471*(7339), 467-472.

Cheli, Y., Ohanna, M., Ballotti, R., & Bertolotto, C. (2009). Fifteen-year quest for microphthalmia-associated transcription factor target genes. *Pigment Cell Melanoma Res, 23*(1), 27-40.

Chen, H., Jiang, L., Xie, Z., Mei, L., He, C., Hu, Z., Xia, K., & Feng, Y. (2010). Novel mutations of PAX3, MITF, and SOX10 genes in Chinese patients with type I or type II Waardenburg syndrome. *Biochem Biophys Res Commun, 397*(1), 70-74.

Chin, L., Garraway, L. A., & Fisher, D. E. (2006). Malignant melanoma: genetics and therapeutics in the genomic era. *Genes Dev, 20*(16), 2149-2182.

Claudio, J. O., Masih-Khan, E., Tang, H., Goncalves, J., Voralia, M., Li, Z. H., Nadeem, V., Cukerman, E., Francisco-Pabalan, O., Liew, C. C., Woodgett, J. R., & Stewart, A. K. (2002). A molecular compendium of genes expressed in multiple myeloma. *Blood, 100*(6), 2175-2186.

Coupland, S. E., Loddenkemper, C., Smith, J. R., Braziel, R. M., Charlotte, F., Anagnostopoulos, I., & Stein, H. (2005). Expression of immunoglobulin transcription factors in primary intraocular lymphoma and primary central nervous system lymphoma. *Invest Ophthalmol Vis Sci, 46*(11), 3957-3964.

Craig, F., Soma, L., Melan, M., Kant, J., & Swerdlow, S. (2008). MUM1/IRF4 expression in the circulating compartment of chronic lymphocytic leukemia. *Leuk Lymphoma, 49*(2), 273-280.

Cronin, J. C., Wunderlich, J., Loftus, S. K., Prickett, T. D., Wei, X., Ridd, K., Vemula, S., Burrell, A. S., Agrawal, N. S., Lin, J. C., Banister, C. E., Buckhaults, P., Rosenberg, S. A., Bastian, B. C., Pavan, W. J., & Samuels, Y. (2009). Frequent mutations in the MITF pathway in melanoma. *Pigment Cell Melanoma Res, 22*(4), 435-444.

Crowther-Swanepoel, D., Broderick, P., Ma, Y., Robertson, L., Pittman, A. M., Price, A., Twiss, P., Vijayakrishnan, J., Qureshi, M., Dyer, M. J., Matutes, E., Dearden, C., Catovsky, D., & Houlston, R. S. (2010). Fine-scale mapping of the 6p25.3 chronic lymphocytic leukaemia susceptibility locus. *Hum Mol Genet, 19*(9), 1840-1845.

Dankort, D., Curley, D. P., Cartlidge, R. A., Nelson, B., Karnezis, A. N., Damsky, W. E., Jr., You, M. J., DePinho, R. A., McMahon, M., & Bosenberg, M. (2009). Braf(V600E) cooperates with Pten loss to induce metastatic melanoma. *Nat Genet, 41*(5), 544-552.

Davies, H., Bignell, G. R., Cox, C., Stephens, P., Edkins, S., Clegg, S., Teague, J., Woffendin, H., Garnett, M. J., Bottomley, W., Davis, N., Dicks, E., Ewing, R., Floyd, Y., Gray, K., Hall, S., Hawes, R., Hughes, J., Kosmidou, V., Menzies, A., Mould, C., Parker, A., Stevens, C., Watt, S., Hooper, S., Wilson, R., Jayatilake, H., Gusterson, B. A., Cooper, C., Shipley, J., Hargrave, D., Pritchard-Jones, K., Maitland, N., Chenevix-Trench, G., Riggins, G. J., Bigner, D. D., Palmieri, G., Cossu, A., Flanagan, A., Nicholson, A., Ho, J. W., Leung, S. Y., Yuen, S. T., Weber, B. L., Seigler, H. F., Darrow, T. L., Paterson, H., Marais, R., Marshall, C. J., Wooster, R., Stratton, M. R., & Futreal, P. A. (2002). Mutations of the BRAF gene in human cancer. *Nature, 417*(6892), 949-954.

Delmas, V., Beermann, F., Martinozzi, S., Carreira, S., Ackermann, J., Kumasaka, M., Denat, L., Goodall, J., Luciani, F., Viros, A., Demirkan, N., Bastian, B. C., Goding, C. R., & Larue, L. (2007). Beta-catenin induces immortalization of melanocytes by suppressing p16INK4a expression and cooperates with N-Ras in melanoma development. *Genes Dev, 21*(22), 2923-2935.

Desterro, J. M., Rodriguez, M. S., Kemp, G. D., & Hay, R. T. (1999). Identification of the enzyme required for activation of the small ubiquitin-like protein SUMO-1. *J Biol Chem, 274*(15), 10618-10624.

Di Bernardo, M. C., Crowther-Swanepoel, D., Broderick, P., Webb, E., Sellick, G., Wild, R., Sullivan, K., Vijayakrishnan, J., Wang, Y., Pittman, A. M., Sunter, N. J., Hall, A. G., Dyer, M. J., Matutes, E., Dearden, C., Mainou-Fowler, T., Jackson, G. H., Summerfield, G., Harris, R. J., Pettitt, A. R., Hillmen, P., Allsup, D. J., Bailey, J. R., Pratt, G., Pepper, C., Fegan, C., Allan, J. M., Catovsky, D., & Houlston, R. S. (2008). A genome-wide association study identifies six susceptibility loci for chronic lymphocytic leukemia. *Nat Genet, 40*(10), 1204-1210.

Do, T. N., Ucisik-Akkaya, E., Davis, C. F., Morrison, B. A., & Dorak, M. T. (2010). An intronic polymorphism of IRF4 gene influences gene transcription in vitro and shows a risk association with childhood acute lymphoblastic leukemia in males. *Biochim Biophys Acta, 1802*(2), 292-300.

Dorvault, C. C., Weilbaecher, K. N., Yee, H., Fisher, D. E., Chiriboga, L. A., Xu, Y., & Chhieng, D. C. (2001). Microphthalmia transcription factor: a sensitive and specific marker for malignant melanoma in cytologic specimens. *Cancer, 93*(5), 337-343.

Duffy, D. L., Iles, M. M., Glass, D., Zhu, G., Barrett, J. H., Hoiom, V., Zhao, Z. Z., Sturm, R. A., Soranzo, N., Hammond, C., Kvaskoff, M., Whiteman, D. C., Mangino, M., Hansson, J., Newton-Bishop, J. A., GenoMel, Bataille, V., Hayward, N. K., Martin, N. G., Bishop, D. T., Spector, T. D., & Montgomery, G. W. (2010). IRF4 variants have age-specific effects on nevus count and predispose to melanoma. *Am J Hum Genet, 87*(1), 6-16.

Duffy, D. L., Zhao, Z. Z., Sturm, R. A., Hayward, N. K., Martin, N. G., & Montgomery, G. W. (2009). Multiple Pigmentation Gene Polymorphisms Account for a Substantial Proportion of Risk of Cutaneous Malignant Melanoma. *J Invest Dermatol, 130*(2), 520-528.

Dynek, J. N., Chan, S. M., Liu, J., Zha, J., Fairbrother, W. J., & Vucic, D. (2008). Microphthalmia-associated transcription factor is a critical transcriptional regulator of melanoma inhibitor of apoptosis in melanomas. *Cancer Res, 68*(9), 3124-3132.

Eisenbeis, C. F., Singh, H., & Storb, U. (1995). Pip, a novel IRF family member, is a lymphoid-specific, PU.1-dependent transcriptional activator. *Genes Dev, 9*(11), 1377-1387.

Eriksson, N., Macpherson, J. M., Tung, J. Y., Hon, L. S., Naughton, B., Saxonov, S., Avey, L., Wojcicki, A., Pe'er, I., & Mountain, J. (2010). Web-based, participant-driven studies yield novel genetic associations for common traits. *PLoS Genet, 6*(6), e1000993.

Ernfors, P. (2010). Cellular origin and developmental mechanisms during the formation of skin melanocytes. *Exp Cell Res, 316*(8), 1397-1407.

Exome Variant Server, N. G. E. S. P. E., Seattle, WA (URL: http://evs.gs.washington.edu/EVS/). (July 2013 accessed).

Fecher, L. A., Amaravadi, R. K., & Flaherty, K. T. (2008). The MAPK pathway in melanoma. *Curr Opin Oncol, 20*(2), 183-189.

Fecher, L. A., Amaravadi, R. K., Schuchter, L. M., & Flaherty, K. T. (2009). Drug targeting of oncogenic pathways in melanoma. *Hematol Oncol Clin North Am, 23*(3), 599-618.

Feldman, A. L., Law, M., Remstein, E. D., Macon, W. R., Erickson, L. A., Grogg, K. L., Kurtin, P. J., & Dogan, A. (2009). Recurrent translocations involving the IRF4 oncogene locus in peripheral T-cell lymphomas. *Leukemia, 23*(3), 574-580.

Finn, L., Markovic, S. N., & Joseph, R. W. (2012). Therapy for metastatic melanoma: the past, present, and future. *BMC Med, 10*(23), 1-10.

Flaherty, K. T., Hodi, F. S., & Bastian, B. C. (2010). Mutation-driven drug development in melanoma. *Curr Opin Oncol, 22*(3), 178-183.

Frame, S., & Cohen, P. (2001). GSK3 takes centre stage more than 20 years after its discovery. *Biochem J, 359*(Pt 1), 1-16.

Friedberg, J. W., & Fisher, R. I. (2008). Diffuse large B-cell lymphoma. *Hematol Oncol Clin North Am, 22*(5), 941-952, ix.

Gallagher, S. J., Rambow, F., Kumasaka, M., Champeval, D., Bellacosa, A., Delmas, V., & Larue, L. (2012). Beta-catenin inhibits melanocyte migration but induces melanoma metastasis. *Oncogene, 32*(27), 2230-2238.

Garber, K. (2013). Melanoma combination therapies ward off tumor resistance. *Nat Biotechnol, 31*(8), 666-668.

Garraway, L. A., & Sellers, W. R. (2006). Lineage dependency and lineage-survival oncogenes in human cancer. *Nat Rev Cancer, 6*(8), 593-602.

Garraway, L. A., Widlund, H. R., Rubin, M. A., Getz, G., Berger, A. J., Ramaswamy, S., Beroukhim, R., Milner, D. A., Granter, S. R., Du, J., Lee, C., Wagner, S. N., Li, C., Golub, T. R., Rimm, D. L., Meyerson, M. L., Fisher, D. E., & Sellers, W. R. (2005). Integrative genomic analyses identify MITF as a lineage survival oncogene amplified in malignant melanoma. *Nature, 436*(7047), 117-122.

Goding, C. R. (2000). Mitf from neural crest to melanoma: signal transduction and transcription in the melanocyte lineage. *Genes Dev, 14*(14), 1712-1728.

Goding, C. R. (2007). Melanocytes: the new Black. *Int J Biochem Cell Biol, 39*(2), 275-279.

Gray-Schopfer, V., Wellbrock, C., & Marais, R. (2007). Melanoma biology and new targeted therapy. *Nature, 445*(7130), 851-857.

Grossman, A., Mittrucker, H. W., Nicholl, J., Suzuki, A., Chung, S., Antonio, L., Suggs, S., Sutherland, G. R., Siderovski, D. P., & Mak, T. W. (1996). Cloning of human lymphocyte-specific interferon regulatory factor (hLSIRF/hIRF4) and mapping of the gene to 6p23-p25. *Genomics, 37*(2), 229-233.

Gudbjartsson, D. F., Sulem, P., Stacey, S. N., Goldstein, A. M., Rafnar, T., Sigurgeirsson, B., Benediktsdottir, K. R., Thorisdottir, K., Ragnarsson, R., Sveinsdottir, S. G., Magnusson, V., Lindblom, A., Kostulas, K., Botella-Estrada, R., Soriano, V., Juberias, P., Grasa, M., Saez, B., Andres, R., Scherer, D., Rudnai, P., Gurzau, E., Koppova, K., Kiemeney, L. A., Jakobsdottir, M., Steinberg, S., Helgason, A., Gretarsdottir, S., Tucker, M. A., Mayordomo, J. I., Nagore, E., Kumar, R., Hansson, J., Olafsson, J. H., Gulcher, J., Kong, A., Thorsteinsdottir, U., & Stefansson, K. (2008). ASIP and TYR pigmentation variants associate with cutaneous melanoma and basal cell carcinoma. *Nat Genet, 40*(7), 886-891.

Guyonneau, L., Murisier, F., Rossier, A., Moulin, A., & Beermann, F. (2004). Melanocytes and pigmentation are affected in dopachrome tautomerase knockout mice. *Mol Cell Biol, 24*(8), 3396-3403.

Halaban, R., & Moellmann, G. (1990). Murine and human b locus pigmentation genes encode a glycoprotein (gp75) with catalase activity. *Proc Natl Acad Sci U S A, 87*(12), 4809-4813.

Hallack Neto, A. E., Siqueira, S. A., Dulley, F. L., Ruiz, M. A., Chamone, D. A., & Pereira, J. (2009). p63 protein expression in high risk diffuse large B-cell lymphoma. *J Clin Pathol, 62*(1), 77-79.

Han, J., Kraft, P., Nan, H., Guo, Q., Chen, C., Qureshi, A., Hankinson, S. E., Hu, F. B., Duffy, D. L., Zhao, Z. Z., Martin, N. G., Montgomery, G. W., Hayward, N. K., Thomas, G., Hoover, R. N., Chanock, S., & Hunter, D. J. (2008). A genome-wide association study identifies novel alleles associated with hair color and skin pigmentation. *PLoS Genet, 4*(5), e1000074.

Han, J., Qureshi, A. A., Nan, H., Zhang, J., Song, Y., Guo, Q., & Hunter, D. J. (2011). A germline variant in the interferon regulatory factor 4 gene as a novel skin cancer risk locus. *Cancer Res, 71*(5), 1533-1539.

Hans, C. P., Weisenburger, D. D., Greiner, T. C., Gascoyne, R. D., Delabie, J., Ott, G., Muller-Hermelink, H. K., Campo, E., Braziel, R. M., Jaffe, E. S., Pan, Z., Farinha, P., Smith, L. M., Falini, B., Banham, A. H., Rosenwald, A., Staudt, L. M., Connors, J. M., Armitage, J. O., & Chan, W. C. (2004). Confirmation of the molecular classification of diffuse large B-cell lymphoma by immunohistochemistry using a tissue microarray. *Blood, 103*(1), 275-282.

Hauswirth, R., Haase, B., Blatter, M., Brooks, S. A., Burger, D., Drogemuller, C., Gerber, V., Henke, D., Janda, J., Jude, R., Magdesian, K. G., Matthews, J. M., Poncet, P. A., Svansson, V., Tozaki, T., Wilkinson-White, L., Penedo, M. C., Rieder, S., & Leeb, T. (2012). Mutations in MITF and PAX3 cause "splashed white" and other white spotting phenotypes in horses. *PLoS Genet, 8*(4), e1002653.

Havelange, V., Pekarsky, Y., Nakamura, T., Palamarchuk, A., Alder, H., Rassenti, L., Kipps, T., & Croce, C. M. (2011). IRF4 mutations in chronic lymphocytic leukemia. *Blood, 118*(10), 2827-2829.

Hemesath, T. J., Price, E. R., Takemoto, C., Badalian, T., & Fisher, D. E. (1998). MAP kinase links the transcription factor Microphthalmia to c-Kit signalling in melanocytes. *Nature, 391*(6664), 298-301.

Hemesath, T. J., Steingrimsson, E., McGill, G., Hansen, M. J., Vaught, J., Hodgkinson, C. A., Arnheiter, H., Copeland, N. G., Jenkins, N. A., & Fisher, D. E. (1994). microphthalmia, a critical factor in melanocyte development, defines a discrete transcription factor family. *Genes Dev, 8*(22), 2770-2780.

Hirobe, T. (1984). Effects of genic substitution at the brown locus on the differentiation of epidermal melanocytes in newborn mouse skin. *Anat Rec, 209*(4), 425-432.

Hodgkinson, C. A., Moore, K. J., Nakayama, A., Steingrimsson, E., Copeland, N. G., Jenkins, N. A., & Arnheiter, H. (1993). Mutations at the mouse microphthalmia locus are associated with defects in a gene encoding a novel basic-helix-loop-helix-zipper protein. *Cell, 74*(2), 395-404.

Hodis, E., Watson, I. R., Kryukov, G. V., Arold, S. T., Imielinski, M., Theurillat, J. P., Nickerson, E., Auclair, D., Li, L., Place, C., Dicara, D., Ramos, A. H., Lawrence, M. S., Cibulskis, K., Sivachenko, A., Voet, D., Saksena, G., Stransky, N., Onofrio, R. C., Winckler, W., Ardlie, K., Wagle, N., Wargo, J., Chong, K., Morton, D. L., Stemke-Hale, K., Chen, G., Noble, M., Meyerson, M., Ladbury, J. E., Davies, M. A., Gershenwald, J. E., Wagner, S. N., Hoon, D. S., Schadendorf, D., Lander, E. S., Gabriel, S. B., Getz, G., Garraway, L. A., & Chin, L. (2012). A landscape of driver mutations in melanoma. *Cell, 150*(2), 251-263.

Hoefnagel, J. J., Dijkman, R., Basso, K., Jansen, P. M., Hallermann, C., Willemze, R., Tensen, C. P., & Vermeer, M. H. (2005). Distinct types of primary cutaneous large B-cell lymphoma identified by gene expression profiling. *Blood, 105*(9), 3671-3678.

Hoek, K. S., & Goding, C. R. (2010). Cancer stem cells versus phenotype-switching in melanoma. *Pigment Cell Melanoma Res, 23*(6), 746-759.

Hoek, K. S., Schlegel, N. C., Eichhoff, O. M., Widmer, D. S., Praetorius, C., Einarsson, S. O., Valgeirsdottir, S., Bergsteinsdottir, K., Schepsky, A., Dummer, R., & Steingrimsson, E. (2008). Novel MITF targets identified using a two-step DNA microarray strategy. *Pigment Cell Melanoma Res, 21*(6), 665-676.

Hou, L., & Pavan, W. J. (2008). Transcriptional and signaling regulation in neural crest stem cell-derived melanocyte development: do all roads lead to Mitf? *Cell Res, 18*(12), 1163-1176.

Hughes, A. E., Newton, V. E., Liu, X. Z., & Read, A. P. (1994). A gene for Waardenburg syndrome type 2 maps close to the human homologue of the microphthalmia gene at chromosome 3p12-p14.1. *Nat Genet, 7*(4), 509-512.

Iida, S., Rao, P. H., Butler, M., Corradini, P., Boccadoro, M., Klein, B., Chaganti, R. S., & Dalla-Favera, R. (1997). Deregulation of MUM1/IRF4 by chromosomal translocation in multiple myeloma. *Nat Genet, 17*(2), 226-230.

Iniguez-Lluhi, J. A., & Pearce, D. (2000). A common motif within the negative regulatory regions of multiple factors inhibits their transcriptional synergy. *Mol Cell Biol, 20*(16), 6040-6050.

Isaacson, P. G., & Du, M. Q. (2004). MALT lymphoma: from morphology to molecules. *Nat Rev Cancer, 4*(8), 644-653.

Ito, M., Iida, S., Inagaki, H., Tsuboi, K., Komatsu, H., Yamaguchi, M., Nakamura, N., Suzuki, R., Seto, M., Nakamura, S., Morishima, Y., & Ueda, R. (2002). MUM1/IRF4 expression is an unfavorable prognostic factor in B-cell chronic lymphocytic leukemia (CLL)/small lymphocytic lymphoma (SLL). *Jpn J Cancer Res, 93*(6), 685-694.

Jackson, I. J. (1988). A cDNA encoding tyrosinase-related protein maps to the brown locus in mouse. *Proc Natl Acad Sci U S A, 85*(12), 4392-4396.

Jackson, I. J., Chambers, D. M., Tsukamoto, K., Copeland, N. G., Gilbert, D. J., Jenkins, N. A., & Hearing, V. (1992). A second tyrosinase-related protein, TRP-2, maps to and is mutated at the mouse slaty locus. *EMBO J, 11*(2), 527-535.

Jaffe, E. S. (2006). Pathobiology of peripheral T-cell lymphomas. *Hematology Am Soc Hematol Educ Program*, 317-322.

Jakob, J. A., Bassett, R. L., Jr., Ng, C. S., Curry, J. L., Joseph, R. W., Alvarado, G. C., Rohlfs, M. L., Richard, J., Gershenwald, J. E., Kim, K. B., Lazar, A. J., Hwu, P., & Davies, M. A. (2012). NRAS mutation status is an independent prognostic factor in metastatic melanoma. *Cancer, 118*(16), 4014-4023.

Keating, M. J., Chiorazzi, N., Messmer, B., Damle, R. N., Allen, S. L., Rai, K. R., Ferrarini, M., & Kipps, T. J. (2003). Biology and treatment of chronic lymphocytic leukemia. *Hematology Am Soc Hematol Educ Program*, 153-175.

King, R., Googe, P. B., Weilbaecher, K. N., Mihm, M. C., Jr., & Fisher, D. E. (2001). Microphthalmia transcription factor expression in cutaneous benign, malignant melanocytic, and nonmelanocytic tumors. *Am J Surg Pathol, 25*(1), 51-57.

King, R., Weilbaecher, K. N., McGill, G., Cooley, E., Mihm, M., & Fisher, D. E. (1999). Microphthalmia transcription factor. A sensitive and specific melanocyte marker for MelanomaDiagnosis. *Am J Pathol, 155*(3), 731-738.

Klein, U., Casola, S., Cattoretti, G., Shen, Q., Lia, M., Mo, T., Ludwig, T., Rajewsky, K., & Dalla-Favera, R. (2006). Transcription factor IRF4 controls plasma cell differentiation and class-switch recombination. *Nat Immunol, 7*(7), 773-782.

Kondo, T., & Hearing, V. J. (2011). Update on the regulation of mammalian melanocyte function and skin pigmentation. *Expert Rev Dermatol, 6*(1), 97-108.

Kuppers, R. (2009). Molecular biology of Hodgkin lymphoma. *Hematology Am Soc Hematol Educ Program*, 491-496.

Kvaskoff, M., Whiteman, D. C., Zhao, Z. Z., Montgomery, G. W., Martin, N. G., Hayward, N. K., & Duffy, D. L. (2011). Polymorphisms in Nevus-Associated Genes MTAP, PLA2G6, and IRF4 and the Risk of Invasive Cutaneous Melanoma. *Twin Res Hum Genet, 14*(5), 422-432.

Kwon, B. S., Haq, A. K., Pomerantz, S. H., & Halaban, R. (1987). Isolation and sequence of a cDNA clone for human tyrosinase that maps at the mouse c-albino locus. *Proc Natl Acad Sci U S A, 84*(21), 7473-7477.

Lalwani, A. K., Attaie, A., Randolph, F. T., Deshmukh, D., Wang, C., Mhatre, A., & Wilcox, E. (1998). Point mutation in the MITF gene causing Waardenburg syndrome type II in a three-generation Indian family. *Am J Med Genet, 80*(4), 406-409.

Lamason, R. L., Mohideen, M. A., Mest, J. R., Wong, A. C., Norton, H. L., Aros, M. C., Jurynec, M. J., Mao, X., Humphreville, V. R., Humbert, J. E., Sinha, S., Moore, J. L., Jagadeeswaran, P., Zhao, W., Ning, G., Makalowska, I., McKeigue, P. M., O'Donnell, D., Kittles, R., Parra, E. J., Mangini, N. J., Grunwald, D. J., Shriver, M. D., Canfield, V. A., & Cheng, K. C. (2005). SLC24A5, a putative cation exchanger, affects pigmentation in zebrafish and humans. *Science, 310*(5755), 1782-1786.

Larue, L., & Delmas, V. (2006). The WNT/Beta-catenin pathway in melanoma. *Front Biosci, 11*, 733-742.

Law, M. H., Macgregor, S., & Hayward, N. K. (2012). Melanoma genetics: recent findings take us beyond well-traveled pathways. *J Invest Dermatol, 132*(7), 1763-1774.

Lee, Y. J., Kim, D. H., Lee, S. H., Kim, D. W., Nam, H. S., & Cho, M. K. (2011). Expression of the c-Met Proteins in Malignant Skin Cancers. *Ann Dermatol, 23*(1), 33-38.

Leger, S., Balguerie, X., Goldenberg, A., Drouin-Garraud, V., Cabot, A., Amstutz-Montadert, I., Young, P., Joly, P., Bodereau, V., Holder-Espinasse, M., Jamieson, R. V., Krause, A., Chen, H., Baumann, C., Nunes, L., Dollfus, H., Goossens, M., & Pingault, V. (2012). Novel and recurrent non-truncating mutations of the MITF basic domain: genotypic and phenotypic variations in Waardenburg and Tietz syndromes. *Eur J Hum Genet, 20*(5), 584-587.

Lennartsson, J., Voytyuk, O., Heiss, E., Sundberg, C., Sun, J., & Rönnstrand, L. (2005). C-Kit signal transduction and involvement in cancer. *Cancer Therapy, 3*(A), 5-28.

Li, A., Ma, Y., Jin, M., Mason, S., Mort, R. L., Blyth, K., Larue, L., Sansom, O. J., & Machesky, L. M. (2012). Activated mutant NRas(Q61K) drives aberrant melanocyte signaling, survival, and invasiveness via a Rac1-dependent mechanism. *J Invest Dermatol, 132*(11), 2610-2621.

Li, X. H., Kishore, A. H., Dao, D., Zheng, W., Roman, C. A., & Word, R. A. (2010). A Novel Isoform of Microphthalmia-Associated Transcription Factor Inhibits IL-8 Gene Expression in Human Cervical Stromal Cells. *Mol Endocrinol, 24*(8), 1512-1528.

Lin, F. R., Kuo, H. K., Ying, H. Y., Yang, F. H., & Lin, K. I. (2007). Induction of apoptosis in plasma cells by B lymphocyte-induced maturation protein-1 knockdown. *Cancer Res, 67*(24), 11914-11923.

Liu, X. Z., Newton, V. E., & Read, A. P. (1995). Waardenburg syndrome type II: phenotypic findings and diagnostic criteria. *Am J Med Genet, 55*(1), 95-100.

Loercher, A. E., Tank, E. M., Delston, R. B., & Harbour, J. W. (2005). MITF links differentiation with cell cycle arrest in melanocytes by transcriptional activation of INK4A. *J Cell Biol, 168*(1), 35-40.

Lohoff, M., Mittrucker, H. W., Prechtl, S., Bischof, S., Sommer, F., Kock, S., Ferrick, D. A., Duncan, G. S., Gessner, A., & Mak, T. W. (2002). Dysregulated T helper cell differentiation in the absence of interferon regulatory factor 4. *Proc Natl Acad Sci U S A, 99*(18), 11808-11812.

Lowings, P., Yavuzer, U., & Goding, C. R. (1992). Positive and negative elements regulate a melanocyte-specific promoter. *Mol Cell Biol, 12*(8), 3653-3662.

Maldonado, J. L., Fridlyand, J., Patel, H., Jain, A. N., Busam, K., Kageshita, T., Ono, T., Albertson, D. G., Pinkel, D., & Bastian, B. C. (2003). Determinants of BRAF mutations in primary melanomas. *J Natl Cancer Inst, 95*(24), 1878-1890.

Mansky, K. C., Sankar, U., Han, J., & Ostrowski, M. C. (2002). Microphthalmia transcription factor is a target of the p38 MAPK pathway in response to receptor activator of NF-kappa B ligand signaling. *J Biol Chem, 277*(13), 11077-11083.

Marecki, S., Atchison, M. L., & Fenton, M. J. (1999). Differential expression and distinct functions of IFN regulatory factor 4 and IFN consensus sequence binding protein in macrophages. *J Immunol, 163*(5), 2713-2722.

Marecki, S., & Fenton, M. J. (2002). The role of IRF-4 in transcriptional regulation. *J Interferon Cytokine Res, 22*(1), 121-133.

Martinez, A., Pittaluga, S., Rudelius, M., Davies-Hill, T., Sebasigari, D., Fountaine, T. J., Hewitt, S., Jaffe, E. S., & Raffeld, M. (2008). Expression of the interferon regulatory factor 8/ICSBP-1 in human reactive lymphoid tissues and B-cell lymphomas: a novel germinal center marker. *Am J Surg Pathol, 32*(8), 1190-1200.

Maruotti, J., Thein, T., Zack, D. J., & Esumi, N. (2012). MITF-M, a 'melanocyte-specific' isoform, is expressed in the adult retinal pigment epithelium. *Pigment Cell Melanoma Res, 25*(5), 641-644.

Matsuyama, T., Grossman, A., Mittrucker, H. W., Siderovski, D. P., Kiefer, F., Kawakami, T., Richardson, C. D., Taniguchi, T., Yoshinaga, S. K., & Mak, T. W. (1995). Molecular cloning of LSIRF, a lymphoid-specific member of the interferon regulatory factor family that binds the interferon-stimulated response element (ISRE). *Nucleic Acids Res, 23*(12), 2127-2136.

McGill, G. G., Haq, R., Nishimura, E. K., & Fisher, D. E. (2006). c-Met expression is regulated by Mitf in the melanocyte lineage. *J Biol Chem, 281*(15), 10365-10373.

McGill, G. G., Horstmann, M., Widlund, H. R., Du, J., Motyckova, G., Nishimura, E. K., Lin, Y. L., Ramaswamy, S., Avery, W., Ding, H. F., Jordan, S. A., Jackson, I. J., Korsmeyer, S. J., Golub, T. R., & Fisher, D. E. (2002). Bcl2 regulation by the melanocyte master regulator Mitf modulates lineage survival and melanoma cell viability. *Cell, 109*(6), 707-718.

Medic, S., & Ziman, M. (2010). PAX3 expression in normal skin melanocytes and melanocytic lesions (naevi and melanomas). *PLoS One, 5*(4), e9977.

Michaux, L., Wlodarska, I., Rack, K., Stul, M., Criel, A., Maerevoet, M., Marichal, S., Demuynck, H., Mineur, P., Kargar Samani, K., Van Hoof, A., Ferrant, A., Marynen, P., & Hagemeijer, A. (2005). Translocation t(1;6)(p35.3;p25.2): a new recurrent aberration in "unmutated" B-CLL. *Leukemia, 19*(1), 77-82.

Miettinen, M., Fernandez, M., Franssila, K., Gatalica, Z., Lasota, J., & Sarlomo-Rikala, M. (2001). Microphthalmia transcription factor in the immunohistochemical diagnosis of metastatic melanoma: comparison with four other melanoma markers. *Am J Surg Pathol, 25*(2), 205-211.

Miller, A. J., Du, J., Rowan, S., Hershey, C. L., Widlund, H. R., & Fisher, D. E. (2004). Transcriptional regulation of the melanoma prognostic marker melastatin (TRPM1) by MITF in melanocytes and melanoma. *Cancer Res, 64*(2), 509-516.

Miller, A. J., Levy, C., Davis, I. J., Razin, E., & Fisher, D. E. (2005). Sumoylation of MITF and its related family members TFE3 and TFEB. *J Biol Chem, 280*(1), 146-155.

Mittrucker, H. W., Matsuyama, T., Grossman, A., Kundig, T. M., Potter, J., Shahinian, A., Wakeham, A., Patterson, B., Ohashi, P. S., & Mak, T. W. (1997). Requirement for the transcription factor LSIRF/IRF4 for mature B and T lymphocyte function. *Science, 275*(5299), 540-543.

Moskvina, V., Smith, M., Ivanov, D., Blackwood, D., Stclair, D., Hultman, C., Toncheva, D., Gill, M., Corvin, A., O'Dushlaine, C., Morris, D. W., Wray, N. R., Sullivan, P., Pato, C., Pato, M. T., Sklar, P., Purcell, S., Holmans, P., O'Donovan, M. C., Owen, M. J., & Kirov, G. (2010). Genetic Differences between Five European Populations. *Hum Hered, 70*(2), 141-149.

Murakami, H., & Arnheiter, H. (2005). Sumoylation modulates transcriptional activity of MITF in a promoter-specific manner. *Pigment Cell Res, 18*(4), 265-277.

Nan, H., Kraft, P., Qureshi, A. A., Guo, Q., Chen, C., Hankinson, S. E., Hu, F. B., Thomas, G., Hoover, R. N., Chanock, S., Hunter, D. J., & Han, J. (2009). Genome-wide association study of tanning phenotype in a population of European ancestry. *J Invest Dermatol, 129*(9), 2250-2257.

Natkunam, Y., Hsi, E. D., Aoun, P., Zhao, S., Elson, P., Pohlman, B., Naushad, H., Bast, M., Levy, R., & Lossos, I. S. (2007). Expression of the human germinal center-associated lymphoma (HGAL) protein identifies a subset of classic Hodgkin lymphoma of germinal center derivation and improved survival. *Blood, 109*(1), 298-305.

Natkunam, Y., Warnke, R. A., Montgomery, K., Falini, B., & van De Rijn, M. (2001). Analysis of MUM1/IRF4 protein expression using tissue microarrays and immunohistochemistry. *Mod Pathol, 14*(7), 686-694.

Nau, K. C., & Lewis, W. D. (2008). Multiple myeloma: diagnosis and treatment. *Am Fam Physician, 78*(7), 853-859.

Nelson, A. A., & Tsao, H. (2009). Melanoma and genetics. *Clin Dermatol, 27*(1), 46-52.

Niyazi, M., Niyazi, I., & Belka, C. (2007). Counting colonies of clonogenic assays by using densitometric software. *Radiat Oncol, 2*, 4.

Nobukuni, Y., Watanabe, A., Takeda, K., Skarka, H., & Tachibana, M. (1996). Analyses of loss-of-function mutations of the MITF gene suggest that haploinsufficiency is a cause of Waardenburg syndrome type 2A. *Am J Hum Genet, 59*(1), 76-83.

Nonaka, D., Laser, J., Tucker, R., & Melamed, J. (2007). Immunohistochemical evaluation of necrotic malignant melanomas. *Am J Clin Pathol, 127*(5), 787-791.

Oetting, W. S., Fryer, J. P., Shriram, S., & King, R. A. (2003). Oculocutaneous albinism type 1: the last 100 years. *Pigment Cell Res, 16*(3), 307-311.

Otsuka, T., Takayama, H., Sharp, R., Celli, G., LaRochelle, W. J., Bottaro, D. P., Ellmore, N., Vieira, W., Owens, J. W., Anver, M., & Merlino, G. (1998). c-Met autocrine

activation induces development of malignant melanoma and acquisition of the metastatic phenotype. *Cancer Res, 58*(22), 5157-5167.

Palmieri, G., Capone, M., Ascierto, M. L., Gentilcore, G., Stroncek, D. F., Casula, M., Sini, M. C., Palla, M., Mozzillo, N., & Ascierto, P. A. (2009). Main roads to melanoma. *J Transl Med, 7*, 86.

Pham-Ledard, A., Prochazkova-Carlotti, M., Laharanne, E., Vergier, B., Jouary, T., Beylot-Barry, M., & Merlio, J. P. (2010). IRF4 gene rearrangements define a subgroup of CD30-positive cutaneous T-cell lymphoma: a study of 54 cases. *J Invest Dermatol, 130*(3), 816-825.

Pingault, V., Ente, D., Dastot-Le Moal, F., Goossens, M., Marlin, S., & Bondurand, N. (2010). Review and update of mutations causing Waardenburg syndrome. *Hum Mutat, 31*(4), 391-406.

Pogenberg, V., Ogmundsdottir, M. H., Bergsteinsdottir, K., Schepsky, A., Phung, B., Deineko, V., Milewski, M., Steingrimsson, E., & Wilmanns, M. (2012). Restricted leucine zipper dimerization and specificity of DNA recognition of the melanocyte master regulator MITF. *Genes Dev, 26*(23), 2647-2658.

Potterf, S. B., Furumura, M., Dunn, K. J., Arnheiter, H., & Pavan, W. J. (2000). Transcription factor hierarchy in Waardenburg syndrome: regulation of MITF expression by SOX10 and PAX3. *Hum Genet, 107*(1), 1-6.

Pratt, G., Fenton, J. A., Allsup, D., Fegan, C., Morgan, G. J., Jackson, G., Sunter, N. J., Hall, A. G., Irving, J. A., & Allan, J. M. (2010). A polymorphism in the 3' UTR of IRF4 linked to susceptibility and pathogenesis in chronic lymphocytic leukaemia and Hodgkin lymphoma has limited impact in multiple myeloma. *Br J Haematol*(150), 371-373.

Primot, A., Mogha, A., Corre, S., Roberts, K., Debbache, J., Adamski, H., Dreno, B., Khammari, A., Lesimple, T., Mereau, A., Goding, C. R., & Galibert, M. D. (2009). ERK-regulated differential expression of the Mitf 6a/b splicing isoforms in melanoma. *Pigment Cell Melanoma Res, 23*(1), 93-102.

Prince, S., Carreira, S., Vance, K. W., Abrahams, A., & Goding, C. R. (2004). Tbx2 directly represses the expression of the p21(WAF1) cyclin-dependent kinase inhibitor. *Cancer Res, 64*(5), 1669-1674.

Puntervoll, H. E., Yang, X. R., Vetti, H. H., Bachmann, I. M., Avril, M. F., Benfodda, M., Catricala, C., Dalle, S., Duval-Modeste, A. B., Ghiorzo, P., Grammatico, P., Harland, M., Hayward, N. K., Hu, H. H., Jouary, T., Martin-Denavit, T., Ozola, A., Palmer, J. M., Pastorino, L., Pjanova, D., Soufir, N., Steine, S. J., Stratigos, A. J., Thomas, L., Tinat, J., Tsao, H., Veinalde, R., Tucker, M. A., Bressac-de Paillerets, B., Newton-Bishop, J. A., Goldstein, A. M., Akslen, L. A., & Molven, A. (2013). Melanoma prone families with CDK4 germline mutation: phenotypic profile and associations with MC1R variants. *J Med Genet, 50*(4), 264-270.

Read, A. P., & Newton, V. E. (1997). Waardenburg syndrome. *J Med Genet, 34*(8), 656-665.

Rudloff, U., & Samuels, Y. (2009). TYRO3-mediated regulation of MITF: a novel target in melanoma? *Pigment Cell Melanoma Res, 23*(1), 9-11.

Russo, A. E., Torrisi, E., Bevelacqua, Y., Perrotta, R., Libra, M., McCubrey, J. A., Spandidos, D. A., Stivala, F., & Malaponte, G. (2009). Melanoma: molecular pathogenesis and emerging target therapies (Review). *Int J Oncol, 34*(6), 1481-1489.

Saez-Ayala, M., Montenegro, M. F., Sanchez-Del-Campo, L., Fernandez-Perez, M. P., Chazarra, S., Freter, R., Middleton, M., Pinero-Madrona, A., Cabezas-Herrera, J., Goding, C. R., & Rodriguez-Lopez, J. N. (2013). Directed Phenotype Switching as an Effective Antimelanoma Strategy. *Cancer Cell, 24*(1), 105-119.

Salti, G. I., Manougian, T., Farolan, M., Shilkaitis, A., Majumdar, D., & Das Gupta, T. K. (2000). Micropthalmia transcription factor: a new prognostic marker in intermediate-thickness cutaneous malignant melanoma. *Cancer Res, 60*(18), 5012-5016.

Schepsky, A., Bruser, K., Gunnarsson, G. J., Goodall, J., Hallsson, J. H., Goding, C. R., Steingrimsson, E., & Hecht, A. (2006). The microphthalmia-associated transcription factor Mitf interacts with beta-catenin to determine target gene expression. *Mol Cell Biol, 26*(23), 8914-8927.

Schiaffino, M. V. (2010). Signaling pathways in melanosome biogenesis and pathology. *Int J Biochem Cell Biol, 42*(7), 1094-1104.

Sciammas, R., Shaffer, A. L., Schatz, J. H., Zhao, H., Staudt, L. M., & Singh, H. (2006). Graded expression of interferon regulatory factor-4 coordinates isotype switching with plasma cell differentiation. *Immunity, 25*(2), 225-236.

Shaffer, A. L., Emre, N. C., Lamy, L., Ngo, V. N., Wright, G., Xiao, W., Powell, J., Dave, S., Yu, X., Zhao, H., Zeng, Y., Chen, B., Epstein, J., & Staudt, L. M. (2008). IRF4 addiction in multiple myeloma. *Nature, 454*(7201), 226-231.

Shibahara, S., Taguchi, H., Muller, R. M., Shibata, K., Cohen, T., Tomita, Y., & Tagami, H. (1991). Structural organization of the pigment cell-specific gene located at the brown locus in mouse. Its promoter activity and alternatively spliced transcript. *J Biol Chem, 266*(24), 15895-15901.

Shibahara, S., Tomita, Y., Sakakura, T., Nager, C., Chaudhuri, B., & Muller, R. (1986). Cloning and expression of cDNA encoding mouse tyrosinase. *Nucleic Acids Res, 14*(6), 2413-2427.

Shigemura, T., Shiohara, M., Tanaka, M., Takeuchi, K., & Koike, K. (2010). Effect of the mutant microphthalmia-associated transcription factor found in Tietz syndrome on the in vitro development of mast cells. *J Pediatr Hematol Oncol, 32*(6), 442-447.

Slager, S. L., Goldin, L. R., Strom, S. S., Lanasa, M. C., Spector, L. G., Rassenti, L., Leis, J. F., Camp, N. J., Kay, N. E., Vachon, C. M., Glenn, M., Weinberg, J. B., Rabe, K. G., Cunningham, J. M., Achenbach, S. J., Hanson, C. A., Marti, G. E., Call, T. G., Caporaso, N. E., & Cerhan, J. R. (2010). Genetic susceptibility variants for chronic lymphocytic leukemia. *Cancer Epidemiol Biomarkers Prev, 19*(4), 1098-1102.

Smith, S. D., Kelley, P. M., Kenyon, J. B., & Hoover, D. (2000). Tietz syndrome (hypopigmentation/deafness) caused by mutation of MITF. *J Med Genet, 37*(6), 446-448.

Soma, L. A., Craig, F. E., & Swerdlow, S. H. (2006). The proliferation center microenvironment and prognostic markers in chronic lymphocytic leukemia/small lymphocytic lymphoma. *Hum Pathol, 37*(2), 152-159.

Sosman, J. A., Kim, K. B., Schuchter, L., Gonzalez, R., Pavlick, A. C., Weber, J. S., McArthur, G. A., Hutson, T. E., Moschos, S. J., Flaherty, K. T., Hersey, P., Kefford, R., Lawrence, D., Puzanov, I., Lewis, K. D., Amaravadi, R. K., Chmielowski, B., Lawrence, H. J., Shyr, Y., Ye, F., Li, J., Nolop, K. B., Lee, R. J., Joe, A. K., & Ribas, A. (2012). Survival in BRAF V600-mutant advanced melanoma treated with vemurafenib. *N Engl J Med, 366*(8), 707-714.

Steingrimsson, E. (2008). All for one, one for all: alternative promoters and Mitf. *Pigment Cell Melanoma Res, 21*(4), 412-414.

Steingrimsson, E., Copeland, N. G., & Jenkins, N. A. (2004). Melanocytes and the microphthalmia transcription factor network. *Annu Rev Genet, 38*, 365-411.

Strub, T., Giuliano, S., Ye, T., Bonet, C., Keime, C., Kobi, D., Le Gras, S., Cormont, M., Ballotti, R., Bertolotto, C., & Davidson, I. (2011). Essential role of microphthalmia transcription factor for DNA replication, mitosis and genomic stability in melanoma. *Oncogene, 30*(20), 2319-2332.

Sturm, R. A. (2009). Molecular genetics of human pigmentation diversity. *Hum Mol Genet, 18*(R1), R9-17.

Sulem, P., Gudbjartsson, D. F., Stacey, S. N., Helgason, A., Rafnar, T., Magnusson, K. P., Manolescu, A., Karason, A., Palsson, A., Thorleifsson, G., Jakobsdottir, M., Steinberg, S., Palsson, S., Jonasson, F., Sigurgeirsson, B., Thorisdottir, K., Ragnarsson, R., Benediktsdottir, K. R., Aben, K. K., Kiemeney, L. A., Olafsson, J. H., Gulcher, J., Kong, A., Thorsteinsdottir, U., & Stefansson, K. (2007). Genetic determinants of hair, eye and skin pigmentation in Europeans. *Nat Genet, 39*(12), 1443-1452.

Sullivan, R. J., & Flaherty, K. T. (2013). Resistance to BRAF-targeted therapy in melanoma. *Eur J Cancer, 49*(6), 1297-1304.

Sundram, U., Harvell, J. D., Rouse, R. V., & Natkunam, Y. (2003). Expression of the B-cell proliferation marker MUM1 by melanocytic lesions and comparison with S100, gp100 (HMB45), and MelanA. *Mod Pathol, 16*(8), 802-810.

Swoboda, A., Schanab, O., Tauber, S., Bilban, M., Berger, W., Petzelbauer, P., & Mikula, M. (2012). MET expression in melanoma correlates with a lymphangiogenic phenotype. *Hum Mol Genet, 21*(15), 3387-3396.

Tachibana, M. (2000). MITF: a stream flowing for pigment cells. *Pigment Cell Res, 13*(4), 230-240.

Tachibana, M., Perez-Jurado, L. A., Nakayama, A., Hodgkinson, C. A., Li, X., Schneider, M., Miki, T., Fex, J., Francke, U., & Arnheiter, H. (1994). Cloning of MITF, the human homolog of the mouse microphthalmia gene and assignment to chromosome 3p14.1-p12.3. *Hum Mol Genet, 3*(4), 553-557.

Takebayashi, K., Chida, K., Tsukamoto, I., Morii, E., Munakata, H., Arnheiter, H., Kuroki, T., Kitamura, Y., & Nomura, S. (1996). The recessive phenotype displayed by a dominant negative microphthalmia-associated transcription factor mutant is a result of impaired nucleation potential. *Mol Cell Biol, 16*(3), 1203-1211.

Takeda, K., Takemoto, C., Kobayashi, I., Watanabe, A., Nobukuni, Y., Fisher, D. E., & Tachibana, M. (2000a). Ser298 of MITF, a mutation site in Waardenburg syndrome type 2, is a phosphorylation site with functional significance. *Hum Mol Genet, 9*(1), 125-132.

Takeda, K., Yasumoto, K., Takada, R., Takada, S., Watanabe, K., Udono, T., Saito, H., Takahashi, K., & Shibahara, S. (2000b). Induction of melanocyte-specific microphthalmia-associated transcription factor by Wnt-3a. *J Biol Chem, 275*(19), 14013-14016.

Tamura, T., Tailor, P., Yamaoka, K., Kong, H. J., Tsujimura, H., O'Shea, J. J., Singh, H., & Ozato, K. (2005). IFN regulatory factor-4 and -8 govern dendritic cell subset development and their functional diversity. *J Immunol, 174*(5), 2573-2581.

Tassabehji, M., Newton, V. E., Liu, X. Z., Brady, A., Donnai, D., Krajewska-Walasek, M., Murday, V., Norman, A., Obersztyn, E., Reardon, W., & et al. (1995). The mutational spectrum in Waardenburg syndrome. *Hum Mol Genet, 4*(11), 2131-2137.

Thomas, A. J., & Erickson, C. A. (2008). The making of a melanocyte: the specification of melanoblasts from the neural crest. *Pigment Cell Melanoma Res, 21*(6), 598-610.

Thomas, A. J., & Erickson, C. A. (2009). FOXD3 regulates the lineage switch between neural crest-derived glial cells and pigment cells by repressing MITF through a non-canonical mechanism. *Development, 136*(11), 1849-1858.

Thumar, J., Giesen, E., & Kluger, H. M. (2012). Drug targets and predictive biomarkers in the management of metastatic melanoma. *Pharmgenomics Pers Med, 5*, 139-148.

Tietz, W. (1963). A syndrome of deaf-mutism associated with albinism showing dominant autosomal inheritance. *Am J Hum Genet, 15*, 259-264.

Tsao, H., Chin, L., Garraway, L. A., & Fisher, D. E. (2012). Melanoma: from mutations to medicine. *Genes Dev, 26*(11), 1131-1155.

Tsuboi, K., Iida, S., Inagaki, H., Kato, M., Hayami, Y., Hanamura, I., Miura, K., Harada, S., Kikuchi, M., Komatsu, H., Banno, S., Wakita, A., Nakamura, S., Eimoto, T., & Ueda, R. (2000). MUM1/IRF4 expression as a frequent event in mature lymphoid malignancies. *Leukemia, 14*(3), 449-456.

Ugurel, S., Houben, R., Schrama, D., Voigt, H., Zapatka, M., Schadendorf, D., Brocker, E. B., & Becker, J. C. (2007). Microphthalmia-associated transcription factor gene amplification in metastatic melanoma is a prognostic marker for patient survival, but not a predictive marker for chemosensitivity and chemotherapy response. *Clin Cancer Res, 13*(21), 6344-6350.

Uranishi, M., Iida, S., Sanda, T., Ishida, T., Tajima, E., Ito, M., Komatsu, H., Inagaki, H., & Ueda, R. (2005). Multiple myeloma oncogene 1 (MUM1)/interferon regulatory factor 4 (IRF4) upregulates monokine induced by interferon-gamma (MIG) gene expression in B-cell malignancy. *Leukemia, 19*(8), 1471-1478.

Valsami, S., Pappa, V., Rontogianni, D., Kontsioti, F., Papageorgiou, E., Dervenoulas, J., Karmiris, T., Papageorgiou, S., Harhalakis, N., Xiros, N., Nikiforakis, E., & Economopoulos, T. (2007). A clinicopathological study of B-cell differentiation markers and transcription factors in classical Hodgkin's lymphoma: a potential prognostic role of MUM1/IRF4. *Haematologica, 92*(10), 1343-1350.

van der Veen, A. G., & Ploegh, H. L. (2012). Ubiquitin-like proteins. *Annu Rev Biochem, 81*, 323-357.

van Imhoff, G. W., Boerma, E. J., van der Holt, B., Schuuring, E., Verdonck, L. F., Kluin-Nelemans, H. C., & Kluin, P. M. (2006). Prognostic impact of germinal center-associated proteins and chromosomal breakpoints in poor-risk diffuse large B-cell lymphoma. *J Clin Oncol, 24*(25), 4135-4142.

Vance, K. W., Carreira, S., Brosch, G., & Goding, C. R. (2005). Tbx2 is overexpressed and plays an important role in maintaining proliferation and suppression of senescence in melanomas. *Cancer Res, 65*(6), 2260-2268.

Waardenburg, P. J. (1951). A new syndrome combining developmental anomalies of the eyelids, eyebrows and nose root with pigmentary defects of the iris and head hair and with congenital deafness. *Am J Hum Genet, 3*(3), 195-253.

Wada, D. A., Law, M. E., Hsi, E. D., Dicaudo, D. J., Ma, L., Lim, M. S., Souza, A., Comfere, N. I., Weenig, R. H., Macon, W. R., Erickson, L. A., Ozsan, N., Ansell, S. M., Dogan, A., & Feldman, A. L. (2011). Specificity of IRF4 translocations for primary cutaneous anaplastic large cell lymphoma: a multicenter study of 204 skin biopsies. *Mod Pathol, 24*(4), 596-605.

Wan, P., Hu, Y., & He, L. (2011). Regulation of melanocyte pivotal transcription factor MITF by some other transcription factors. *Mol Cell Biochem, 354*(1-2), 241-246.

Wang, N., & Hebert, D. N. (2006). Tyrosinase maturation through the mammalian secretory pathway: bringing color to life. *Pigment Cell Res, 19*(1), 3-18.

Wellbrock, C., & Marais, R. (2005). Elevated expression of MITF counteracts B-RAF-stimulated melanocyte and melanoma cell proliferation. *J Cell Biol, 170*(5), 703-708.

Wellbrock, C., Ogilvie, L., Hedley, D., Karasarides, M., Martin, J., Niculescu-Duvaz, D., Springer, C. J., & Marais, R. (2004). V599EB-RAF is an oncogene in melanocytes. *Cancer Res, 64*(7), 2338-2342.

Wellbrock, C., Rana, S., Paterson, H., Pickersgill, H., Brummelkamp, T., & Marais, R. (2008). Oncogenic BRAF regulates melanoma proliferation through the lineage specific factor MITF. *PLoS One, 3*(7), e2734.

Widlund, H. R., Horstmann, M. A., Price, E. R., Cui, J., Lessnick, S. L., Wu, M., He, X., & Fisher, D. E. (2002). Beta-catenin-induced melanoma growth requires the downstream target Microphthalmia-associated transcription factor. *J Cell Biol, 158*(6), 1079-1087.

Winter, J. N., Gascoyne, R. D., & Van Besien, K. (2004). Low-grade lymphoma. *Hematology Am Soc Hematol Educ Program*, 203-220.

Wu, M., Hemesath, T. J., Takemoto, C. M., Horstmann, M. A., Wells, A. G., Price, E. R., Fisher, D. Z., & Fisher, D. E. (2000). c-Kit triggers dual phosphorylations, which couple activation and degradation of the essential melanocyte factor Mi. *Genes Dev, 14*(3), 301-312.

Yamada, M., Asanuma, K., Kobayashi, D., Moriai, R., Yajima, T., Yagihashi, A., Yamamori, S., & Watanabe, N. (2001). Quantitation of multiple myeloma oncogene 1/interferon-regulatory factor 4 gene expression in malignant B-cell proliferations and normal leukocytes. *Anticancer Res, 21*(1B), 633-638.

Yamaguchi, Y., & Hearing, V. J. (2009). Physiological factors that regulate skin pigmentation. *Biofactors, 35*(2), 193-199.

Yasumoto, K., Yokoyama, K., Shibata, K., Tomita, Y., & Shibahara, S. (1994). Microphthalmia-associated transcription factor as a regulator for melanocyte-specific transcription of the human tyrosinase gene. *Mol Cell Biol, 14*(12), 8058-8070.

Yasumoto, K., Yokoyama, K., Takahashi, K., Tomita, Y., & Shibahara, S. (1997). Functional analysis of microphthalmia-associated transcription factor in pigment cell-specific transcription of the human tyrosinase family genes. *J Biol Chem, 272*(1), 503-509.

Yavuzer, U., Keenan, E., Lowings, P., Vachtenheim, J., Currie, G., & Goding, C. R. (1995). The Microphthalmia gene product interacts with the retinoblastoma protein in vitro and is a target for deregulation of melanocyte-specific transcription. *Oncogene, 10*(1), 123-134.

Yokoyama, S., Woods, S. L., Boyle, G. M., Aoude, L. G., Macgregor, S., Zismann, V., Gartside, M., Cust, A. E., Haq, R., Harland, M., Taylor, J. C., Duffy, D. L., Holohan, K., Dutton-Regester, K., Palmer, J. M., Bonazzi, V., Stark, M. S., Symmons, J., Law, M. H., Schmidt, C., Lanagan, C., O'Connor, L., Holland, E. A., Schmid, H., Maskiell, J. A., Jetann, J., Ferguson, M., Jenkins, M. A., Kefford, R. F., Giles, G. G., Armstrong, B. K., Aitken, J. F., Hopper, J. L., Whiteman, D. C., Pharoah, P. D., Easton, D. F., Dunning, A. M., Newton-Bishop, J. A., Montgomery, G. W., Martin, N. G., Mann, G. J., Bishop, D. T., Tsao, H., Trent, J. M., Fisher, D. E., Hayward, N. K., & Brown, K. M. (2011). A novel recurrent mutation in MITF predisposes to familial and sporadic melanoma. *Nature, 480*(7375), 99-103.

Yoshida, S., Nakazawa, N., Iida, S., Hayami, Y., Sato, S., Wakita, A., Shimizu, S., Taniwaki, M., & Ueda, R. (1999). Detection of MUM1/IRF4-IgH fusion in multiple myeloma. *Leukemia, 13*(11), 1812-1816.

Zdarsky, E., Favor, J., & Jackson, I. J. (1990). The molecular basis of brown, an old mouse mutation, and of an induced revertant to wild type. *Genetics, 126*(2), 443-449.

Zinzani, P. L., Dirnhofer, S., Sabattini, E., Alinari, L., Piccaluga, P. P., Stefoni, V., Tani, M., Musuraca, G., Marchi, E., Falini, B., Baccarani, M., & Pileri, S. A. (2005). Identification of outcome predictors in diffuse large B-cell lymphoma. Immunohistochemical profiling of homogeneously treated de novo tumors with nodal presentation on tissue micro-arrays. *Haematologica, 90*(3), 341-347.

Paper I :
Christine Grill, Kristín Bergsteinsdóttir, Margrét H. Ögmundsdóttir, Vivian Pogenberg, Alexander Schepsky, Matthias Wilmanns, Veronique Pingault, and Eiríkur Steingrímsson

MITF mutations associated with pigment deficiency syndromes and melanoma have different effects on protein function
Hum. Mol. Genet. (2013) 22 (21): 4357-4367
first published online June 20, 2013 doi:10.1093/hmg/ddt285

Online available at : http://hmg.oxfordjournals.org/

HMG Advance Access published June 26, 2013

Human Molecular Genetics, 2013 **1–11**
doi:10.1093/hmg/ddt285

MITF mutations associated with pigment deficiency syndromes and melanoma have different effects on protein function

Christine Grill[1], Kristín Bergsteinsdóttir[1], Margrét H. Ögmundsdóttir[1], Vivian Pogenberg[2], Alexander Schepsky[1], Matthias Wilmanns[2], Veronique Pingault[3] and Eiríkur Steingrímsson[1,*]

[1]Department of Biochemistry and Molecular Biology, BioMedical Center, Faculty of Medicine, University of Iceland, Vatnsmyrarvegi 16, 101 Reykjavik, Iceland, [2]European Molecular Biology Laboratory, Hamburg Unit, Notkestrasse 85, 22603 Hamburg, Germany and [3]INSERM Unit U955, Department of Genetics, Créteil F-94000, France

Received April 16, 2013; Revised May 27, 2013; Accepted June 11, 2013

The basic-helix–loop–helix-leucine zipper (bHLHZip) protein MITF (microphthalmia-associated transcription factor) is a master regulator of melanocyte development. Mutations in the MITF have been found in patients with the dominantly inherited hypopigmentation and deafness syndromes Waardenburg syndrome type 2A (WS2A) and Tietz syndrome (TS). Additionally, both somatic and germline mutations have been found in MITF in melanoma patients. Here, we characterize the DNA-binding and transcription activation properties of 24 MITF mutations found in WS2A, TS and melanoma patients. We show that most of the WS2A and TS mutations fail to bind DNA and activate expression from melanocyte-specific promoters. Some of the mutations, especially R203K and S298P, exhibit normal activity and may represent neutral variants. Mutations found in melanomas showed normal DNA-binding and minor variations in transcription activation properties; some showed increased potential to form colonies. Our results provide molecular insights into how mutations in a single gene can lead to such different phenotypes.

INTRODUCTION

Microphthalmia-associated transcription factor (MITF) is a bHLHZip transcription factor which belongs to the MYC supergene family. MITF plays an important role in melanocytes, where it has been shown to be involved in regulating many diverse events, including proliferation, differentiation, apoptosis, DNA replication, mitosis and genome stability (reviewed in 1 and 2). Mice which lack MITF have white coat color due to the absence of melanocytes (reviewed in 3).

Mutations in the human MITF gene have been found in patients with the hypopigmentation and deafness syndromes Waardenburg (WS) and Tietz (TS) (reviewed in 3–5). Both syndromes are listed as rare diseases by the Office of Rare Diseases Research (USA) and Orphanet (Europe). WS is an auditory-pigmentary syndrome named after the Dutch ophthalmologist Petrus Waardenburg (6). Four types of WS have been described, all with similar clinical features including sensorineural hearing loss, hypopigmentation of skin (usually patches of hypopigmentation) and hair and pigmentary disturbances of the irises (hypoblastic blue irides and/or heterochromia). In contrast to WS type 1 (WS1), WS2 patients do not show dystopia canthorum (eyelid anomaly; lateral displacement of the inner canthi of the eye) (6–8). The phenotype of WS3 and WS4 patients is similar to WS1 but with additional hypoplasia of limb muscles (WS3) or Hirschprung's disease (WS4). WS2 is inherited in an autosomal-dominant fashion (8). Mutations in MITF have been found in a subset of WS2 patients, categorized as type 2A. WS1 and WS3 have been shown to be due to mutations in PAX3, and WS4 to be due to mutations in the receptor–ligand pair EDN3/EDNRB or in the transcription factor SOX10 (reviewed in 9). SOX10 mutations have also been found in some cases of WS2, termed WS2E (reviewed in 9). TS is another rare hypopigmentation disorder characterized by profound congenital hearing loss and generalized hypopigmentation and is inherited in a fully penetrant autosomal-dominant fashion. MITF mutations have been found in TS patients (5,10–12).

*To whom correspondence should be addressed at: Department of Biochemistry and Molecular Biology, BioMedical Center, Faculty of Medicine, University of Iceland, Vatnsmyrarvegi 16, 101 Reykjavik, Iceland. Tel: +354 5254270; Email: eirikurs@hi.is

© *The Author 2013. Published by Oxford University Press. All rights reserved.*
For Permissions, please email: journals.permissions@oup.com

In addition to being essential during melanocyte development, MITF also plays an important role in melanoma. Overexpression of MITF has been shown in cutaneous melanomas (13,14) and MITF gene amplification has been observed in about 30% of metastatic melanoma (15). Somatic mutations in MITF have been found in metastatic melanoma samples (16) and recently, a germline mutation was found in families where several members had melanoma (17,18). MITF has been proposed to fulfill all the criteria of a lineage-survival oncogene (reviewed in 19). As human MITF mutations are found in both auditory-pigmentary disorders and melanomas, it is of importance to understand how mutations in the same transcription factor can lead to such different phenotypes.

Here, we analyzed the DNA-binding and transcription activation ability of 18 MITF mutations found in WS2 and TS patients and 6 MITF mutations found to date in melanoma patients. Our results show that 11 of the 18 mutations associated with WS2 and TS failed to bind DNA and were unable to activate expression from melanocyte-specific promoters. On the other hand, the MITF mutations found in melanoma patients were able to bind DNA and activate expression from melanocyte-specific promoters; some showed increased potential to form colonies. Our functional analysis of human MITF mutations reveals novel insights into their ability to bind DNA, activate transcription and form colonies.

RESULTS

The human MITF mutations studied

A summary of all known human missense MITF mutations found in WS2A and TS patients as well as in melanomas is provided in Table 1, together with information on their location within the protein, the phenotypes assigned to the mutations, the mode of inheritance and the reference describing their characterization. All these mutations were originally identified in genomic DNA. Sometimes, the same mutation has been described in different families (such as R214X, R217del and R217I) and is therefore mentioned accordingly in Table 1. Figure 1A shows the location of the mutations in the protein. In addition to missense mutations, we included the R217del mutation which deletes three nucleotides leading to a deletion of arginine 217 and two stop mutations which result in truncated MITF proteins (R214X and R259X). The R214X mutation results in a protein which truncates in the basic region (BR), whereas R259X truncates in the helix–loop–helix domain.

Table 1. Summary of Mitf mutations in WS and TS and melanomas used in this study

Mutation	Location	Disease	Authors	Phenotype/remarks	Inheritance
E87R	AD	Melanoma	Cronin *et al.* (16)	Metastatic melanomas with BRAF (V600E) mutation	Somatic
L135V	AD	Melanoma	Cronin *et al.* (16)	Metastatic melanomas	Somatic
L142F	AD	Melanoma	Cronin *et al.* (16)	Metastatic melanomas	Somatic
R203K	BR	WS2	Tassabehji *et al.* (5)	Typical WS2. Mutation found in proband does not segregate with disease	Neutral variant
K206Q	BR	WS2	Leger *et al.* (12)	36-year female; SNHL, white forelock blue irides	Familial
N210K	BR	Tietz	Smith *et al.* (10)	Deafness, blonde hair, white eyelashes & eyebrows, cutaneous hypopigmentation	Familial
I212M	BR	Tietz/WS2	Welch *et al.* (43)	Blue eyes, hypopigmentation of hair and skin, 14 of 28 affected members have SNHL	Familial
I212S	BR	WS2	Leger *et al.* (12)	9-year male; generalized hypopigmentation, freckles, blue irides, premature graying	Familial
E213D	BR	WS2	Leger *et al.* (12)	33-year female; SNHL, white forelock, premature graying, blue irides	*De novo*
R214X	BR	WS2	Lalwani *et al.* (42)	SNHL, heterochromia of the irides, premature graying, white forelock, a three-generation WS2 family	Familial
-	-	WS2	Nobukuni *et al.* (40)	SNHL, heterochromia of the irides, white forelock, early graying	Familial
R216K	BR	WS2	Leger *et al.* (12)	21-year female; SNHL, white forelock, fair skin, blue irides	*De novo*
R217del	BR	Tietz	Leger *et al.* (12)	3-year female; SNHL, generalized hypopigmentation, blue irides	Familial
-	-	WS2	Chen *et al.* (41)	Three affected families	Familial
-	-	Tietz	Tassabehji *et al.* (5)	SNHL, blonde/red hair color, pale skin, blue irides; dominant pedigree	Familial
-l	-	Tietz	Shigemura *et al.* (11)	15-year male, generalized hypopigmentation, blue irides, blonde hair and eyebrows	Familial
R217I	BR	Tietz	Léger *et al.* (12)	3-year female; SNHL, generalized hypopigmentation, blue irides and white forelock	Familial
-	-	WS2	Chen *et al.* (41)	SNHL, blue irides, premature graying	*De novo*
R217G	BR	WS2	Chen *et al.* (41)	No data available	n/a
I224S	HLH	WS2	Pingault *et al.* (9)	6-year female; SNHL, white forelock, heterochromia of the irides	Familial
G244R	HLH	Melanoma	Cronin *et al.* (16)	Metastatic melanomas with BRAF (V600E) mutation	Somatic
S250P	HLH	WS2	Tassabehji *et al.* (5)	Female patient; unilateral hearing loss, premature graying	Familial
Y253C	HLH	WS2	Read *et al.* (8)	No data available	n/a
R259X	HLH	WS2	Nobukuni *et al.* (40)	SNHL, heterochromia of the irides, white forelock, early graying	Familial
N278D	ZD	WS2	Tassabehji *et al.* (5)	Female patient; SNHL, inherited from unaffected father	Familial
L283P	ZD	WS2	This study	30-year female; SNHL, heterochromia of the irides	Familial
S298P	AD	WS2	Tassabehji *et al.* (5)	Affected patient comes from a three-generation history of WS2	Neutral variant
E318K	AD	Melanoma	Bertolotto *et al.* (17)	Five of 62 melanoma and renal cell carcinoma patients harbor the E318K mutation	Germline
D380N	AD	Melanoma	Cronin *et al.* (16)	Metastatic melanomas with a BRAF (V600E) mutation	Somatic

AD, activation domain; BR, basic region; HLH, helix–loop–helix; ZD, zipper domain; SNHL, sensorineural hearing loss, n/a not available.

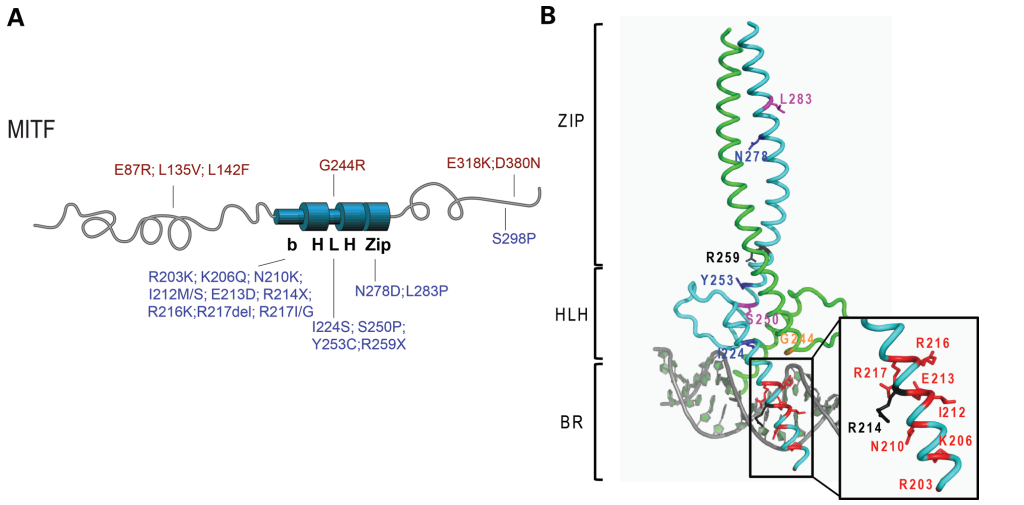

Figure 1. MITF mutations found in melanoma, WS2A and TS patients. (**A**) A graphic depiction of the human MITF protein with the location of the mutations indicated. The mutations found in melanoma patients are indicated in red (on top). These mutations are located at the amino- and carboxyl ends, and only one mutation is located in the helix–loop–helix domain (G244R). The mutations found in WS2A and TS patients are indicated in blue (on the bottom). Most of these mutations are located in the BR of MITF and in the HLH and zipper domains. The WS2A mutation S298P is located at the carboxyl end of MITF. (**B**) Structure of the bHLHZip region of MITF showing the location of the mutant residues. To separate mutations leading to TS and WS2A syndromes and those causing melanoma, the respective mutations are mapped on two different molecules of the dimeric MITF structure. The TS/WS2A mutations on the first protomer in cyan are highlighted in the following colors: residues mutated into stop codons, black; residues mutated into prolines, magenta; residues when mutated affecting direct DNA contacts, red; residues when mutated affecting protein–protein interactions, blue. In sharp contrast, only one melanoma-inducing mutation has been found within the bHLHZip region for which the structure of MITF was determined. This mutation (G244) has been highlighted in orange on the second MITF protomer, colored in green.

These mutations were included in the study as negative controls as we expected them to be functionally inactive. MITF mutations associated with WS2A and TS (indicated in blue) are located in the basic (11 of 18), helix–loop–helix (4 of 18) and zipper (2 of 18) domains of the protein; one mutation (S298P) is located in the carboxy terminal region of MITF (Fig. 1A). Mutations associated with melanoma (indicated in red) are primarily located in the amino (three of six) and carboxyl (two of six) ends of MITF, but also in the bHLHZip region (one of six) (Fig. 1A); all but one are somatic mutations. The only germline mutation associated with melanoma is E318K. Figure 1B shows where mutations, which affect the bHLHZip region, are located in the MITF structure (20).

For functional analysis, all the mutations were re-created in a mouse *Mitf* expression construct which produces the melanocyte-specific M-MITF protein (reviewed in 3). Sequence alignment of the mouse and human MITF proteins showed 94% identity; all the mutant sites are completely conserved between the two species (Supplementary Material, Fig. S1). In addition, we created two different E213D mutations [the original c.639A>C mutation identified by (21) and a c.639A>T mutation (not found in WS2A patients) both of which result in a substitution for aspartic acid] and the N278P mutation which introduces a helical breaker in the leucine zipper segment of the protein.

Eleven out of 18 WS2A and TS mutations failed to bind DNA

To determine DNA-binding ability of the wild-type and mutant MITF proteins, electrophoretic mobility shift assays (EMSAs) were performed using a double-stranded oligonucleotide with a central E-box (CACGTG) as a probe. The proteins were expressed using an *in vitro* translation system; expression analyzed using western blot analysis and protein levels adjusted to eliminate differences in DNA-binding studies (Supplementary Material, Fig. S2).

As shown in Figure 2, 6 of the 11 mutations which affect the BR of MITF (E213D, R214X, R216K, R217Del, R217I, R217G) failed to bind the E-box DNA sequence (CACGTG). The R203K and N210K mutant proteins were able to bind to the E-box probe equal to wild-type MITF, whereas the K206Q mutant protein showed some but decreased binding ability (Fig. 2A). Changing residue I212 to either methionine (I212M) or serine (I212S) did not affect the ability to bind the E-box sequence (Fig. 2B). Mutations in the HLH domain (I224S, S250P and R259X) induced loss of DNA binding (Fig. 2B and C). Interestingly, the tyrosine-to-cysteine substitution at residue 253 was able to bind DNA, albeit weakly (Fig. 2C). Mutations affecting the zipper domain (N278D/P and L283P) also failed to bind DNA. The L283P mutation is a novel non-truncating MITF mutation found in a WS2A patient (Table 1). The only WS2A mutation located at the C-terminal region of MITF, S298P, did not affect the DNA-binding ability. In summary, 11 out of the 18 WS2A and TS mutations investigated failed to bind DNA.

MITF also binds strongly to the TCATGTG sequence, sometimes referred to as the M-box sequence (20). In order to investigate if the MITF mutant proteins which showed E-box binding (R203K, K206Q, N210K, I212M, I212S and S298P) can also bind this sequence, gel shift assays were performed using

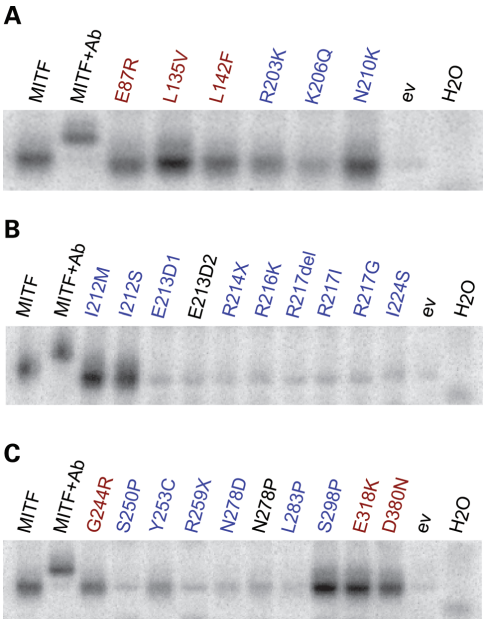

Figure 2. MITF mutations and their ability to bind the E-box. (**A**–**C**) EMSAs showing the binding of wild-type and mutant MITF proteins to the E-box sequence (CACGTG). In each case, Lane 1 shows binding of the wild-type MITF protein, and Lane 2 shows a supershift where the C5 MITF antibody was added. Empty vector pcDNA3.1 (ev) and water (H_2O) were loaded as negative controls. Melanoma mutations are indicated in red, whereas WS2A and TS mutations are indicated in blue. The synthetic E213D2 and N278P mutations are indicated in black. Representative data from three separate experiments are shown.

TCATGTG as a probe. As was seen with the E-box probe, the R203K, N210K and S298P mutations can bind the M-box sequence similar to wild–type, whereas K206Q has severely impaired DNA-binding ability (Supplementary Material, Fig. S3). Consistent with previous results (20), the two I212 mutations (I212M/S) showed less binding to the M-box than to the E-box (Supplementary Material, Fig. S3). In summary, our results show that most mutations associated with WS2A and TS failed to bind DNA. The exceptions are R203K, N210K and S298P which show normal-level DNA binding, and the Y253C and K206Q mutations which show reduced but significant DNA binding. The two I212 mutations, I212M and I212S, affect the ability of MITF to bind the M-box but not the E-box. This position has been suggested to determine the ability of MITF to bind the M-box sequence (20).

DNA-binding ability of MITF mutations found in melanoma is similar to wild-type MITF

Gel shift assays were also used to determine the DNA-binding ability of MITF mutations found in melanoma patients. The E87R, L135V, L142F, G244R, E318K and D380N mutations did not affect the DNA-binding ability of MITF to either the E-box (Fig. 2A and C) or the M-box (Supplementary Material, Fig. S3). Interestingly, the L135V protein showed increased DNA binding when compared with wild-type MITF (Fig. 2A and Supplementary Material, Fig. S3).

Reduced transcription activation potential of WS2A and TS mutants

In order to investigate whether the MITF mutants were able to activate gene expression, we performed reporter gene assays with several different MITF target promoters. MITF has been shown to activate expression from the melanocyte-specific tyrosinase (TYR), tyrosinase-related protein 1 (TYRP1) and dopachrome tautomerase (DCT) promoters (22–24) (Supplementary Material, Fig. S4). HEK293T cells, which do not express MITF endogenously, were cotransfected with the respective promoter constructs and MITF expression constructs (wild type or mutant) and effects on expression determined using luciferase reporter assays. Supplementary Material, Figure S5 shows that all the transfected cells express the MITF protein. Figure 3A shows fold activation by the mutant proteins when compared with wild-type MITF for the four different promoters used. Consistent with the results of the DNA-binding assays, 11 of the 18 mutations which affect the basic (E213D1/2, R214X, R216K, R217Del, R217I and R217G), the HLH (I224S, S250P and R259X) and zipper domains (N278D/P and L283P) of MITF failed to activate expression from the TYR promoter ($P < 0.05$). The R206Q and the Y253C mutant proteins showed a significantly reduced ability to activate tyrosinase expression [48 and 71% compared with wild-type MITF ($P < 0.05$)], consistent with the reduced ability to bind DNA. The two I212 mutations (I212M and I212S) also showed a significantly reduced ability to activate expression from the TYR promoter ($P < 0.05$). The TYR promoter contains one E-box and one M-box. Since both mutant proteins bound the E-box at similar levels as the wild-type MITF protein but showed reduced binding to the M-box, this suggests either that the M-box is more important for activating TYR expression or that these sites act cooperatively. Alternatively, the I212 mutations may affect transactivation ability of MITF. Surprisingly, the R203K, N210K and S298P mutations, which are all able to bind the E-box, showed significantly increased transcription activity compared with wild-type MITF ($P < 0.05$). Indeed, the activation of tyrosinase by the R203K and N210K mutations was 1.5- and 2.2-fold compared with wild-type MITF ($P = \leq 5 \times 10^{-4}$ and $< 9.3 \times 10^{-6}$, respectively), whereas the S298P mutation activated TYR 1.3-fold compared with wild-type MITF ($P = 0.042$).

We also determined the ability of the mutations to activate expression of the pigment-cell specific TYRP1 promoter (Fig. 3A). The mutations either completely failed to activate expression from this promoter (R214X, R216K, R217Del, R217I, R217G, I224S, S250P, R259X, N278D, N278P and L283P) or showed significant reduction (R203K, K206Q, N210K, I212M/S, E213D and Y253C) in activation when compared with wild type ($P < 0.05$). The hyperactivation observed with the R203K, N210K and S298P mutant proteins from the TYR promoter was not observed using the TYRP1 reporter nor with the other reporters used in the study (see below). In fact, all the three mutations showed reduced TYRP1 activation when compared with wild-type MITF (Fig. 3A).

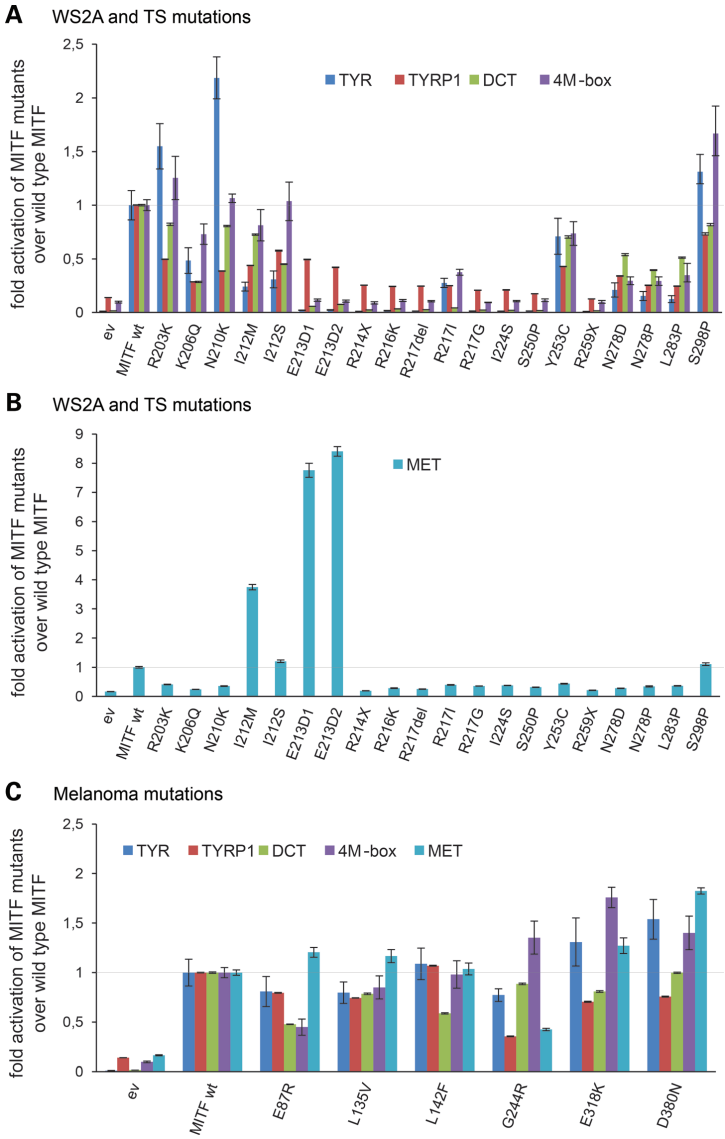

Figure 3. Transcriptional activity of MITF mutations associated with WS2A, TS and melanoma. (**A**) Transcription activation ability of WS2A and TS mutant proteins from the TYR, TYRP1, DCT and 4M-box promoters. The data are shown as fold activation of MITF mutants over wild-type MITF. Error bars indicate the standard error of mean. (**B**) Transcription activation ability of WS2A and TS mutations from the MET promoter. The I212M and E213D mutations show hyperactivation from the MET promoter. The data are shown as fold activation of MITF mutants over wild-type MITF. Error bars indicate the standard error of mean. (**C**) Transcription activation ability of the melanoma mutations from the TYR, TYRP1, DCT, 4M-box and MET promoters. All cotransfection assays were repeated twice in six replicates and fold induction calculated over MITF wild type.

Similar to what was observed with the TYR promoter, MITF mutations which affect the basic and HLH regions failed to activate expression from the DCT promoter (Fig. 3A). The K206Q, I212S, N278D, N278P and L283P mutations showed reduced activation, whereas the E213D, R214X, R216K, R217Del, R217I, R217G, I224S and R259X mutations showed a complete lack of

activation ($P < 0.05$). The R203K, N210K and S298P mutations showed somewhat reduced transcription activation potential (82.4, 80.7 and 81%, respectively) when compared with the wild-type MITF protein, but the difference was not statistically significant. As these mutations lead to increased TYR activation, this suggests that the mutant proteins can have promoter-specific effects on transcription. The I212M and Y253C proteins showed slightly but significantly reduced transcription activation of DCT (72.7 and 70.5%, respectively, compared with wild-type MITF, $P < 0.05$).

MITF robustly activates expression of a synthetic promoter consisting of four tandem M-box sequences (23). The R203K, N210K and I212M/S mutations were able to activate expression from this promoter construct at levels similar to wild-type MITF (Fig. 3A), whereas the K206Q mutation showed reduced activation (73.1% compared with wild-type MITF, $P = 0.0075$). The only mutation which showed hyperactivation from this synthetic promoter was S298P, which showed a 1.67-fold increase ($P < 0.05$). The remaining mutations (E213D, R214X, E216K, R217Del, R217I, R217G, I224S, S250P, Y253C, R259X, N278D, N278P and L283P) failed to activate the 4M-box construct ($P < 0.05$).

The proto-oncogene MET, which encodes the cell-surface receptor for hepatocyte growth factor (25), has been implicated in renal cell carcinoma (26) and in late stages of melanoma (27). Chromatin-immunoprecipitation coupled to high throughput sequencing of a human melanoma cell line (501mel) revealed that MET is a target of MITF and that MITF is able to activate expression from the MET promoter (17,28) (Supplementary Material, Fig. S4b). Most of the MITF mutations associated with WS2A and TS (R203K, K206Q, N210K, R214X, R216K, R217Del, R217I, R217G, I224S, S250P, Y253C, R259X, N278D/P and L183P) were unable to activate expression from the MET promoter ($P < 0.05$) (Fig. 3B). The I212S and S298P mutations showed activation potential similar to wild-type MITF (1.2- and 1.1-fold, respectively). Although the R203K, K206Q, N210K and Y253C proteins were able to bind DNA, they were unable to activate expression from the MET promoter. Surprisingly, the I212M and E213D mutations showed strong activation of the MET promoter, 3.7- and 8-fold activation compared with wild-type MITF, respectively (Fig. 3B). The I212M mutation alters the DNA-binding profile of MITF, such that it binds less to the M-box than to E-box sequences (20), whereas the E213D mutation cannot bind the E-box sequence.

To summarize, our results suggest that 11 of the 18 mutations associated with WS2A and TS located within the BR (E213D, R214X, R216K, R217Del, R217I and R217G), the HLH domain (I224S, S250P and R259X), and the three mutations affecting the zipper domain (N278D and L283P) fail to activate expression from melanocyte-specific promoters such as TYR TYRP1, DCT and the synthetic 4M-box promoter (Fig. 3A and B). However, mutations at the beginning of the BR (R203K and N210K) and the S298P mutation at the C-terminus can still activate expression from many pigment-cell specific promoters. Importantly, 2 of the 18 mutations lead to a promoter-specific increase in expression, most notably the MET promoter.

Mutations associated with melanoma have promoter-specific effects on transcription

We also tested the transcription activation ability of MITF mutations associated with melanoma. Interestingly, these mutations had promoter-specific effects on transcription activation, and the effects depended on where in the protein the mutations are located (Fig. 3C). The E87R mutation showed statistically significant reduced activation from the TYR, TYRP1, DCT and 4M-box promoters and L135V for TYR, TYRP1 and DCT ($P < 0.05$). However, both proteins activated MET at normal levels. The L142F mutant protein showed a normal level of transcription activation from all promoters tested, except DCT, which was reduced to ~50% of the levels seen in wild-type MITF (Fig. 3C). The G244R mutation, located in the HLH domain of MITF, showed varied promoter-specific effects with reduced activation of TYR, TYRP1 and MET promoters, normal activation of DCT and increased expression of the synthetic 4M-box promoter (1.35-fold induction; $P < 0.05$). Interestingly, the two mutations located in the carboxyl end of MITF, E318K and D380N showed significantly increased activation potential from the TYR (1.3- and 1.5-fold, respectively), 4M-box (1.7- and 1.4-fold, respectively) and MET (1.3- and 1.82-fold, respectively) promoters; activation of TYRP1 was reduced in both cases whereas activation of DCT was not statistically different from wild type (Fig. 3C).

Nuclear localization

Since the results of the transcription activation assays were performed in cell-based assays using HEK293T cells, it was possible that the effects observed in those assays were due to altered nuclear localization of the mutant proteins. Thus, we determined the nuclear localization of all the MITF mutations by transfecting HEK293T cells with each of the mutant proteins and then used the 1D2 monoclonal anti-MITF antibody (29) to determine subcellular localization. The results show that all the mutations are primarily located in the nuclei (Supplementary Material, Fig. S6), except the two deletion mutations R214X and R259X which also have a major cytoplasmic component as seen by staining with the C5 anti-MITF antibody (the 1D2 antibody recognizes the C-end of MITF which is missing from the two mutants). Surprisingly, the R217del mutation which has been shown to affect nuclear localization of MITF in NIH3T3 and 293T cells (30) was nuclear in our assay using either the 1D2 or C5 antibodies.

Clonogenicity

In order to investigate whether the MITF mutants associated with melanoma have clonogenic properties that differ from the wild-type protein, we created stable HEK293 cell lines carrying the MITF mutations E87R, L142F, G244R and D380N. As controls, we also created stable lines expressing wild-type MITF and empty vector. All the lines created expressed the respective proteins at similar levels (Supplementary Material, Fig. S7). In order to investigate the clonogenic potential of these mutant proteins, we seeded 2500 cells in three replicates and cultured the cells for

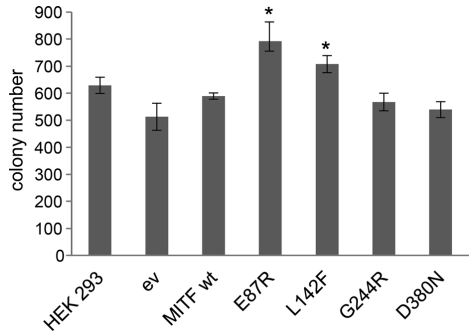

Figure 4. Clonogenic behavior of MITF mutations associated with melanoma. Untransfected HEK293 cells, empty vector and wild-type MITF transfected cells showed similar clonogenic potential. The slight differences observed were not statistically significant. The melanoma mutations E87R and L142F showed significantly ($P < 0.05$, indicated by asterisks) higher clonogenic potential than wild-type MITF. The G244R and D380N mutations behaved like wild-type MITF.

1 week. Cells transfected with an empty vector or wild-type MITF showed similar clonogenic potential as HEK293 cells alone (Fig. 4). Although there were slight variations in the colony formation of empty vector transfected cells and untransfected HEK293 cells, these differences were not statistically significant (Fig. 4). As shown in Figure 4, the melanoma mutations E87R and L142F showed significantly higher clonogenicity than wild-type MITF (34 and 20% increase, respectively). However, the G244R and D380N mutations showed the same clonogenic behavior as wild-type MITF.

DISCUSSION

Our analysis of the DNA-binding and transcription activation potential of human MITF mutations associated with melanoma and WS2A and TS is summarized in Table 2. Eleven of 18 WS2A and TS mutations showed no DNA-binding or transcription activation potential. Many of the mutations affect residues in the DNA-binding domain which make specific contacts with DNA, including E213 and R217 as well as R216, which does not make direct contacts with DNA but is conserved in the MITF subfamily of bHLHZip proteins (20). The exact role of R216 is not clear, and it is surprising that changing this residue for lysine, another basic amino acid, has this large effect on DNA binding. The R217del, R214X and R259X mutations have no affinity for DNA (Fig. 2) (20) and, therefore, serve as negative controls. The R214X mutation is missing a significant portion of the DNA-binding domain and all the rest of the protein, and can thus not bind DNA. The R259X mutation is missing everything following the HLH domain and presumably cannot form DNA-binding homodimers. Consistent with that conclusion, other mutations affecting the structure of the HLH and ZIP regions also affect the DNA-binding ability of MITF. This includes the S250P, L283P, I224S and N278D mutations. In the structure of MITF, N278 plays an important role in forming hydrogen bonds in one of the heptad repeats of the leucine zipper, thus connecting the two MITF protomers (20). Consequently, DNA-binding ability is abolished when this residue is mutated to aspartate (Fig. 2C). Mutating N278, S250 and L283 to proline, an amino acid that cannot be accommodated in an α-helix, disrupts proper folding of the respective regions and, therefore, impairs the dimerization ability of MITF. Due to its location in the hydrophobic core of the HLH domain, we expect the I224S mutation to disrupt the nearby three-dimensional structure as well. The fact that mutations affecting dimerization of MITF lead to dominant phenotypes suggests that haploinsufficiency can lead to WS2A and TS.

Surprisingly, a third of the WS2A and TS mutations showed normal or near-normal DNA-binding and transcription activation ability. The R203K and K206Q mutations showed somewhat reduced DNA binding, whereas the N210K, I212M, I212S and S298P mutations all showed normal-level binding to the E-box sequence. All six mutations showed significant transcription activation ability from some of the promoters tested, especially R203K, N210K and S298P, which activate expression of some promoters at normal levels and some at increased levels. The R203K mutation was originally described in a patient who inherited it from his unaffected mother (5). The family had a four-generation history of WS2, but only one member harbored the R203K mutation (5). This, together with the fact that the R203K mutant protein behaves like the wild-type MITF protein suggests that this is a neutral variant and not a disease-causing mutation. The side chain of the R203 residue was not visible in the structure of the MITF protein (20), and at present its role is not entirely clear. Residues 210–221 of MITF have been suggested to contain a nuclear localization signal (30). The I212N mutation is able to enter the nucleus (30) and so is the R217I mutation (31). The nuclear localization potential of the other mutations affecting this region has not been tested; all fail to bind DNA *in vitro*, except N210K.

The N210K mutation was originally identified in a family where affected family members were reported as born 'snow-white' but gradually gained some pigmentation; they had blue eye color and bilateral congenital sensorineural and profound hearing loss (10). Surprisingly, the N210K mutant protein retains significant DNA-binding and transcriptional activity. Interestingly, this position has been shown to be mutated to serine (N210S) in macchiato Franches-Montagnes horses (also called Freiberger). MITF is 97.9% conserved between humans and horses; the N210 position is conserved (Supplementary Material, Fig. S8). An EMSA showed that the N210S mutation had reduced ability to bind the M-box probe (32). The N210S mutation thus has more severe effects on protein function *in vitro* than the N210K mutation. Consistent with this, lysine is a positively charged and long-chained residue that has the ability to maintain the hydrogen bond with DNA in which the wild-type residue is involved, whereas serine, a neutral and short-chained residue, does not. Both the human and horse mutations are inherited in a dominant fashion and both have severe effects on the phenotype, particularly with respect to effects on hearing. The different effects on function are therefore surprising and call for further investigations.

The S298P mutation is located at the carboxyl end of the leucine zipper of MITF. It has been suggested that S298 might be phosphorylated by GSK3β, and that substituting serine for either alanine or proline destroys MITF as a substrate for GSK3β (33). GSK3β phosphorylates many of its substrates

Table 2. Summary of DNA-binding assays and transcriptional activation analysis of MITF and MITF mutants; WS2A and TS mutations indicated in blue and melanoma mutations are indicated in red [shown in percentages which represent densitometric scans of EMSA gels (DNA-binding) and transcriptional activation ratios]

	DNA binding assays		Co-transfection assays				
	E-box*	M-box**	TYR	TYRP1	DCT	4M-box	MET
MITF	100	100	100	100	100	100	100
E87R	95	120	81	80	48	45	121
L135V	261	205	80	74	79	85	117
L142F	126	93	109	107	59	98	104
R203K	92	59	155	50	82	125	41
K206Q	39	30	49	29	29	73	24
N210K	107	83	219	39	81	106	35
I212M	135	69	24	44	73	81	375
I212S	104	78	31	58	45	104	121
E213D1	20	n/d	2	50	6	12	776
E213D2	24	n/d	2	42	8	11	841
R214X	19	n/d	1	26	2	9	19
R216K	20	n/d	1	24	3	11	28
R217del	21	n/d	1	25	3	11	25
R217I	21	n/d	28	25	4	38	40
R217G	25	n/d	1	21	2	9	36
I224S	20	n/d	1	21	2	11	37
G244R	100	n/d	77	36	89	135	43
S250P	15	n/d	1	18	2	11	31
Y253C	54	n/d	71	43	71	74	43
R259X	23	n/d	1	13	2	10	21
N278D	33	n/d	21	34	54	30	28
N278P	28	n/d	15	26	40	29	34
L283P	18	n/d	12	24	50	35	36
S298P	145	232	131	73	81	167	111
E318K	104	123	131	71	81	176	127
D380N	99	108	154	76	100	140	182
	>150	80-150	50-80	20-50	<20		

*CACGTG
** CTCATGTG

via the optimal consensus site S/T-X-X-X-S/T, where S and T are phosphoserine and phosphothreonine and X any amino acid (34,35). Interestingly, S298 does not fulfill all the criteria of a GSK3β substrate (36). Takeda *et al*. (2000) showed that the S298A or S298P MITF mutations severely affected binding to the M-box sequence and ability to activate expression from the TYR promoter, whereas substituting serine 302 with alanine had no effect on the ability to activate TYR (33). Our results, showing that S298P has normal DNA binding, are not consistent with the results of Takeda *et al*. (33). Similarly, substituting S298 with alanine and performing cotransfection assays with the TYR, 4M-box, TYRP1 and MET promoter constructs revealed no statistically significant difference from wild-type MITF (Supplementary Material, Fig. S9). Analysis of the Exome Variant Server database (http://evs.gs.washington.edu/EVS/) shows that a C/T polymorphism (rs104893747) which changes serine to proline at residue 298 in MITF is prevalent in European Americans and has a minor allele frequency of 0.046%. This polymorphism was not found in sequenced African Americans. The prevalence of all WSs combined is estimated to be 1/42 000 of the population (8), suggesting that rs104893747 is much more frequent than all WSs. This, together with our results showing that the S298P mutation has no major effect on function, suggests that this is a rare polymorphism in Caucasian populations that is functionally equivalent to the wild-type protein. The phenotype assigned to the S298P polymorphism must therefore be due to another non-identified non-coding mutation in the MITF gene, or to a mutation in another gene associated with WS.

The I212M and I212S mutations showed normal ability to bind the E-box whereas ability to bind the M-box was reduced (Fig. 2, Supplementary Material, Fig. S3). This is consistent with the results of Pogenberg *et al*. who showed that the I212 position is critical for allowing MITF to bind the M-box sequence (20). Mutating this site alters the target gene profile of MITF, leading to an imbalance in the activation of target genes, as observed by the hyperactivation of the MET promoter by the I212M mutation and the reduced ability to activate the TYR, TYRP1 and DCT promoters. Surprisingly, both mutations are able to activate expression of the 4M-box promoter. An imbalance in target gene selection is a novel model for how mutations can lead to WS2A and TS.

Paradoxically, despite severely affecting DNA binding of MITF and reducing activation from TYR, TYRP1, DCT and 4M-box promoters, the E213D mutations lead to hyperactivation of the MET promoter. It is possible that this mutant protein can

bind sequences other than the E-box to activate expression of the MET promoter. It is also possible that this mutation activates MET through another mechanism that does not involve direct binding to DNA. Interestingly, the I212M and E213D mutations, both of which hyperactivate the MET promoter, affect adjacent residues of the basic DNA-binding domain. The hyperactivation data suggest that mutations in MITF can have specific effects on gene expression or function, despite severely affecting the ability of MITF to bind the E-box.

We also analyzed the functional effects of somatic MITF mutations identified in melanoma tumor tissues; E87R, L135V, L142F, G244R and D380N (16) and a recently described germline mutation, E318K (17,18). Our results show that all the melanoma mutations were able to bind the E-box probe at normal levels, and most were capable of activating expression from melanocyte-specific promoters, although minor differences were observed, depending on both the mutation involved and the promoter investigated. Critically, four mutations (E87R, L135V, E318K and D380N) tended to increase activation from the MET promoter; this increase was statistically significant only for the D380N mutation (Fig. 3C). One of these mutations, L135V, showed increased DNA-binding ability, but this was not reflected in effects on transcription activation. The two mutations located in the C-terminus of MITF, E318K and D380N significantly increased transactivation potential of the tyrosinase and 4M-box promoters, but only D380N showed statistically significant activation of the MET promoter, suggesting that these mutations lead to increased but promoter-dependent transcription activation potential of MITF. This is consistent with the results of Bertolotto *et al*. (2011) who showed that the E318K mutation led to increased transcription activation of the HIF1α and synthetic 3M-box reporters (17). Consistent with our results, Bertolotto *et al*. did not observe any difference between wild-type MITF and the E318K mutant with respect to activation of the MET promoter (17). Although the E87R and L135V mutations tend to increase activation from the MET promoter, both mutations lead to reduced transcription activation potential from the pigment-specific promoters. This indicates that the effects of these two mutations are more subtle than the effects of the E318K and D380N mutations and may affect target genes differently. The L135V and L142F mutations are located within a proposed activation domain of MITF (37,38). Consistent with that both mutants showed significantly decreased transcriptional activation of the TYRP, TYRP1 and DCT promoters. The germline mutation E318K has recently been associated with melanoma and occurs within a SUMOylation consensus motif, IKQE. Since SUMOylation is generally reported to have inhibitory effects with respect to transcriptional activation, a mutation inhibiting SUMOylation may lead to activation of protein function (17,18,23).

The clonogenic assays showed that the E87R and L142F mutations increased clonogenic potential of MITF, whereas the D380N mutation did not. Unfortunately, very little is known about the functional role of the N and C domains of MITF. However, our results suggest that these domains have distinct function, and that they can lead to melanoma through different pathways, either leading to increased proliferation through mechanisms depending on the N-end of MITF, or by affecting transcription activation potential through features of the C-end of MITF. How these effects are mediated is not known at present.

In summary, we have shown that 11 of 18 MITF mutations associated with WS2A and TS, located in the bHLH-ZIP domains of the MITF protein, fail to bind DNA and activate melanocyte-specific promoters in cotransfection assays. The remaining seven mutations either have normal or reduced DNA-binding and transcription activity. The MITF mutations found in melanoma behave similar to the wild-type MITF protein in terms of DNA binding. However, these mutations affect transactivation potential and possess the ability to form colonies in clonogenic assays. Clearly, the amino- and carboxyl domains of MITF, where these mutations are located, play an important role in transactivation ability of MITF and the oncogenic role of MITF. The roles that these domains play in MITF function need further analysis.

MATERIALS AND METHODS

Cell culture

HEK 293 (ATTC; CRL-1573) and HEK293T cells were maintained in Dulbeccós modified Eagle Medium (GIBCO), supplemented with 10% fetal bovine serum, 100 U of penicillin/ml and 100 μg of streptomycin/ml and cultured in a humidified incubator at 37°C with 5% CO_2. HEK293T cells are derived from HEK293 cells but contain the large T antigen and are resistant to Geneticin.

Cotransfection assays

HEK 293T cells (1×10^5) were seeded in 96-well plates and transfected with 35 ng of Luciferase reporter construct (TYR, TYRP1, DCT, 4M-box and MET) and 15 ng wild-type or mutant mouse MITF constructs using ExGen 500 *in vitro* transfection reagent (Fermentas). pRenilla (1.5 ng) was used to normalize luciferase activity. Twenty-four hours after transfection, cells were lysed with passive lysis buffer (Promega) and assayed for firefly and *Renilla* luciferase activity according to manufacturer's instructions (Promega). Transfection experiments were carried out in six replicates each time and repeated at least twice. Measurements were taken with a Modulus II microplate reader (Turner Biosystems). Luciferase signals were normalized to corresponding *Renilla* signals and results expressed as fold activation over wild-type MITF. Error bars show the standard error of mean and significance was calculated via Student's *t*-test ($P < 0.05$ have been considered statistically significant).

Mutagenesis

Mutations were created in an expression vector (pcDNA3.1) containing the wild-type mouse MITF gene using the QuickChange Lightning site-directed mutagenesis kit from Stratagene and verified by Sanger sequencing. The QuickChange primer design program provided by Agilent Technologies was used to design the primers (listed in Supplementary Material, Table S1).

Protein expression

Wild-type and mutant MITF proteins were synthesized using the TNT quick coupled transcription/translation system according to manufacturer's protocol (Promega). TNT proteins were

analyzed by electrophoresis on 8% SDS–polyacrylamide gels. After electroblotting the proteins on a polyvinylidine difluoride membrane, membranes were incubated with an MITF antibody (C5, Thermo Scientific) and β-actin (13E5, Cell Signaling) overnight at 4°C in phosphate buffered saline (PBS) with 5% milk. The membranes were scanned on an Odyssey reader (Li-Core), and the bands quantitated and compared by intensity comparison to wild-type MITF (Supplementary Material, Fig. S2). To ensure equal protein loading on the EMSA gel, protein amounts were adjusted accordingly. For determining expression of transfected MITF proteins in cotransfection assays, constructs expressing wild-type and mutant MITF proteins were transfected into HEK293T cells and the cells lysed in RIPA buffer. Electrophoresis and electroblotting were performed as described above followed by incubation with the 1D2 antibody overnight at 4°C in PBS with 5% milk.

EMSA

The double stranded oligonucleotides encompassing MITF-binding sequences E-box 5′-AAAGAGTAG**CACGTG**CTA CTCAGA-3′ and M-box 5′-AAAGAGG**CTCATGTG**CTA-ACCAGA-3′ were ^{32}P-dCTP-end-labeled (PerkinElmer) using the Klenow fragment (Fermentas) and subsequently purified using Sephadex G50. TNT expressed proteins were incubated in 2 mM spermidine, 2 mM $MgCl_2$, 10% fetal calf serum, 2 ng/μl poly(dI)(dC)) for 15 min on ice. For supershift assays, 0.5 μl Mitf antibody (C5, Thermo Scientific) was added and incubated for 30 min on ice. The labeled probe was incubated with binding buffer (39) for a couple of minutes at room temperature and added to the TNT protein. After a 10 min incubation period, the DNA–protein complexes were resolved by electrophoresis on a 4.2% non-denaturating polyacrylamide gel in 0.25 × TBE buffer for 2–2.5 h at 130 V. In addition to the empty vector (pcDNA3.1) control, a water negative control was also included. The gel was incubated overnight on a storage phosphor screen and the gel scanned on a Typhoon 8610 imager (Molecular Dynamics). Intensity of bands was determined using ImageQuant.

Nuclear localization

HEK293T cells were seeded in 8-well chamber slides (4×10^5 cells/well) and transfected with 1 μg DNA using Fugene HD transfection reagent (Promega). The following day, the cells were fixed with 4% formalin for 15 min at room temperature, permeabilized in 0.1% Triton-x100 for 8 min, washed 3 times in PBS before blocking in PBS containing 0.05% Triton-X100, 0.25% BSA (PBT) and 5% normal goat serum. Cells were incubated with the C5 (Thermo scientific) or 1D2 anti-MITF antibodies overnight at 4°C, washed three times in PBT, incubated with a Cy3-labeled secondary antibody for 1 h at room temperature, washed three times in PBT and incubated for 15 min in TO-PRO-3 (Invitrogen). Cells were rinsed with PBS, slides mounted with Fluoroshield (Sigma) and imaged on a Zeiss 510 confocal microscope.

Clonogenic assays

HEK 293 cells (ATTC; CRL-1573) were transfected with wild-type and mutant MITF proteins using ExGene (Fermentas) transfection reagent according to manufacturer's protocol. After 48 h, cells were treated with 1–2 mg/ml Geneticin (G418). After several weeks under constant Geneticin selection, cells were counted (Countess) and reseeded in six-well plates at a density of 2500 cells/well. To ensure that the proteins are expressed, western blot analysis of whole cell lysates was performed (Supplementary Material, Fig. S5). After 1 week of incubation, plates were stained with 0.5% crystal violet. Plates were scanned and colonies counted via the open access program Clonocounter. Clonogenic assays were performed in triplicates and repeated twice. Error bars show the standard error of mean, and the significance was calculated using Student's *t*-test. *P*-values <0.05 were considered statistically significant.

SUPPLEMENTARY MATERIAL

Supplementary Material is available at *HMG* online.

ACKNOWLEDGEMENTS

We thank Colin Goding, Heinz Arnheiter and Lionel Larue for thoughtful comments on the manuscript. We acknowledge Dr Sandrine Marlin (Hospital Trousseau, Paris, France) for communicating clinical data. We thank Richard Frederickson for providing the template for Figure 1A. The authors thank the NHLBI GO Exome Sequencing Project and its ongoing studies which produced and provided exome variant calls for comparison: the Lung GO Sequencing Project (HL-102923), the WHI Sequencing Project (HL-102924), the Broad GO Sequencing Project (HL-102925), the Seattle GO Sequencing Project (HL-102926) and the Heart GO Sequencing Project (HL-103010).

Conflict of interest statement: None declared.

FUNDING

This work was supported by grants from the Icelandic Research Fund and the Research Fund of the University of Iceland (E.S.).

REFERENCES

1. Cheli, Y., Ohanna, M., Ballotti, R. and Bertolotto, C. (2009) Fifteen-year quest for microphthalmia-associated transcription factor target genes. *Pigment Cell Melanoma Res.*, **23**, 27–40.
2. Strub, T., Giuliano, S., Ye, T., Bonet, C., Keime, C., Kobi, D., Le Gras, S., Cormont, M., Ballotti, R., Bertolotto, C. *et al.* (2011) Essential role of microphthalmia transcription factor for DNA replication, mitosis and genomic stability in melanoma. *Oncogene*, **30**, 2319–2332.
3. Steingrimsson, E., Copeland, N.G. and Jenkins, N.A. (2004) Melanocytes and the microphthalmia transcription factor network. *Annu. Rev. Genet.*, **38**, 365–411.
4. Hughes, A.E., Newton, V.E., Liu, X.Z. and Read, A.P. (1994) A gene for Waardenburg syndrome type 2 maps close to the human homologue of the microphthalmia gene at chromosome 3p12-p14.1. *Nat. Genet.*, **7**, 509–512.
5. Tassabehji, M., Newton, V.E., Liu, X.Z., Brady, A., Donnai, D., Krajewska-Walasek, M., Murday, V., Norman, A., Obersztyn, E., Reardon, W. *et al.*

(1995) The mutational spectrum in Waardenburg syndrome. *Hum. Mol. Genet.*, **4**, 2131–2137.
6. Waardenburg, P.J. (1951) A new syndrome combining developmental anomalies of the eyelids, eyebrows and nose root with pigmentary defects of the iris and head hair and with congenital deafness. *Am. J. Hum. Genet.*, **3**, 195–253.
7. Tietz, W. (1963) A syndrome of deaf-mutism associated with albinism showing dominant autosomal inheritance. *Am. J. Hum. Genet.*, **15**, 259–264.
8. Read, A.P. and Newton, V.E. (1997) Waardenburg syndrome. *J. Med. Genet.*, **34**, 656–665.
9. Pingault, V., Ente, D., Dastot-Le Moal, F., Goossens, M., Marlin, S. and Bondurand, N. (2010) Review and update of mutations causing Waardenburg syndrome. *Hum. Mutat.*, **31**, 391–406.
10. Smith, S.D., Kelley, P.M., Kenyon, J.B. and Hoover, D. (2000) Tietz syndrome (hypopigmentation/deafness) caused by mutation of MITF. *J. Med. Genet.*, **37**, 446–448.
11. Shigemura, T., Shiohara, M., Tanaka, M., Takeuchi, K. and Koike, K. (2010) Effect of the mutant microphthalmia-associated transcription factor found in Tietz syndrome on the in vitro development of mast cells. *J. Pediatr. Hematol. Oncol.*, **32**, 442–447.
12. Leger, S., Balguerie, X., Goldenberg, A., Drouin-Garraud, V., Cabot, A., Amstutz-Montadert, I., Young, P., Joly, P., Bodereau, V., Holder-Espinasse, M. *et al.* (2012) Novel and recurrent non-truncating mutations of the MITF basic domain: genotypic and phenotypic variations in Waardenburg and Tietz syndromes. *Eur. J. Hum. Genet.*, **20**, 584–587.
13. King, R., Weilbaecher, K.N., McGill, G., Cooley, E., Mihm, M. and Fisher, D.E. (1999) Microphthalmia transcription factor. A sensitive and specific melanocyte marker for MelanomaDiagnosis. *Am. J. Pathol.*, **155**, 731–738.
14. King, R., Googe, P.B., Weilbaecher, K.N., Mihm, M.C. Jr and Fisher, D.E. (2001) Microphthalmia transcription factor expression in cutaneous benign, malignant melanocytic, and nonmelanocytic tumors. *Am. J. Surg. Pathol.*, **25**, 51–57.
15. Garraway, L.A., Widlund, H.R., Rubin, M.A., Getz, G., Berger, A.J., Ramaswamy, S., Beroukhim, R., Milner, D.A., Granter, S.R., Du, J. *et al.* (2005) Integrative genomic analyses identify MITF as a lineage survival oncogene amplified in malignant melanoma. *Nature*, **436**, 117–122.
16. Cronin, J.C., Wunderlich, J., Loftus, S.K., Prickett, T.D., Wei, X., Ridd, K., Vemula, S., Burrell, A.S., Agrawal, N.S., Lin, J.C. *et al.* (2009) Frequent mutations in the MITF pathway in melanoma. *Pigment Cell Melanoma Res.*, **22**, 435–444.
17. Bertolotto, C., Lesueur, F., Giuliano, S., Strub, T., de Lichy, M., Bille, K., Dessen, P., d'Hayer, B., Mohamdi, H., Remenieras, A. *et al.* (2011) A SUMOylation-defective MITF germline mutation predisposes to melanoma and renal carcinoma. *Nature*, **480**, 94–98.
18. Yokoyama, S., Woods, S.L., Boyle, G.M., Aoude, L.G., Macgregor, S., Zismann, V., Gartside, M., Cust, A.E., Haq, R., Harland, M. *et al.* (2011) A novel recurrent mutation in MITF predisposes to familial and sporadic melanoma. *Nature*, **480**, 99–103.
19. Garraway, L.A. and Sellers, W.R. (2006) Lineage dependency and lineage-survival oncogenes in human cancer. *Nat. Rev. Cancer*, **6**, 593–602.
20. Pogenberg, V., Ogmundsdottir, M.H., Bergsteinsdottir, K., Schepsky, A., Phung, B., Deineko, V., Milewski, M., Steingrimsson, E. and Wilmanns, M. (2012) Restricted leucine zipper dimerization and specificity of DNA recognition of the melanocyte master regulator MITF. *Genes Dev.*, **26**, 2647–2658.
21. Leger, S., Balguerie, X., Goldenberg, A., Drouin-Garraud, V., Cabot, A., Amstutz-Montadert, I., Young, P., Joly, P., Bodereau, V., Holder-Espinasse, M. *et al.* (2012) Novel and recurrent non-truncating mutations of the MITF basic domain: genotypic and phenotypic variations in Waardenburg and Tietz syndromes. *Eur. J. Hum. Genet*, **20**, 584–587.
22. Bentley, N.J., Eisen, T. and Goding, C.R. (1994) Melanocyte-specific expression of the human tyrosinase promoter: activation by the microphthalmia gene product and role of the initiator. *Mol. Cell Biol.*, **14**, 7996–8006.
23. Murakami, H. and Arnheiter, H. (2005) Sumoylation modulates transcriptional activity of MITF in a promoter-specific manner. *Pigment Cell Res.*, **18**, 265–277.
24. Lowings, P., Yavuzer, U. and Goding, C.R. (1992) Positive and negative elements regulate a melanocyte-specific promoter. *Mol. Cell Biol.*, **12**, 3653–3662.
25. Bottaro, D.P., Rubin, J.S., Faletto, D.L., Chan, A.M., Kmiecik, T.E., Vande Woude, G.F. and Aaronson, S.A. (1991) Identification of the hepatocyte growth factor receptor as the c-met proto-oncogene product. *Science*, **251**, 802–804.
26. Schmidt, L., Duh, F.M., Chen, F., Kishida, T., Glenn, G., Choyke, P., Scherer, S.W., Zhuang, Z., Lubensky, I., Dean, M. *et al.* (1997) Germline and somatic mutations in the tyrosine kinase domain of the MET proto-oncogene in papillary renal carcinomas. *Nat. Genet.*, **16**, 68–73.
27. Natali, P.G., Nicotra, M.R., Di Renzo, M.F., Prat, M., Bigotti, A., Cavaliere, R. and Comoglio, P.M. (1993) Expression of the c-Met/HGF receptor in human melanocytic neoplasms: demonstration of the relationship to malignant melanoma tumour progression. *Br. J. Cancer*, **68**, 746–750.
28. Strub, T., Giuliano, S., Ye, T., Bonet, C., Keime, C., Kobi, D., Le Gras, S., Cormont, M., Ballotti, R., Bertolotto, C. *et al.* (2011) Essential role of microphthalmia transcription factor for DNA replication, mitosis and genomic stability in melanoma. *Oncogene*, **30**, 2319–2332.
29. Bharti, K., Liu, W., Csermely, T., Bertuzzi, S. and Arnheiter, H. (2008) Alternative promoter use in eye development: the complex role and regulation of the transcription factor MITF. *Development*, **135**, 1169–1178.
30. Takebayashi, K., Chida, K., Tsukamoto, I., Morii, E., Munakata, H., Arnheiter, H., Kuroki, T., Kitamura, Y. and Nomura, S. (1996) The recessive phenotype displayed by a dominant negative microphthalmia-associated transcription factor mutant is a result of impaired nucleation potential. *Mol. Cell Biol.*, **16**, 1203–1211.
31. Zhang, H., Luo, H., Chen, H., Mei, L., He, C., Jiang, L., Li, J.D. and Feng, Y. (2012) Functional analysis of MITF gene mutations associated with Waardenburg syndrome type 2. *FEBS Lett*, **586**, 4126–4131.
32. Hauswirth, R., Haase, B., Blatter, M., Brooks, S.A., Burger, D., Drogemuller, C., Gerber, V., Henke, D., Janda, J., Jude, R. *et al.* (2012) Mutations in MITF and PAX3 cause 'splashed white' and other white spotting phenotypes in horses. *PLoS Genet.*, **8**, e1002653.
33. Takeda, K., Takemoto, C., Kobayashi, I., Watanabe, A., Nobukuni, Y., Fisher, D.E. and Tachibana, M. (2000) Ser298 of MITF, a mutation site in Waardenburg syndrome type 2, is a phosphorylation site with functional significance. *Hum. Mol. Genet.*, **9**, 125–132.
34. Fiol, C.J., Wang, A., Roeske, R.W. and Roach, P.J. (1990) Ordered multisite protein phosphorylation. Analysis of glycogen synthase kinase 3 action using model peptide substrates. *J. Biol. Chem.*, **265**, 6061–6065.
35. Wang, Q.M., Park, I.K., Fiol, C.J., Roach, P.J. and DePaoli-Roach, A.A. (1994) Isoform differences in substrate recognition by glycogen synthase kinases 3 alpha and 3 beta in the phosphorylation of phosphatase inhibitor 2. *Biochemistry*, **33**, 143–147.
36. Frame, S. and Cohen, P. (2001) GSK3 takes centre stage more than 20 years after its discovery. *Biochem. J.*, **359**, 1–16.
37. Sato, S., Roberts, K., Gambino, G., Cook, A., Kouzarides, T. and Goding, C.R. (1997) CBP/p300 as a co-factor for the microphthalmia transcription factor. *Oncogene*, **14**, 3083–3092.
38. Vachtenheim, J. and Drdova, B. (2004) A dominant negative mutant of microphthalmia transcription factor (MITF) lacking two transactivation domains suppresses transcription mediated by wild type MITF and a hyperactive MITF derivative. *Pigment Cell Res.*, **17**, 43–50.
39. Beuret, L., Flori, E., Denoyelle, C., Bille, K., Busca, R., Picardo, M., Bertolotto, C. and Ballotti, R. (2007) Up-regulation of MET expression by alpha-melanocyte-stimulating hormone and MITF allows hepatocyte growth factor to protect melanocytes and melanoma cells from apoptosis. *J. Biol. Chem.*, **282**, 14140–14147.
40. Nobukuni, Y., Watanabe, A., Takeda, K., Skarka, H. and Tachibana, M. (1996) Analyses of loss-of-function mutations of the MITF gene suggest that haploinsufficiency is a cause of Waardenburg syndrome type 2A. *Am. J. Hum. Genet.*, **59**, 76–83.
41. Chen, H., Jiang, L., Xie, Z., Mei, L., He, C., Hu, Z., Xia, K. and Feng, Y. (2010) Novel mutations of PAX3, MITF, and SOX10 genes in Chinese patients with type I or type II Waardenburg syndrome. *Biochem. Biophys. Res. Commun.*, **397**, 70–74.
42. Lalwani, A.K., Attaie, A., Randolph, F.T., Deshmukh, D., Wang, C., Mhatre, A. and Wilcox, E. (1998) Point mutation in the MITF gene causing Waardenburg syndrome type II in a three-generation Indian family. *Am. J. Med. Genet.*, **80**, 406–409.
43. Welch, K.O., Smith, S.D., Hoover, D., Arnos, K.S., Kelley, P.M. and Pandya, A. (2002) A variant of Tietz syndrome caused by a mutation in the basic domain of the MITF gene. 2002 ASHG Annual Meeting, Baltimore, MD, USA.

Grill et al., Supplementary Figure 1

```
Mmus   MLEMLEYSHYQVQTHLENPTKYHIQQAQRHQVKQYLSTTLANKHASQVLSSPCPNQPGDH
Hsap   MLEMLEYNHYQVQTHLENPTKYHIQQAQRQQVKQYLSTTLANKHANQVLSLPCPNQPGDH
       *******.*********************:***************.**** *********

Mmus   AMPPVPGSSAPNSPMAMLTLNSNCEKEAFYKFEEQSRAESECPGMNTHSRASCMQMDDVI
Hsap   VMPPVPGSSAPNSPMAMLTLNSNCEKEGFYKFEEQNRAESECPGMNTHSRASCMQMDDVI
       .*************************.********.************************

Mmus   DDIISLESSYNEEILGLMDPALQMANTLPVSGNLIDLYSNQGLPPPGLTISNSCPANLPN
Hsap   DDIISLESSYNEEILGLMDPALQMANTLPVSGNLIDLYGNQGLPPPGLTISNSCPANLPN
       ***************.*******.*****************.**********************

Mmus   IKRELTACIFPTESEARALAKERQKKDNHNLIERRRRFNINDRIKELGTLIPKSNDPDMR
Hsap   IKRELTACIFPTESEARALAKERQKKDNHNLIERRRRFNINDRIKELGTLIPKSNDPDMR
       ************************.***.**********.*********.***************

Mmus   WNKGTILKASVDYIRKLQREQQRAKDLENRQKKLEHANRHLLLRVQELEMQARAHGLSLI
Hsap   WNKGTILKASVDYIRKLQREQQRAKELENRQKKLEHANRHLLLRIQELEMQARAHGLSLI
       ****.*******.**********.******:************.*****.:**********.***

Mmus   PSTGLCSPDLVNRIIKQEPVLENCSQELVQHQADLTCTTTLDLTDGTITFTNNLGTMPES
Hsap   PSTGLCSPDLVNRIIKQEPVLENCSQDLLQHHADLTCTTTLDLTDGTITFNNNLGTGTEA
       ******************.********.:*:**:******************.***** .*:

Mmus   SPAYSIPRKMGSNLEDILMDDALSPVGVTDPLLSSVSPGASKTSSRRSSMSAEETEHAC
Hsap   NQAYSVPTKMGSKLEDILMDDTLSPVGVTDPLLSSVSPGASKTSSRRSSMSMEETEHTC
       . ***:* ****:*******.*:**************************** *****:*
```

Grill et al., Supplementary Figure 2

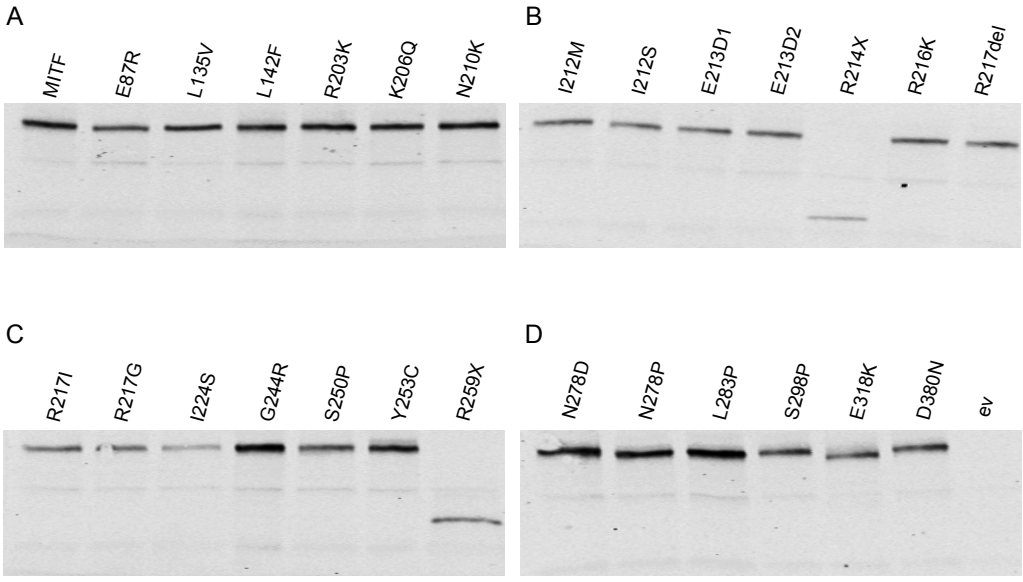

Grill et al., Supplementary Figure 3

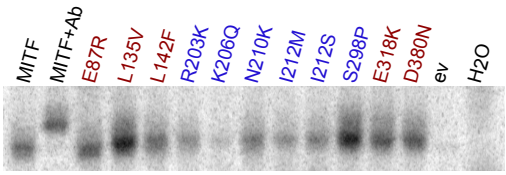

Grill et al., Supplementary Figure 4

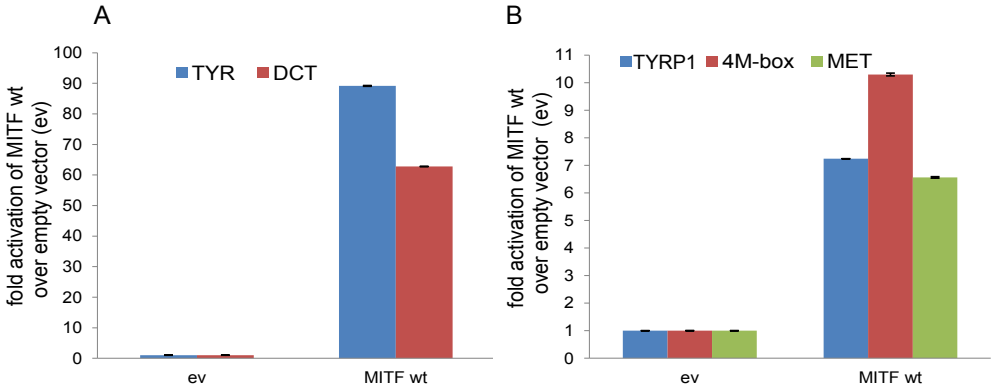

Grill et al., Supplementary Figure 5

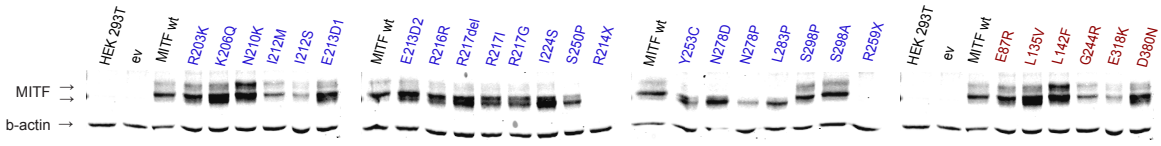

Grill et al., Supplementary Figure 6

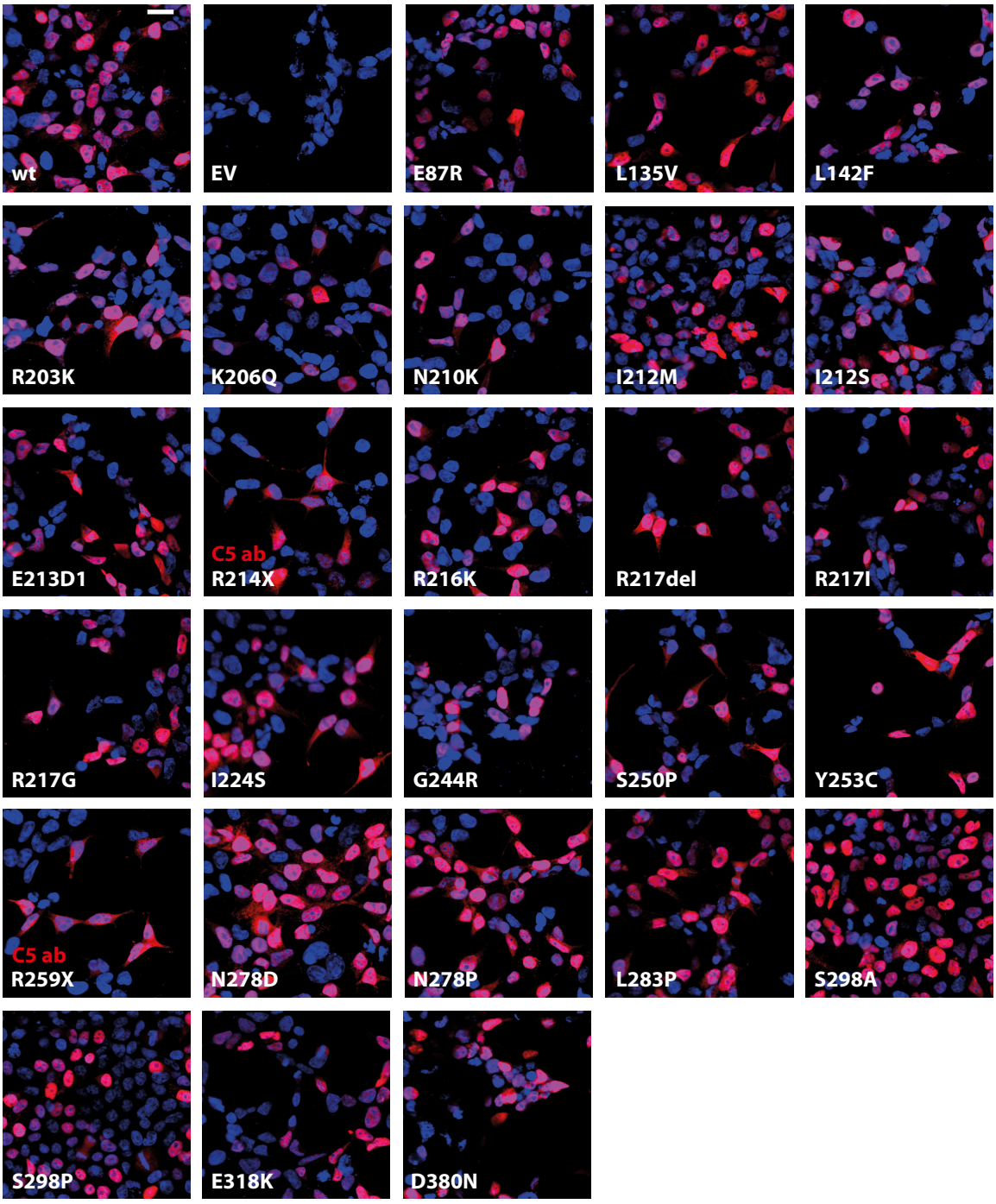

Grill et al., Supplementary Figure 7

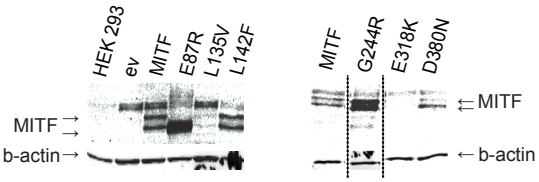

Grill et al., Supplementary Figure 8

```
human          MLEMLEYNHYQVQTHLENPTKYHIQQAQRQQVKQYLSTTLANKHANQVLSLPCPNQPGDH
horse          MLEMLEYNHYQVQTHLENPTKYHIQQAQRQQVKQYLSTTLANKHANQVLSLPCPNQPGDH
               ************************************************************

human          VMPPVPGSSAPNSPMAMLTLNSNCEKEGFYKFEEQNRAESECPGMNTHSRASCMQMDDVI
horse          VMPPVPGSSAPNSPMAMLTLNSNCEKEGFYKFEEQNRAESECPSMNTHSRASCMQMDDVI
               ******************************************.*****************

human          DDIISLESSYNEEILGLMDPALQMANTLPVSGNLIDLYGNQGLPPPGLTISNSCPANLPN
horse          DDIISLESSYNEEILGLMDPALQMANTLPVSGNLIDLYSNQGLPPPGLTISNSCPANLPN
               ************************************.***********************

human          IKRELTACIFPTESEARALAKERQKKDNHNLIERRRRFNINDRIKELGTLIPKSNDPDMR
horse          IKRELTACIFPTESEARALAKERQKKDNHNLIERRRRFNINDRIKELGTLIPKSNDPDMR
               ******************************************************************

human          WNKGTILKASVDYIRKLQREQQRAKELENRQKKLEHANRHLLLRIQELEMQARAHGLSLI
horse          WNKGTILKASVDYIRKLQREQQRAKELENRQKKLEHANRHLLLRIQELEMQARAHGLSLI
               ************************************************************

human          PSTGLCSPDLVNRIIKQEPVLENCSQDLLQHHADLTCTTTLDLTDGTITFNNNLGTGTEA
horse          PSTGLCSPDLVNRIIKQEPALENCNQDLLQHHADLTCTTTLDLTDGTISFNNNLGTGTES
               ******************.****.**********************:**********:

human          NQAYSVPTKMGSKLEDILMDDTLSPVGVTDPLLSSVSPGASKTSSRRSSMSMEETEHTC
horse          NQAYSIPAKMGSKLEDILMDDTLSPVGVTDPLLSSVSPGASKTSSRRSSMSMEETEHAC
               *****:*:**************************************************:*
```

Grill et al., Supplementary Figure 9

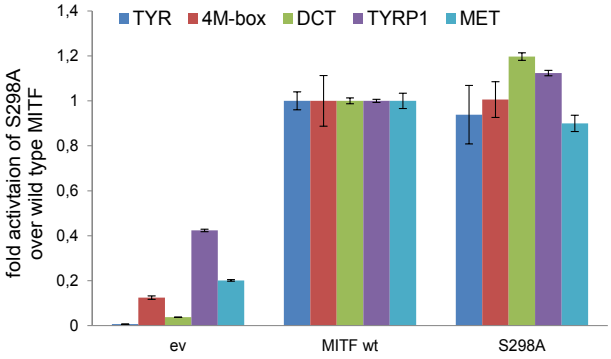

Supplementary Figure Legends

Supplementary Figure 1. Alignment of human and mouse MITF proteins. Indicated in red are residues mutated in our analysis. All those residues are fully conserved between human and mouse.

Supplementary Figure 2. MITF wild type and mutant protein expression. (A-D) Western analysis showing the wild type and mutant MITF proteins used in the EMSA studies. The proteins were generated using the TNT system and were then loaded on an 8% SDS-PAGE gel and incubated with MITF antibody (C5, Thermo). Differences have been adjusted to load equal amounts on the EMSA gel.

Supplementary Figure 3. DNA-binding ability of selected mutations to the M-box. Electrophoretic mobility shift assay using an M-box probe with a core sequence of TCATGTG. Lane 1 shows binding of the wild type MITF protein and lane 2 shows a supershift where the C5 MITF antibody was added. Empty vector pcDNA3.1 (ev) and water (H_2O) were loaded as negative controls. Melanoma mutations are indicated in red and WS2A and TS mutations in blue.

Supplementary Figure 4. Activation of melanocyte-specific promoters by MITF. (A) Cotransfection assays of wild type MITF protein together with reporter constructs containing the tyrosinase and DCT promoters. (B) Cotransfection assays of wild type MITF protein together with the TYRP1, 4M-box and MET promoters. Fold activation was calculated over empty vector (pcDNA3.1) and repeated twice in 6 replicates.

Supplementary Figure 5. Expression of transfected MITF proteins in cotransfection assays.

Western analysis of lysates stained with the 1D2 anti-MITF and the anti-Actin antibodies.

Supplementary Figure 6. Nuclear localization of wild type and mutant MITF proteins.

Nuclear localization of wild type and mutant MITF proteins as seen by 1D2 or C5 antibody staining upon transfection of HEK293T cells with the indicated constructs. MITF is indicated in red and the

TOPRO nuclear marker in blue. All the figures were stained with the 1D2 antibody except the R214X and R259X which were stained with the C5 antibody. Scale bar in wt represents 20 µm and applies to all panels.

Supplementary Figure 7. Expression of MITF and MITF mutant proteins in stable cell lines. HEK293 cells were transfected with empty vector, wild type MITF and selected MITF mutants and subsequently treated with Geneticin. Whole cell lysates were used to load on an SDS-PAGE gel. After transfer, Western blots were incubated with C5 MITF antibody (Thermo). All resulting cell lines express MITF or mutant MITF, except L135V and E318K which were excluded from further studies. Unfortunately, we were not able to generate stable cell lines for the L135V and the E318K mutations and therefore were not able to include those in the clonogenic assay. MITF was expressed as a double band (between 60-70kDa) and β-actin (Cell signaling) was used as a loading control. Untransfected HEK293 cells did not show any endogenous MITF expression, and neither did empty vector transfected cells. A double 75-80 kD band was observed in all transfected cells including those transfected with empty vector controls.

Supplementary Figure 8. Alignment of human and horse MITF proteins. Sequence alignment reveals 97.9% conservation of human and horse MITF proteins. Indicated in red is the asparagine at position 210 (N210).

Supplementary Figure 9. Activation of melanocyte-specific promoters by S298A. Cotransfection assays of the mutant S298A together with reporter constructs containing the TYR, 4M-box, DCT and TYRP1 promoters. The data are shown as fold activation of MITF mutants over wild type MITF. Error bars indicate the standard error of mean.

Supplementary Tables

Supplementary Table1. Primer sequences used for mutagenesis. Bold indicates site of mutagenesis.

Primer name	Sequence
E87R-F	5'-atgctcactcttaactccaactgtgaaaaa**ag**ggcattttataagtttgag-3'
E87R-R	5'-ctcaaacttataaaatgcc**ct**tttttcacagttggagttaagagtgagcat-3'
L135V-F	5'-gcctggaatcaagttataatgaagaaatt**g**tgggcttgatggatc-3'
L135V-R	5'-gatccatcaagccca**c**aatttcttcattataacttgattccaggc-3'
L142F-F	5'-ttgatggatccggcctt**c**caaatggcaaatacgtt-3'
L142F-R	5'-aacgtatttgccatttg**g**aaggccggatccatcaa-3'
R203K-F	5'-gcaagagcattggctaaagaga**a**gcagaaaaaggaca-3'
R203K-R	5'-tgtccttttctgc**t**tctctttagccaatgctcttgc-3'
K206Q-F	5'-agcattggctaaagagaggcagaaa**c**aggacaatcacaa-3'
K206Q-R	5'-ttgtgattgtcct**g**tttctgcctctctttagccaatgct-3'
N210K-F	5'-agaggcagaaaaaggacaatcacaa**g**ttgattgaacgaag-3'
N210K-R	5'-cttcgttcaatcaa**c**ttgtgattgtccttttttctgcctct-3'
I212M-F	5'-gaaaaaggacaatcacaacttgat**g**gaacgaagaagaagatttaacata-3'
I212M-R	5'-tatgttaaatcttcttcttcgttc**c**atcaagttgtgattgtccttttttc-3'
I212S-F	5'-ggcagaaaaaggacaatcacaacttga**g**tgaacgaagaagaa-3'
I212S-R	5'-ttcttcttcgttca**c**tcaagttgtgattgtccttttttctgcc-3'
E213D1-F	5'-ggcagaaaaaggacaatcacaacttgattga**c**cgaagaagaagattta-3'
E213D1-R	5'-taaatcttcttcttcg**g**tcaatcaagttgtgattgtccttttttctgcc-3'
E213D2-F	5'-ggcagaaaaaggacaatcacaacttgattga**t**cgaagaagaagattta-3'
E213D2-R	5'-taaatcttcttcttcg**a**tcaatcaagttgtgattgtccttttttctgcc-3'
R214X-F	5'-aaggacaatcacaacttgattgaa**t**gaagaagaagatttaacataaacg-3'
R214X-R	5'-cgtttatgttaaatcttcttcttca**t**tcaatcaagttgtgattgtcctt-3'
R216K-F	5'-acaatcacaacttgattgaacgaagaa**a**aagatttaacataaacgacc-3'
R216K-R	5'-ggtcgtttatgttaaatctt**t**ttcttcgttcaatcaagttgtgattgt-3'
R217del-F	5'-acaacttgattgaacgaagaagatttaacataaacgaccgcattaa-3'
R217del-R	5'-ttaatgcggtcgtttatgttaaatcttcttcgttcaatcaagttgt-3'
R217I-F	5'-caacttgattgaacgaagaagaa**t**atttaacataaacgaccgcatta-3'
R217I-R	5'-taatgcggtcgtttatgttaaat**a**ttcttcttcgttcaatcaagttg-3'
R217G-F	5'-caacttgattgaacgaagaaga**gg**atttaacataaacgaccgcat-3'
R217G-R	5'-atgcggtcgtttatgttaaatc**c**tcttcttcgttcaatcaagttg-3'
I224S-F	5'-tttaacataaacgaccgca**g**taaggagctaggtactctg-3'
I224S-R	5'-cagagtacctagctcctta**c**tgcggtcgtttatgttaaa-3'
G244R-F	5'-catgcggtggaacaag**a**gaaccattctcaaggc-3'
G244R-R	5'-gccttgagaatggttc**t**cttgttccaccgcatg-3'
S250P-F	5'-aaccattctcaaggcc**c**ctgtggactacatccg-3'
S250P-R	5'-cggatgtagtccacag**gg**ggccttgagaatggtt-3'
Y253C-F	5'-ggcctctgtggact**g**catccggaagttgc-3'
Y253C-R	5'-gcaacttccggatg**c**agtccacagaggcc-3'
R259X-F	5'-gactacatccggaagttgcaa**ta**ggaacagcaacgagctaa-3'
R259X-R	5'-ttagctcgttgctgttcc**ta**ttgcaacttccggatgtagtc-3'
N278D-F	5'-ctggagcatgcg**g**accggcacctgc-3'
N278D-R	5'-gcaggtgccggt**c**cgcatgctccag-3'
N278P-F	5'-gctggagcatgcg**cc**ccggcacctgctg-3'
N278P-R	5'-cagcaggtgccgg**gg**cgcatgctccagc-3'
L283P-F	5'-cggcacctgctgc**c**cagagtacaggag-3'
L283P-R	5'-ctcctgtactctg**gg**cagcaggtgccg-3'
S298P-F	5'-ggctagagcgcatggactt**c**cccttatcccatc-3'
S298P-R	5'-gatgggataagggg**g**aagtccatgcgctctagcc-3'
E318K-F	5'-ctggtgaatcggatcatcaagcaa**a**aaccagttcttga-3'
E318K-R	5'-tcaagaactggtt**t**tgcttgatgatccgattcaccag-3'
D380N-F	5'-ggaagacatcctgatg**a**acgatgccctctcacc-3'
D380N-R	5'-ggtgagagggcatcgt**t**catcaggatgtcttcc-3'

Paper II:
IRF4 affects human pigmentation by regulating expression of tyrosinase through an MITF and TFAP2A-dependent pathway.

Praetorius C.[#], Grill C.[#], Stacey SN., Metcalf AM., Robinson KC., Gorkin DU., Van Otterloo E., Kim RSQ., Mishva PJ., Davis SR., Guo T., Zaidi MR., Sigurdsson MJ., Melzer PS., Merlino G., Larue L., Loftus S., Adams DR., Pavan WJ., McCallion AS., Cornell RA., Smith AG., Fisher DE., Strum RA., Steingrimsson E.
[#] Equal contribution.

IRF4 affects human pigmentation by regulating expression of Tyrosinase through a MITF and TFAP2A-dependent pathway

Christian Praetorius[1,#], Christine Grill[1,#], Simon N. Stacey[2], Alexander M. Metcalf[3], David U. Gorkin[4,5], Kathleen C. Robinson[6], Eric Van Otterloo[7], Reuben S.Q. Kim[3,8], Kristin Bergsteinsdottir[1], Margret H. Ogmundsdottir[1], Erna Magnusdottir[1], Pravin J. Mishra[9], Sean R. Davis[10], Theresa Guo[9], M. Raza Zaidi[9], Agnar S. Helgason[2], Martin I. Sigurdsson[1], Paul S. Melzer[10], Glenn Merlino[9], Valerie Petit[11], Lionel Larue[11], Stacie K. Loftus[12], David R. Adams[13], Ulduz Sobhiafshar[14], N. C. Tolga Emre[14], William J. Pavan[12], Robert Cornell[7], Aaron G. Smith[3,8], Andrew S. McCallion[4], David E. Fisher[6], Kari Stefansson[2], Richard A. Sturm[3], Eiríkur Steingrímsson[1,*]

[1]Department of Biochemistry and Molecular Biology, Biomedical Center, Faculty of Medicine,University of Iceland, Vatnsmyrarvegur 16, 101 Reykjavik.

[2]Decode Genetics, Sturlugata 8, 101 Reykjavik, Iceland.

[3]Institute for Molecular Bioscience, University of Queensland, Brisbane, Qld 4072, Australia.

[4]McKusick-Nathans Institute of Genetic Medicine, Johns Hopkins University School of Medicine, 733 N. Broadway, Baltimore, MD 21205, USA.

[5]Predoctoral Training Program in Human Genetics, Johns Hopkins University School of Medicine, Baltimore, Maryland 21205, USA

[6]Department of Dermatology, Massachusetts General Hospital, Harvard Medical School, Boston, MA 02114, USA.

[7]Anatomy and Cell Biology, University of Iowa, 357 Medical Research Center, Iowa City, IA 52242-1101, USA.

[8]The School of Biomedical Sciences, University of Queensland, Brisbane, Qld 4072, Australia.

[9]Laboratory of Cancer Biology and Genetics, National Cancer Institute, Bldg 37, Room 5002, 37 Convent Drive, Bethesda, MD 20892, USA.

[10]Genetics Branch, National Cancer Institute, Bldg 37, Room 6138, 37 Convent Drive, Bethesda, MD 20892, USA.
[11]Institut Curie, Centre de Recherche, Developmental Genetics of Melanocytes, Orsay, France.

[12]Genetic Disease Research Branch, National Human Genome Research Institute, National Institutes of Health, Bethesda, MD 20892, USA
[13]Medical Genetics Branch, National Human Genome Research Institute, National Institutes of Health, Bethesda, MD 20892, USA
[14]Laboratory of Genome Regulation, Department of Molecular Biology and Genetics, Boğaziçi University, Bebek 34342, Istanbul, Turkey

# Equal contribution.
*Corresponding author:
Eiríkur Steingrímsson
Tel +354 525 4270
eirikurs@hi.is

Abstract

Sequence polymorphisms linked to human diseases and phenotypes in genome-wide association studies often affect non-coding regions. A single nucleotide polymorphism (SNP) within an intron of the gene encoding Interferon Regulatory Factor 4 (IRF4), a transcription factor with no known role in melanocyte biology, is strongly associated with sensitivity of skin to sun exposure, freckles, blue eyes and brown hair color. Here we demonstrate that this SNP lies within an enhancer of IRF4 transcription in melanocytes. The allele associated with this pigmentation phenotype impairs binding of the TFAP2A transcription factor which, together with the melanocyte master regulator MITF, regulates activity of the enhancer. Assays in zebrafish and mice reveal that IRF4 cooperates with MITF to activate expression of Tyrosinase (TYR), an essential enzyme in melanin synthesis. Our findings provide a clear example of a non-coding polymorphism that affects a phenotype by modulating a developmental gene regulatory network.

Introduction

Human pigmentation is a complex process involving melanocytes which synthesize the pigment melanin in melanosomes, cell organelles that are transferred to neighbouring keratinocytes, where they form a cap over nuclei, thus protecting them from negative effects of ultra violet radiation (UVR). Pigmentation is not only one of the most distinguishing features of humans but also serves an important protective role. In humans, pigmentation decreases with increasing distance from the equator, presumably due to a balance between the pressure to optimize the amount of available UVR for the generation of vitamin D3 and the protection from UVR-mediated damage, which may result in increased risk of cutaneous malignancies. This has led to positive selection for less pigmented skin, hair and eyes in areas distant from the equator. The major difference between dark- and light-skinned individuals is due to differences in the number, size and density of the melanin-containing melanosomes; the number of melanocytes is roughly the same (reviewed in Sturm, (2009)).

The genetics of pigmentation is complex and involves several genes and pathways. It has been best characterized in the mouse where 171 of nearly 400 loci implicated in pigmentation have been functionally characterized (http://www.espcr.org/micemut/). These pigmentation genes affect various steps in the formation of melanocytes from the neural crest (e.g. *Mgf*, *Kit* and *Mitf*), the generation of components of melanosomes and pigment

(e.g. *pMel17/Silver* and *Tyr*) or the transport of melanosomes along microtubules in the dendrites before delivery to adjacent keratinocytes (e.g. *MyoVa*, *Rab27* and *Mlph*). Most genes involved in pigmentation are transcriptionally regulated by the bHLHZip transcription factor MITF, the master regulator of melanocytes (reviewed in Steingrimsson et al., (2004)).

Genome wide association studies (GWAS) have identified several Single Nucleotide Polymorphism (SNPs) involved in human pigmentation, including SNPs on chromosome 6 near the *DUSP22, IRF4,* and *EXOC2* genes, none of which were previously implicated in pigmentation (Sulem et al., 2007; Han et al., 2008; Sulem et al., 2008). The SNP showing the strongest association is located in intron 4 of *IRF4* (Han et al., 2008). IRF4 belongs to the interferon regulatory factors, a wing-helix-turn-helix family of transcription factors that regulate interferon (IFN)-inducible genes (Paun and Pitha, 2007). Although IRF4 does not depend on interferon stimulation, it binds to the IFN-stimulated response element (ISRE) within IFN-responsive genes (Matsuyama, 1995; Grossman et al., 1996; Escalante et al, 1998). *Irf4* mutant mice completely lack germinal centers and plasma cells and show severely reduced immunoglobulin levels in the serum; no defects in pigmentation were reported (Mittrucker et al., 1997). In a subset of multiple myeloma patients, *IRF4* is translocated downstream of the immunoglobulin heavy-chain regulatory regions (Iida et al., 1997; Tsuboi et al., 2000). Interestingly, in this disease, *IRF4* acts as a lineage survival oncogene regardless of translocation status (Shaffer et al., 2008). Polymorphisms in the *IRF4* gene are associated with chronic lymphocytic leukemia (CLL) (Di Bernardo et al., 2008) and with non-hematopoietic diseases including celiac disease (Dubois et al., 2010), and progressive supranuclear palsy (Hoglinger et al., 2011). Finally, IRF4 was recently shown to be critical for transcriptional response to nutrient availability in adipocytes (Eguchi et al., 2011).

A few reports have linked *IRF4* to pigment cells. *IRF4* is expressed in melanocytes in the skin and in the G361 melanoma cell line (Grossman et al., 1996) as well as in most melanomas (Sundram,2003). Importantly, IRF4 is associated with human pigmentation (Sulem et al., 2007; Han et al., 2008) and IRF4 expression correlates with MITF expression in melanoma cells (Hoek et al. 2008). Here we show that *IRF4* is involved in pigmentation, that the melanocyte master regulator MITF activates expression of the *IRF4* gene and that this activation depends on the presence of the Transcription Factor Activator Protein alpha (TFAP2A). A naturally occurring sequence variant associated with human pigmentation overlaps the TFAP2A binding site, impairs binding by this

transcription factor and consequently lowers induction of IRF4 expression. Together, the MITF and IRF4 proteins cooperatively activate expression of the gene encoding the pigmentation enzyme Tyrosinase (TYR). This activation depends on MITF and IRF4 binding sites in the TYR promoter. Thus, we have established a direct link between a polymorphism in an intron in the *IRF4* gene and reduced expression of an enzyme essential for pigmentation.

Results

Fine mapping of the IRF4 locus implicates rs12203592 as a functional variant affecting pigmentation

Several sequence variants in the *IRF4* locus have been associated with freckling, sun sensitivity, eye and hair color and with nevus counts, with rs12203592-[T/C] showing the strongest association (Sulem et al., 2007; Han et al., 2008; Duffy et al., 2010). The rs12203592-T minor allele is most common in individuals of European descent; it is not seen in sub-Saharan Africans or in East Asians (Figure S1). Analysis of sequenced vertebrate species shows that this position is occupied by C, suggesting that it is the ancestral allele.

In order to fine map the pigmentation trait associations at the *IRF4* locus, we used whole genome sequencing data derived from 2,230 Icelanders sequenced to an average coverage of at least 10x. This yielded approximately 38.5 million SNP and small indel (insertion or deletion) variants genome-wide, 16,280 of which were located in the region around *IRF4* (0-1 Mb on chromosome 6). Using imputation assisted by long-range haplotype phasing (Kong et al., 2008; Kong et al., 2009; Holm et al., 2011), we determined the genotypes of these 16,280 variants in 95,085 individuals who had been typed using Illumina SNP chips. We then tested each variant for association with eye color, hair color, freckling and sun sensitivity, observing numerous significant signals (Figure 1). The strongest signals in the *IRF4* region came from the association of rs12203592-T with presence of freckles, brown hair and high sensitivity of skin to sun exposure (Figure 1, Table S1). The second most significant variant association was for rs62389424-A with freckles ($P = 1.1 \times 10^{-81}$, nearly 40 orders of magnitude less significant than the corresponding signal from rs12203592-T ($P = 2.0 \times 10^{-120}$). The rs62389424 variant is correlated with rs12203592 with an r^2 of 0.65. Two other SNPs in the region have r^2 values in excess of 0.2 with rs12203592 and they also gave association signals with similar phenotypes (Table S2). When, in a multivariate analysis, the associations were conditioned on the effect of rs12203592, the signals from the three correlated SNPs became non-significant (Table S2). Indeed, once rs12203592 was taken into account in the multivariate analysis, no variant in the *IRF4* region retained a significant signal after Bonferroni correction for the number of tests (Figure 1). We note in this context that the signal from the originally reported pigmentation variant at this locus, rs1540771-T (Sulem et al., 2007) was also captured by rs12203592 (Table S2).

Thus, the associations at the *IRF4* locus with freckles, hair color, sun sensitivity and eye color could all be accounted for by rs12203592 and no other variant detected by sequencing explains the effect with a similar level of significance.

Intron 4 of IRF4 contains a melanocyte-specific enhancer element

rs12203592 is located in intron 4 of the IRF4 gene, suggesting that this SNP might alter the function of a *cis*-regulatory element. Data from the ENCODE consortium (Thurman et al., 2012) shows that rs12203592 overlaps a peak of DNase I hypersensitivity (HS), a property of active regulatory elements, in human primary melanocytes and three human melanoma lines (Figure 2a). Moreover, rs12203592 does not overlap a DNase I HS peak in 158 of 165 (96%) non-melanocyte-derived cell types examined by ENCODE, suggesting that the regulatory activity in this region is specific to the melanocyte lineage. In a subset of 49 ENCODE cell types assayed by the Crawford group (Duke University) for both DNase I HS and global gene expression, *IRF4* is expressed at high levels only in cell types of melanocyte (n=3) and lymphocyte origin (n=8). The corresponding patterns of DNase I HS in these cell types suggest that *IRF4* expression in lymphocytes and melanocytes are directed by distinct sets of regulatory elements (Figure 2b). In addition, the position orthologous to rs12203592 in the mouse genome directly overlaps a melanocyte enhancer (Gorkin et al., 2012) since it is occupied by p300 and marked by H3K4me1 in the melanocyte line melan-Ink4a-Arf (Sviderskaya et al., 2002) (Figure 2c).

To confirm that the intronic sequence containing rs12203592 acts as a melanocyte-specific enhancer we sub-cloned a 450 bp fragment containing the rs12203592-C allele upstream of a minimal promoter driving luciferase, and assayed its activity in both the mouse melan-Ink4a-Arf and human SK-MEL-28 cell lines. The fragment showed strong enhancer activity, directing >35-fold higher luciferase expression than the minimal promoter alone in melan-Ink4a-Arf, and >200-fold in SK-MEL-28 (Figure 3a, b). We next asked whether the genotype at rs12203592 affects enhancer activity. In both melan-Ink4a-Arf and SK-MEL-28, the presence of the rs12203592-T allele significantly reduced the enhancer activity of the fragment (P<0.008) (Figure 3a, b).

We further assayed the sequence containing rs12203592 *in vivo* using transgenic zebrafish. We engineered a vector containing the entire human *IRF4* intron 4 sequence upstream of a minimal promoter and the gene encoding Green Fluorescent Protein (GFP). We created two versions of the vector, with either the T or C allele at

rs12203592; as above, the remainder of the sequence was identical in both constructs. We injected these constructs, or a negative control construct lacking any human genomic sequence, into zebrafish embryos at the 2-cell stage, incubated them 48 hour post fertilization, and scored them for the presence of GFP-positive cells. In embryos injected with the negative control construct we did not detect GFP-positive melanocytes (0/40 embryos) (Figure 3c). In embryos injected with the *IRF4* intron 4 reporter construct containing the ancestral rs12203592-C allele, we detected GFP-positive melanocytes in about 20% of embryos (8/40 embryos, 17 melanocytes total from the 8 embryos), consistent with the mosaicism expected in transient transgenic embryos (Figure 3c, d). By contrast, in embryos injected with the reporter containing rs12203592-T, only 9% of the embryos had detectable GFP-positive melanocytes (4/44 embryos, only 6 melanocytes total). The difference in the total number of melanocytes is statistically significant (p=0,0023, unpaired t-test). We did not detect expression in other tissues, beyond transient, scattered expression which was seen in all three constructs and has been reported by others (Bessa et al., 2009). We conclude that *IRF4* intron 4 contains a melanocyte enhancer, likely directing *IRF4* expression in these cells, and that the rs12203592-T allele reduces the activity of this enhancer.

MITF activates IRF4 gene expression

ChIP sequencing and gene expression studies have suggested that MITF may be involved in regulating *IRF4* gene expression (Hoek et al., 2008, Strub et al., 2011). We analyzed *Irf4* expression in mice lacking *Mitf* and focused on the heart because cells that normally express *Mitf* are still present in the heart of $Mitf^{mi\text{-}vga9}$ homozygous mutants, whereas melanocytes are absent resulting in white coat color (Hodgkinson et al., 1993). *Irf4* gene expression was dramatically reduced in *Mitf* mutants compared to wild type controls (Figure 4a) consistent with the possibility that *Irf4* is regulated by MITF. To determine whether *IRF4* is a target of MITF in the melanocyte lineage, we used shRNA to knock down *MITF* and *IRF4* mRNAs in human 501mel melanoma cells which normally express these genes. Transfecting these cells with shRNA directed against *MITF* reduced *MITF* mRNA expression to 45% (Figure 4b) and MITF protein levels to 41% (Figures 4c and S2) of those seen in untreated cells or cells treated with a scrambled control shRNA. In cells treated with shMITF, the expression of *IRF4* mRNA and protein were dramatically reduced (to 50% and 25%, respectively). shRNA against *IRF4* resulted in reduction in

IRF4 mRNA and protein expression to 40% and 20% of control levels, respectively, whereas *MITF* expression was unaffected (Figures 4c and S2). The expression of *DCT* (encoding Dopachrome tautomerase) and TYR, two known MITF target genes (Yasumoto et al., 2002; Yasumoto et al., 1994), was also reduced upon shMITF treatment whereas shIRF4 treatment only affected the expression of *TYR* (Figure 4b). TYR protein expression was reduced upon treatment with shMITF, shIRF4 and shAP2A, as well as with all shRNAs together (Figures S2). Knocking down TFAP2A did not affect MITF expression. We also tested this relationship in an overexpression assay. Untransfected 501mel melanoma cells express *MITF* but low levels of both *TYR* and *IRF4* mRNAs whereas HEK293T cells do not express *MITF* endogenously and also lack expression of *TYR* and *IRF4*. In both cell lines, overexpression of mouse *Mitf* (*mMitf*) strongly induced the levels of *TYR* and *IRF4* (Figure 4d). Analysis of the expression of MITF and IRF4 in 22 melanoma cell lines revealed a positive correlation between MITF and IRF4 ($p=0.0003$, Pearson correlation coefficient, Figure S3a). These results indicate that MITF directly or indirectly regulates *IRF4* expression. They also suggest that *TYR* expression depends on IRF4.

rs12203592 alters the function of a melanocyte enhancer in IRF4 through disruption of a TFAP2A binding site

The rs12203592 polymorphism is located 66 bp from 3 sites recently shown to be occupied by MITF in ChIP-sequencing studies (Figure 5a) (Strub et al., 2011). ChIP performed in 501mel and MITF-transfected 293T cells showed that MITF binds to intron 4 of *IRF4* (Figure 5b). Interestingly, the rs12203592-T polymorphism occurs in a predicted binding site (GGCAAA) for TFAP2A (Do et al., 2010) which was recently shown to be involved in melanocyte differentiation in zebrafish (van Otterloo et al., 2010). To determine if TFAP2A can bind this sequence, we performed anti-TFAP2A ChIP in 501mel cells (homozygous for rs12203592-C) and showed that TFAP2A binds to the intron 4 element in the *IRF4* gene (Figure 5c). Furthermore, gel shift assays showed that TFAP2A binds oligos carrying the TFAP2A motif from *IRF4* intron 4 only when the oligos harbor the rs12203592-C allele. It did not bind the rs12203592-T variant, nor when the binding site was altered completely (Figure 5d). Addition of antibody resulted in a supershift only in presence of the wild-type oligo. Binding of MITF to the neighbouring MITF sites was not affected by the SNP (Figure S3b). These results show that TFAP2A

binds the ancestral sequence (rs12203592-C) in intron 4 of *IRF4* but fails to bind to the rs12203592-T variant.

To determine if TFAP2A plays a role in the activity of the *IRF4* enhancer, we performed reporter assays using intron 4 of *IRF4* as regulatory element. 501mel melanoma cells were co-transfected with the reporter constructs and with plasmids encoding MITF, TFAP2A or both. Neither MITF nor TFAP2A alone elevated expression from this element above basal levels (Figure 5e). However, when both MITF and TFAP2A were expressed simultaneously, transcription was increased 6-fold (Figure 5e), suggesting that the proteins have cooperative effects on the activity of this enhancer. This is further supported by the shRNA experiments which showed that knocking down TFAP2A reduces IRF4 expression (Figure 4b and c). Removing all three MITF binding sites together (intron 4-3xE) lead to background-level expression (Figure 5e). Importantly, when the rs12203592-T variant was introduced into the reporter construct (intron 4-rs), the cooperation seen between MITF and TFAP2A was reduced to levels close to background (Figure 5e). This suggests that MITF requires TFAP2A in order to induce expression from the intron 4 element and that the rs12203592-T polymorphism abolishes the MITF-mediated activation.

To determine whether the rs12203592-T variant affects *IRF4* expression in melanocytes, RNA and protein were isolated from melanocytes differentiated from human neonatal foreskin melanoblasts from Australian subjects (Cook et al., 2009). RT-qPCR showed a significantly lower ($p<0,01$, unpaired t-test) expression of *IRF4* mRNA in cells homozygous for the rs12203592-T polymorphism than in cells homozygous for the ancestral C (Figure 5f, Figure S3c). IRF4 protein levels in cells from T/T individuals were considerably reduced compared to that of cells from C/C individuals (Figure 5g).

To determine whether the rs12203592 polymorphism affects expression of the transcript on the chromosome on which the variation resides we used an allele discrimination assay. We used RT-qPCR on human primary melanocytes heterozygous for the *IRF4* 3'UTR SNP rs872071-A/G. The rs872071-G allele resides 15kb distal to rs12203592 and is present on the haplotype on which the rs12203592-T allele arose, thus allowing for comparison of IRF4 allele specific expression levels, controlling for potential trans-factor variations that may contribute to expression level differences between individuals. We observed no difference in IRF4 allelic expression in rs12203592-C/C homozygous melanocytes, as represented by the rs872071-A/G allele

ratio (Figure S4). In contrast, cells heterozygous for the rs12203592 C/T alleles exhibit a significantly higher rs872071-A/G allele ratio ($p<0.01$) consistent with reduced transcription occurring from IRF4 rs872071-G alleles in phase with rs12203592-T.

Several alternate products are made from the IRF4 gene, including transcripts which initiate in intron 4 (Figure S5a), leading to an mRNA containing internal ATGs (lacking Kozak consensus sequences) and the tentative production of a truncated protein lacking the N-terminal DNA-binding domain. To determine the major product in the melanocyte, RT-qPCR analysis with transcript specific primers was performed on RNA isolated from foreskin melanoblasts from Australian subjects. This showed that the major *IRF4* product in melanocytes is the full length transcript; the smaller alternative product was barely detectable (Figure S5b). Similarly, in mouse melanoblasts isolated from E15.5 and E17.5 embryos and melanocytes from P1 and P7 neonatal pups (Debbache et al., 2012), the full-length *Irf4* transcript was the only transcript detected at all developmental stages (Figure S6). We therefore conclude that the regulatory element in intron 4 affects the production of the full-length *IRF4* transcript.

IRF4 and MITF cooperatively regulate TYR expression

To determine how IRF4 levels might affect pigmentation we searched the promoter sequences of several pigmentation genes for the IRF4 binding motif. Several potential IRF4 binding motifs were found in the *TYR* promoter, on either side of known MITF binding sites previously shown to be essential for gene activation (Figure 6a) (Yasumoto et al., 1994; Bertolotto et al., 1996). To investigate the relationship between IRF4 and the expression of several pigmentation genes, two human melanocyte strains with high expression of *IRF4* were independently transfected with siRNA targeting *IRF4* for 48 hours, followed by total RNA extraction and RT-qPCR. These results combined show that expression of *IRF4* was reduced on average to 40% of cells treated with negative control siRNA (Figure 6b). Interestingly, the expression of *TYR* was reduced to 50% compared to untreated control whereas the expression of the pigmentation genes *SLC45A2 (MATP)*, *SLC24A5* and *DCT* were largely unaffected (Figure 6b). Similarly, knockdown of *IRF4* affected expression of *TYR* but not of *DCT* in 501mel melanoma cells (Figure 2b, c). This suggests that IRF4 is involved in regulating *TYR* expression but does not affect expression of SLC45A2 or SLC24A5. The expression of IRF4 correlates with the

expression of TYR in 22 melanoma cell lines (p=0.0007, Pearson correlation coefficient, Figure S3a).

Co-transfection assays in HEK293T cells (which do not express MITF) showed that whereas MITF can activate expression of the *TYR* gene, the IRF4 protein is unable to do so on its own (Figure 6c). However, in the presence of both MITF and IRF4, cooperative effects were observed with increasing amounts of IRF4 (Figure 6c). A mutant MITF protein with defective DNA-binding ability resulted in less activation and reduced cooperativity (Figure S7a). Similar effects were observed when the E-box was mutated (Figure S7b), confirming that the cooperativity is mediated through MITF. Quantitative ChIP experiments in Skmel28 (Figure 6d) and Skmel5 (Figure S7c) melanoma cells showed that IRF4 binds the proximal TYR promoter as well as a more distant region.

Irf4 ***affects pigmentation in mice***

No pigment phenotypes were reported in mice with a targeted deletion of *Irf4* (Mittrucker et al., 1997). We analyzed the expression of *Mitf*, *Tfap2a*, *Irf4* and *Tyr* in melanoblasts isolated from E15.5, E17.5, P2 and P7 mouse embryos (Debbache et al., 2012). *Mitf* and *Tfap2a* are both expressed at the embryonic and postnatal stages whereas *Irf4* is detected at a low level at the two postnatal stages (Figure 7a). *Tyr* is expressed at all stages but the level of expression increases at the postnatal stages and is ten-fold higher at P7 than at the earlier stages (Figure 7a). This expression pattern is consistent with our data that MITF and TFAP2A regulate *IRF4* expression and MITF and IRF4 regulate *TYR* expression. Since early stages of development do not express *Irf4*, this also suggests that IRF4 is mostly involved in melanocyte differentiation. To determine if *Irf4* plays a role in mouse melanocytes, mice carrying an *Irf4-flox* cassette (*Irf4 f*) (Klein et al., 2006) were crossed to mice expressing the Cre-recombinase under control of the *Tyr* promoter (*Tyr::Cre*) (Delmas et al., 2003). This led to the lack of *Irf4* expression in *Tyr* expressing cells, but no apparent pigmentation phenotype, similar to the *Irf4* null mice (Mittrucker et al., 1997). In order to test the relationship between *Mitf* and *Irf4* in the mouse, we crossed the *Tyr*::*Cre*/^{0}; *Irf4* f/f mice to mice carrying the dominant negative allele *Mitf*$^{Mi\text{-}White}$ (*Mitf*$^{Mi\text{-}Wh}$). Mice heterozygous for this allele (*Mitf*$^{Mi\text{-}Wh}$/+) have a partial deficiency of *Mitf* and exhibit a stable, grey coat color with white belly spot. Interestingly, the *Tyr*::*Cre*/^{0}; *Irf4* f/f; *Mitf*$^{Mi\text{-}Wh}$/+ mice showed distinctly lighter coat color than seen in *Mitf*$^{Mi\text{-}Wh}$/+ mice which are negative for the *Tyr-Cre* transgene (*Irf4 f/f*;

Mitf$^{Mi\text{-}Wh}$/+) (Figure 7b). This confirms that IRF4 plays a role in mouse pigmentation, like in humans, and that the effects of *Irf4* in the mouse also depend on *Mitf*. In humans, the *IRF4* variant rs12203592-T is linked to brown hair color (Sulem et al., 2007) (Table S1). Thus, reduced *IRF4* expression alone is sufficient for lighter hair color in humans whereas in mice MITF function also needs to be reduced to see effects on pigmentation. This suggests that there may be species-specific differences between mice and humans in terms of requirement for *MITF* and *IRF4* in melanocytes of the hair.

Discussion

Genome-wide association studies have yielded a long list of sequence variants correlated with a wide range of human phenotypes. Most of these variants are located in non-coding regions of the genome, and do not alter the amino-acid sequence of proteins or have known regulatory functions. Two steps are essential in order to characterize the biology behind such associations. First, the association signals must be fine-mapped using full sequence data. Second, the biological processes involved must be unravelled experimentally. In this study, we have taken both steps to shed light on the functional consequences of the IRF4 non-coding variant rs12203592 on pigmentation.

Our work proposes a model describing how IRF4 acts in cooperation with MITF to influence pigmentation phenotypes (Figure 7c). In melanocytes, MITF and TFAP2A cooperatively activate *IRF4* expression through an enhancer element in intron 4. In turn, IRF4 and MITF cooperate to activate transcription of *TYR*. The rs12203592-T allele reduces binding of TFAP2A to its cognate site in intron 4 of *IRF4*, thereby suppressing the induction of IRF4 expression and, as a consequence, impairing the cooperative induction of *TYR*. This leads to the pigmentation phenotypes associated with the rs12203592-T allele. The effects of this variant must be cell-type specific since Do et al. (2010) have shown that it leads to increased *IRF4* promoter activity in Burkitt lymphoma B cells (Raji), HEK293T human embryonic kidney cells and the NCI-H295R human adrenal cells. Consistent with our results, they showed that TFAP2A binds with higher affinity to the C allele than to the T allele (Do et al., 2010). Thus, the cell-type specific effects must be mediated by transcription factors other than TFAP2A.

In humans, genetic variants in different genes have particular effects on pigmentation traits. For example, *MC1R* and *ASIP* variants have major effects on freckling, sun sensitivity and red hair, whereas they have relatively little effect on eye color (Sulem et al., 2007; Sulem et al., 2008). The rs12203592-T variant of *IRF4* also has major effects on freckling and sun sensitivity, but is associated with brown (over blond) hair and has a notable effect on eye color (Table S1). The results presented here suggest that *IRF4*, like *MC1R* and *ASIP*, exerts its major effects on pigmentation traits through the master regulator MITF. However some divergence in pathways must occur, in order to account for the differences in effects on pigmentation traits. We have shown that *TYR* is a target of MITF-IRF4 cooperative activation. However, *TYRP1* and *DCT* are targets of MITF activation that do not appear to be responsive to IRF4. Clearly, the MITF-IRF4

cooperation only occurs in a subset of MITF responsive genes. A broader search of MITF target genes for potential IRF4 responsiveness might shed light on the pattern of pigmentation traits affected by *IRF4*.

Freckles represent clusters of concentrated melanin in the skin, without an increase in melanocyte numbers. Freckles are either light brown or red but usually become darker and more visible upon exposure to sunlight. GWAS studies have shown that variations in MC1R, ASIP, TYR, and BNC2, in addition to IRF4, are associated with freckles (Sulem et al., 2007; Sulem et al., 2008; Eriksson et al., 2010). Mutations in the *MC1R* gene have been highly associated with the formation of freckles (Bastiaens et al., 2001). In addition to regulating TYR and IRF4 gene expression, MITF is also known to regulate expression of *MC1R* (Adachi et al., 2000; Smith et al., 2001; Aoki and Moro, 2002). This suggests the possibility that, like with TYR, IRF4 cooperates with MITF in regulating expression of *MC1R* in melanocytes. Indeed, ChIP-seq studies show that MITF binds MC1R regulatory sequences (Strub et al., 2011).

The effects of both TFAP2A and IRF4 are mediated through MITF which is needed both for the TFAP2A-mediated activation of *IRF4* and the IRF4-mediated activation of *TYR*. ChIP-seq studies suggest that MITF regulates *TFAP2A* as well as *IRF4* (Strub et al., 2011). The cooperative effects of MITF and IRF4 suggest that these proteins might physically interact on the *TYR* promoter. TFAP2A is expressed in a variety of both mesenchymal and epithelial cell types. It is not known how MITF and TFAP2A interact in the regulation of IRF4. Since the binding sites are physically close to each other, it is possible that both proteins are part of a larger complex formed at the site. Together, these data suggest that transcription factors which are expressed in multiple cell types can form cell-type specific complexes to govern differentiation.

Several studies have shown that polymorphisms identified as susceptibility loci in GWAS studies affect the binding of particular transcription factors, in some cases leading to differences in expression of a nearby target gene (Meyer et al., 2008; Rahimov et al., 2008; Pomerantz et al., 2009; Schodel et al., 2012; Tuupanen et al., 2009). However, the effects of the gene expression differences have not been characterized and, more importantly, the biological effects on the phenotype are only implied in these studies. A recent example is provided by the rs12913832 polymorphism in intron 86 of the *HERC2* gene which shows a strong association with human eye color and pigmentation. Since the pigment gene *OCA2* is located 21kb downstream of *HERC2* it has been speculated

that this polymorphism is located in a distal regulatory element of OCA2 and may affect binding of the transcription factors HLTF, LEF1 and MITF (Visser et al., 2012). This results in the formation of a loop between the HERC2 enhancer and the OCA2 promoter, thus affecting OCA2 expression. The rs12913832-C allele prevents HLTF from binding to the element, thus reducing loop formation. The regulation of OCA2 expression may be more complex however, with separate regulatory elements responsible for eye and skin color (Beleza et al., 2013). Here we have gone one step further and shown the effects of transcription factor binding on gene expression and how this gene expression difference leads to effects on human pigmentation.

Materials and Methods

Whole genome sequence analysis

Icelandic population samples and phenotypic information: Icelandic adults were recruited as cases, family members or controls thorough a series of cardiovascular, oncology, neurology and metabolic studies conducted by deCODE Genetics. Blood samples were taken for DNA isolation upon recruitment. The studies were approved by the National Bioethics Committee of Iceland and the Icelandic Data Protection Commission. Personal identifiers associated with phenotypic information, blood samples and genotypes were encrypted using a third party encryption system. Each participant completed a questionnaire that included questions about natural eye color categories (blue/gray, green or black/brown), natural hair color categories (red/reddish, blond, dark blond/light brown or brown/black) and the presence of freckles at any time. Sun sensitivity was assessed using the Fitzpatrick skin-type score (Fitzpatrick, 1988), where the lowest score (I) represents very fair skin that is sensitive to UVR and the highest score represented in native Icelanders (IV) represents dark skin that tans rather than burns in reaction to UVR exposure. Individuals scoring I or II were classified as being sensitive to sun whereas individuals scoring III and IV were classified as not being sensitive to sun.

SNP chip genotyping: The Icelandic chip-typed samples were genotyped with Illumina Human Hap300, HumanHap CNV370, HumanHap 610, 1M, Omni1-Quad, Omni 2.5 or Omni Express bead chips at deCODE Genetics. SNPs were excluded if they had (i) yield less than 95%, (ii) minor allele frequency less than 1% in the population (iii) significant deviation from Hardy-Weinberg equilibrium in the controls ($P < 0.001$), (iv) if they produced and excessive inheritance error rate (over 0.001), (v) if there was a substantial difference in allele frequency between the chip types (SNPs from a single chip platform were excluded if that resolved all differences, but otherwise from all chip platforms). All samples with a call rate below 97% were excluded from the analysis. For the HumanHap series of chips 308,840 SNPs were used for long rang phasing, whereas for the Omni series of chips 642,079 SNPs were included. The final set of SNPs used for long-range phasing was composed of 785,863 SNPs.

Whole genome sequencing and imputation: Sequence data was obtained from about 2,230 Icelanders using methods described previously (Holm et al., 2011). Sequencing was carried out to an average depth of at least 10x. This resulted in the identification of

approximately 38.5 million SNPs and small indels that were available for imputation. Long range phasing, imputation and association testing (by logistic regression) was done as described previously (Kong et al., 2008; Kong et al., 2009; Holm et al., 2011; Stacey et al., 2011). For conditional analysis of the IRF4 region the rs12203592-T allele count of each individual was given as a covariate in the logistic regression.

Acknowledgements

We thank Thorunn Rafnar, Magnus Karl Magnusson, Unnur Thorsteinsdottir, Colin R. Goding and Thorarinn Gudjonsson for critical comments on the manuscript. This work was supported by grants from NIH (5R01 AR043369-16), Melanoma Research Alliance, Dr. Miriam and Sheldon Adelson Medical Research Foundation, US-Israel Binational Science Foundation (to DEF), from Ligue Nationale Contre le Cancer (Equipe labellisée) and INCa (to LL), from the Icelandic Research Fund the Research Fund of the University of Iceland (to ES), from the Haskolasjodur Student Fund (ES, CP and CG), from the Jules Verne Fund (ES and LL), by the National Institute of General Medical Sciences (GM071648) and National Institute of Neurological Disease and Stroke (NS062972) to ASM, by the National Human Genome Research Institute's (NHGRI) Intramural Research Program (WJP, SL) and by an NSF Graduate Research Fellowship to DUG.

Declaration of Contribution

ES conceived and designed the study; SNS, AH and KS analyzed whole genome sequence data and the frequency of *IRF4* variants, AMM, RSQK, AGS and RAS characterized expression of *IRF4* and other genes in cultured human melanocytes, DUG, ASM, SKL, DRA and WJP identified and characterized the enhancer element in intron 4 of *IRF4* and performed the allele-specific expression analysis, EVO and RC performed experiments in zebrafish, CP analyzed the effects of MITF and TFAP2A on regulation of *IRF4* and other target genes and CG, MHO and KB determined the involvement of IRF4 and MITF in *TYR* regulation, EM, US and NCTE performed ChIP on the TYR promoter, PJM, TG, MRZ, SRD, PSM and GM analyzed expression of *MITF*, *TFAP2A*, *IRF4* and *TYR* in mouse melanocytes and VP and LL in human melanoma cells. KCR, LL and DEF characterized the interaction between MITF and IRF4 in mouse pigmentation. CP and ES wrote the manuscript. All authors approved the final version of the manuscript.

Conflicts of Interest

The authors declare that they have no conflict of interest.

References

Adachi, S., Morii, E., Kim, D., Ogihara, H., Jippo, T., Ito, A., Lee, Y.M., and Kitamura, Y. (2000). Involvement of mi-transcription factor in expression of alpha-melanocyte-stimulating hormone receptor in cultured mast cells of mice. Journal of immunology *164*, 855-860.

Aoki, H., and Moro, O. (2002). Involvement of microphthalmia-associated transcription factor (MITF) in expression of human melanocortin-1 receptor (MC1R). Life Sci *71*, 2171-2179.

Bastiaens, M., ter Huurne, J., Gruis, N., Bergman, W., Westendorp, R., Vermeer, B.J., and Bouwes Bavinck, J.N. (2001). The melanocortin-1-receptor gene is the major freckle gene. Hum Mol Genet *10*, 1701-1708.

Beleza, S., Johnson, N.A., Candille, S.I., Absher, D.M., Coram, M.A., Lopes, J., Campos, J., Araujo, II, Anderson, T.M., Vilhjalmsson, B.J*., et al.* (2013). Genetic architecture of skin and eye color in an African-European admixed population. PLoS Genet *9*, e1003372.

Bertolotto, C., Bille, K., Ortonne, J.P., and Ballotti, R. (1996). Regulation of tyrosinase gene expression by cAMP in B16 melanoma cells involves two CATGTG motifs surrounding the TATA box: implication of the microphthalmia gene product. J Cell Biol *134*, 747-755.

Bessa, J., Tena, J.J., de la Calle-Mustienes, E., Fernandez-Minan, A., Naranjo, S., Fernandez, A., Montoliu, L., Akalin, A., Lenhard, B., Casares, F*., et al.* (2009). Zebrafish enhancer detection (ZED) vector: a new tool to facilitate transgenesis and the functional analysis of cis-regulatory regions in zebrafish. Developmental dynamics : an official publication of the American Association of Anatomists *238*, 2409-2417.

Cook, A.L., Chen, W., Thurber, A.E., Smit, D.J., Smith, A.G., Bladen, T.G., Brown, D.L., Duffy, D.L., Pastorino, L., Bianchi-Scarra, G*., et al.* (2009). Analysis of cultured human melanocytes based on polymorphisms within the SLC45A2/MATP, SLC24A5/NCKX5, and OCA2/P loci. J Invest Dermatol *129*, 392-405.

Debbache, J., Zaidi, M.R., Davis, S., Guo, T., Bismuth, K., Wang, X., Skuntz, S., Maric, D., Pickel, J., Meltzer, P*., et al.* (2012). In vivo role of alternative splicing and serine phosphorylation of the microphthalmia-associated transcription factor. Genetics *191*, 133-144.

Delmas, V., Martinozzi, S., Bourgeois, Y., Holzenberger, M., and Larue, L. (2003). Cre-mediated recombination in the skin melanocyte lineage. Genesis *36*, 73-80.

Di Bernardo, M.C., Crowther-Swanepoel, D., Broderick, P., Webb, E., Sellick, G., Wild, R., Sullivan, K., Vijayakrishnan, J., Wang, Y., Pittman, A.M*., et al.* (2008). A genome-wide association study identifies six susceptibility loci for chronic lymphocytic leukemia. Nature genetics *40*, 1204-1210.

Do, T.N., Ucisik-Akkaya, E., Davis, C.F., Morrison, B.A., and Dorak, M.T. (2010). An intronic polymorphism of IRF4 gene influences gene transcription in vitro and shows a risk association with childhood acute lymphoblastic leukemia in males. Biochim Biophys Acta *1802*, 292-300.

Dubois, P.C., Trynka, G., Franke, L., Hunt, K.A., Romanos, J., Curtotti, A., Zhernakova, A., Heap, G.A., Adany, R., Aromaa, A*., et al.* (2010). Multiple common variants for celiac disease influencing immune gene expression. Nature genetics *42*, 295-302.

Duffy, D.L., Iles, M.M., Glass, D., Zhu, G., Barrett, J.H., Hoiom, V., Zhao, Z.Z., Sturm, R.A., Soranzo, N., Hammond, C*., et al.* (2010). IRF4 variants have age-specific effects on nevus count and predispose to melanoma. Am J Hum Genet *87*, 6-16.

Eguchi, J., Wang, X., Yu, S., Kershaw, E.E., Chiu, P.C., Dushay, J., Estall, J.L., Klein, U., Maratos-Flier, E., and Rosen, E.D. (2011). Transcriptional control of adipose lipid handling by IRF4. Cell metabolism *13*, 249-259.

Eriksson, N., Macpherson, J.M., Tung, J.Y., Hon, L.S., Naughton, B., Saxonov, S., Avey, L., Wojcicki, A., Pe'er, I., and Mountain, J. (2010). Web-based, participant-driven studies yield novel genetic associations for common traits. PLoS genetics *6*, e1000993.

Escalante, C.R., Yie, J., Thanos, D., and Aggarwal, A.K. (1998). Structure of IRF-1 with bound DNA reveals determinants of interferon regulation. Nature *391*, 103-106.

Fitzpatrick, T.B. (1988). The validity and practicality of sun-reactive skin types I through VI. Archives of dermatology *124*, 869-871.

Gorkin, D.U., Lee, D., Reed, X., Fletez-Brant, C., Bessling, S.L., Loftus, S.K., Beer, M.A., Pavan, W.J., and McCallion, A.S. (2012). Integration of ChIP-seq and machine learning reveals enhancers and a predictive regulatory sequence vocabulary in melanocytes. Genome research.

Grossman, A., Mittrucker, H.W., Nicholl, J., Suzuki, A., Chung, S., Antonio, L., Suggs, S., Sutherland, G.R., Siderovski, D.P., and Mak, T.W. (1996). Cloning of human lymphocyte-specific interferon regulatory factor (hLSIRF/hIRF4) and mapping of the gene to 6p23-p25. Genomics *37*, 229-233.

Han, J., Kraft, P., Nan, H., Guo, Q., Chen, C., Qureshi, A., Hankinson, S.E., Hu, F.B., Duffy, D.L., Zhao, Z.Z*., et al.* (2008). A genome-wide association study identifies novel alleles associated with hair color and skin pigmentation. PLoS genetics *4*, e1000074.

Hodgkinson, C.A., Moore, K.J., Nakayama, A., Steingrimsson, E., Copeland, N.G., Jenkins, N.A., and Arnheiter, H. (1993). Mutations at the mouse microphthalmia locus are associated with defects in a gene encoding a novel basic-helix-loop-helix-zipper protein. Cell *74*, 395-404.

Hoek, K.S., Schlegel, N.C., Eichhoff, O.M., Widmer, D.S., Praetorius, C., Einarsson, S.O., Valgeirsdottir, S., Bergsteinsdottir, K., Schepsky, A., Dummer, R*., et al.* (2008). Novel MITF targets identified using a two-step DNA microarray strategy. Pigment Cell Melanoma Res *21*, 665-676.

Hoglinger, G.U., Melhem, N.M., Dickson, D.W., Sleiman, P.M., Wang, L.S., Klei, L., Rademakers, R., de Silva, R., Litvan, I., Riley, D.E*., et al.* (2011). Identification of common variants influencing risk of the tauopathy progressive supranuclear palsy. Nature genetics *43*, 699-705.

Holm, H., Gudbjartsson, D.F., Sulem, P., Masson, G., Helgadottir, H.T., Zanon, C., Magnusson, O.T., Helgason, A., Saemundsdottir, J., Gylfason, A*., et al.* (2011). A rare variant in MYH6 is associated with high risk of sick sinus syndrome. Nature genetics *43*, 316-320.

Iida, S., Rao, P.H., Butler, M., Corradini, P., Boccadoro, M., Klein, B., Chaganti, R.S., and Dalla-Favera, R. (1997). Deregulation of MUM1/IRF4 by chromosomal translocation in multiple myeloma. Nature genetics *17*, 226-230.

Klein, U., Casola, S., Cattoretti, G., Shen, Q., Lia, M., Mo, T., Ludwig, T., Rajewsky, K., and Dalla-Favera, R. (2006). Transcription factor IRF4 controls plasma cell differentiation and class-switch recombination. Nat Immunol *7*, 773-782.

Kong, A., Masson, G., Frigge, M.L., Gylfason, A., Zusmanovich, P., Thorleifsson, G., Olason, P.I., Ingason, A., Steinberg, S., Rafnar, T*., et al.* (2008). Detection of sharing by descent, long-range phasing and haplotype imputation. Nature genetics *40*, 1068-1075.

Kong, A., Steinthorsdottir, V., Masson, G., Thorleifsson, G., Sulem, P., Besenbacher, S., Jonasdottir, A., Sigurdsson, A., Kristinsson, K.T., Jonasdottir, A.*, et al.* (2009). Parental origin of sequence variants associated with complex diseases. Nature *462*, 868-874.

Meyer, K.B., Maia, A.T., O'Reilly, M., Teschendorff, A.E., Chin, S.F., Caldas, C., and Ponder, B.A. (2008). Allele-specific up-regulation of FGFR2 increases susceptibility to breast cancer. PLoS biology *6*, e108.

Mittrucker, H.W., Matsuyama, T., Grossman, A., Kundig, T.M., Potter, J., Shahinian, A., Wakeham, A., Patterson, B., Ohashi, P.S., and Mak, T.W. (1997). Requirement for the transcription factor LSIRF/IRF4 for mature B and T lymphocyte function. Science *275*, 540-543.

Paun, A., and Pitha, P.M. (2007). The IRF family, revisited. Biochimie *89*, 744-753.

Pomerantz, M.M., Ahmadiyeh, N., Jia, L., Herman, P., Verzi, M.P., Doddapaneni, H., Beckwith, C.A., Chan, J.A., Hills, A., Davis, M.*, et al.* (2009). The 8q24 cancer risk variant rs6983267 shows long-range interaction with MYC in colorectal cancer. Nat Genet *41*, 882-884.

Rahimov, F., Marazita, M.L., Visel, A., Cooper, M.E., Hitchler, M.J., Rubini, M., Domann, F.E., Govil, M., Christensen, K., Bille, C.*, et al.* (2008). Disruption of an AP-2alpha binding site in an IRF6 enhancer is associated with cleft lip. Nat Genet *40*, 1341-1347.

Schodel, J., Bardella, C., Sciesielski, L.K., Brown, J.M., Pugh, C.W., Buckle, V., Tomlinson, I.P., Ratcliffe, P.J., and Mole, D.R. (2012). Common genetic variants at the 11q13.3 renal cancer susceptibility locus influence binding of HIF to an enhancer of cyclin D1 expression. Nat Genet *44*, 420-425, S421-422.

Shaffer, A.L., Emre, N.C., Lamy, L., Ngo, V.N., Wright, G., Xiao, W., Powell, J., Dave, S., Yu, X., Zhao, H.*, et al.* (2008). IRF4 addiction in multiple myeloma. Nature *454*, 226-231.

Smith, A.G., Box, N.F., Marks, L.H., Chen, W., Smit, D.J., Wyeth, J.R., Huttley, G.A., Easteal, S., and Sturm, R.A. (2001). The human melanocortin-1 receptor locus: analysis of transcription unit, locus polymorphism and haplotype evolution. Gene *281*, 81-94.

Stacey, S.N., Sulem, P., Jonasdottir, A., Masson, G., Gudmundsson, J., Gudbjartsson, D.F., Magnusson, O.T., Gudjonsson, S.A., Sigurgeirsson, B., Thorisdottir, K.*, et al.* (2011). A germline variant in the TP53 polyadenylation signal confers cancer susceptibility. Nature genetics *43*, 1098-1103.

Steingrimsson, E., Copeland, N.G., and Jenkins, N.A. (2004). Melanocytes and the Microphthalmia Transcription Factor Network. Annu Rev Genet *38*, 365-411.

Strub, T., Giuliano, S., Ye, T., Bonet, C., Keime, C., Kobi, D., Le Gras, S., Cormont, M., Ballotti, R., Bertolotto, C.*, et al.* (2011). Essential role of microphthalmia transcription factor for DNA replication, mitosis and genomic stability in melanoma. Oncogene *30*, 2319-2332.

Sturm, R.A. (2009). Molecular genetics of human pigmentation diversity. Human molecular genetics *18*, R9-17.

Sulem, P., Gudbjartsson, D.F., Stacey, S.N., Helgason, A., Rafnar, T., Jakobsdottir, M., Steinberg, S., Gudjonsson, S.A., Palsson, A., Thorleifsson, G.*, et al.* (2008). Two newly identified genetic determinants of pigmentation in Europeans. Nat Genet *40*, 835-837.

Sulem, P., Gudbjartsson, D.F., Stacey, S.N., Helgason, A., Rafnar, T., Magnusson, K.P., Manolescu, A., Karason, A., Palsson, A., Thorleifsson, G.*, et al.* (2007). Genetic determinants of hair, eye and skin pigmentation in Europeans. Nat Genet *39*, 1443-1452.

Sundram, U., Harvell, J.D., Rouse, R.V., and Natkunam, Y. (2003). Expression of the B-cell proliferation marker MUM1 by melanocytic lesions and comparison with S100, gp100 (HMB45), and MelanA. Mod Pathol *16*, 802-810.

Sviderskaya, E.V., Hill, S.P., Evans-Whipp, T.J., Chin, L., Orlow, S.J., Easty, D.J., Cheong, S.C., Beach, D., DePinho, R.A., and Bennett, D.C. (2002). p16(Ink4a) in melanocyte senescence and differentiation. Journal of the National Cancer Institute *94*, 446-454.

Thurman, R.E., Rynes, E., Humbert, R., Vierstra, J., Maurano, M.T., Haugen, E., Sheffield, N.C., Stergachis, A.B., Wang, H., Vernot, B*., et al.* (2012). The accessible chromatin landscape of the human genome. Nature *489*, 75-82.

Tsuboi, K., Iida, S., Inagaki, H., Kato, M., Hayami, Y., Hanamura, I., Miura, K., Harada, S., Kikuchi, M., Komatsu, H*., et al.* (2000). MUM1/IRF4 expression as a frequent event in mature lymphoid malignancies. Leukemia : official journal of the Leukemia Society of America, Leukemia Research Fund, UK *14*, 449-456.

Tuupanen, S., Turunen, M., Lehtonen, R., Hallikas, O., Vanharanta, S., Kivioja, T., Bjorklund, M., Wei, G., Yan, J., Niittymaki, I*., et al.* (2009). The common colorectal cancer predisposition SNP rs6983267 at chromosome 8q24 confers potential to enhanced Wnt signaling. Nat Genet *41*, 885-890.

Van Otterloo, E., Li, W., Bonde, G., Day, K.M., Hsu, M.Y., and Cornell, R.A. (2010). Differentiation of zebrafish melanophores depends on transcription factors AP2 alpha and AP2 epsilon. PLoS Genet *6*.

Visser, M., Kayser, M., and Palstra, R.J. (2012). HERC2 rs12913832 modulates human pigmentation by attenuating chromatin-loop formation between a long-range enhancer and the OCA2 promoter. Genome research *22*, 446-455.

Yang, Y., Shaffer, A.L., 3rd, Emre, N.C., Ceribelli, M., Zhang, M., Wright, G., Xiao, W., Powell, J., Platig, J., Kohlhammer, H*., et al.* (2012). Exploiting synthetic lethality for the therapy of ABC diffuse large B cell lymphoma. Cancer cell *21*, 723-737.

Yasumoto, K., Takeda, K., Saito, H., Watanabe, K., Takahashi, K., and Shibahara, S. (2002). Microphthalmia-associated transcription factor interacts with LEF-1, a mediator of Wnt signaling. Embo J *21*, 2703-2714.

Yasumoto, K., Yokoyama, K., Shibata, K., Tomita, Y., and Shibahara, S. (1994). Microphthalmia-associated transcription factor as a regulator for melanocyte-specific transcription of the human tyrosinase gene. Molecular and cellular biology *14*, 8058-8070.

Figure legends

Figure 1: Association with pigmentation traits of variants in the IRF4 region (0-1Mb on chromosome 6) as determined by whole genome sequencing and imputation into SNP chip typed individuals. Black points show the unadjusted association values, yellow points show association values adjusted for the effect of rs12203592. The X axis is the genomic coordinate (hg18 Build 36). The Y axes are the association $-\log_{10}$ P values for Sun Sensitivity (yes/no, upper panel), Brown vs Blond Hair Color (second panel), and Freckling (yes/no, third panel). The position of rs12203592 is indicated. The fourth panel shows the local recombination rates in cM/Mb. The lowest panel indicates the locations of known genes in the region, from UCSC.

Figure 2. rs12203592 disrupts a conserved melanocyte enhancer at *IRF4*.

a) UCSC genome browser view of 25 KB region around *IRF4* (hg19 coordinates chr6:388,750-413,750). DNase-seq signal (orange) in human epidermal melanocytes, Colo829, Mel 2183, and RPMI-7951 generated by ENCODE. b) Top: Graph shows *IRF4* expression level as measured by ENCODE in 49 cell types (Duke Affymetrix exon arrays). Bottom: UCSC genome browser view of 25 KB region around *IRF4* (hg19 coordinates chr6:388,750-413,750) in corresponding cell lines. Melanocyte-specific DNase HS peak overlapping rs12203592 labeled 'M'; Lymphoid-specific DNase HS peaks labeled 'L'; DNase HS overlapping the IRF4 promoter (labeled 'P'). Cell types shown are (top to bottom) human epidermal melanocytes, Colo829, Mel 2183, GM12878, GM12891, GM12892, GM19238, GM19238, GM19240, GM18507, and CLL. c) UCSC genome browser view of 25 KB region around *Irf4* (mm9 coordinates chr13:30,838,000-30,863,000). The ChIP-seq signals for EP300 (green) and H3K4me1 (blue) in the mouse melanocyte line melan-Ink4a-Arf from Gorkin et al., 2012.

Figure 3: Intron 4 of IRF4 drives expression in melanocytes

a-b) Results of the luciferase assays in melan-Ink4a-Arf and SK-MEL-28 cells. Pr=promoter; Luc=Luciferase reporter gene; *IRF4* enh= 450 bp fragment from the 4th intron of IRF4 containing rs12203592. '*IRF4* enh' fragments are identical except for the base at position rs12203592 as indicated ('C' is the ancestral allele, 'T' is the derived allele). The X-axis shows fold luciferase activity relative to the minimal promoter alone, which is normalized to 1. P-values calculated by Kolmogorov–Smirnov test. The result is

also highly significant by other non-parametric tests (P=0.007937 by Wilcoxon Rank-Sum test for both melan-Ink4a-Arf and SK-MEL-28), and by the standard parametric t-test (P=0.001686 for melan-Ink4a-Arf; P=0.01032 for SK-MEL-28). Each bar represents the average of five biological replicates per reporter construct. Error bars represent standard deviation. c) Reporter constructs containing either the rs12203592-C version of the IRF4 intron 4 element (IRF4) or the rs12203592-T version (IRF4snp) upstream of the GFP reporter after transfection into zebrafish. The numbers represent the number of melanophores (blue) and embryos (red) seen to be positive for GFP. The difference between the melanophores containing the wild-type allele of intron 4 of IRF4 compared to the mutant allele (rs12203592) is statistically significant (p=0,0023, unpaired t-test). d) Image showing a GFP positive zebrafish embryo with a GFP positive melanophore in the inset.

Figure 4: MITF regulates expression of IRF4.

a) The expression of the *Mitf* and *Irf4* mRNAs is reduced in hearts from *Mitf*$^{mi\text{-}vga9}$ mutant mice, as determined by qPCR analysis. b) Expression of the *MITF*, *IRF4*, *TFAP2a*, *DCT* and *TYR* genes upon treatment with shRNA against *MITF*, *IRF4*, *TFAP2A* and negative control in 501mel melanoma cells as determined by qPCR analysis. c) Western blot showing expression of the MITF, TFAP2A, IRF4 and β-actin proteins in 501mel cells after shRNA treatment. Intensity quantification is relative to actin loading control. d) Overexpression of the mouse Mitf (mMitf) cDNA (expressed from pcDNA3.1) in 501mel melanoma cells and in HEK293T embryonic kidney cells affects expression of the TYR and IRF4 mRNAs as assayed by RT-qPCR, whereas β-actin expression is unchanged. mMitf was detected with species-specific primers which only recognize the mouse *Mitf* gene.

Figure 5: MITF and TFAP2A affect *IRF4* expression by binding regulatory elements in intron 4.

a) Schematic view of the IRF4 gene. The sequence shows comparison of MITF and TFAP2A binding sites in intron 4 of IRF4 between humans (H sap), gorilla (G gor), chimpanzee (P tro) and mouse (M mus). The location of the rs12203592 polymorphism is indicated. b) ChIP analysis of a GST-tagged MITF protein (a-GST AB) performed in 501mel cells. Primers specific for HSPA1B (neg. control), TYR (pos. control), and intron 4 of IRF4 are indicated. The GST-tagged Mitf only precipitated TYR and IRF4 sequences. c) ChIP analysis of TFAP2A in 501mel

cells. PCR products specific for TGFA (pos. control), HSPA1B (neg. control) and intron 4 of IRF4 are shown. TFAP2A only precipitated TGFA and INT4 sequences. d) Gel shift analysis showing the binding of TFAP2A to the ancestral sequence (INT4-wt) in intron 4 of IRF4 (coordinates chr6: 396309-396333 in build GRCh37.p5 of the human genome) but not to the rs12203592-T sequence (INT4-RS) or to a completely mutated sequence (INT4-mut). e) Luciferase reporter assays performed in 501mel melanoma cells using intron 4 of IRF4 as a reporter. The ancestral IRF4 intron 4 sequence (intron 4, blue), the rs12203592-T polymorphic sequence (intron 4-rs), a sequence where all MITF binding sites were mutated (intron 4-3xE) and a sequence containing mutated MITF sites and the rs12203592-T polymorphism (intron 4-3xE+rs) were tested. The luciferase reporters were co-transfected with the wild type MITF and TFAP2A proteins and with a dominant negative version of MITF ($MITF^{mi}$). Statistical analysis ($p<0.0001$) was done using unpaired t-test. f) Cells homozygous for the ancestral allele (CC) express significantly higher levels of IRF4 than cells homozygous for the rs12203592-T polymorphism (TT). Fold expression data is represented relative to pooled mean TT expression. Statistical analysis was performed using analysis of variance (***, $p < 0.001$). g) A western blot showing expression of the IRF4 protein in melanocytes from CC and TT individuals. Intensity quantification is relative to GAPDH loading control. Note the decrease of basal IRF4 protein in the TT melanocyte cell lines.

Figure 6: MITF and IRF4 regulate expression of TYR.

a) Schematic view of the human TYR promoter showing the sequence of the MITF and potential IRF4 binding sites. b) Expression of IRF4, TYR, MATP, SLC24A5 and DCT as determined by qPCR, after treatment with siIRF4 or control siRNAs. Fold expression of each gene is represented relative to cells transfected with negative siRNA (arbitrarily set to 1). Data represent the mean ± range of two experiments using two primary melanocytes (QF1438 and QF1424). c) Luciferase reporter assay using wild-type TYR promoter as reporter construct and co-transfected with constructs expressing the MITF and IRF4 proteins. Statistical analysis was performed using the t-test. d) IRF4 binds the TYR locus. Chromatin immunoprecipitation real time PCR (ChIP-qPCR) analysis of IRF4 binding at sites proximal (around transcription start site; pTYR) and more distal (~1800 bp upstream of transcription start site; dTYR) to TYR coding region and other control loci in SK-MEL-28 melanoma cell line and in negative control OCI-Ly-19, a germinal center type B-cell lymphoma (GCB-DLBCL) cell line previously shown to lack IRF4 expression (Yang et al., 2012). Primer pair amplifying a region upstream of the SUB1 locus was used as a positive control, since this region showed strong IRF4 binding both

in multiple myeloma (Shaffer et al., 2008), and activated B-cell type B-cell lymphoma (Yang et al., 2012) cell lines. NegA is a region on chromosome 7, used as a negative control for IRF4 binding, due to lack of observable IRF4 binding in previous studies with multiple myeloma and ABC-DLBCL cell lines. Error bars depict standard error of the mean.

Figure 7: IRF4 is involved in regulating pigmentation in mice.

a) The expression plot shows presence and clear differences in the expression of *Mitf*, *Tcfap2a*, *Irf4* and *Tyr* at different developmental time points, E15.5, E17.5, P1 and P7, measured in FPKM. Indicated expression levels of a transcript are proportional to the number of reads sequenced from that transcript after normalizing for respective transcript's length. RNA from E15.5 embryos is shown in blue bars, E17.5 embryos in red, P1 pups in green and P7 in violet. b) Mice where *Irf4* has been conditionally knocked out in heterozygotes for the semidominant $Mitf^{Mi\text{-}Wh}$ mutation. $Mitf^{Mi\text{-}Wh}$ heterozygotes which are simultaneously lacking *Irf4* show lighter coat color (left) than mice which are wild type for *Irf4* (right). c) Model depicting the relationship between MITF, TFAP2A and IRF4 in melanocytes and their effects on the expression of *TYR*. MITF and TFAP2A bind together to the intron 4 element in the *IRF4* gene and regulate the expression of *IRF4* from the upstream promoter. MITF and IRF4 then bind to and activate expression of TYR, leading to normal pigmentation. The rs12203592-T polymorphism leads to reduced IRF4 activation and thus reduced TYR expression which consequently leads to sun sensitivity and blue eyes.

Figure 1

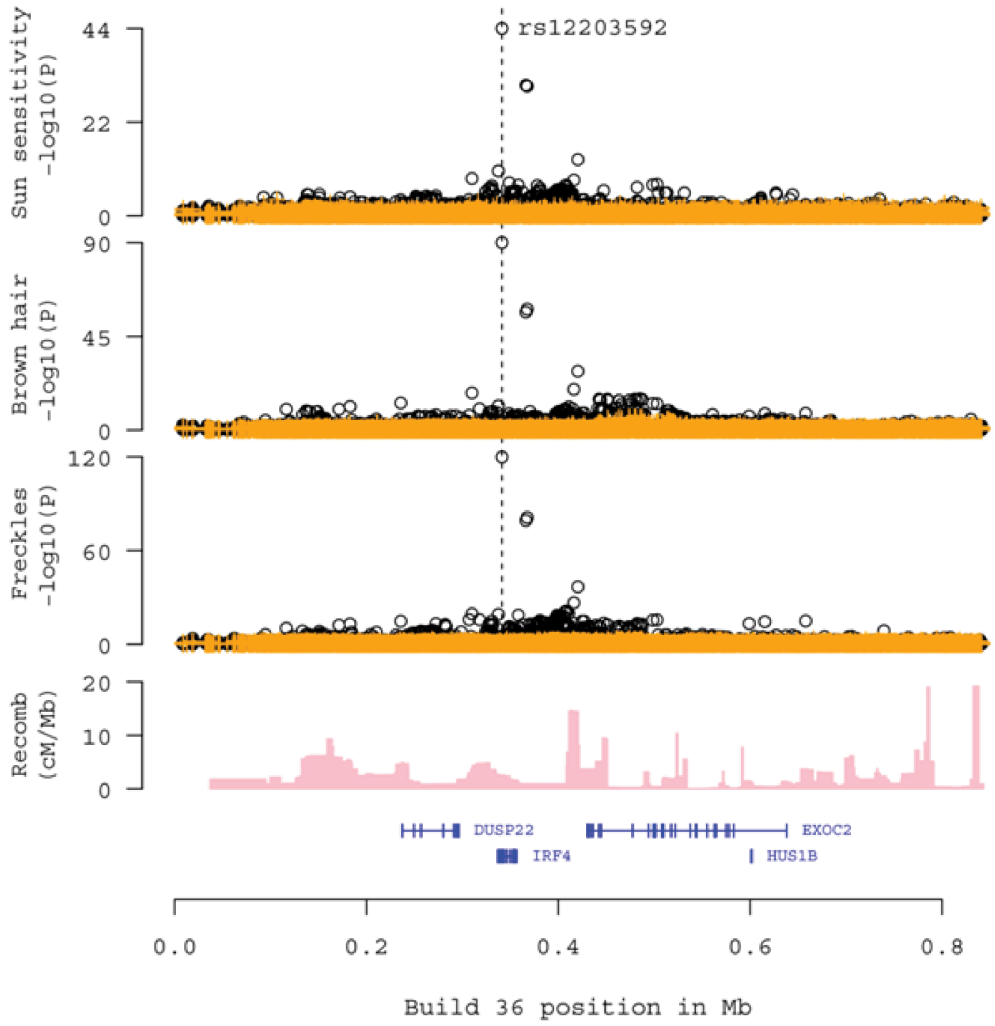
rs12203592
Sun sensitivity
-log10(P)
44
22
0
Brown hair
-log10(P)
90
45
0
Freckles
-log10(P)
120
60
0
Recomb
(cM/Mb)
20
10
0
DUSP22
EXOC2
IRF4
HUS1B
0.0
0.2
0.4
0.6
0.8
Build 36 position in Mb

Figure 2

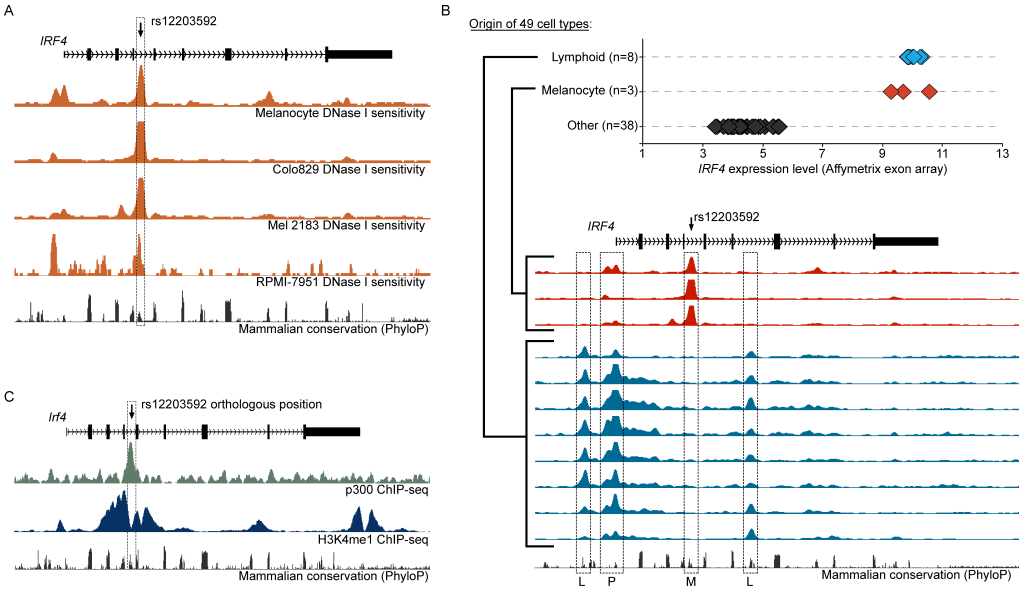
A
rs12203592
IRF4
Melanocyte DNase I sensitivity
Colo829 DNase I sensitivity
Mel 2183 DNase I sensitivity
RPMI-7951 DNase I sensitivity
Mammalian conservation (PhyloP)
B
Origin of 49 cell types:
Lymphoid (n=8)
Melanocyte (n=3)
Other (n=38)
1
3
5
7
9
11
13
IRF4 expression level (Affymetrix exon array)
IRF4
rs12203592
L
P
M
L
Mammalian conservation (PhyloP)
C
rs12203592 orthologous position
Irf4
p300 ChIP-seq
H3K4me1 ChIP-seq
Mammalian conservation (PhyloP)

Figure 3

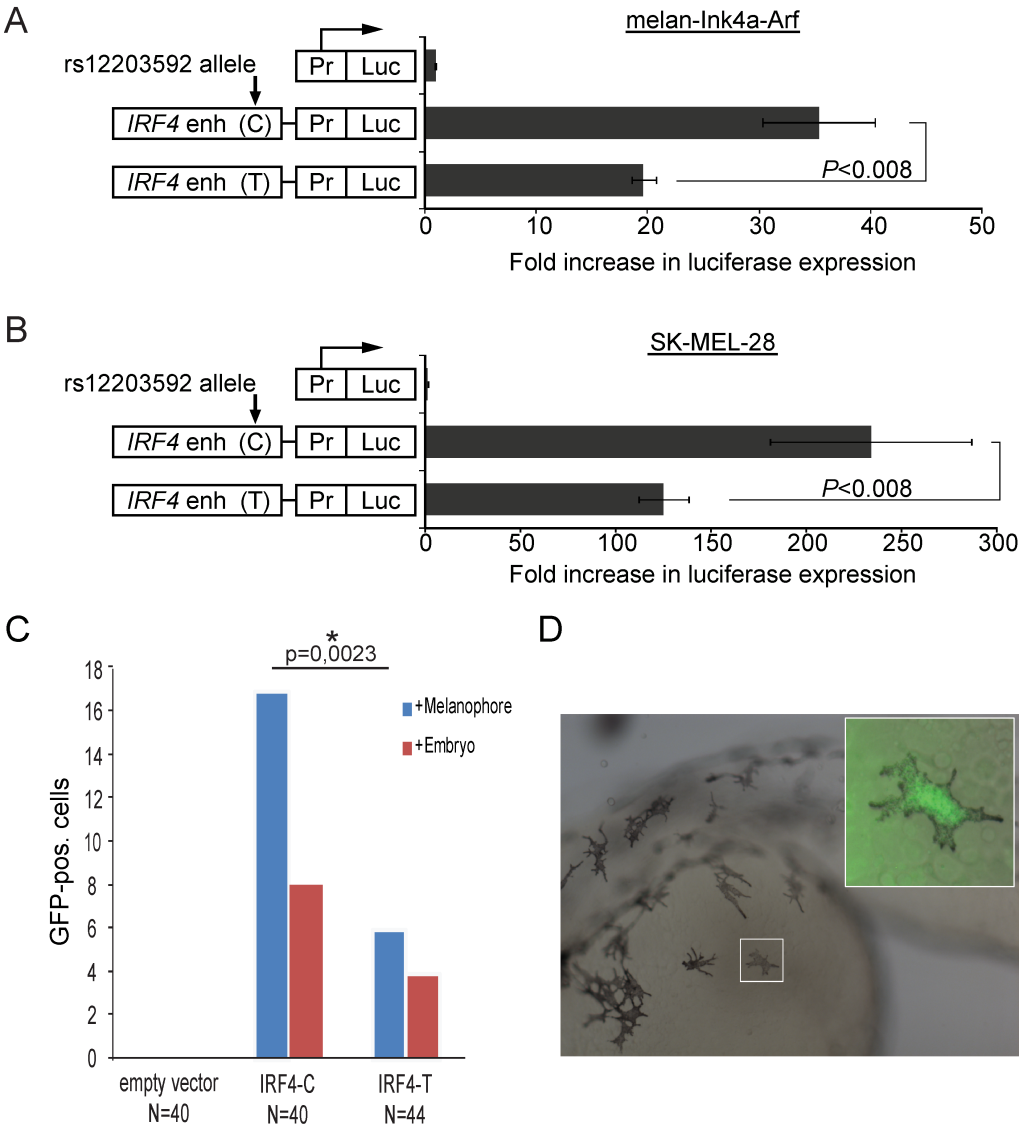
A
melan-Ink4a-Arf
rs12203592 allele
Pr
Luc
IRF4 enh (C)
IRF4 enh (T)
P<0.008
0
10
20
30
40
50
Fold increase in luciferase expression
B
SK-MEL-28
rs12203592 allele
Pr
Luc
IRF4 enh (C)
IRF4 enh (T)
P<0.008
0
50
100
150
200
250
300
Fold increase in luciferase expression
C
*
p=0,0023
+Melanophore
+Embryo
GFP-pos. cells
0
2
4
6
8
10
12
14
16
18
empty vector
N=40
IRF4-C
N=40
IRF4-T
N=44
D

Figure 4

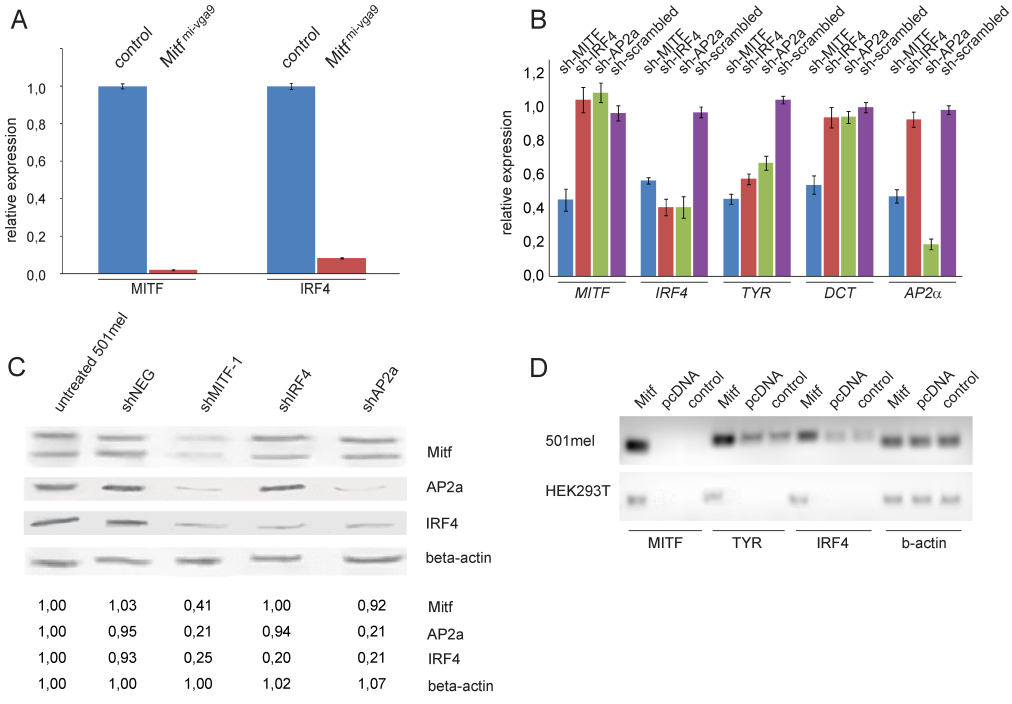
A
control
Mitf mi-vga9
control
Mitf mi-vga9
relative expression
1,0
0,8
0,6
0,4
0,2
0,0
MITF
IRF4
B
sh-MITF
sh-IRF4
sh-AP2a
sh-scrambled
relative expression
1,2
1,0
0,8
0,6
0,4
0,2
0,0
MITF
IRF4
TYR
DCT
AP2α
C
untreated 501mel
shNEG
shMITF-1
shIRF4
shAP2a
Mitf
AP2a
IRF4
beta-actin
1,00 1,03 0,41 1,00 0,92 Mitf
1,00 0,95 0,21 0,94 0,21 AP2a
1,00 0,93 0,25 0,20 0,21 IRF4
1,00 1,00 1,00 1,02 1,07 beta-actin
D
Mitf
pcDNA
control
501mel
HEK293T
MITF
TYR
IRF4
b-actin

Figure 5

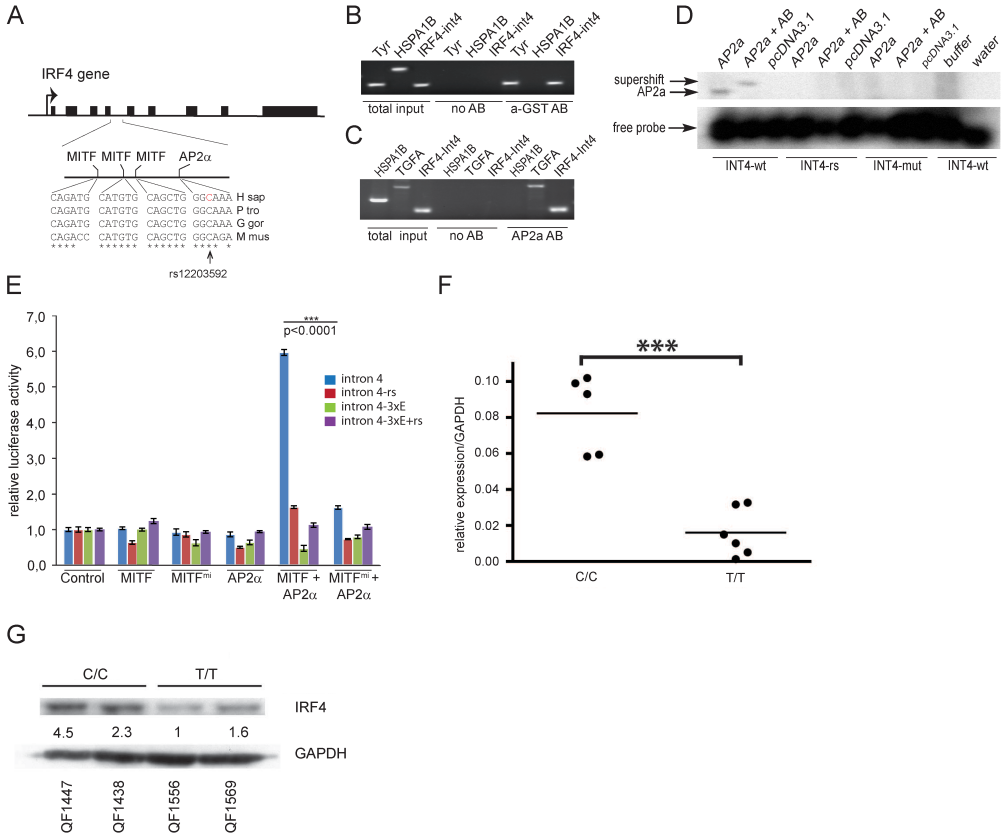
A
IRF4 gene
MITF MITF MITF AP2α
CAGATG CATGTG CAGCTG GGCAAA H sap
CAGATG CATGTG CAGCTG GGCAAA P tro
CAGATG CATGTG CAGCTG GGCAAA G gor
CAGACC CATGTG CAGCTG GGCAGA M mus
rs12203592
B
Tyr HSPA1B IRF4-int4
total input
no AB
a-GST AB
C
HSPA1B TGFA IRF4-int4
total input
no AB
AP2a AB
D
AP2a
AP2a + AB
pcDNA3.1
buffer
water
supershift AP2a
free probe
INT4-wt
INT4-rs
INT4-mut
E
relative luciferase activity
p<0.0001
intron 4
intron 4-rs
intron 4-3xE
intron 4-3xE+rs
Control
MITF
MITFmi
AP2α
MITF + AP2α
MITFmi + AP2α
F
relative expression/GAPDH
C/C
T/T
G
C/C
T/T
IRF4
GAPDH
4.5
2.3
1
1.6
QF1447
QF1438
QF1556
QF1569

Figure 6

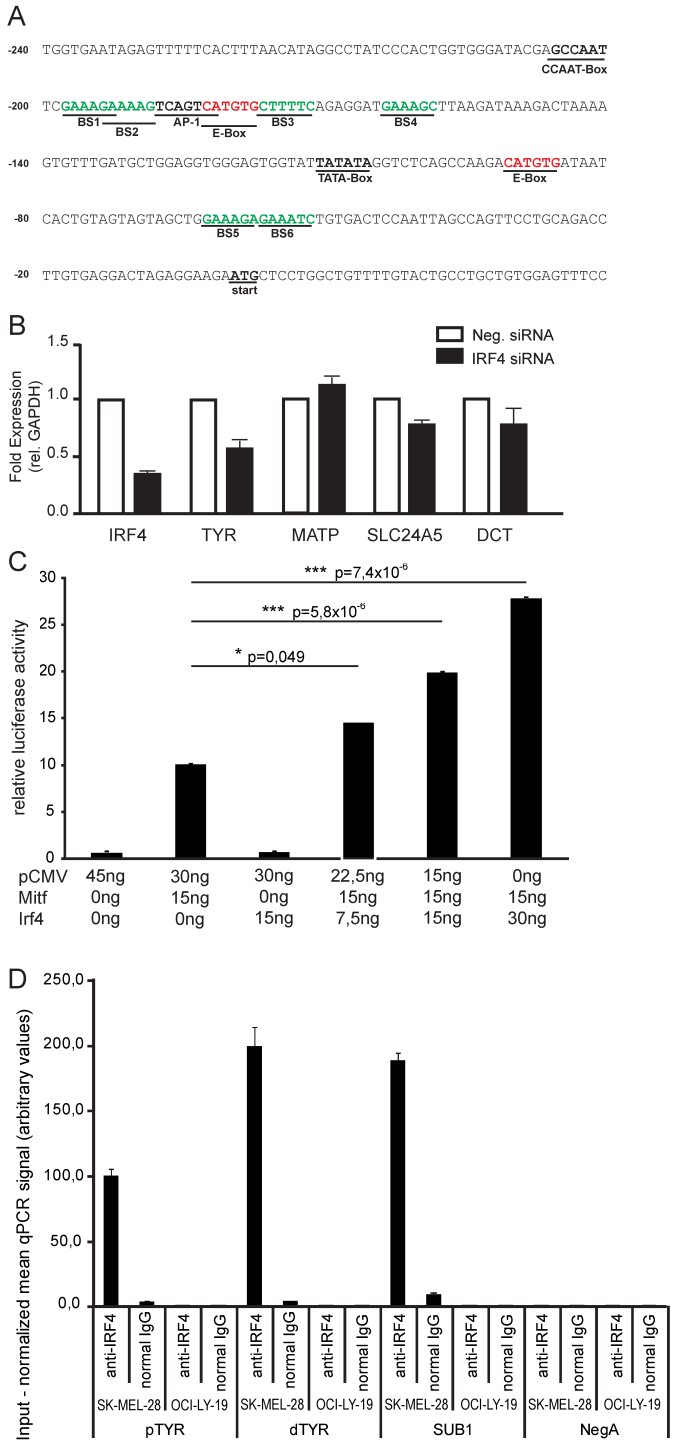
A
-240 TGGTGAATAGAGTTTTTCACTTTAACATAGGCCTATCCCACTGGTGGGATACGAGCCAAT
CCAAT-Box
-200 TCGAAAGAAAAGTCAGTCATGTGCTTTTCAGAGGATGAAAGCTTAAGATAAAGACTAAAA
BS1 BS2 AP-1 E-Box BS3 BS4
-140 GTGTTTGATGCTGGAGGTGGGAGTGGTATTATATAGGTCTCAGCCAAGACATGTGATAAT
TATA-Box E-Box
-80 CACTGTAGTAGTAGCTGGAAAGAGAAATCTGTGACTCCAATTAGCCAGTTCCTGCAGACC
BS5 BS6
-20 TTGTGAGGACTAGAGGAAGAATGCTCCTGGCTGTTTTGTACTGCCTGCTGTGGAGTTTCC
start
B
Neg. siRNA
IRF4 siRNA
Fold Expression (rel. GAPDH)
1.5
1.0
0.5
0.0
IRF4
TYR
MATP
SLC24A5
DCT
C
*** p=7,4x10-6
*** p=5,8x10-5
* p=0,049
relative luciferase activity
30
25
20
15
10
5
0
pCMV 45ng 30ng 30ng 22,5ng 15ng 0ng
Mitf 0ng 15ng 0ng 15ng 15ng 15ng
Irf4 0ng 0ng 15ng 7,5ng 15ng 30ng
D
Input - normalized mean qPCR signal (arbitrary values)
250,0
200,0
150,0
100,0
50,0
0,0
anti-IRF4
normal IgG
SK-MEL-28
OCI-LY-19
pTYR
dTYR
SUB1
NegA

Figure 7

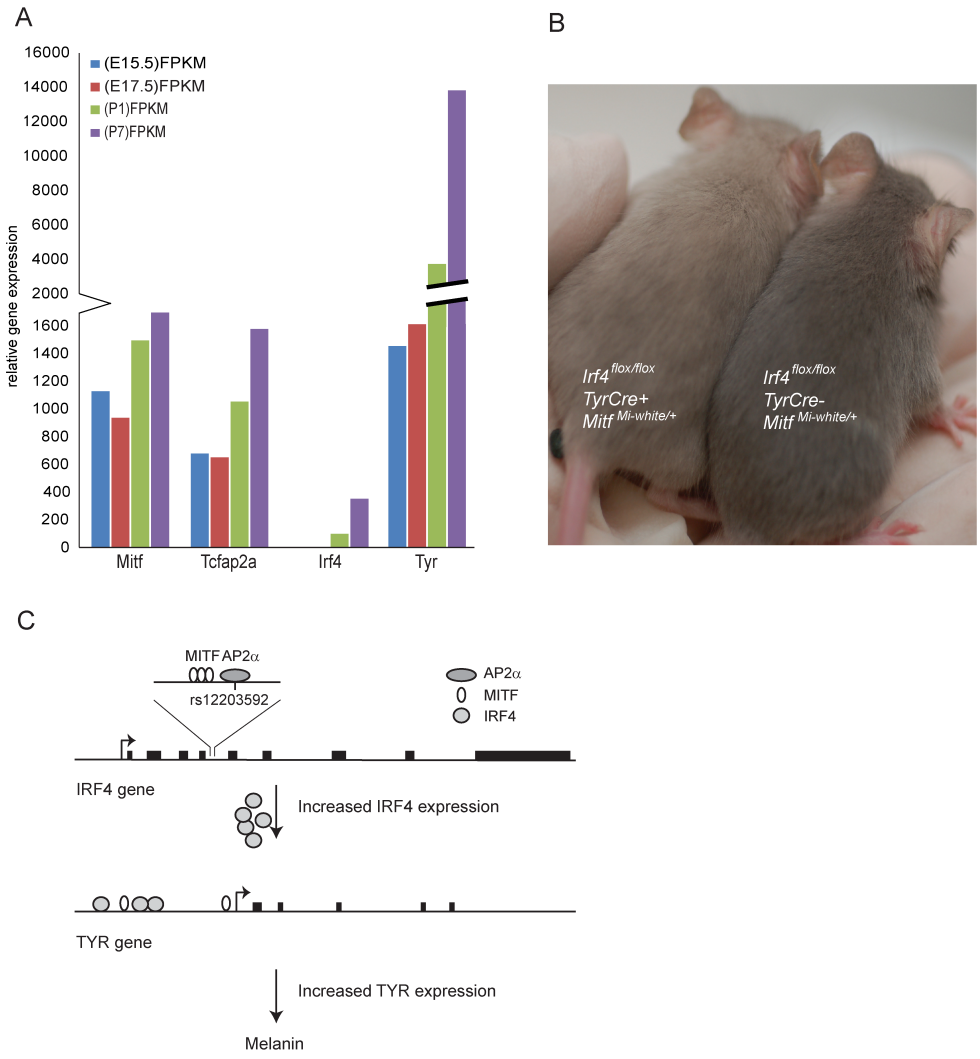
A
16000
14000
12000
10000
8000
6000
4000
2000
1600
1400
1200
1000
800
600
400
200
0
relative gene expression
(E15.5)FPKM
(E17.5)FPKM
(P1)FPKM
(P7)FPKM
Mitf
Tcfap2a
Irf4
Tyr
B
Irf4 flox/flox
TyrCre+
Mitf Mi-white/+
Irf4 flox/flox
TyrCre-
Mitf Mi-white/+
C
MITF AP2α
rs12203592
AP2α
MITF
IRF4
IRF4 gene
Increased IRF4 expression
TYR gene
Increased TYR expression
Melanin

Praetorius et al.

Supplemental Information

Table of contents:

Supplemental Figures

Supplemental Figure 1: Geographical distribution of allele frequencies for rs12203592

Allele frequencies of the rs12203592 polymorphism in several human populations from around the world. Information about allele frequencies and geographical coordinates of human populations were obtained from the ALFRED database (http://alfred.med.yale.edu) (Rajeevan et al., 2012), with the exception of the Icelandic population, for which the frequency of rs12203592 was determined as described in the materials and methods section. The percentage is shown as a circle with the wild-type C allele in yellow and the T derived allele in blue.

Supplemental Figure 2.

Western blot showing expression of the MITF (Thermo Fisher C5), TFAP2A (abcam ab52222), IRF4 (Cell Signalling, IRF4 (CST #4299), TYR (Santa Cruz sc-7833) and β-actin (Millipore C4 MAB1501R) proteins in 501mel cells after shRNA treatment.

Supplemental Figure 3.

a) Correlation of IRF4 and TYR expression levels with the SNP genotype of rs12203592 in melanoma cell lines. b) EMSA showing the binding of the wild-type MITF protein to an oligo containing the M-box (first two lanes) and to longer oligos from intron 4 of IRF4 which contain the three MITF binding sites as well as the TFAP2A binding site, with (IRF4-Int4-RS) and without the SNP (IRF4-Int4-wt). Supershifts with a MITF-specific antibody are indicated, confirming the specificity of the gel shifts. Western blot shows equal loading of the MITF-wt, delR217 and empty vector proteins. c) Relative expression of IRF4 in cultured primary melanocytes: Expression of IRF4 relative to GAPDH in melanocytes cultured from individuals homozygous for the ancestral rs12203592-C allele (CC) or the rs12203592-T allele (TT). QF1383, QF1438, QF1447, QF1459, QF1558, QF1424, QF1101, QF1359, QF1392, QF1556, QF1564, and QF1569 represent melanocytes from different individuals. Relative expression data represent the means and standard deviations of technical triplicates from single experiments (n=1).

Supplemental Figure 4. *IRF4* allelic expression variation is correlated with the rs12203592-T allele

The rs872701 SNP is located in the 3'UTR of IRF4. In order to determine if the rs12203592 SNP affects expression of the gene in cis, allelic RT-qPCR was performed using primary melanocytes to determine relative allelic expression ratios for IRF4 3'UTR SNP rs872701-A alleles relative to rs872701-G alleles.

The rs872071–A/-G allele ratios are plotted relative to heterozygous DNA from primary melanocyte line C-002-25P. Genotypes for rs87201 and rs12203592 are indicated below. A total of four heterozygous rs872701 DNA samples control for potential allele specific amplification and probe binding bias (white). In cells homozygous for the rs12203592-C ancestral SNP (light grey), there is little difference in expression between rs872071–A and rs872071-G alleles. In cells heterozygous for the rs12203592 C/T polymorphism (dark grey), the relative rs872071-A/rs872071-G allele ratio is significantly higher ($p<0.01$) by two-way ANOVA followed by Scheffe's post hoc analysis, indicating that altered allelic IRF4 expression is correlated with rs12203592–T derived alleles.

Supplemental Figure 5. The alternative *IRF4*-transcript

a) Schematic drawing of the IRF4 gene showing the structure of the gene. The arrowhead denotes the transcription start site, red markers show the MITF binding sites in intron 4, the green marker the rs12203592 polymorphism. The exons are marked as black boxes, the introns as a line. The different alternative IRF4 transcripts described to date are shown. b) Expression of *IRF4* isoforms in foreskin melanocytes from Australian subjects. The full length product is detected by IRF4, the short versions by primer pair pr55.

Supplemental Figure 6. RNA-sequencing of the IRF4 gene at various stages of mouse development.

RNA-Seq analysis of the Irf4 transcript in embryonic E15.5 and E17.5, and neonatal P1 and P7 melanoblasts/melanocytes isolated from the iDct-GFP transgenic line. Only the full-length transcript was expressed at all stages, and the expression increased in the neonatal melanocytes as compared to the embryonic melanoblasts, presumably according to the differentiation stage.

Supplemental Figure 7. Activation of the TYR promoter

a) Luciferase reporter assay using wild-type TYR promoter as reporter, co-transfected with the MITF, $Mitf^{mi\text{-}white}$ and IRF4 expression constructs. b) Luciferase reporter assay using TYR promoter with mutated E-boxes as reporter and co-transfected with MITF, $Mitf^{mi\text{-}white}$ and IRF4 expression constructs. c) Chromatin immunoprecipitation real time PCR (ChIP-qPCR) analysis of IRF4 binding at sites proximal (around transcription start site; pTYR) and distal (~1800 bp upstream of transcription start site; dTYR) to the TYR coding region and other control loci in SK-MEL-5 melanoma cell line. Primer pairs amplifying a region upstream of the SUB1 locus was used as a positive control since this region showed strong IRF4 binding both in multiple myeloma (Shaffer et al., 2008), and activated B-cell type B-cell lymphoma (Yang et al., 2012) cell lines. NegA is a region on chromosome 7, used as a

negative control for IRF4 binding due to lack of observable IRF4 binding in previous studies with multiple myeloma and ABC-DLBCL cell lines. Error bars depict standard error of the mean.

Supplemental Tables

Supplemental Table 1: Association of rs12203592-T with pigmentation traits in Icelanders

Phenotype[a]	OR[b]	95% CI[b]	P value[b]	Allele	Allele frequency[c]	N[d]
Freckles (present vs absent)	3.22	(2.92, 3.55)	2.00×10^{-120}	T	0.130	14,996
Hair Color (blond vs brown)	0.17	(0.15, 0.21)	8.60×10^{-90}	T	0.130	6,582
Sun Sensitivity (yes vs no)	1.87	(1.72, 2.05)	3.20×10^{-44}	T	0.130	14,910
Eye Color (blue vs brown)	1.57	(1.32, 1.86)	2.10×10^{-7}	T	0.130	12,897
Hair Color (red vs non-red)	1.26	(1.08, 1.47)	0.0041	T	0.130	15,418
Eye Color (blue vs green)	1.13	(1.00, 1.27)	0.043	T	0.130	13,771

[a]Phenotyping was carried out as described in Sulem et al, 2007. [b]P values, OR, and 95% confidence intervals (CI) were determined by long-range phasing and impuation into chip-typed individuals, as described in Holm et al. 2011. [c]The estimated allele frequency in the Icelandic population. [d]N is the number of indivduals with information for the respective trait.

Supplemental Table 2: Association IRF4 region SNPs with Pigmentation Traits without and with adjustment for effect of rs12203592-T

						Unadjusted			Adjusted for rs12203592		
Phenotype[a]	SNP	Allele	Allele frequency[b]	Location[c]	r^2 vs rs12203592[d]	OR[b]	95% CI[b]	P value[b]	OR[b]	95% CI[b]	P value[b]
Freckles	rs12203592	T	0.130	chr6:341321	NA	3.22	(2.92, 3.55)	2.0×10^{-120}	NA	NA	NA
(present vs absent)	rs62389423	A	0.107	chr6:366281	0.647101	2.79	(2.51, 3.11)	7.5×10^{-80}	1.06	(0.88, 1.28)	0.53
	rs62389424	A	0.109	chr6:367631	0.647801	2.79	(2.51, 3.09)	1.1×10^{-81}	1.11	(0.93, 1.33)	0.26
	rs1540771	T	0.467	chr6:411033	0.097303	1.32	(1.25, 1.40)	1.5×10^{-20}	1.08	(1.01, 1.15)	0.02
	rs12210050	T	0.163	chr6:420489	0.257611	1.71	(1.58, 1.86)	2.5×10^{-37}	1.09	(0.98, 1.20)	0.1
Hair Color	rs12203592	T	0.130	chr6:341321	NA	0.17	(0.15, 0.21)	8.6×10^{-90}	NA	NA	
(blond vs brown)	rs62389423	A	0.107	chr6:366281	0.647101	0.23	(0.19, 0.28)	9.9×10^{-57}	0.98	(0.71, 1.37)	0.93
	rs62389424	A	0.109	chr6:367631	0.647801	0.23	(0.19, 0.28)	3.3×10^{-58}	0.91	(0.66, 1.25)	0.57
	rs1540771	T	0.467	chr6:411033	0.097303	0.72	(0.66, 0.79)	8.4×10^{-12}	0.95	(0.86, 1.04)	0.27
	rs12210050	T	0.163	chr6:420489	0.257611	0.47	(0.41, 0.53)	1.1×10^{-28}	0.86	(0.73, 1.01)	0.068
Sun Sensitivity	rs12203592	T	0.130	chr6:341321	NA	1.87	(1.72, 2.05)	3.2×10^{-44}	NA	NA	
(yes vs no)	rs62389423	A	0.107	chr6:366281	0.647101	1.78	(1.61, 1.96)	4.4×10^{-31}	1.06	(0.90, 1.25)	0.49
	rs62389424	A	0.109	chr6:367631	0.647801	1.76	(1.60, 1.94)	8.3×10^{-31}	1.05	(0.90, 1.24)	0.52
	rs1540771	T	0.467	chr6:411033	0.097303	1.15	(1.08, 1.21)	4.5×10^{-6}	1.01	(0.95, 1.07)	0.83
	rs12210050	T	0.163	chr6:420489	0.257611	1.35	(1.25, 1.46)	8.1×10^{-14}	1.02	(0.93, 1.12)	0.61

[a]Phenotyping was carried out as described in Sulem et al, 2007. [b]The estimated allele frequency in the Icelandic population. [c]HG18 build 36. [d]P values, OR, 95% confidence intervals (CI) and r2 values were determined by long-range phasing and imputation into chip-typed individuals, as described in Holm et al. 2011

Supplemental Table 3: Oligos used for the experiments (noted in 5' -> 3' direction)

Primer	species	forward	reverse
Mitf	Hsap	CTATGCTTACGCTTAACTCCA	TACATCATCCATCTGCATACAG
Mitf	Mmus	CAAATGATCCAGACATGCGG	TGCTCCAGCTTCTTCTGTC
IRF-4	Hsap	ACAGCAGTTCTTGTCAGAG	GAGGTTCTACGTGAGCTG
IRF-4	Mmus	CAGCTCATGTGGAACCTC	GGAAGAATGACGGAGGGA
Tyr	Hsap	CCATGACAAATCCAGAACCC	GGACTAGCAAATCCTTCCAG
DCT	Hsap	ACTGGAACTTTGCCACTG	TCATCCAAGCTATCACAGAC
TFAP2a	Hsap	GAGGTCCCGCATGTAGAA	CCGAAGAGGTTGTCCTTGT
ActB	Hsap	AAATCTGGCACCACACCT	GTCTCAAACATGATCTGGGTC
ActB	Mmus	TACCAACTGGGACGACAT	GTCTCAAACATGATCTGGGTC
IRF4 intron 4 qPCR primer	Hsap	ACCCACCAAAGTGGATGAAA	CGCCTGTTGGAATATGCTTC
IRF4 intron 4 AP2a BS	Hsap	CTTCAGGCTTTCTTGATGTGAA	GGAGGATCATAAAGGACAATGG
HSPA1B promoter	Hsap	CATGGAGACCAACACCTTC	CTTTCCCCTTCTGAGCCAAT
TGFA promoter	Hsap	TAGCCGCCTTCCTATTTCC	AAAGACGCAGACTAGGCA
Tyr promoter	Hsap	ACGAGCCAATTCGAAAGAAA	CACAGATTTCTCTTTCCAGCTAC
IRF4-Int4 wildtype	Hsap	GGTAAAAGAAGGCAAATTCCCCTGT	ACAGGGGAATTTGCCTTCTTTTAC
IF4-Int4 RS12203592	Hsap	GGTAAAAGAAGGTAAATTCCCCTGT	ACAGGGGAATTTACCTTCTTTTAC
IRF4-Int4 AP2A site mutated	Hsap	GGTAAAAGAATTACGATTCCCCTGT	ACAGGGGAATCGTAATTCTTTTAC
Proximal Tyrosinase Primers	Hsap	GTGGGATACGAGCCAATTCGAAAGA	CCCACCTCCAGCATCAAACACTTTT
Distal Tyrosinase Primers	Hsap	TAAGCCTCCTTGTGGAGATCATGTG	TGTGTGGGTGAAGAGGAAGAGAAGT
Negative Control Primer Pair A	Hsap	AATATGTACATCAGGCAATCGGCTCTTC	CAACTGGAATCAGATCCACTTCATGGAAA
SUB1 upstream Primers	Hsap	CTTAGAGAACCGAAACCCAAACCTACA	TGCAACCCTTCCTGCTTTAACAAGTTT
IRF4-Int4 primer	Hsap	ATTTGCTATGGCTGCTCCAA	CACCGGGTAAAGGAGTGCAGGAGA
Mouse screening primers			
IRF4 screening primer	Mmus	AATACTGAGCTGCAGTCTAGC	TGTTGCTGGTGGAGAGGAAG
			GACCACTACCAGCAGAACAC
TyrCre screening primer		GTCACTCCAGGGGTTGCTGG	CCGCCGCATAACCAGTGA

Materials and Methods

Allelic Discrimination Test

Primary Human melanocytes, C-002-25P (Invitrogen) and UDP3138, UDP629, UP1033, UDP3588, UDP3138, UDP1026, and HPS163 (generously provided by Dr. William Gahl) were cultured as indicated by Cullinane et al. (2011). Control lymphoblast cell lines GM12044 and GM12873 were grown per Coriell culture conditions. DNA was isolated from cell lines using Puregene reagents (Gentra Systems). RNA was isolated from cells plated in 6-well dishes grown to 80% confluence, harvested in Trizol (Invitrogen), followed by chloroform extraction and RNA phase purification using Qiagen RNeasy mini kit (Qiagen). DNase I (Invitrogen) treated RNA (800 ng) was used to synthesize cDNA in a 40ul reaction using High-Capacity cDNA Reverse Transcription Kit as per manufacturer's instructions (Applied Biosystems). Allelic discrimination RT-qPCR was performed using rs872701 TAQMAN SNP genotyping assay and TAQMAN GTXpress Master Mix in 20ul reactions under fast conditions with a StepOnePlus Real Time machine (Applied Biosystems). Allelic discrimination for DNA controls was performed in triplicate and RT-qPCR for cell lines was performed for using at least three independent biological replicates, each assayed in triplicate. Relative concentrations for each allele were calculated using the Standard Curve Method, with the standard curve representing allele concentration ratio mixes spanning the range of 90% C/10% T to 10% C /90% T alleles for rs872701. Genotyping of cell lines for rs12203592 and rs872701 was performed using TAQMAN SNP genotyping assay as described above followed by allelic discrimination analysis using 7500Fast Machine (Applied Biosystems).

Cloning.

The intron 4 element of IRF4 was amplified with PCR from human genomic DNA (Promega, #G3041). The primers contained overhanging MluI (forward primer) and XhoI (reverse primer) sites to allow directed cloning into the pGL3b vector (Promega). The resulting plasmid was verified by sequencing. Mutations were introduced by using the *QuikChange Lightning* Site-Directed *Mutagenesis* Kit (Agilent) according to the manufacturer's instructions. Oligo sequences used for generating the mutations are listed in Supplemental Table 3. The IRF4 expression construct was provided by Dr. Singh (Brass et al., 1996) and the TFAP2A expression construct by Dr. Bar-Eli (Tellez et al., 2003).

The 450 bp enhancer fragments were synthesized and sequence-verified (Genewiz, Inc). We used the human reference genome (hg19 coordinates chr6:396,143-396,593) to determine the sequence of the fragments, but the reference 'C' allele at rs12203592 was replaced with a 'T' as indicated in text and figures. The two enhancer fragments were otherwise identical. We included Gateway-compatible recombination arms (Fu et al., 2008) on either side of the enhancer sequence, and used the Gateway LR reaction (Invitrogen) to insert the enhancer fragment upstream of a minimal

promoter in the reporter plasmid pE1B for luciferase assays (Antonellis et al., 2008), or the ZED vector for zebrafish enhancer assays (Bessa et al., 2009).

Cell culture and transfections

Cell lines (501mel, SK-MEL-28 and HEK293T cells) were cultured in DMEM (Life Technologies) with the addition of 10% fetal bovine serum (Life Technologies), 2mM Glutamax (Life Technologies) and antibiotics (100 IU penicillin and 100 µg Streptomycin, Life Technologies). The 501mel cells were a kind gift from Ruth Halaban. For transfections, Exgene 500 (Fermentas) was used according to the manufacturer's instructions. For selection after shRNA-plasmid transfections, puromycin was used at the final concentration of 5 µg/ml. For the overexpression of Mitf in 501mel and 293T cells the cells were seeded in 6 well plates. Then they were transfected as described above with a construct containing the mouse Mitf cDNA in pCDNA3.1 and cultivated for 24 hours. After this period the total RNA was extracted as described, cDNA prepared and Q-RT-PCR performed with primers specific for mouse Mitf and for human TYR and IRF4.

Primary melanoblast strains were established from human neonatal foreskin tissue and grown as described (Cook et al., 2003). The melanoblast media was removed and replaced with melanocyte growth media and differentiated over a seven-day period (Cook et al., 2009), however cholera toxin was removed from the media for the final three days of the differentiation process. Accordingly all results presented in this article were derived from differentiated cells. Genotyping of the rs12203592 SNP for each strain was determined using iPLEX Gold chemistry on a MALDI-TOF Mass Spectrometer (Sequenom, San Diego, CA, USA) (Duffy et al., 2010a; Duffy et al., 2010b), with confirmation of genotype in cultured cells performed by an allelic discrimination assay (#C_31918199_10, Taqman primers, Applied Biosystems) using a 7500 real-time PCR system (Applied Biosystems, Foster City, USA).

RNA extraction, cDNA synthesis and quantitative PCR analysis:

For RNA extraction, heart tissues from homozygous C57BL/6J-*Mitf*$^{mi\text{-}vga9}$ mice as well as controls were collected and frozen in liquid nitrogen until RNA extraction. RNA was also extracted from confluent cultures of 501mel and SKmel28 cells. Total RNA was extracted from tissues (and cells) using Trizol (Invitrogen) according to the manufacturer's instructions. The resulting RNA was dissolved in 50µl nuclease-free water and RNA concentration determined using Nanodrop ND-1000. The RNA was treated with DNAseI (Qiagen) and cleaned up using the RNeasy Kit (Qiagen). For cDNA synthesis, 2µg of RNA where resverse transcribed using the RevertAid First Strand cDNA synthesis kit (Fermentas). Gene expression was analyzed using quantitative RT-PCR. For each PCR reaction, 0.5 µl of the cDNA synthesis reaction (correlating to 50ng of RNA) were incubated with primers and the Maxima Sybr

Green mastermix (Fermentas) according to instructions of the manufacturer. Samples were run on an ABI 7500 PCR machine and analyzed afterwards with the REST2009 software package (Pfaffl et al., 2002). List of primers used is shown in Supplemental Table 3. Expression was normalised to GAPDH. For gene expression analysis we assayed for the following genes: MITF, IRF4, TFAP2a, TYR and DCT. IRF4 expression in the Australian human melanocyte strains was determined using a TaqMan IRF4 Gene Expression Assay (Hs00180031-m1 – Applied Biosystems).

Real-time RT-PCR of IRF4, TYR and MITF transcript levels

Total RNA was extracted from cells in culture with TRIzol reagent (Invitrogen) followed by chloroform extraction and isopropanol precipitation. Two microgram of total RNA were reverse transcribed using the M-MLV RT system (Invitrogen). For each sample, 2 µl cDNA were used in a reaction volume of 25 µl containing iTaq™ Universal SYBR® Green supermix (Bio-Rad) and 300 nM of the following primers: TBP-sense 5' CAC GAA CCA CGG CAC TGA TT 3'; TBP-antisense 5' TTT TCT TGC TGC CAG TCT GGA C 3'; MITF-M-sense 5' ACC GTC TCT CAC TGG ATT GG 3'; MITF-M-antisense 5' TAC TTG GTG GGG TTT TCG AG 3' ; IRF4-sense 5' ACA GCA GTT CTT GTC AGA G 3'; IRF4-antisense 5' GAG GTT CTA CGT GAG CTG 3'; TYR-sense 5' CCA TGA CAA ATC CAG AAC CC 3'; TYR-antisense 5' GGA CTA GCA AAT CCT TCC AG 3'. The results reported are standardized to TBP.

Sequencing of intron4 of IRF4

Genomic DNA was extracted from cells in culture and intron 4 of IRF4 was amplified with DyNAzyme II DNA polymerase (Thermo scientific) using the following primers: IRF4-intron4-sense 5' ATT TGC TAT GGC TGC TCC AA 3'; IRF4-intron4-antisense 5' GGG TAA AGG AGT GCA GGA GA 3'. The 460 bp amplified band was gel-extracted for each sample using the QIAquick gel extraction kit (Qiagen). The purified PCR products were sequenced by Eurofins MWG Operon with the same primers used for the PCR amplification.

shRNA and siRNA mediated knockdown of Mitf/IRF4/AP2a:

Cells were seeded in 6-well plates (100.000 cells per well) the day before transfection. The shRNA and controls where purchased from Openbiosystems (Mitf V2THS_76565 and V2LHS_257541; IRF4 V3LHS_377530 and V3LHS_377531; TFAP2a V3LHS_344899, neg. control RHS4346) and transfected into the cells using Exgen500 (Fermentas). The most effective knockdown was obtained by combining 2 shRNAs for each gene. The day after transfection, the media was changed and Puromycin added to a final concentration of 5µg/ml. The selection was continued until all the cells in the control wells were dead. The treated cells where then grown to 80-90% confluency and total RNA isolated and quantified using qPCR as described above.

After differentiating two highly IRF4 expressing cell lines QF1438 (CC) and QF1424 (CT) for eight days, the cells were transfected using 200 pmol of siRNA molecules using Lipofectamine 2000 (Invitrogen)

and cells were lysed after 48 hr, following differentiation from melanoblasts for eight days. The predesigned annealed siRNA's were purchased from Applied Biosystems (negative control, Applied Biosystems Cat # AM4635, SILENCER Negative Control siRNA#1 (40nmol) and Dharmacon (IRF4 specific siRNA, Dharmacon Cat # L-019668-00-005 On-target plus SMART pool siRNA Target Gene: IRF4 (Human)). Total cellular RNA was harvested and analysed by RT-qPCR, normalized to GAPDH.

Luciferase reporter assays

The SK-MEL-28 and 501mel cell lines were propagated according to guidelines from the American Tissue Culture Collection (ATCC), and melan-Ink4a-Arf according to guidelines from the Wellcome Trust Functional Genomics Cell Bank (Sviderskaya et al., 2002). Cells were plated at a density of 40,000 cells per well one day prior to transfection. Each well was transfected using 2 µl of Lipofectamine 2000 and 400 ng of the appropriate firefly luciferase reporter plasmid, and 8 ng of pHRL renilla luciferase reporter plasmid as internal control for transfection efficiency. The total concentration of transfected DNA was equalized using empty vector. Cells were lysed 48 hours after transfection and assayed with the Dual-Luciferase Reporter Assay System (Promega), and measurements made on a Tecan Genios Pro plate reader. At least three biological replicates were performed per construct per cell line, with each replicate performed using a unique plasmid prep and clone (i.e. unique colony from transformation after LR reaction). This was done to rule out the possibility that differences in DNA prep quality could be causing the observed difference in activity betweeen alleles. For co-transfection studies using the IRF4 reporter constructs, 10^4 cells were seeded onto 96 well plates. After the cells attached to the surface they were transfected with expression and reporter constructs using Exgene 500 (Fermentas), 50ng of the reporter constructs and 15ng of the Mitf/IRF4/TFAP2A plasmids and grown for 24h. The medium was removed completely and the cells lysed with 1x passive lysis buffer for 20min at room-temperature. Afterwards the luciferase activity was measured using the Dual-glo luciferase kit (Promega) according to the manufacturer's instructions. Samples were measured in six replicates with three independent experiments.

Protein analysis

Cells were grown in 6 well plates in the presence of the shRNA constructs as described, grown to 80-90% confluency and then lysed with RIPA buffer in the presence of protease inhibitors. Cell extracts where then denaturated with SDS-sample buffer and loaded on SDS-gels. For the western blots the gels where blocked with 5% milk in PBS-T, incubated with the appropriate antibody (Mitf: Thermo Fisher C5, TFAP2A: abcam ab52222, IRF4: Millipore 06-1047, TYR: Santa Cruz sc-7833, beta-actin: Millipore C4 MAB1501R), washed and incubated with the secondary antibody from Li-cor Biosystems (fluorescently labeled anti-mouse (IRDye 800CW Goat anti-Mouse), anti-rabbit (IRDye 800CW

Donkey anti-Rabbit) or anti-goat (IRDye 800CW Donkey Anti-Goat). The blots were scanned on a Li-cor Odyssey infrared scanner. Bands were quantified using the ImageJ software package.

Chromatin immunoprecipitation

501mel cells were transfected with GST-tagged Mitf or TFAP2A expression constructs. After reaching ~80% confluency, chromatin was cross-linked with formaldehyde, sonicated and pre-incubated with protein A/G-Sepharose beads (GE Healthcare). Pre-cleared chromatin samples were incubated with an antibody against the protein of interest (Mitf-GST or TFAP2A), human serum or no antibody. After overnight incubation the beads were isolated and the chromatin purified. Specific primers against the targeted regions (see Supplemental Table 2) were used to analyze binding to DNA.

For characterizing binding of IRF4 to the TYR promoter, 20-40 million cells were cross-linked with 1% formaldehyde on a shaking platform for 10 minutes at room temperature, and the cross-linking reaction stopped by incubation with 0.125M glycine for 5 minutes at room temperature. Cells were then washed two times in PBS, resuspended in ChIP lysis buffer (50 mM HEPES, 150 mM NaCl, 1% Triton-X 100, 0.1% Na-deoxycholate, 1mM EDTA) supplemented with SDS (0.25% final) and protease inhibitor cocktail (Roche 11873580001), incubated on ice for 1 hour, and sonicated for 16 cycles (each for 1 min. at 80% duty cycle and 85% power output) with an MS72 tip-fitted Bandelin Sonoplus HD2070 sonicator. Sonicated lysates were cleared by centrifugation for 5 min. at 13 krpm. Soluble chromatin lysate derived from ~5 million cells was diluted three-fold with ChIP lysis buffer with protease inhibitor cocktail, and was incubated with 50µl of an equal volume mix of Protein G and Protein A magnetic beads (Dynal, Life Technologies) pre-bound with 5µg anti-IRF4 antibody (Santa Cruz, sc-6059) or normal goat IgG (sc-2028) for 45 min. at room temperature. Bead-bound immune complexes were then washed 6 times each for 1 min at room temperature with shaking using 0.8 ml of the following: ChIP Lysis Buffer (2 times), ChIP Lysis Buffer with 500mM NaCl (2 times), and TE (2 times). The washed, bead-bound immune complexes and corresponding sonicated lysates (to be used as non-enriched 'input control') were then boiled for 10 min. in TE, treated with RNase A (Sigma Aldrich R4875; 0.1 µg/µl final) for 45 minutes at 39^{o}C (input controls only), treated with Proteinase K (Sigma Aldrich; 200ng/µl final) for 30 min. at 55^{o}C, boiled again for 10 min, and the DNA residing in the supernatant was purified using silica-based spin columns (Macherey Nagel # 740609, or Zymo Research D5205). Purified enriched DNA and input control DNA were then diluted 25- to 100-fold, and subjected to real-time PCR amplification in triplicates with region-specific primer pairs (sequences given below) on a PikoReal instrument (Thermo Scientific). qPCR reactions without template DNA were set up for each primer pair in order to rule out DNA contamination or unspecific amplification. The resulting qPCR data from each ChIP were then analyzed with the $\Delta\Delta$Ct method (taking into account the amplification efficiencies of the individual primer pairs as assessed by

standard curves generated with DNA dilution series), normalized to corresponding input DNA samples' data, and plotted.

DNA binding assay

Electrophoretic Mobility Shift Assay (EMSA) was performed using proteins expressed in the TNT-T7 Coupled Reticulocyte Lysate System (Promega, WI) according to the manufacturer's recommendations. 2 µl of *in vitro* translated proteins were analyzed by electrophoresis on 8% SDS-polyacrylamide gels and electro-transferred to nitrocellulose (Odyssey) membranes. Membranes were incubated with antibodies against MITF (C5 , MS-771, NeoMarkers) or TFAP2A (Abcam) and then with secondary antibodies conjugated to IRDye-800 (Licor Biosciences). The blotted proteins were detected and quantified using the Odyssey infrared imaging system. Equivalent protein quantities were added to gel shift assays.

For generating probes for the EMSA assays, the following primers and their reverse complementary strands wee synthesized (including a G-overhang at the 5'-end), annealed, ^{32}P-labeled, purified and used for EMSA analysis. Oligonucleotides carrying the sequence of the potential TFAP2A binding site (GGTAAAAGAAGGCAAATTCCCCTGT), the same sequence including the rs12203592 polymorphism (GGTAAAAGAAGGTAAATTCCCCTGT) and sequence where the entire binding site was mutated (GGTAAAAGAATTACGATTCCCCTGT). The probe is located at position chr6: 396309-396333 in build GRCh37.p5 of the human genome. For determining the DNA-binding ability of MITF, the following probes were generated: Mbox: 5'-AAAGCTAGTCATGTGCTTTTCAGA-3'. IRF4-Int4-wt: 5-TGGGAAACAGATGTTTTGTGGAAGTGGAAGATTTTGGAAGTAGTGCCT TATCATGTGAAACCACAGGGCAGCTGATCTCTTCAGGCTTTCTTGATGTGAATGACAGCTTTGTTTCATCCACTT TGGTGGGTAAAAGAAGG**C**AAATTCCCCTGT and IRF4-Int4-RS: 5-TGGGAAACAGATGTTTTGTGGAAGTGGAAGATTTTGGAAGTAGTGCCT TATCATGTGAAACCACAGGGCAGCTGATCTCTTCAGGCTTTCTTGATGTGAATGACAGCTTTGTTTCATCCACTT TGGTGGGTAAAAGAAGG**T**AAATTCCCCTGT.

For the MITF protein, 2 µl of TNT translated proteins were preincubated in buffer containing: 20 ng of poly(dI-dC), 10% fetal calf serum, 2 mM $MgCl_2$, and 2 mM spermidine for 15 min on ice. The TFAP2A protein was made using the TNT system (Promega) and the probes incubated in reaction buffer as described (Li et al., 2006). For supershift assay, 1.0 µg anti-TFAP2a (Abcam) antibody was added and incubated on ice for 30 min. For the MITF protein we followed the procedure of Pogenberg et al. (2012). For supershift assay, 1.0 µg anti-MITF (C5, MS-771, NeoMarkers) antibody was added and incubated on ice for 30 min. For both TFAP2A and MITF, the resulting DNA-protein complexes were resolved on 4.2% non-denaturing polyacrylamide gels, placed on a storage phosphor screen and then scanned on a Typhoon Phosphor Imager 8610 (Molecular Dynamics).

Reporter construct in Zebrafish.

Both versions of the rs12203592 polymorphism (wildtype C and mutant T) in the human Intron 4 of Irf4 were cloned initially into a pENTR shuttle vector and subsequently Gateway cloned into a zebrafish GFP-reporter plasmid, previously described (Bessa et al., 2009) (primers: forward, 5'-ATTTGCTATGGCTGCTCCAA-3' and reverse, 5'-CACCGGGTAAAGGAGTGCAGGAGA-3'). The plasmid was then micro-injected into the single cell of fertilized zebrafish eggs and the fish grown to the larval stage. For cell counts the embryos were divided into smaller groups, mounted, and scored blindly by an unbiased observer. The counts included both total number of embryos with at least one GFP+ melanocyte and total number of melanocytes within a group. Epinephrine treatment has been described previously (Fisher et al., 2006). Images were taken on a Nikon AZ100 Multizoom microscope with NIS-elements software. This work was performed under an approved protocol (FI10M369), reviewed by the Universisty of Iowa Institutional Animal Care and Use Committee.

Gene expression analysis in mouse melanocytes.

GFP-expressing melanoblasts/melanocytes from bitransgenic (iDct-GFP, strain FVB/N) E15.5 and E17.5 embryos and P1 and P7 postnatal pups were isolated via Fluorescence-Activated Cell Sorting (FACS), utilizing previously published protocols (Zaidi et al., 2011; Debbache et al., 2012). Total RNA was isolated from these FACS-sorted melanoblasts/melanocytes according to standard Illumina RNA-Seq paired-end protocol and sequenced on the Illumina GAIIx to 80 bp per read. The sequences were aligned using the genomic short-read nucleotide alignment program (Wu and Nacu, 2010) to mouse genome assembly mm9.

Conditional IRF4 mice.

Mice with loxP sites flanking exons 1 and 2 of IRF4,(Klein et al., 2006), were obtained from Jackson labs and crossed with mice expressing Cre recombinase under the control of the TYR promoter, (Delmas et al., 2003), resulting in excision of IRF4 in the melanocyte lineage. Mice were photographed at 4 weeks of age. Mice were housed in accordance with MGH and US National Institutes of Health guidelines. Genotyping primers were: IRF4F: 5'-AATACTGAGCTGCAGTCTAGC-3', IRF4R1: 5'-TGTTGCTGGTGGAGAGGAAG-3', IRF4R2: 5'-GACCACTACCAGCAGAACAC-3', TyrCreF: 5'-GTCACTCCAGGGGTTGCTGG-3', and TyrCreR: 5'-CCGCCGCATAACCAGTGA-3'. Both transgenic strains had been backcrossed onto a C57Bl6 background.

Supplementary References

Antonellis, A., Huynh, J.L., Lee-Lin, S.Q., Vinton, R.M., Renaud, G., Loftus, S.K., Elliot, G., Wolfsberg, T.G., Green, E.D., McCallion, A.S*., et al.* (2008). Identification of neural crest and glial enhancers at the mouse Sox10 locus through transgenesis in zebrafish. PLoS genetics *4*, e1000174.

Brass, A.L., Kehrli, E., Eisenbeis, C.F., Storb, U., and Singh, H. (1996). Pip, a lymphoid-restricted IRF, contains a regulatory domain that is important for autoinhibition and ternary complex formation with the Ets factor PU.1. Genes Dev *10*, 2335-2347.

Cook, A.L., Donatien, P.D., Smith, A.G., Murphy, M., Jones, M.K., Herlyn, M., Bennett, D.C., Leonard, J.H., and Sturm, R.A. (2003). Human melanoblasts in culture: expression of BRN2 and synergistic regulation by fibroblast growth factor-2, stem cell factor, and endothelin-3. J Invest Dermatol *121*, 1150-1159.

Cullinane, A.R., Curry, J.A., Carmona-Rivera, C., Summers, C.G., Ciccone, C., Cardillo, N.D., Dorward, H., Hess, R.A., White, J.G., Adams, D*., et al.* (2011). A BLOC-1 mutation screen reveals that PLDN is mutated in Hermansky-Pudlak Syndrome type 9. Am J Hum Genet *88*, 778-787.

Duffy, D.L., Zhao, Z.Z., Sturm, R.A., Hayward, N.K., Martin, N.G., and Montgomery, G.W. (2010b). Multiple pigmentation gene polymorphisms account for a substantial proportion of risk of cutaneous malignant melanoma. J Invest Dermatol *130*, 520-528.

Fisher, S., Grice, E.A., Vinton, R.M., Bessling, S.L., Urasaki, A., Kawakami, K., and McCallion, A.S. (2006). Evaluating the biological relevance of putative enhancers using Tol2 transposon-mediated transgenesis in zebrafish. Nature protocols *1*, 1297-1305.

Fu, C., Wehr, D.R., Edwards, J., and Hauge, B. (2008). Rapid one-step recombinational cloning. Nucleic acids research *36*, e54.

Li, H., Goswami, P.C., and Domann, F.E. (2006). AP-2gamma induces p21 expression, arrests cell cycle, and inhibits the tumor growth of human carcinoma cells. Neoplasia *8*, 568-577.

Pfaffl, M.W., Horgan, G.W., and Dempfle, L. (2002). Relative expression software tool (REST) for group-wise comparison and statistical analysis of relative expression results in real-time PCR. Nucleic acids research *30*, e36.

Pogenberg, V., Ogmundsdottir, M.H., Bergsteinsdottir, K., Schepsky, A., Phung, B., Deineko, V.,Milewski, M., Steingrimsson, E., and Wilmanns, M. (2012). Restricted leucine zipper dimerization and specificity of DNA recognition of the melanocyte master regulator MITF. Genes & development *26*, 2647-2658.

Rajeevan, H., Soundararajan, U., Kidd, J.R., Pakstis, A.J., and Kidd, K.K. (2012). ALFRED: an allele frequency resource for research and teaching. Nucleic Acids Res *40*, D1010-1015.

Steingrimsson, E., Arnheiter, H., Hallsson, J.H., Lamoreux, M.L., Copeland, N.G., and Jenkins, N.A. (2003). Interallelic complementation at the mouse Mitf locus. Genetics *163*, 267-276.

Tellez, C., McCarty, M., Ruiz, M., and Bar-Eli, M. (2003). Loss of activator protein-2alpha results in overexpression of protease-activated receptor-1 and correlates with the malignant phenotype of human melanoma. The Journal of biological chemistry *278*, 46632-46642.

Wu, T.D., and Nacu, S. (2010). Fast and SNP-tolerant detection of complex variants and splicing in short reads. Bioinformatics *26*, 873-881.

Zaidi, M.R., Davis, S., Noonan, F.P., Graff-Cherry, C., Hawley, T.S., Walker, R.L., Feigenbaum, L., Fuchs, E., Lyakh, L., Young, H.A*., et al.* (2011). Interferon-gamma links ultraviolet radiation to melanomagenesis in mice. Nature *469*, 548-553.

Supplementary Figure 1

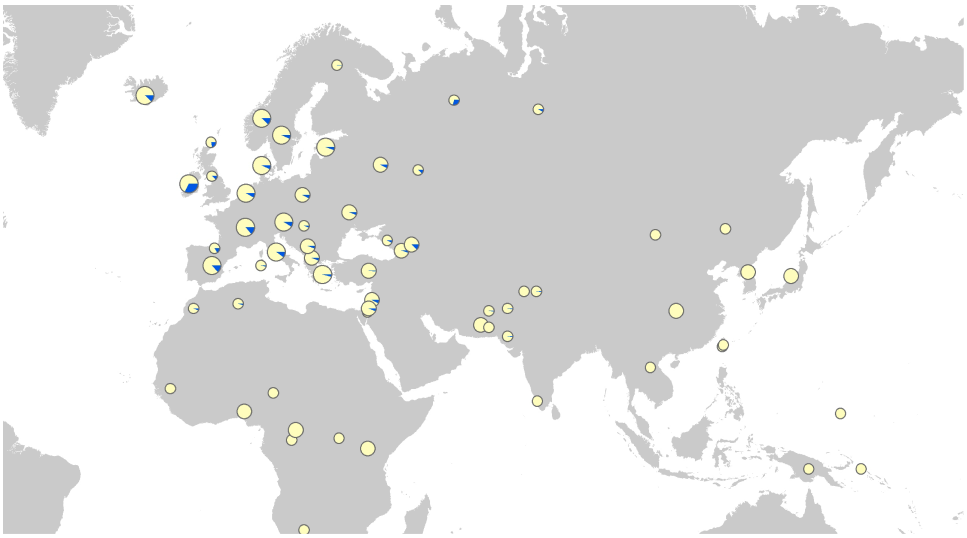

Supplementary Figure 2

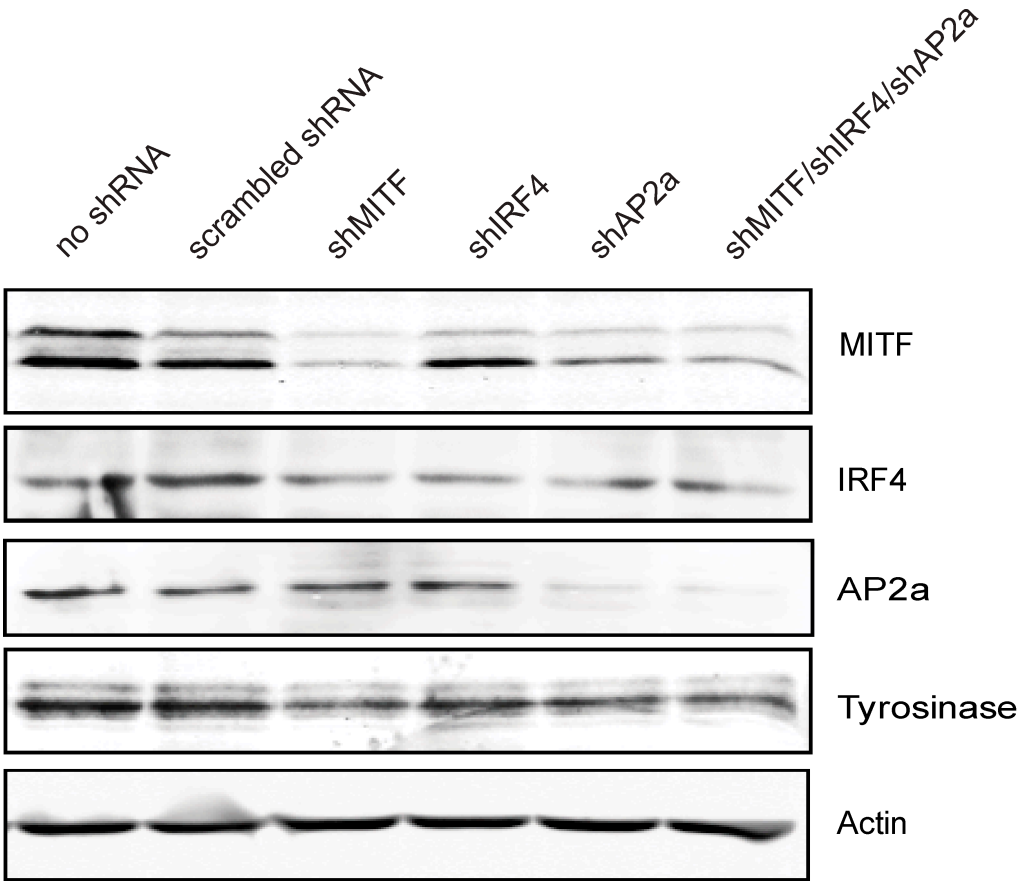

Supplementary Figure 3

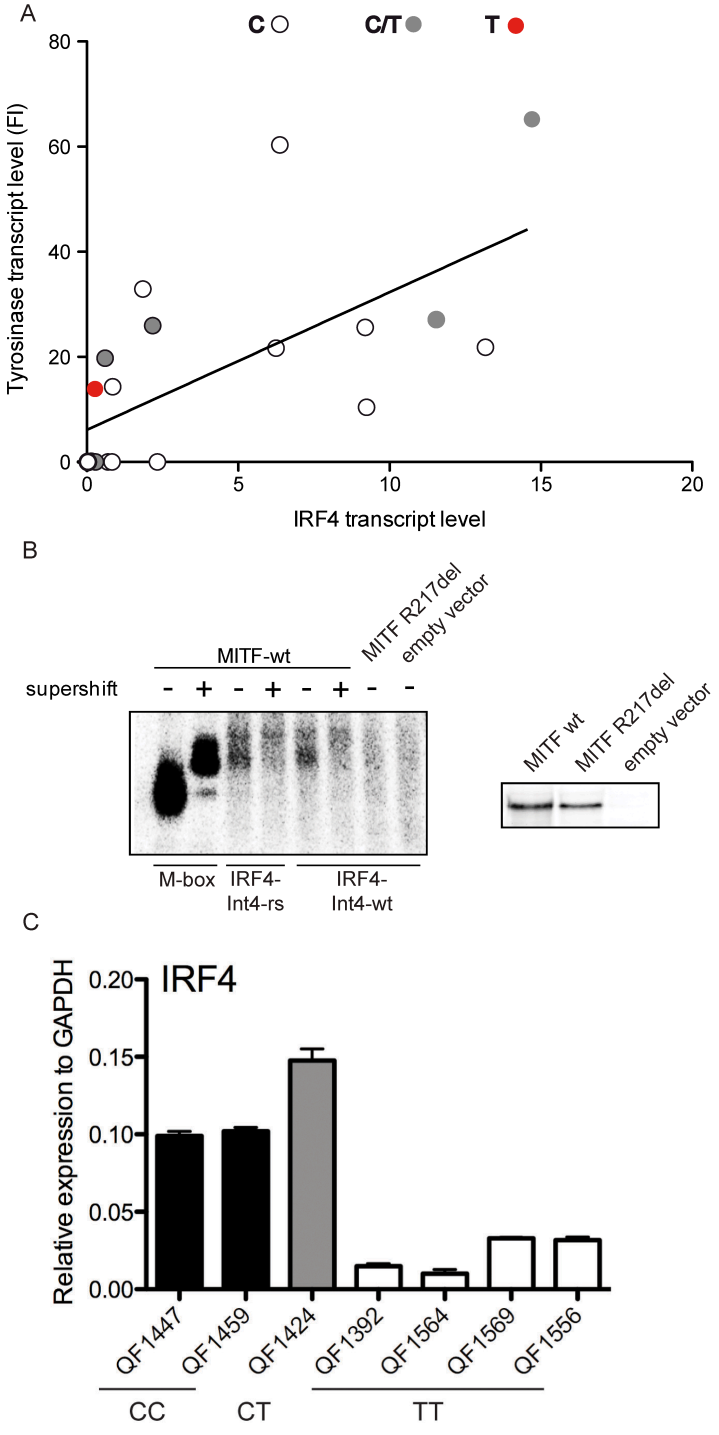

Supplementary Figure 4

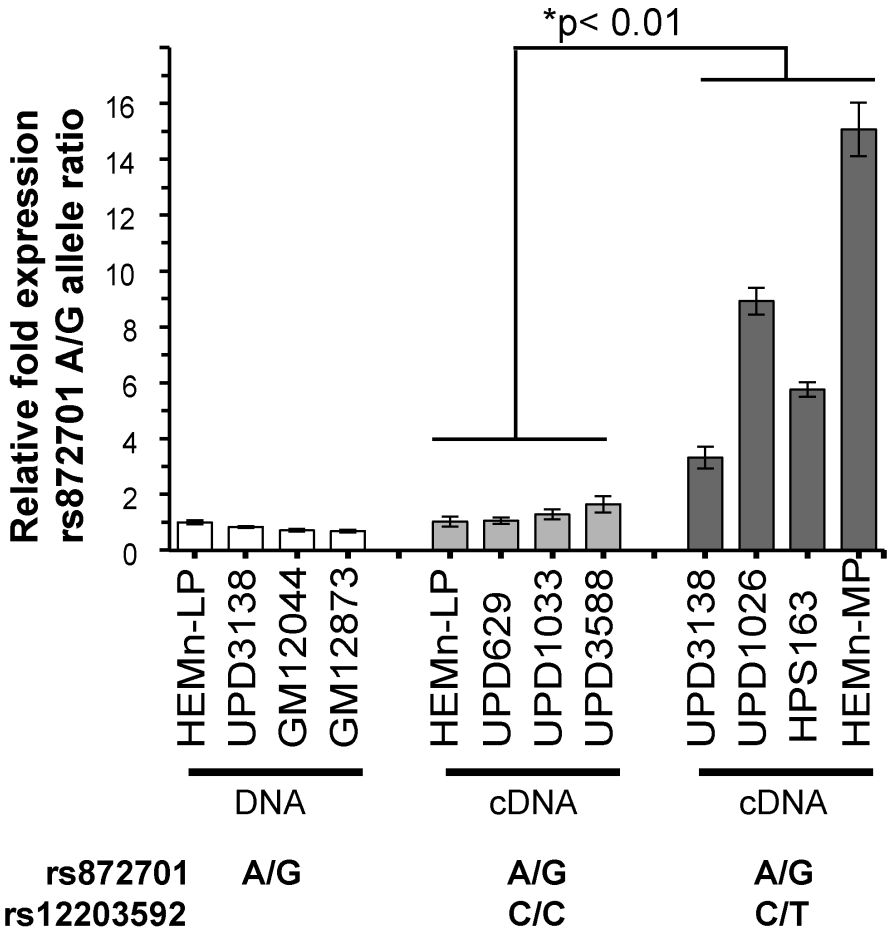

Supplementary Figure 5

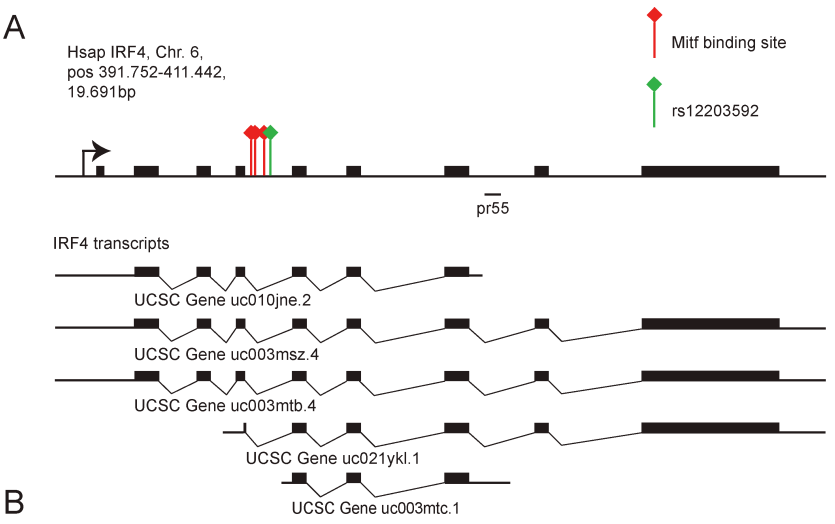

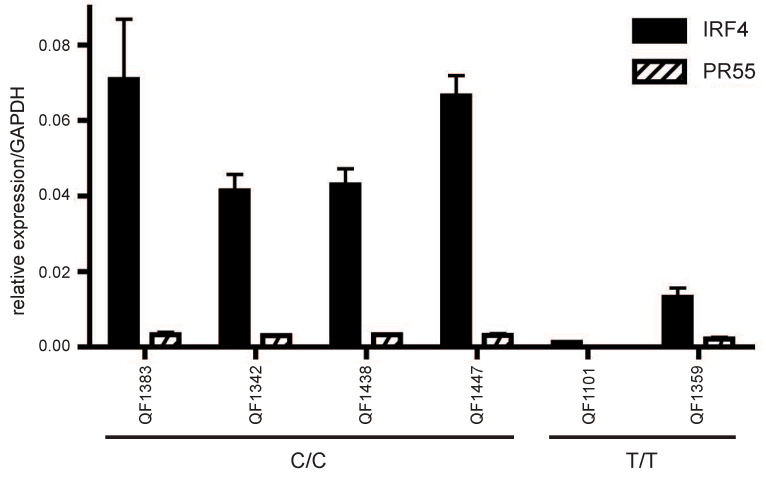

Supplementary Figure 6

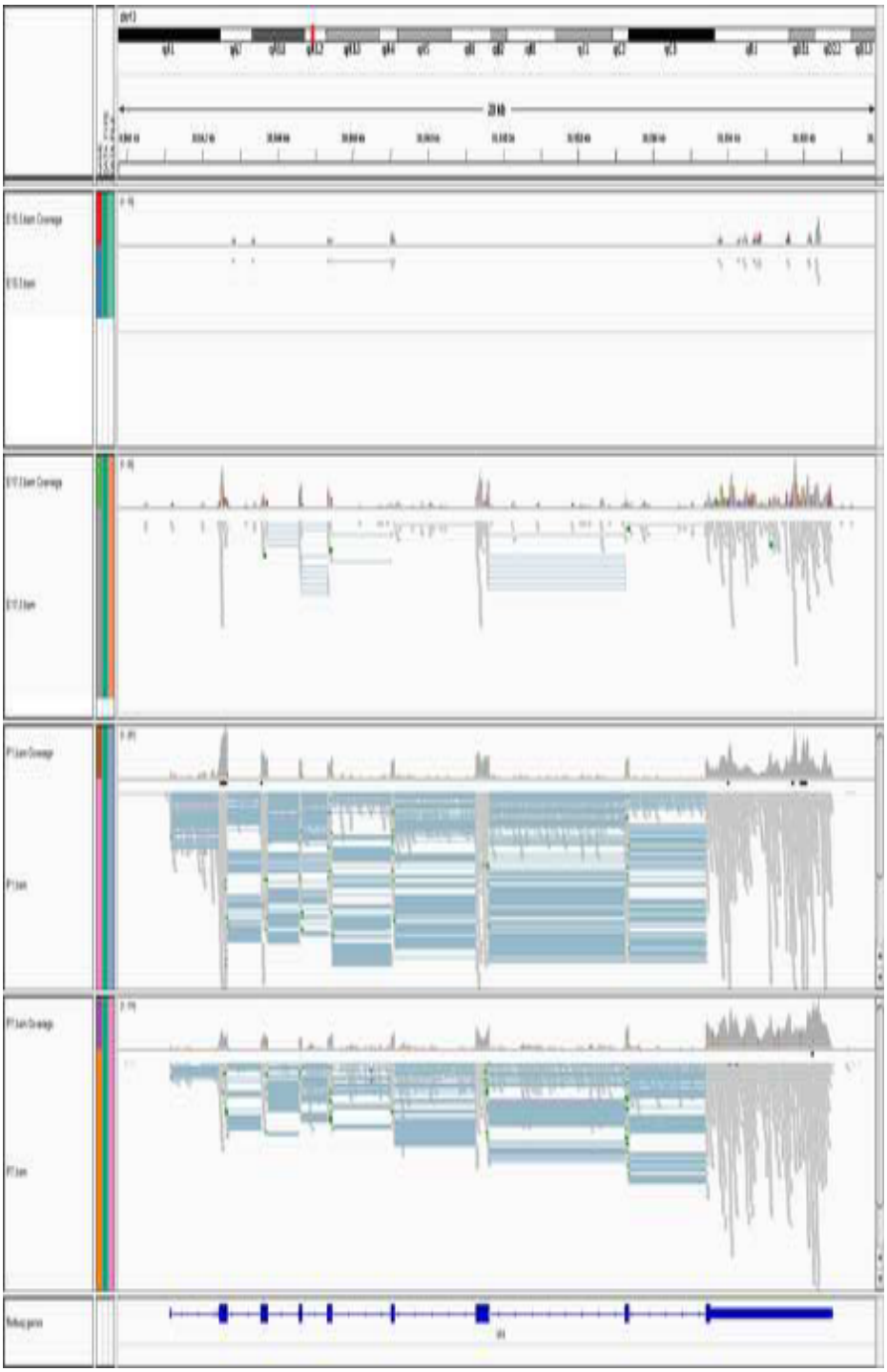

Supplementary Figure 7